

Sheffield Hallam University

The design and analysis of static pallet racking systems.

CROSBIE, Matthew William James.

Available from the Sheffield Hallam University Research Archive (SHURA) at:

<http://shura.shu.ac.uk/19514/>

A Sheffield Hallam University thesis

This thesis is protected by copyright which belongs to the author.

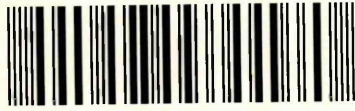
The content must not be changed in any way or sold commercially in any format or medium without the formal permission of the author.

When referring to this work, full bibliographic details including the author, title, awarding institution and date of the thesis must be given.

Please visit <http://shura.shu.ac.uk/19514/> and <http://shura.shu.ac.uk/information.html> for further details about copyright and re-use permissions.

CITY CAMPUS, POND STREET,
SHEFFIELD, S1 1WR.

101 617 295 8



REFERENCE

ProQuest Number: 10694395

All rights reserved

INFORMATION TO ALL USERS

The quality of this reproduction is dependent upon the quality of the copy submitted.

In the unlikely event that the author did not send a complete manuscript and there are missing pages, these will be noted. Also, if material had to be removed, a note will indicate the deletion.



ProQuest 10694395

Published by ProQuest LLC (2017). Copyright of the Dissertation is held by the Author.

All rights reserved.

This work is protected against unauthorized copying under Title 17, United States Code
Microform Edition © ProQuest LLC.

ProQuest LLC.
789 East Eisenhower Parkway
P.O. Box 1346
Ann Arbor, MI 48106 – 1346

**THE DESIGN AND ANALYSIS OF STATIC
PALLET RACKING SYSTEMS**

Matthew William James Crosbie

A thesis submitted in partial fulfilment of the requirements of
Sheffield Hallam University
for the degree of Master of Philosophy

December 1998

Collaborating Organisation : Redirack UK Ltd.



LEVEL 1

Declaration

I wish to declare that, except for commonly understood and accepted ideas, or where specific reference is made to the research of other authors, the contents of this thesis are my own original work. The work has not been previously submitted, in part or in whole, to any University for any degree, Diploma, or other qualification.

Abstract

The essential purpose of a pallet racking system is to support the largest load possible in relation to its self weight, while maintaining ready access to individual pallets and preventing damage to stored goods. This should be achieved within the constraints imposed by design and safety considerations. This basic requirement has ensured that most current rack designs consist of thin-walled ($< 3\text{mm}$) steel elements whose self weight typically accounts for between 2% to 3% of the total weight of the structure. In general, the design is complicated by the semi-rigid nature of beam/upright and upright/floor connections, and by the use of perforated upright members in large, multi-storey sway frames.

Currently, a UK code exists (SEMA) to design racking installations using a permissible stress philosophy. However, the development of limit state design in conjunction with advances in computing power and the emergence of the single European market have combined to create an environment in which the development of a new European design code has become logical and desirable. A code has been developed at the request of the European industrial pallet racking manufacturers association (FEM), to take account of the latest developments in steel design. When the FEM code has been fully evaluated (to April 2000), and assuming that no modifications are necessary, it will be implemented as a Euro-norm with the intention of replacing all of the national codes in Europe. This thesis is intended to form a part of that evaluation process.

The purpose of this document is to examine the performance of a single manufacturers industrial pallet racking system in relation to the FEM code. In the first instance, this involved the design and application of suitable experimental procedures, followed by the completion of a sufficient number of tests to generate a reliable statistical characterisation of each of the components in the system. Approximately 2000 tests were completed during the course of this exercise. An approach was subsequently established using this characteristic test data, and based on the recommendations contained within the FEM, in order to predict the load capacity of any given racking system. To this end, the use of finite element predictive software was investigated, typically incorporating second order analysis techniques to the treatment of sway frames with loose and semi-rigid connections. This 'novel' design approach has been documented using a detailed worked example. Any considerations necessary for the purposes of design are included within a full design procedure.

The European code has subsequently been compared to the national SEMA code, in order that an assessment can be made of the accuracy and limitations of each. This includes an investigation into the key differences between test methodologies and the interpretation of experimental results. In addition, twenty eight structures possessing a broad range of rack geometries have been analysed using each code, in order that conclusions can be drawn on the consequences for the UK racking industry of designing to a new European code. This investigation has calculated a mean reduction in load carrying capacity of 15.2% for FEM designed rack, with a range distributed between a 12.8% increase in capacity to a 36.5% reduction. This is the first indication available as to the effect of the implementation of the FEM code on the load capacity of racking.

Finally, a sensitivity analysis has been performed on twenty four further structures to identify some of the critical factors that are most influential in determining the load carrying capacity of a rack, based on the design approach already identified. Variables included: beam end connector looseness; moment capacity and rotational stiffness; floor connector stiffness and upright yield stress.

Acknowledgements

I would like to thank the following people for their assistance and encouragement during the writing of this thesis. Firstly my supervisors, Prof. Graham Cockerham and Dr. Neil Taylor who have given me invaluable support and guidance, Jack Holden, whose clear insight and unlimited patience have made its writing possible, and Dr. M. Godley at Oxford Brookes University, (co-author of the FEM code) whose knowledge of this subject area is unparalleled.

The influence of my friends has been invaluable, although not necessarily of any relevance to this thesis. I would therefore like to express my appreciation to the following people :

Paul "mine's a pernod and coke" Hutchinson, who would like me to mention that I owe everything to him!

Rod 'international man of mystery' Taylor for throwing up on my stairs, and Ozma "I'm a doctor not a pea brain" Omar, for hoovering it up.

Steve Cousins for ensuring my complete safety while I was writing up, and for doing that great poster for my wedding.

..... and not forgetting Marcus Bridges, Tim Bowers and Ged Carden without whom no Saturday night is complete.

Sincere thanks must also go to my family:

To my brother, Philip (o' fish) for his monosyllabic phone conversations, for ringing me last Sunday morning at 8am to tell me he was going to work! and for his sincerity, wit and genuinely decent, charming personality. Special thanks must go to 'roids for trying to change him for the better, against all the odds.

To my wife, Sandra for paying half the mortgage, doing most of the decorating (in the bathroom) and for having a juicy, red pair of kissable lips.

And last, but by no means least to my dad, for being there, keeping me cheerful and for being a great dad!

Finally, I would like to dedicate this thesis to my mum. Unfortunately, she is not around to see it completed, but had she been, I'm sure it would have made her very proud.

List of Symbols

A	accidental action	r	internal bending radius
A/S _o	cross sectional area	S	shear force
A _{eff}	effective cross sectional area	s	system length
A _g	gross cross sectional area	s	standard deviation
A _{ph}	accidental horiz. placement force	s _w	system length of web
A _{pv}	accidental vert. placement force	t	thickness of material
b	width of upright/sample	t _t	Observed core thickness at test
b _o	width of flat element	V	shear force
b _p	notional plane width of element	V	vertical load
D	spacing of upright in a frame	V _{cr}	elastic critical value of critical load
E	modulus of elasticity	W	section modulus
e	effective bearing width of baseplate	W	total load on a beam
f	strength	W _f	max. frame capacity
f _{cu}	characterist. concrete cube strength		
f _t	observed yield strength (test)	α	imperfection factor
f _u	ultimate tensile strength	β	beam coefficient
f _y	nominal yield strength	β	correction factor for thickness.
G	shear modulus	β	amplif. factor for 2 nd order effects
G _k	characteristic value of dead load	γ	partial safety factor (PSF)
H	frame height	γ _A	PSF - accidental actions
h	storey height	γ _f	load factor
h _p	length, longest plane web element	γ _G	PSF - permanent actions
h _w	depth of web normal to flange	γ _M	material factor
h _l	length of web between system lines	γ _Q	PSF - variable actions
I	second moment of area	δ	deflection
I _T	St Venant torsional constant	ε	strain
I _w	warping constant	θ	rotation
i	radius of gyration	λ	slenderness ratio
i _o	polar radius of gyration	λ	non-dimensional slenderness ratio
K	effective length factor	ν	Poisson's ratio
k _b	connector stiffness	ρ	density
k _e	effective connector stiffness	τ	shear strength
l	length	φ	sway imperfection
l	effective length or buckling length	φ _o	initial sway imperfection
L	span	φ ₁	looseness of connector
L _o	original gauge length	χ	stress reduction factor for buckling
M	bending moment		
N	axial force		Subscripts
N	no. of 90° bends in section	b	buckling
n	number of tests	c	compression
n _b	number of bays	cr	critical
n _s	number of storeys	d	design
Q	variable action	FT	flexural torsional
Q _f	concentrated load on floor	g	gross
Q _h	horiz. load/crane at guide rail level	i	test number
Q _{ph}	horizontal placement load	k	characteristic
Q _{pv}	vertical placement load	LT	lateral torsional
Q _u	unit load	m	mean value
q	distributed load	n	corrected value
R	resistance	R	resistance
R _m	mean value of adjusted test results	S	strength
R _n	corrected failure loads	T	torsional
R _t	observed failure load	t	observed test value

Contents

	Page No.
Declaration	ii
Abstract	iii
Acknowledgments	v
List of Symbols	vi
Contents	vii
Chapter 1 Introduction	
1.1. General outline	1
1.2. A new European design code	2
1.3. Objectives of the research	3
Chapter 2 Literature Review	
2.1. General outline	5
2.2. Cold-reduced material	6
2.3. Enhanced yield of perforated section	7
2.4. Generation of design column curves	8
2.5. Limit state design considerations	9
2.6. Down-aisle sway stability	10
2.7. Semi-rigid connections	12
2.8. Summary	13
Chapter 3 Product Configuration and Referencing	
3.1. Introduction	14
3.2. Manufacturing processes	
3.2.1. Outline	14
3.2.2. Roll forming	15
3.2.3. Punch press	15
3.2.4. Blanking and forming	15
3.2.5. Reducing mill	15
3.2.6. Welding	16
3.2.7. Painting	17
3.3. Frame properties	18
3.4. Beam properties	20
3.5. Material tensile testing	
3.5.1. General outline	21
3.5.2. Sample preparation	22

3.5.3. Test methodology	24
3.5.4. Discussion	26

Chapter 4 The Determination of Individual Upright Characteristics through Experimentation

4.1. General outline	29
4.2. Stub column compression test	
4.2.1. Introduction	30
4.2.2. Test geometry	30
4.2.3. Methodology	31
4.2.4. Discussion	33
4.3. Results and analysis	
4.3.1. Introduction	36
4.3.2. Material and geometric corrections	36
4.3.3. Characteristic values of failure load	38
4.3.4. Effective area of uprights	40
4.3.5. Results summary	40
4.4. Compression tests on uprights	
4.4.1. General outline	41
4.4.2. Test arrangement	41
4.4.3. Test measurement	47
4.4.4. Discussion	47
4.5. Results and analysis	
4.5.1. Material and geometric corrections	50
4.5.2. Calculation of column buckling curve	52
4.6. Tests for Shear stiffness of frames	
4.6.1. General outline	57
4.6.2. Test arrangement	57
4.6.3. Test measurement	59
4.6.4. Discussion	59
4.7. Results and analysis	
4.7.1. Introduction	60
4.7.2. Calculation of transverse shear stiffness	61
4.7.3. Calculation of effective area of frame bracing	61
4.8. Bending test on upright section	
4.8.1. General outline	64
4.8.2. Test arrangement	65
4.8.3. Data capture	66
4.9. Results and analysis	
4.9.1. Introduction	70
4.9.2. Material and geometric corrections	70
4.9.3. Characteristic moment of resistance and results summary	71
4.10. Floor connector test	
4.10.1. General outline	72
4.10.2. Test arrangement	72
4.10.3. Test methodology	73

	4.10.4. Data acquisition	75
4.11.	Results and analysis	
	4.11.1. Introduction	77
	4.11.2. Consideration of the statistical treatment of results	78
	4.11.3. Calculation of floor connector design moment and stiffness	79
Chapter 5	The Determination of Beam End Connector Characteristics through Experimentation	
5.1.	General outline	83
5.2.	Bending tests on beam end connectors	
	5.2.1. Introduction	84
	5.2.2. Test arrangement	84
	5.2.3. Instrumentation	86
	5.2.4. Data acquisition	86
	5.2.5. Discussion	88
5.3.	Results and analysis	
	5.3.1. Introduction	92
	5.3.2. Material and geometric corrections	92
	5.3.3. The relationship between the design moment and stiffness	92
	5.3.4. Calculation of beam end connector design moment	94
	5.3.5. Calculation of beam end connector design stiffness	95
5.4.	Looseness test on beam end connectors	
	5.4.1. Introduction	98
	5.4.2. Test arrangement	100
	5.4.3. Test measurements	101
5.5.	Results and analysis	
	5.5.1. Calculation of design looseness	103
	5.5.2. Discussion	105
5.6.	Shear tests on beam end connectors	
	5.6.1. Introduction	107
	5.6.2. Test arrangement	107
	5.6.3. Data acquisition	109
	5.6.4. Discussion	110
5.7.	Results and analysis	
	5.7.1. Evaluation of characteristic shear strength	112
5.8.	Shear tests on beam end connector locks	
	5.8.1. Introduction	114
	5.8.2. Test arrangement	114
	5.8.3. Data acquisition	116
	5.8.4. Discussion	118
5.9.	Results and analysis	
	5.9.1. Evaluation of characteristic shear strength	119
5.10.	Bending tests on beams	
	5.10.1. Introduction	120
	5.10.2. Test arrangement	120
	5.10.3. Data capture	122

	5.10.4. Discussion	123
5.11.	Results and analysis	
	5.11.1. Calculation of beam rotation at service load	127
	5.11.2. Calculation of beam characteristic moment of resistance	127
Chapter 6	Racking System Design to FEM 10.2.02 using Finite Element Analysis	
6.1.	General outline	129
6.2.	The effect of second order analysis	130
6.3.	System design using finite element analysis	
	6.3.1. Model generation	131
	6.3.2. Treatment of semi-rigid joints in F.E. software	132
	6.3.3. The rotational limit for the combin40 element	135
6.4.	Design procedure	
	6.4.1. Introduction	137
	6.4.2. Section properties	137
	6.4.3. Calculations and considerations necessary for the construction of an F.E. model	139
	6.4.4. Frame imperfections	141
	6.4.5. Member imperfections	142
	6.4.6. Bracing system imperfections	142
	6.4.7. Accidental vertical load	143
	6.4.8. Accidental horizontal load	143
	6.4.9. Load combinations	144
	6.4.10. Additional load cases	149
6.5.	Design checks	
	6.5.1. Frame design checks	151
	6.5.2. Bending and axial compression check	151
	6.5.3. Bending and axial compression without lateral-torsional buckling	152
	6.5.4. Bending and axial compression with lateral-torsional buckling	154
	6.5.5. Design of bracing in upright frame	155
	6.5.6. Sway limit in the down aisle direction in the serviceability limit state	157
	6.5.7. Floor connector check	157
6.6.	Beam design checks	
	6.6.1. Beam end connector check	159
	6.6.2. Moment of resistance of members not subject to lateral buckling	160
	6.6.3. Beam design with respect to shear	160
	6.6.4. Design strength of beams with respect to web crippling	161
	6.6.5. Beam design with respect to horizontal placement loading	162
	6.6.6. Combined bending moment and shear force	163

6.6.7.	Combined bending moment and concentrated load	163
6.6.8.	Beam deflection check in the serviceability limit state	163
6.7.	Summary and conclusions	164
Chapter 7	A Comparison of Rack Performance based on the Limit State Approach of FEM and the Permissible Stress Approach of SEMA	
7.1.	General outline	165
7.2.	Treatment of experimental data	
7.2.1.	Introduction	166
7.2.2.	Beam end connector performance	166
7.2.3.	Beam end connector looseness	173
7.2.4.	Floor connector performance	176
7.2.5.	Upright capacity	178
7.3.	SEMA design	
7.3.1.	Introduction	180
7.3.2.	Rack dimensioning and section properties	180
7.3.3.	Beam design	180
7.3.4.	Frame design	182
7.3.5.	Overall rack stability	184
7.3.6.	Summary of the major design and analysis differences between codes	185
7.4.	Racking system design comparisons	187
7.5.	Impact of design changes to the development of the rack	
7.5.1.	Introduction	192
7.5.2.	Variations in beam end connector looseness	193
7.5.3.	Variations in beam end connector moment capacity and stiffness	195
7.5.4.	Variations in nominal material yield strengths	197
7.5.4.	Variations in floor connector stiffness	199
7.6.	Summary and conclusions	200
Chapter 8	Conclusions and Further Work	
8.1.	General outline	202
8.2.	Summary and conclusions	202
8.3.	Further work	205
	References	207
	Appendix A : Standard drawings	
	Appendix B : Concrete design mix (floor connector test), floor connector test rig	
	Appendix C : Equal area calculation method	
	Appendix D : Statistical correction factor table (k_s)	
	Appendix E : 4 level, 6 bay down and cross-aisle rack in Ansys 5.4, Visual basic sub-routines for SEMA design program, deformed rack geometry	

Chapter 1

Introduction

1.1. General outline

During the manufacture-to-consumption cycle, approximately 40% of all commercially produced goods are stored on industrial pallet racking systems [1]*. In the UK, the growth in the development and use of these structures has been predominantly in response to the ever increasing number of out-of-town developments, warehouses and distribution centres springing up around the country.

The essential purpose of any adjustable pallet racking system is to maximise the load capacity of the structure within a specified 'storage cube', while maintaining ready access to individual pallets and preventing damage to stored goods. There is an expectation that these goals can and should be achieved, whilst minimising the associated costs to the customer. Simply stated, economic imperatives dictate that within the constraints imposed by design and safety considerations, a rack must be manufactured to support the largest load possible in relation to the self weight of the system. This basic requirement has ensured that most current rack designs consist of thin-walled steel elements whose self weight typically accounts for between 2% to 3% of the total weight of the structure. Advances in the design of these typically slender structures with the development of limit state design have combined with the emergence of the European single market to create an environment in which the development of a new Europe-wide design code has become a logical and desirable outcome.

* Numbers in square brackets refer to references listed at the end of this thesis.

1.2. A new European design code

This dissertation examines the impact of the Federation Europeenne de la Manutention (FEM) code 10.2.02. 'Recommendations for the Design of Steel Static Pallet Racking and Shelving' [2], on the design of racking structures in the UK. The intention is that the code in the form of a Euronorm should replace existing national codes across Europe by April 2000. This allows for an 18 month period of evaluation of the code, of which this document forms a part.

The code attempts to reflect the current state-of-the-art in terms of steel design good practice and as a result borrows sufficiently from 'Eurocode 3 : Design of Steel Structures' to form the basis for its design methodology. This approach has been tempered however, by the particular problems associated with the design of racking systems. These include the use of perforated, thin-walled steel uprights in large, multi-storey sway frames incorporating 'loose' connections. In conjunction with this, is the necessity to consider the semi-rigid nature of the joints which form both the beam to upright interface and the interface between the upright and the ground. The design approach adopted in the code is therefore based on an empirical assessment of the behaviour of the individual components that make up a rack, and this approach is reflected in this document.

The FEM code is based on limit state design and is intended to replace the national SEMA (Storage Equipment Manufacturers Association) code [3] which uses a permissible stress design philosophy and is currently in use in the UK. Across the European Union, it is expected that by the start of the next millennium, or shortly thereafter the FEM code will provide the standard design criteria by which all racking structures will be assessed. The broad intention of this thesis is to measure the impact of the introduction of such a code on the pallet racking industry in this country with

reference to a single manufacturing company, and to explore the possibility of improving rack design to exploit the advantages arising from a new approach.

1.3. Objectives of research

The following objectives have been identified for the purposes of this research :

- To examine the structural behaviour of thin-walled, cold formed steel sections either perforated or non-perforated through the design and application of suitable experimental testing procedures, within the guidelines set down by the FEM code. A sufficient number of tests will be completed to generate a reliable statistical characterisation for individual components of various cross sectional geometry and for combinations of components where semi-rigid joints are formed.
- To establish an approach to pallet racking design on the basis of recommendations contained within the new code using characteristic data obtained through experimentation in order to predict the failure and/or the loading capacity of racking systems using this 'novel' design methodology.
- To investigate the use of finite element modelling as predictive software, particularly with regard to the use of second order analysis techniques and the treatment of semi-rigid joints in sway frames.
- To employ manual calculation techniques contained within the current national design standard in order that a comparison may be made between the accuracy and limitations of each of the available codes. This comparison should include a broad range of design examples in order to allow generalised conclusions to be drawn, on the consequences for the UK racking industry of designing to a novel European code.
- To examine on the basis of a sensitivity analysis, the critical factors that determine the load carrying capacity of a range of racking structures, based on the design approach

adopted by the new code and as a direct consequence to modify the rack design appropriately to maximise its performance.

These objectives were achieved during the course of this research.

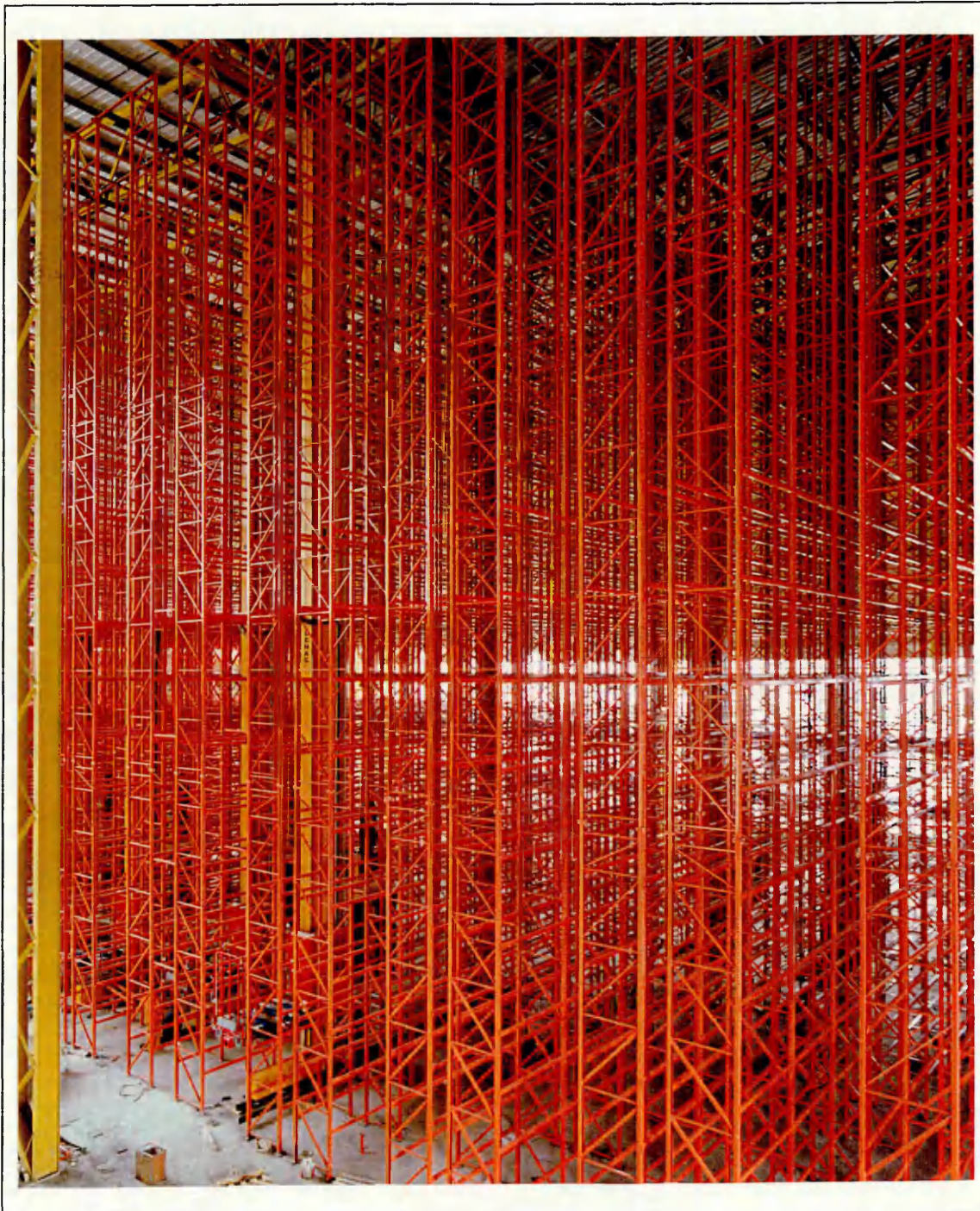


Fig. 1.1. The construction of a 25m high racking installation

Chapter 2

Literature Review

2.1. General outline

A racking structure is typically composed of thin-walled members, cold-formed into beams and uprights, which are connected together using semi-rigid joints at the beam-upright interface. Typically, each structure is attached to a (concrete) floor using a steel baseplate which is also considered to have partial rigidity. The nature of racking is such, that the behaviour of these joints is crucial to its' stability and load carrying capacity.

Until recently, with the increase in the ability of the computer to provide fast and accurate solutions to complex non-linear analyses, it has not been possible to develop anything other than approximate manual solutions [3] for racking system design, using a very limited number of load conditions. However, the Storage Equipment Manufacturers Association (SEMA) code, the UK's code of practice for the last twenty years, has proved more than adequate for the design needs of the industry up to this point in time. These guidelines are based on BS449 [4] which was revised in April 1975 to include a specification for "The use of Cold-Formed Steel Sections in Building" [5].

This standard adopts a permissible stress approach to design which was embraced by the SEMA code of practice, although further adaptation was necessary in order that the particular behavioural qualities of racking should be taken fully into account. Special consideration has been given to the behaviour of the compression members which are invariably cold-formed, perforated, thin-walled (typically 3mm or less in thickness) sections, and additionally to the connections at both the floor and beam level. Typically, these possess an amount of rotational stiffness and as a result are considered to be semi-rigid, with the beam end connectors having an additional, potential degree of looseness. Both beams and frames may be manufactured from cold-rolled material.

The chapter headings contained within the FEM are indicative of the design approach that it advocates. These included : the general scope of the code; the safety philosophy, and consideration of loads and imperfections on the system; member design considerations; global analysis of beam pallet racks; and finally the approach to testing. Shelving design has also been incorporated within the code, but is not included within the remit of this document.

2.2. Cold-reduced material

A significant problem with using cold-reduced steels, which is not addressed by the SEMA code is the relationship between the ultimate and the yield stress (f_u/f_y). This has been taken up by the FEM [2]. Some manufacturers have historically used these steels in their uprights and beams in order to improve the performance of their sections by enhancing their yield strength values. With the emergence of the new code this issue was examined in the light of the Eurocode [6] recommendation that the ratio between the two values should be no less than 1.2. Strictly adhered to this would mean a reliance purely on hot rolled materials for use in the manufacture of racking systems, and the redesign of many racking systems.

When steel is cold reduced its ductility is diminished when compared with that normally associated with mild steel, making it much more brittle. In addition to this, the process has the effect of increasing both the yield point and the ultimate tensile strength of the material. This has immediate benefits both in terms of component testing and in the subsequent design unity checks. However, as a consequence there is also a corresponding reduction in the ratio between these values. This can fall to as little as 1.05 or less. Clearly, the effect of this is to seriously undermine the inherent factor of safety of the material, and under normal circumstances this should give serious cause for concern.

Although there is an historical precedent in the pallet racking industry over many years which supports the use of cold reduced materials and products, until the development of the FEM code no specific work had been undertaken into the relative merits of cold reduced steels. Comparative research conducted by Davies and Cowen [7] using ‘conventional steel’ and cold reduced steel in two full-scale tests, concluded that “the cold-reduced steel performed in every respect in a similar manner to the conventional steel and that there was no reduction in performance as a consequence of the reduced ductility.” As a result of this work, a view has been taken by the industry that cold-reduced steels may be used in the manufacture of racking, and a clause to this effect has been included in the FEM code. The ratio of f_w/f_y may be as small as 1.05 (FEM Cl.1.8.3.c.). It is worth mentioning here that despite the inclusion of this clause and the conclusions of the research, there seems to be a move away from the use of cold-rolled steels, particularly in the manufacture of uprights.

2.3. Enhanced Yield of Perforated Sections

Consideration for enhancing the nominal value of yield stress for perforated sections within the limits outlined above, has not been addressed by the FEM design procedures. Cl. 1.9. allows an increase in yield for non-perforated members only, based on the effects of cold-forming and the number of 90° bends (partial or complete) in the section. It is suggested here that a modified version of this formula (also contained in current British standards [8]) should be considered as a method of more accurately assessing the true value of the yield stress in the steel component being considered. The formula as it appears in the FEM is :

$$f_{ya} = f_{yb} + \left(\frac{CNt^2}{A_g} \right) (f_u - f_{yb})$$

In the equation above, 'N' is the number of full or partial 90° bends in the section with an internal radius $\leq 5t$, where 't' is the net thickness of the steel. 'f_u' is the minimum ultimate tensile strength. 'C' is a coefficient whose value is dependent on the methods used to form the section (for rolled material C = 7), and 'f_{yb}' and 'f_{ya}' are the nominal yield of the material and the average yield of the cold formed section respectively. 'A_g' would remain (conservatively) as the gross cross-sectional area of the member under consideration.

In the case of perforated upright sections therefore, the modified formula would take account of bends that remained unaffected by perforations and by implication, ignore those in and adjacent to the central stiffener of the upright. For example, the upright sections being examined by this document would use a reduced value of 'N', which would become four instead of seven or eight, as they would have been if the section were un-perforated. The effect of the introduction of this modified approach to establishing the yield stress of a perforated section would provide only a marginal increase in its value (approximately 5%). However, this is a significant improvement based, as it is, purely on the cross sectional shape of the upright and the conditions under which it is rolled. It also has the advantage of recognising improvements in material properties that have already been acknowledged for non-perforated members and should be considered for use in the FEM.

2.4. Generation of Design Column Curves

The effective prediction of the elastic buckling loads of perforated compression members without recourse to testing was not available to SEMA committee. The main thrust of the SEMA code was therefore to design on the basis of component testing, and in the case of uprights to reduce the experimental column failure curve to a permissible axial stress against slenderness curve for the purposes of design. The generation of column

curves under the FEM code can now be approached in one of three ways. Firstly, by using a full theoretical procedure which until the development of finite element shell analysis was not possible. This would take a considerable amount of time to develop and would in any event need a degree of confirmatory testing to be undertaken. Secondly, column curves can be generated based on stub column compression tests using the distortional buckling check contained within Cl.5.4.6. of the FEM and the methodology outlined in Cl.3.5.(3)., and continued in Cl.3.5.2 and Cl.3.5.3. This design process has a tendency, for obvious reasons, to be overly conservative, and as a result can severely effect the load capacity of the rack. For the uprights examined within this document the results where reduced by in excess of 20% [9] when compared with actual test data. It is clear then that the most satisfactory way in which to assess the performance of the perforated uprights against a range of slenderness values is still to use reliable testing techniques.

2.5. Limit State Design Considerations

The effect of basing the new (FEM) Euro code on limit state design, in contrast to the permissible stress design of the SEMA code has been that the load factors, and in particular the variable action load factor, have been inherited from Eurocode 3 (upon which much of the FEM is based). As a consequence, the value of the variable action load factor was set at 1.5 in the ultimate limit state, in accordance with Table 2.2 ENV 1993-1-1 :1992 [10]. However, this was revised down to 1.4 in the February 1998 draft of the code for two specific reasons. Firstly, the technical committee of Section X in consultation with the national manufacturers' associations, believed that there was a key difference between the variable actions associated with steel structures design contained within EC3, and those contained within the FEM. The value of each load factor reflects the accuracy with which a given load can be estimated. In the case of pallet rack, each

system is designed for a specific pallet loading to suit the requirements specified by a customer. Under these circumstances, there is a degree of certainty attached to the loading of these structures which was not reflected in the original choice of safety factor, and which is not present in the design of the type of structures with which EC3 and BS5950 are dealing.

The second reason for the revision to 1.4 followed a comparison with a code being developed by the Rack Manufacturers' Institute (RMI) in the USA [11]. This is based on US national building and cold-formed steel standards [12-15] and is intended as a revision to their 1990 edition. This code is at a similar stage of development but uses a 'product load factor' equivalent to the variable action load factor contained within the FEM of 1.4. It has been foreseen that at some point in the future it may be desirable for the American and the European codes to be harmonised, particularly with the increased globalisation of the racking industry. Under these circumstances, and for the reasons outlined above the variable action load factor has been revised down to 1.4.

It is worth mentioning here that the RMI code in its updated form, will still make provision for the use of permissible stress design. This contrasts with the European code, which is intended (following its 'full' introduction) to eliminate this approach to rack design from the UK with the complete withdrawal and replacement of the SEMA code. The American code states that limit state and permissible stress designs "are equally acceptable although they may not produce identical designs", (Cl.2.).

2.6. Down-aisle sway stability

The down-aisle sway stability of these systems has been approximated by a number of methods which are intended to provide a simplified approach to racking design without

the need to rely on exhaustive finite element design procedures. Lewis [16] developed a simplified approach to pallet racking analysis in 1991. Included in this model were the semi-rigid behaviour typified by the beam end connectors, but the assumption was made that the uprights were connected to the ground using pinned connections. Obviously, this procedure ignores the benefits of having a rotational stiffness associated with the base of the upright and as a consequence produces an overly conservative analytical approach.

Stark and Tilburgs [17] model, based on a single internal upright was contained within an early draft of the FEM code. Providing flexibility only below the first beam level with a fully rigid upright above. In contrast to Lewis' model this analytical approach becomes unconservative when applied to rack with limited height to first beam, or indeed as the system becomes progressively taller. This is particularly true when p - δ effects are taken into account.

A much improved model was proposed and developed by Davies [18,19]. Based in part on the earlier work of Horne [20], it analyses the down-aisle stability of racking using a single column as a substitute frame. The development of an approximate analysis based on the flexibility of the lowest two levels of rack (neglecting any further upright flexibility) is done on the basis that "the critical storey with the highest sway index is usually the first or second". This approach takes account of the semi-rigid behaviour of the connectors, the rotational stiffness of the baseplate and the second order effects which characterise the design procedure contained within the FEM code.

The Davies model has been further adapted by Feng, Godley and Beale [21] and an effective method for the computerised buckling analysis of multi-bay rack with variable numbers of storeys has been developed. This approach claims "good agreement with the

'exact analysis', a second order plane frame program developed by Davies in a previous paper [19].

2.7. Semi-Rigid Connections

The semi-rigid nature of the connections between the upright and the beam, and at the interface between the upright and the floor are factors which dominate the design of racking structures. Much of the research conducted into the behaviour of these joints has tended to concentrate on the upright/beam connections. This work has been summarised by Jones, Kirby and Nethercot [22].

As early as 1936 [23], the design of connections based on semi-rigid analysis was appreciated, although it was not immediately adopted as a result of the obvious and substantial manual calculation requirements. The assumption that all joints could be taken to be either pinned or fully-fixed predominated therefore, regardless of the knowledge that an inherent degree of stiffness is found in the majority of joints that are present in most structures. Later, much more in depth work has been undertaken into the effects of semi-rigidity in connections, including in respect of their effect on the buckling behaviour of simple plane frames [24], and their influence on the stability of single-bay, double storey plane frames [25]. Further work has been undertaken by Monforton and Wu [26] assuming a linear moment-rotation relationship at the joints, and therefore a single stiffness value for the connections. However this work has been improved upon and adapted to take account of the inherently non-linear behaviour of connectors in analyses by Ang and Morris [27], Ackroyd and Gerstle [28], and Lui and Chen [29].

There has however been a less substantial body of work dealing with the rotational stiffness of baseplates, and their variation with axial load and subgrade, particularly in relation to static pallet racking design. The methodology contained within the FEM is based in essence on the work of Feng [30] which outlines (amongst other things) a suitable test procedure with which to determine and characterise the rotational behaviour of the baseplate in relation to variations in axial load.

2.8. Summary

This section of the thesis has examined the approach of previous standards, research and specifications adopted and embodied by the emerging FEM code. In the light of some of the previously developed work explored here, which relates particularly to static pallet racking, it has been possible to examine certain aspects of this 'novel' design treatment in order to clarify specific areas which differ in emphasis or intent from current more general design standards. In addition, there have been suggestions incorporated into this section, which have been added to and developed in later chapters of this document, which if incorporated, are intended to refine the code as a direct consequence of the work undertaken here.

Chapter 3

Product Configuration and Referencing

3.1. Introduction

Throughout this document reference has been made to upright and beam sections, using the supplying company's standard product referencing system. To avoid any confusion, the coding has been expanded on here and in Appendix A, to provide a clearer understanding of the geometric and material properties that are associated with each 'reference'. This chapter has been divided into four sections :

- Manufacturing processes, which has been included to provide a background knowledge of the various stages of production through which the steel must pass before becoming a racking system.
- Frame properties, which identifies some of the key upright, bracing and baseplate properties (material and geometric).
- Beam properties, which identifies some of the key beam and connector properties (material and geometric).
- Material tensile testing, which includes a methodology and discussion on the characteristic tensile behaviour of the parent steels used in the manufacture of the racking system component parts.

3.2. Manufacturing Processes

3.2.1. Outline

Flow diagram 3.1. explains in very general terms, the processes by which the steel used in the manufacturing of pallet racking systems finds its way into the finished product. Following on from this is a more detailed explanation of the main stages in the manufacturing process.

3.2.2. Roll Forming

Each coil of steel weighs around two tonnes and is fed onto the roll forming mill from a double capstan, which minimises delays in changing from one coil to another. The strip steel is fed through a series of rolls which progressively form it into the required section (beam or upright). When formed, the section is automatically cut to length using a 60T (fly wheel) shear. The system used means that a high degree of precision can be achieved but with upto 38m/minute being formed in this way [31]. The bracing used in the manufacture of frames is produced in a similar way, but on a smaller scale using a mini roll form line.

3.2.3. Punch Press

Uprights are fed through a semi-automatic, 100T hydraulic press which punches connector holes along the entire length of the section. This allows the racking systems to be sold as ‘adjustable pallet racking’ (APR) as the connectors can be fixed at any point along the upright length.

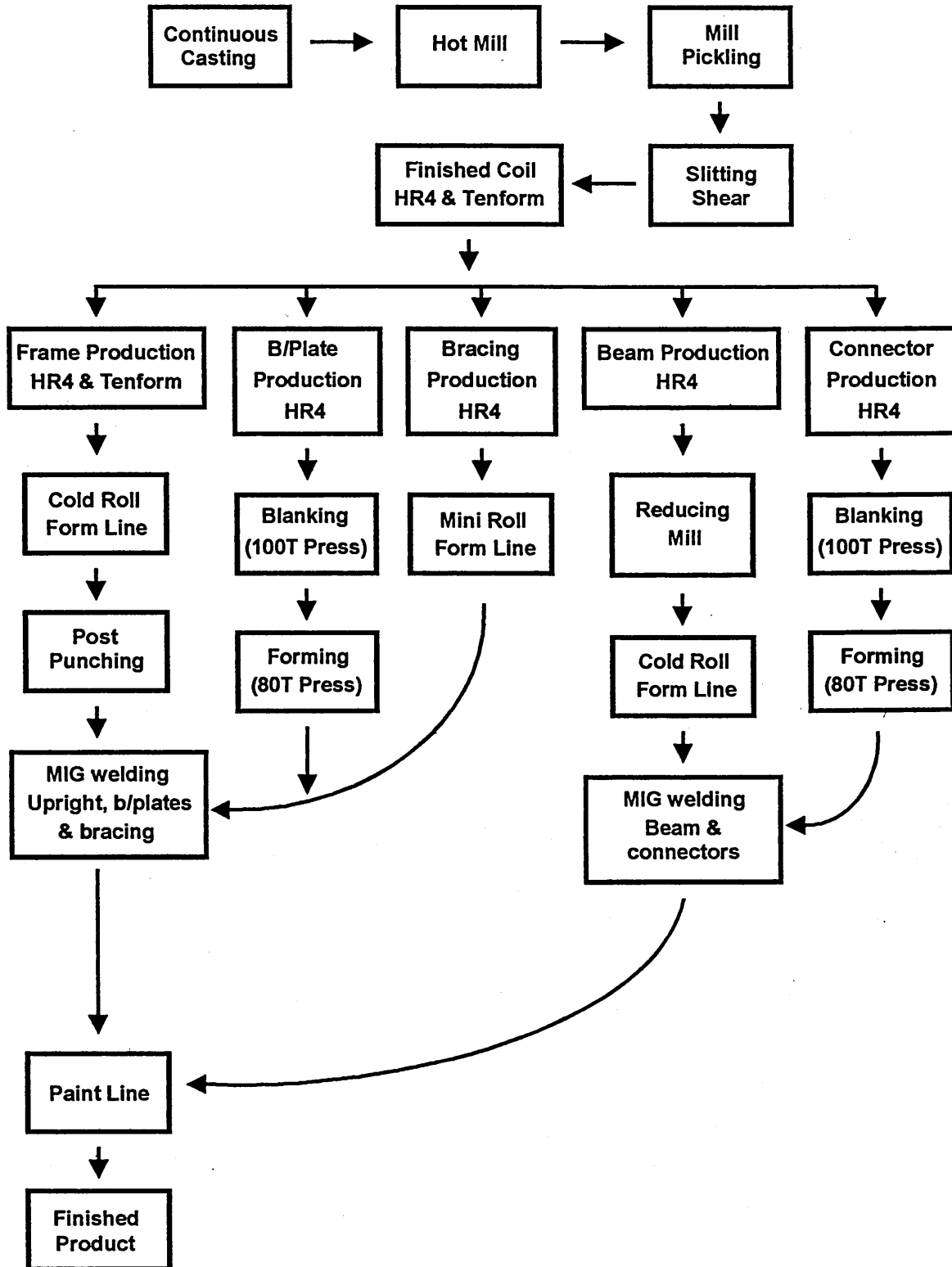
3.2.3. Blanking and Forming

Baseplates and beam end connectors are ‘blanked’ into the required shape from the basic coil, using a 100T press. The beam end connector blanks are then bent into shape using an 80T forming press.

3.2.4. Reducing Mill

Prior to roll forming, the beam steel is cold reduced. As a consequence, the materials yield properties are greatly enhanced, from HR4 [32] at 170 N/mm², to a minimum requirement of 417 N/mm². The following table shows coil thicknesses before and after being passed through the reducing mill together with the reduction in thickness as a percentage of the initial thickness :

Manufacturing Process



Diag. 3.1. Processes used in the manufacture of pallet rack

Beam Section	Pre-reduction coil thickness (mm)	Post-reduction coil thickness (mm)	Post/Pre (%)
50 O/S	2.325	1.78	76.6
76 O/S	2.325	1.78	76.6
95(1.78) B/B	2.325	1.78	76.6
110 B/B	2.325	1.78	76.6
130 (1.78) B/B	2.325	1.78	76.6
145 B/B	2.325	1.78	76.6
80 B/B	1.9	1.57	82.6
95 (1.57) B/B	1.9	1.57	82.6
130 (1.57) B/B	1.9	1.57	82.6

Table 3.1. Beam section coil reductions

3.2.5. Welding

MIG (metal-inert-gas) welding is employed for welding both beams and frames. A mixture of argon and CO₂ is used as a gas shield (88% argon, 12% carbon dioxide). This mixture stabilises the arc, increases the penetration of the weld and cuts spatter to a minimum. Beams are welded on an automatic welding machine using a fillet weld to attach the beam end connectors. A further spot weld is applied to the back of box beams to ensure that the C-sections remain nested under high loads. In contrast, manually operated jigs are used to weld bracing and baseplates to the uprights to form frames.

3.2.6. Painting

After they have been welded, all beams and frames are transferred to the paintline. The first part of the line consists of a three-stage automatic process to clean and prepare the sections. The steel is degreased and phosphate crystals are applied to its surface to increase paint adhesion. Sections are then pass through a cold rinse and into a drying oven after which they are ready for painting.

The paint is applied using hot, airless, electrostatic guns, with the sections being negatively charged to attract paint evenly over their entire surface (the paint is positively

charged). Following this, components are passed through a flash-off tunnel to remove any solvent vapours and are then stove enameled to produce a hard, durable finish.

3.3. Frame Properties

There are seven types of frame in the product range and the nomenclature associated with each can be broken down into three distinct parts :

- A frame falls into one of two categories, SD (Standard Duty) or HD (Heavy Duty). This relates to the external dimensions of the section. Obviously the heavy duty sections have a more robust cross section (see Appendix A).
- Within these two categories the frames are coded depending on the gauge of steel used in their manufacture. For example, an SD17 frame would use a standard duty cross section with 1.7mm gauge steel (external dimensions are maintained independently of the gauge width). Similarly, an HD25 frame would employ a heavy duty section with 2.5mm gauge steel.
- Finally, a material code is attached to the frame description to distinguish uprights manufactured from tenform (high yield) steel, from uprights made from HR4. This is done by adding a 'T' to the end of the description. For instance, an HD25T frame has the same dimensions and uses the same gauge of steel as an HD25 frame, but uses a tenform steel with a much higher yield stress.

Each frame type used in production has been listed below, together with the strip width and thickness of the coils from which they are made. The roll condition and grade of steel along with the nominal coil yield stress have also been tabulated.

Upright Section	Roll condition & grade	Strip width & thickness (mm)	Nominal Yield Stress (N/mm ²)
SD17	HR4	203 x 1.7	250
SD25	HR4	200 x 2.5	250
SD25T	Tenform - XF350	200 x 2.5	350
HD25	HR4	260 x 2.5	250
HD25T	Tenform - XF350	260 x 2.5	350
HD30	HR4	256 x 3.0	250
HD30T	Tenform - XF350	256 x 3.0	350

Table 3.2. Upright section coil data

All frames are constructed using a common bracing section, welded in a Z-form pattern (see Appendix A). The bracing consists of ties and diagonals fillet welded to the upright lips in standard panel widths of 1200mm. It is cut to length to allow frames ranging between 600mm and 1500mm in width to be manufactured to order.

Two types of baseplates are commonly produced (see Appendix A). The ‘narrow aisle’ baseplate is used (for rack designed to the current SEMA code) in cases where design advantages accrue from using a baseplate with a relatively high degree of rotational stiffness. This reduces the slenderness ratio of the upright and consequently increases the permissible axial stress. In cases where this is not crucial (generally on racks of limited height) a ‘standard aisle’ baseplate is used. All baseplates are welded rather than bolted to the uprights. The following table outlines strip widths and material properties used for the manufacture of both types of baseplate and the bracing section :

Section Details	Roll condition & grade	Strip width & thickness (mm)	Minimum Yield Stress (N/mm ²)
Bracing	-	94 x 1.57	417
Narrow Aisle B/Plate	HR4	200 x 6.0	170
Standard Aisle B/Plate	HR4	125 x 4.0	170

Table 3.3. Upright ancillaries - coil data

3.4. Beam Properties

There are nine separate beam types available in the product range, manufactured in lengths of between 900mm and 4800mm, in 75mm increments. Seven of these are box beams (B/B) of variable depth and gauge, which use two C-sections nested together to form the required shape (see Appendix A). The other two are open sections (O/S), which are formed from a single coil and are classed as light duty beams. All of the beams are classified by depth, gauge of material (if different from 1.78mm) and whether the section is boxed or open :

Beam Duty	Strip width & thickness (mm)	Minimum Yield Stress (N/mm ²)
50 O/S	166 x 1.78	417
76 O/S	213 x 1.78	417
80 (1.6) B/B	181 x 1.6	417
95 (1.6) B/B	196 x 1.6	417
95 B/B	196 x 1.78	417
110 B/B	208 x 1.78	417
130 (1.6) B/B	231x1.6	417
130 B/B	231x1.78	417
145 B/B	247x1.78	417

Table 3.4. Upright section coil data

There is only one type of connector commonly in use with all beam sections although the left and right handed versions of these are treated separately for the purposes of design. Both C-section and open section beams are typically welded flush to the top of the connector although 'down welding' is occasionally required. This is generally done when it is necessary for a given beam level to fall between the pitches of the upright (to fit an additional level into a given height of rack, for instance). Standard pitches are punched at 75mm centres, but in these cases more flexibility is required, and the beams can then be down welded by anything from 1mm to 74mm (65mm for 145 B/B).

As with the connector, only one type of locking pin is used across the product range. Developed to secure the beams against accidental uplift, they are positioned through a 'locking hole' above the central connector lug into the front face of the upright. The table below outlines the strip widths and material properties used in the manufacture of both the connector (left and right hand) and the locking pin :

Section Details	Roll condition & grade	Strip width & thickness (mm)	Minimum Yield Stress (N/mm ²)
Connector	HR4	116 x 3.0	170
Locking Pin	HR4	41.275 x 3.5	170

Table 3.5. Beam ancillaries - coil data

3.5. Material Tensile Testing

3.5.1. General Outline

In subsequent chapters design tests have been performed in an effort to obtain basic performance data on the component parts that make up an industrial pallet racking system. In an effort to eliminate inconsistencies in the results, variations in material yield stress were determined for the following tests :

- Stub Column Compression Tests
- Compression Tests on Uprights
- Bending Tests on Beam End Connectors
- Shear Tests on Beam End Connectors
- Bending Test on Upright Section
- Bending Test on Beams

In contrast, corrections for yield stress were deemed unnecessary for assessing results in the following cases :

- Shear Stiffness of Frames Test
- Looseness Test on Beam End Connectors
- Floor Connector Test

When tensile testing was undertaken, the method used corresponded with that outlined in BS EN 10002-1 Tensile Testing of Metallic Materials : 1990 as specified by Cl.5.2.1. of the FEM code. The results have been included with the relevant test in the experimental sections of this document.

3.5.2. Sample Preparation

Samples of steel 500mm long were taken from all coils used in the production of test pieces, prior to rolling. Using this 'parent' material, tensile test specimens were then blanked to the required shape [33] on a press, using a punch and dye set. Subsequently, each sample was sanded along its edges (using a fine emery cloth) to remove any surface imperfections such as stress razors. Fig. 3.1 shows the dimensions of the resultant tensile test sample :

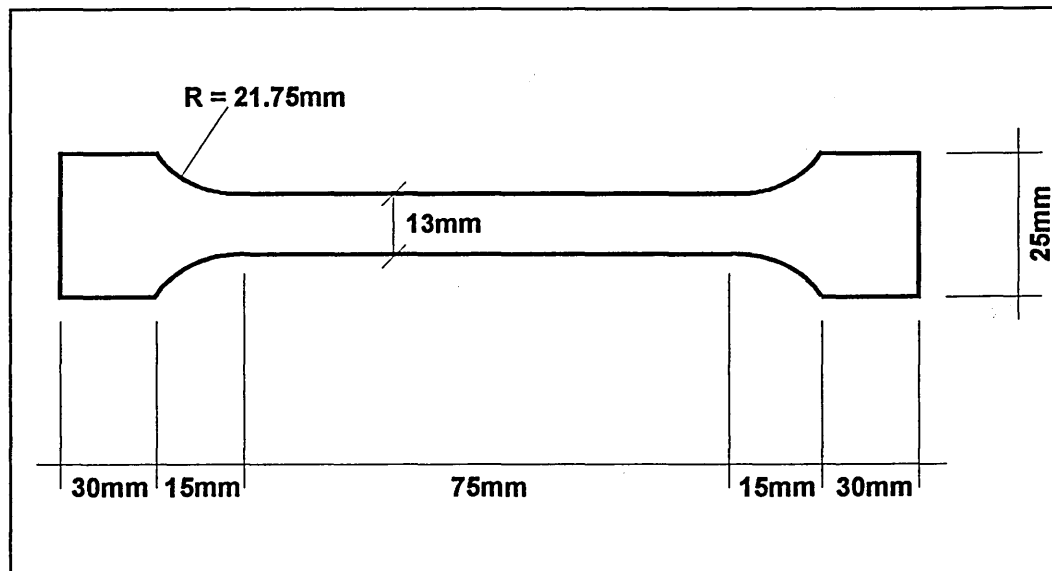


Fig. 3.1 Tensile test sample - dimensions

The parallel length of the section was standard (75mm) for all samples, as it was manufactured using a press. The implication of this was that it was not possible to produce a proportional test piece, because of the variability of the cross sectional area (widths of strip steel ranged between 1.7mm and 3.0mm). This has been demonstrated

below, with reference to the relevant formulae. Dimensions of proportional test samples were calculated as follows :

$$S_o = 13 \times t$$

$$L_o = k\sqrt{S_o}$$

$$L_c = L_o + 2b$$

Where S_o is the cross sectional area of the sample, t is the sample thickness, L_o is the original gauge length (>20mm), k is 5.65 (see Cl.6.1.1.) and L_c and b are the parallel length of the sample and the width of parallel length of the sample respectively.

As a result of sample thickness variations and their effect on the calculation of the parallel length of the sample, a standard non-proportional test piece was produced from a single dye, in accordance with Annex A of the European standard (see Table 3.1) :

Tensile test samples	Width (mm)	Original Gauge Length, L_o (mm)	Parallel Length, L_c (mm)	Free Length between grips (mm)
Type 1 test piece	12.5 ± 1	50	75	> 87.5
Actual Sample values	13.0	50	75	100

Table 3.6. A comparison of actual sample dimensions with those contained in Table 4 of BS EN 10002-1 : 1990

In addition to these dimensional requirements, the standard specifies that “the parallel length (L_c) ... shall be connected to the ends by means of transition curves with a radius of at least 12mm” and that the “width of these ends shall be at least 20mm and not more than 40mm”. It is evident from Fig. 3.1 these values have been strictly adhered to.

The length axis of the specimens corresponded with the direction of rolling of the coiled steel and the orientation of the longitudinal fibres in the cold-formed members. Blanks were taken from the middle of the coil width and wherever possible near the end of the coil, in accordance with FEM code Cl.1.8.5.(a) *Testing of Steels with no Guaranteed Mechanical Properties.*

3.5.3. Test Methodology

A standard micrometer was used to measure the cross section of each test piece to an accuracy of 0.01mm. Three values of width and three of thickness were taken in the middle and at the ends of the parallel section of the sample. These were then averaged and a single value for the cross sectional area of the specimen was derived.

After preparation of the samples had been completed, they were placed individually into an Instron (4200 series) tensile testing machine which is pictured overleaf in Plate 3.1. This machine was capable of automatically controlling the rate of strain, which approximated to 0.00083 mm/sec during testing, and of processing the resultant data. It measured the tensile force applied to the specimens electronically together with the displacement of the 'wedge' grips. As a result, a plot of the stress/strain graph together with some of the basic material properties of the sample, including 0.2% proof stress, were output automatically. However, this method of testing was not sufficiently accurate to determine quantities such as Young's modulus . This was due to possible slippage in the clamps and elastic elongation of the wider parts of the sample.

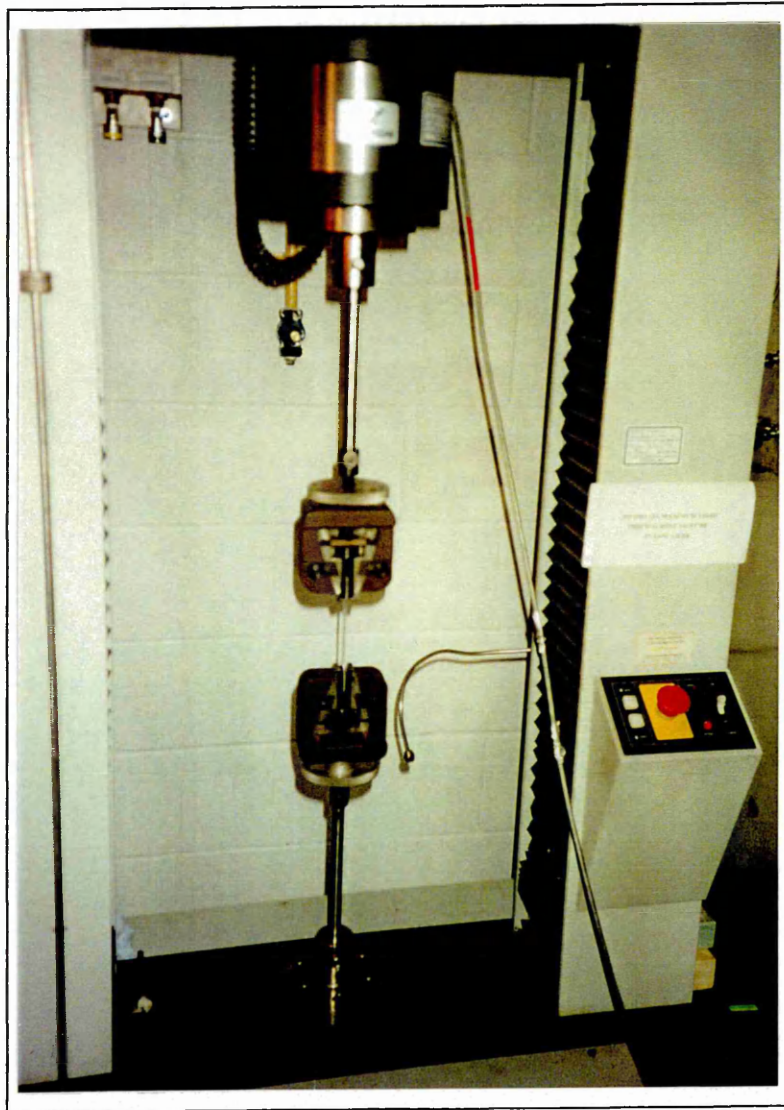


Plate 3.1. Instron tensile testing machine

3.5.4. Discussion

Throughout this document, uniform stress (N/mm^2) within the test sample is defined as the ratio of tensile force to the sample's initial cross-sectional area :

$$\sigma = P/A$$

Similarly the strain (recorded on the test plots in mm/mm), is defined as the ratio of the change in length of the sample to its initial length :

$$\varepsilon = \Delta L/L$$

For correction purposes the yield stress was of primary concern during this series of tests. However, in cases where more information on the general properties of steel was needed, standard properties taken from FEM Cl.1.8.4.3. were used. These properties have been used throughout this document :

- Modulus of Elasticity - $E = 210000 \text{ N/mm}^2$
- Shear Modulus - $G = E/[2(1+\nu)] \text{ N/mm}^2$
- Poisson's Ratio - $\nu = 0.3$
- Coefficient of linear thermal expansion - $\alpha = 12 \times 10^{-6} \text{ per}^\circ\text{C}$
- Density - $\rho = 7850 \text{ kg/m}^3$

Typically, failure was induced within the parallel length (L_c) of the sample, where the stress distribution was uniform and the sample was subject only to pure tension. Despite this, it was apparent that two distinct modes of failure could be observed during testing. It was clear that the steel used in the manufacture of the beam C-sections behaved very differently from that used in the uprights and connectors. A comparison of the graphical output from each 'type' of test can be seen below.

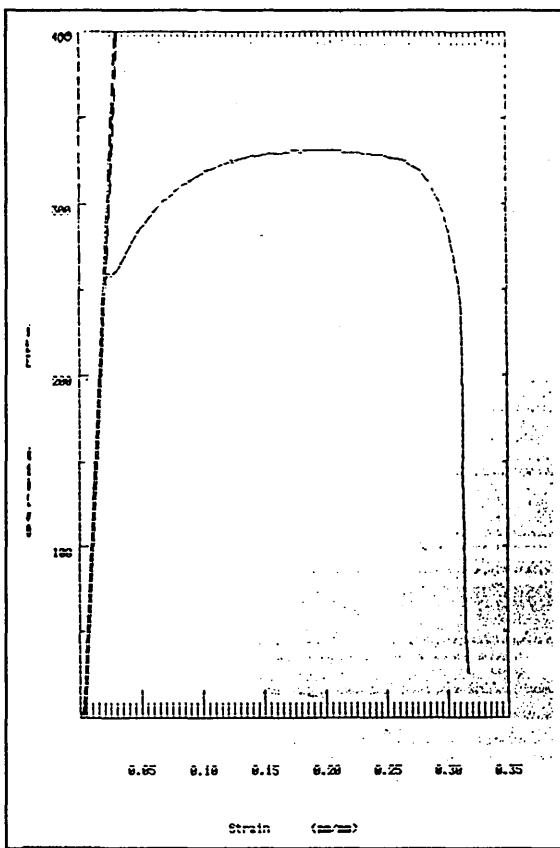


Fig. 3.2 Tensile test on Upright steel

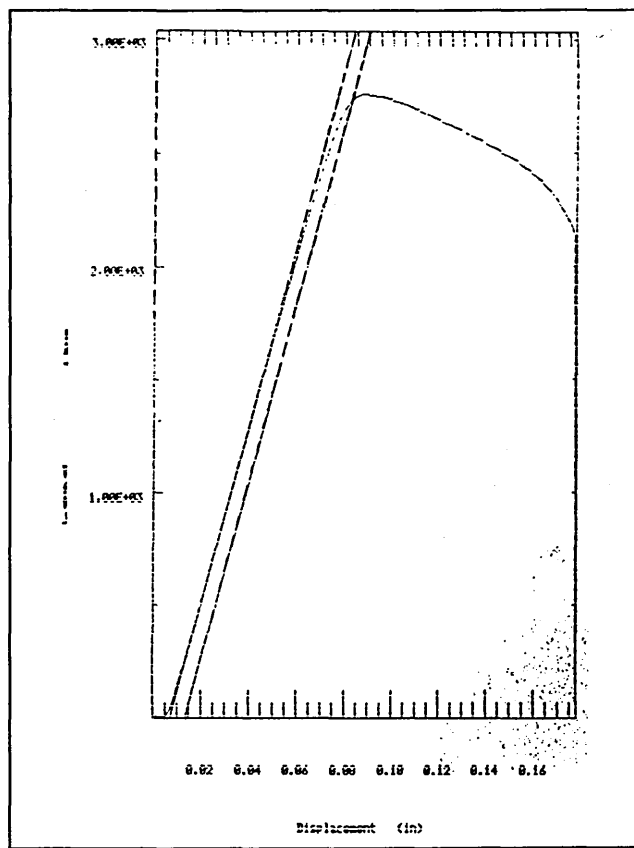


Fig. 3.3 Tensile test on beam steel

It is apparent from the output above, that there are distinct differences between the behaviour of the beam steel and the upright steel (tenform and HR4) during tensile testing. In the first instance, although both sets of data appear to obey Hooke's Law ($\sigma = E\epsilon$), and display linear elastic characteristics during the initial portion of the test, there is no discernible yield point visible on Fig. 3.3. In cases such as these, a line parallel to the initial portion of the curve and offset by a standard amount of strain (0.002 or 0.2%) was constructed. As a consequence the point at which this line crossed the test data line was taken to be the 'actual yield stress' for the purposes of FEM analysis. This point is commonly known as the 0.2% proof stress.

Secondly, it is clear that the ductility associated with the upright steel in Fig. 3.2 is not present in Fig. 3.3. A reduction in strain hardening is a distinct feature of the cold reduced material used in the manufacture of beam sections. Ductility is defined as the "extent to which a material can

sustain plastic deformation without rupture” [34], and it is clear that steel which exhibits brittle tendencies will be less well able to cope with the large plastic deformations induced by operations such as cold roll forming. In addition to this, it is apparent from the graphs that substantial changes to the mechanical properties, other than a reduction in ductility of the steel, have occurred. The process of cold reducing has the effect of increasing both the yield point and the ultimate tensile strength of the material. However, “the percentage increase in tensile strength is much smaller than the increase in yield strength, with a consequent smaller reduction in the spread between [the two] ”[34]. One of the consequences of this, which can be seen from comparing the graphs, is that the inherent factor of safety in the material itself is diminished. If loads become too large a ductile material will tend to distort visibly. In this case action could be taken to remove load before failure occurred. However, in the case of more brittle (cold reduced) materials such as those used in the beam sections, there is less distortion prior to failure. The issues raised here with regard to structural integrity are addressed in the code by ensuring that the ratio of characteristic ultimate tensile strength to characteristic yield strength is greater than 1.05 (FEM Cl.1.8.3.), as is the case here. In addition, because the capacity of the majority of beams is deflection limited at the serviceability limit state, stresses in the beams are never sufficiently high to pose a design problem.

Chapter 4

The Determination of Individual Upright Characteristics through Experimentation

4.1. General Outline

To enable the design of a system of racking through Finite Element Analysis (FEA) or any other numerical method, it is first necessary to determine the characteristics of the component parts. Basic performance data having been obtained, a full examination of the systems behaviour during its operating life can thereby be determined. A total number of eleven specific tests were carried out to obtain this performance data. This chapter examines the upright behaviour through five of these tests, including :-

1. Stub Column Tests
2. Compression Tests on Frames
3. Tests for Shear Stiffness of Frames
4. Bending Tests on Frames
5. Tests on Floor Connections

The tests outlined above were exhaustive for the product range supplied. All possible combinations of beam, upright and baseplate were examined to produce a complete set of data which would allow predictive software (and user) to vary any chosen set of parameters during the design of a racking system.

4.2. Stub Column Compression Test

4.2.1. Introduction

The purpose of this test is “ to observe the influence of such factors as perforations and local buckling on the compressive strength of a short column ” (FEM-CI.5.3.1.), in order to determine the following for each class of upright :

- centroidal axis position
- characteristic failure load
- effective area of section (A_{eff})

The implications of this test series are self-evidently far ranging, as the position of the centroidal axis forms the basis for all subsequent upright/frame compression tests, while the individual failure loads are integral to the construction of the design column curves.

4.2.2. Test Geometry

To form the test pieces, sections of upright incorporating five pitches of perforations were cut normal to their longitudinal axis, midway between two sets of perforations. Following this, the section (375mm in length) was adjusted for springback using base and cap plates 4mm thick, which were welded to each end of the stub. Ball bearings 30mm in diameter were positioned above and below each specimen and applied load axially through two identical plates (150mm x 100mm x 35mm) which were indented to a depth of 5mm to seat each bearing. The test specimen dimensions are shown overleaf in Fig.

4.1.

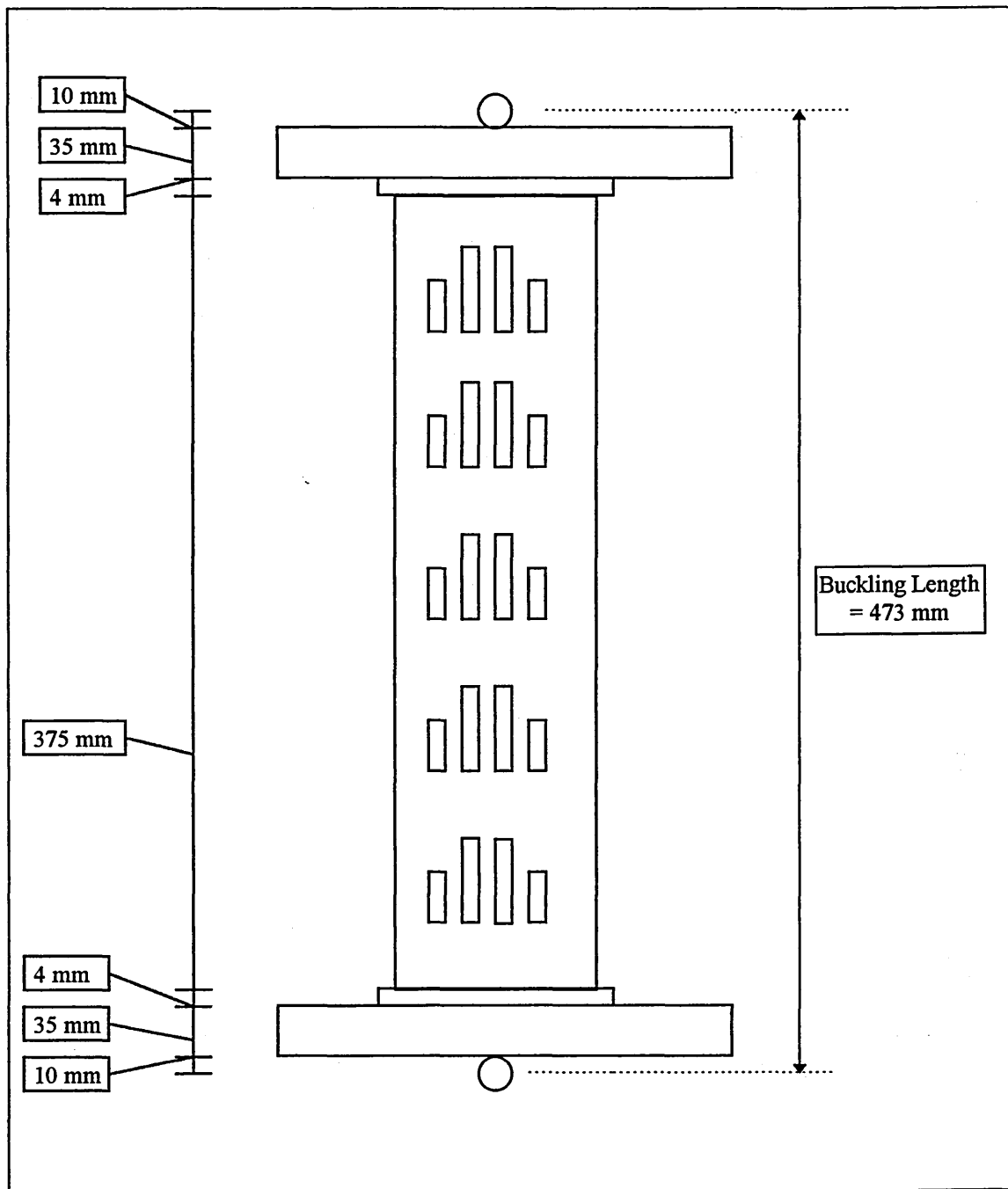


Fig. 4.1. Stub Compression Test Dimensions

4.2.3. Methodology

A total of 115 tests were performed on six separate sections of upright in accordance with the recommendations of the FEM code 10.2.02. Each separate section of coil material used had at least two tensile tests performed on it to determine the actual yield stress of the samples being tested. In addition, actual material thickness' were determined

using a standard micrometer accurate to 0.01mm. Tests were carried out using a servo-hydraulically controlled ESH universal testing machine capable of applying compressive loads of up to 275KN. The rate of compression was controlled by a ramp generator and was set to 0.05 mm/sec.

During testing all sections were arranged to ensure that “the position of the ball bearings in relation to the cross section [was] the same at both ends” (FEM-C1.5.3.3.). The test pieces were loaded axially along their line of symmetry at a variable distance, from the front face of each upright, in order to maximise the failure load. Crucial to the results of the tests was the verticality of the samples with respect to the ball bearings together with the accuracy of their positioning. Initially, this was ensured using a system of dial gauges. However, the set up procedure for each test was an unnecessarily complex and time consuming one, and so this method was quickly replaced (test 28-115) with a mechanical stop system which was designed to slide quickly into place (for upright location) and out again during testing. This system together with an upright sample ready for test is shown overleaf (see Plate 4.1.).

Throughout the test procedure the centroidal axis was taken to be along the line of symmetry for each upright and at a “test determined distance” referenced from the front face. An initial guess for this distance was the centre of gravity for the gross cross sectional area of each sample. Using the mechanical stop it was possible to vary this distance accurately to maximise the failure loads during testing and thereby pinpoint the exact “co-ordinates” of the centroidal axes with some confidence. Subsequently, the characteristic failure load could be derived from a series of tests through these newly determined co-ordinates, repeatability allowing a greater degree of statistical confidence to be placed on the results.

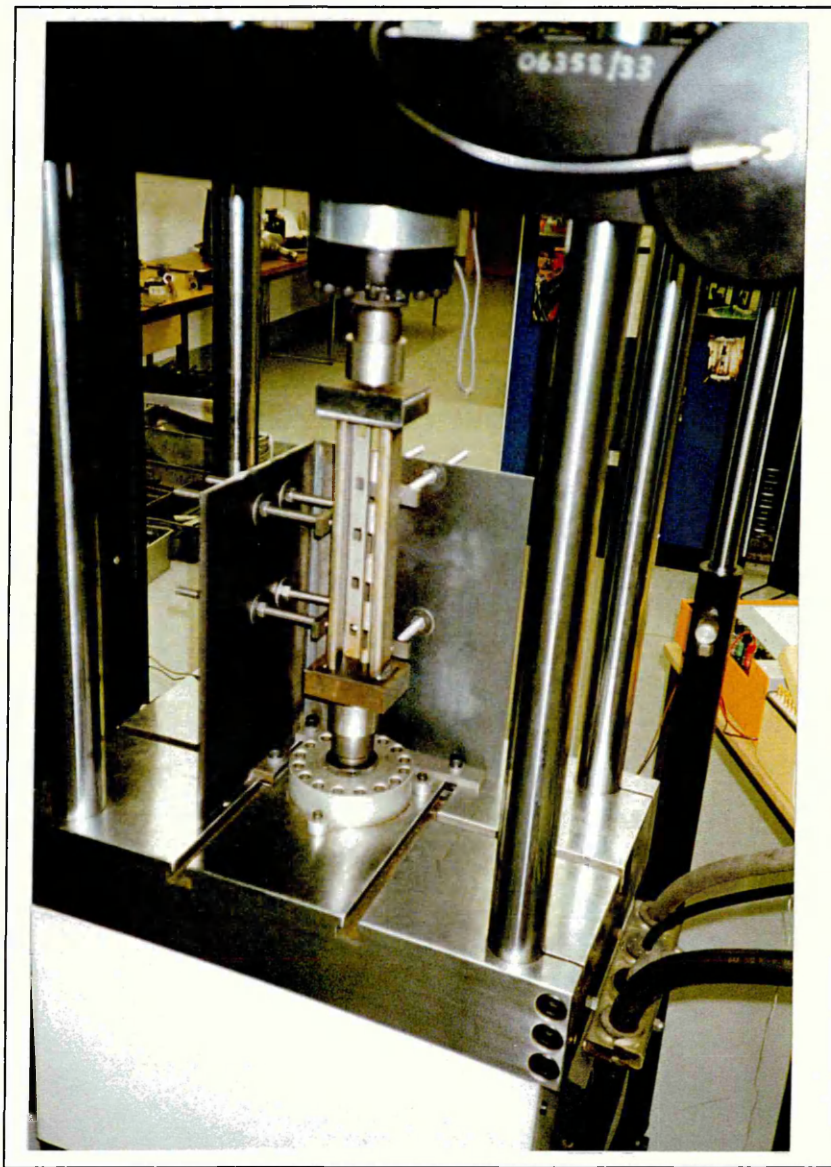


Plate 4.1. Stub column section ready for testing together with upright locator

4.2.4. Discussion

Plate 4.2. has been included to exemplify a typical mode of failure for many of the uprights tested. This was characterised by a backward buckling of the stub together with a central web crippling failure (see Plates 4.3.-4.5.). A second significant mode of failure was typified by an inward buckling of the rear lips in conjunction with a bulging outward of the web of the column.

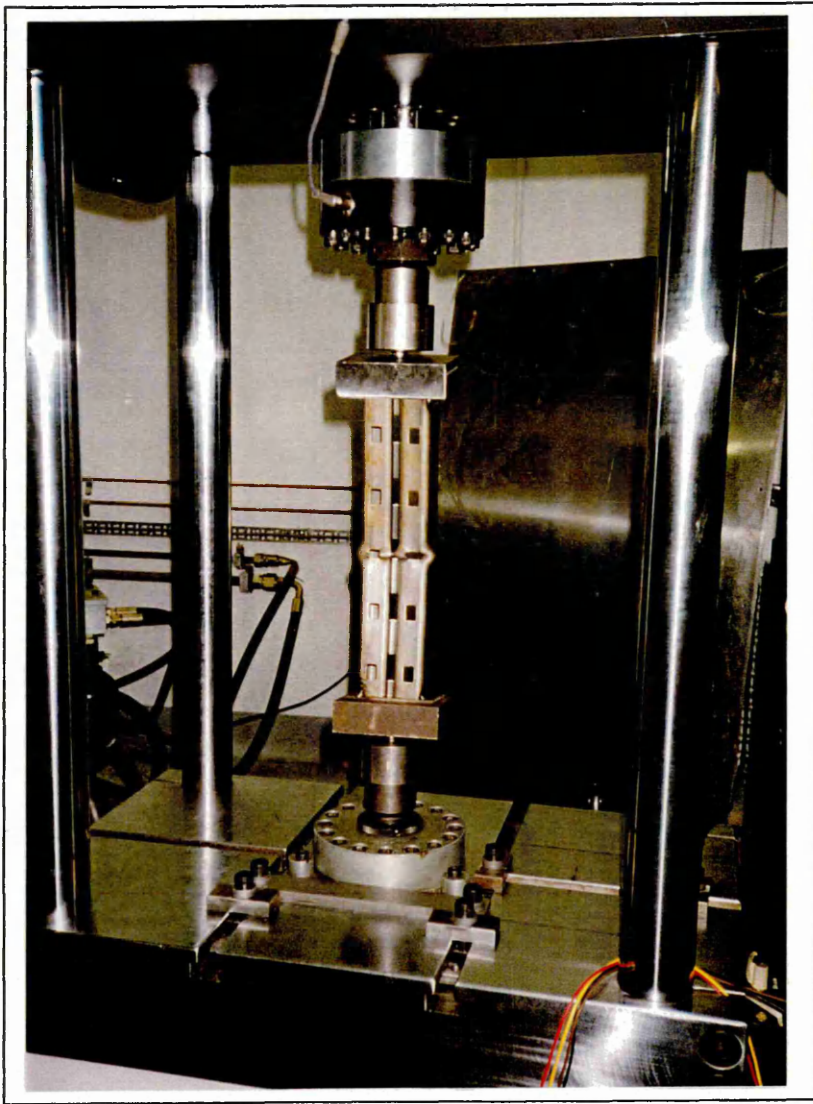


Plate 4.2. Stub column failure

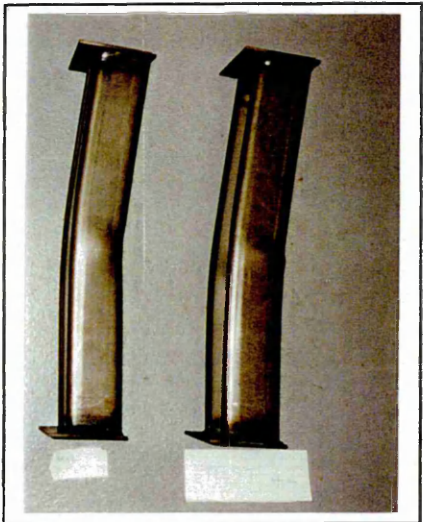
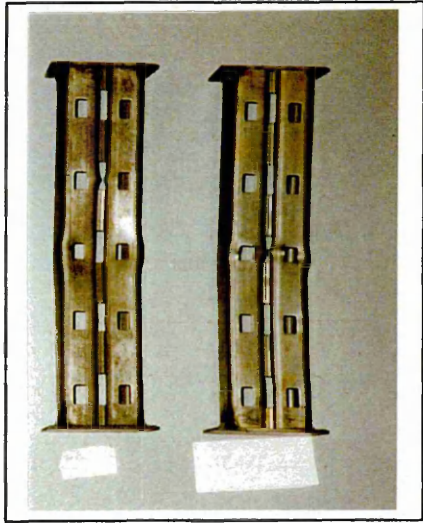


Plate 4.3.-4.5.
Stub column section failure

4.3. Results and Analysis

4.3.1. Introduction

Analysis has been undertaken here and throughout this document using values for notional plane width (b_p) as defined below. These values have been calculated in accordance with Cl.3.2.1, Fig. 3.1 and Fig. D.2 of the FEM, taking the effect of corner radii into account.

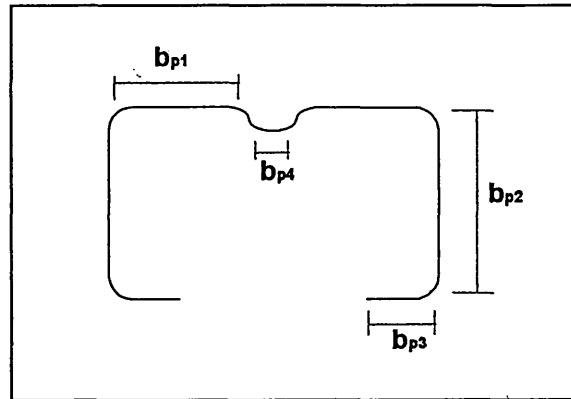


Fig. 4.2. Notional upright plane widths

- Heavy duty upright values :

b_{p1}	:	30.6 mm	(stiffened)
b_{p2}	:	60.6 mm	(stiffened)
b_{p3}	:	21.8 mm	(unstiffened)
b_{p4}	:	26.9 mm	(stiffened)

- Standard duty upright values :

b_{p1}	:	33.2 mm	(stiffened)
b_{p2}	:	47.5 mm	(stiffened)
b_{p3}	:	13.6 mm	(unstiffened)
b_{p4}	:	(intermediate stiffener)	

4.3.2. Material and geometric corrections

Material and geometric corrections to the observed failure loads were undertaken using the formulae outlined below :

$$R_{ni} = R_{ti} \left(\frac{f_y}{f_t} \right)^\alpha \left(\frac{t}{t_t} \right)^\beta \quad (4.1.)$$

where R_{ni} and R_{ti} are corrected and observed failure loads respectively for test ‘i’, f_t and f_y are observed and nominal yield stresses respectively, and t_t and t are the observed and design thickness’. In general, values of yield stress measured from tests were found to exceed nominal values. In these cases $\alpha = 1$ down-rating the value of R_{ni} accordingly ($\alpha = 0$ when $f_y \geq f_t$). To adjust R_{ti} for thickness, the thickness ratio is raised to the power β , which is itself dependent on the limiting values of the width to thickness ratios detailed below :

$$\text{Stiffened elements :- } \left\{ \frac{b_p}{t} \right\}_{\text{lim}} = 0.64 \sqrt{\frac{4E}{f_t}} \quad \left(\geq \frac{b_p}{t} \right) \quad (4.2.)$$

$$\text{Unstiffened elements :- } \left\{ \frac{b_p}{t} \right\}_{\text{lim}} = 0.64 \sqrt{\frac{0.43E}{f_t}} \quad \left(\geq \frac{b_p}{t} \right) \quad (4.3.)$$

Thin-walled sections employed as compression members in a racking system may suffer significant effects as a result of local buckling. The limitations imposed here reflect the importance of the ‘b/t ratio’ in determining each sections susceptibility to this mode of failure. “Compression elements supported on (one or) two longitudinal edges may be assumed to be fully effective if the breadth to thickness ratio” (Cl.3.3) limitations outlined above are satisfied.

The maximum flat-width-to-thickness ratios for each upright section are as follows :

	SD17	SD25	HD25	HD30	SD25T	HD25T	HD30T
Maximum notional plane width - stiffened element (mm)	47.5	47.5	60.6	60.6	47.5	60.6	60.6
b_p/t ratio	27.94	19	24.24	20.2	19	24.24	20.2
Maximum notional plane width - unstiffened element (mm)	13.6	13.6	21.8	21.8	13.6	21.8	21.8
b_p/t ratio	8	5.44	8.72	7.27	5.44	8.72	7.27

Table 4.1. Flat-width-to-thickness ratios for each upright

The results of each test have been graphically illustrated in Fig. 4.3.-4.8. It can clearly be demonstrated that the mean corrected failure load varies significantly in response to a variation in the distance of the application of the load from the front face of each upright. In each case, the highest load was taken to be indicative of the optimal position for the centroidal axes, and was used in all subsequent upright compression tests.

4.3.3. Characteristic values of failure load

In general, the calculation of a characteristic failure load from test results on a single upright was statistically treated to reflect a 75% confidence level that 95% of any future tests would be higher than the characteristic value (R_k) :

$$R_k = R_m - k_s s \quad (4.4.)$$

' R_m ' is the mean of at least three adjusted test results (n), ' k_s ' is the confidence level coefficient (see App. C) and ' s ' is the sample standard deviation :

$$s = \sqrt{\frac{1}{n-1} \sum_{i=1}^n (R_{ni} - R_m)^2} \quad (4.5.)$$

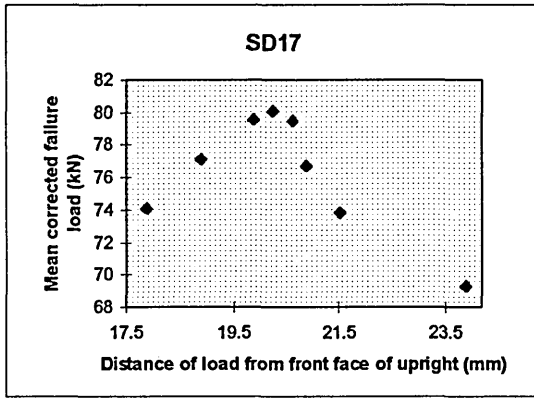


Fig. 4.3. SD17 upright summary

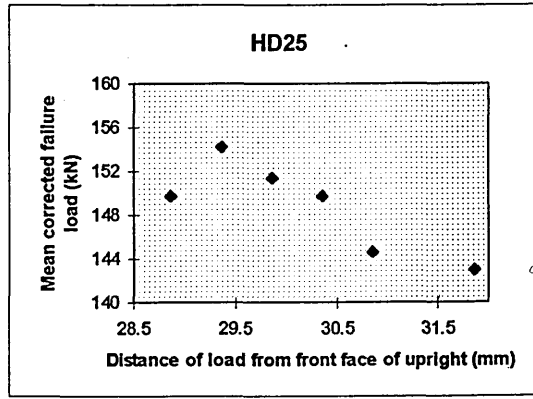


Fig. 4.4. HD25 upright summary

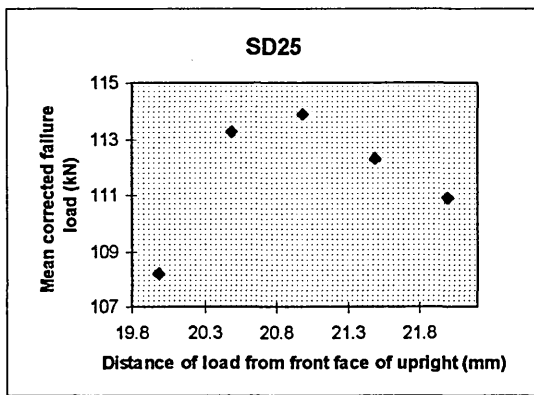


Fig. 4.5. SD25 upright summary

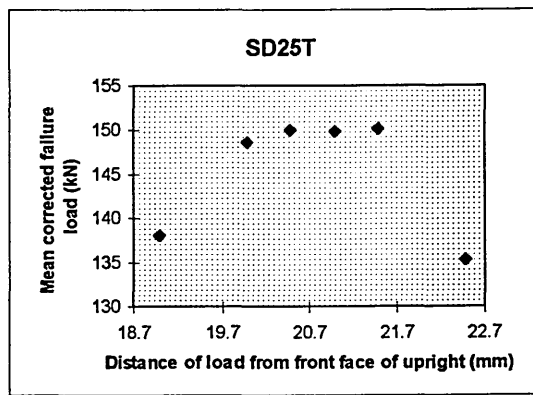


Fig. 4.6. SD25T upright summary

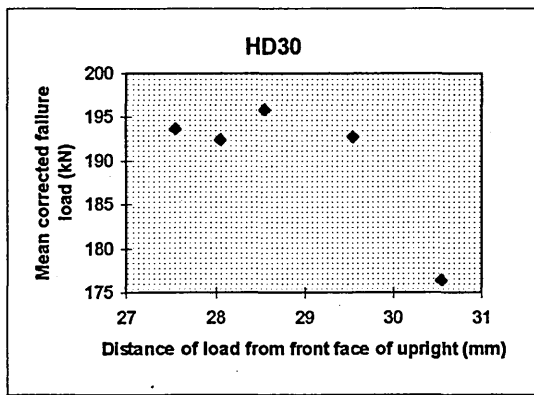


Fig. 4.7. HD30 upright summary

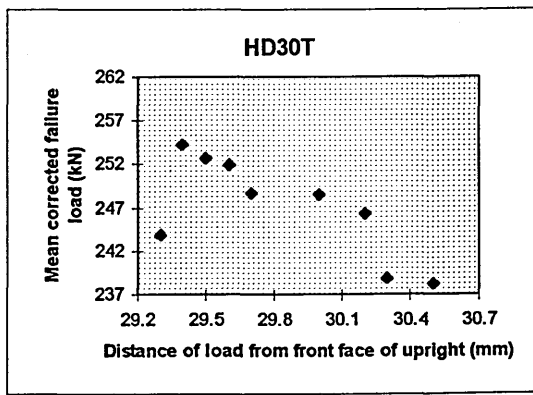


Fig. 4.8. HD30T upright summary

Fig. 4.3.-4.8. Graphical illustration of stub column test results

4.3.4. Effective area of uprights

Having first derived the characteristic value of failure load, an effective area for each section can be calculated as follows, where f_y is the nominal yield stress :

$$A_{\text{eff}} = \frac{R_k}{f_y} \quad (4.6.)$$

Values of A_{eff} obtained from this test have been compared with values obtained from the upright compression tests in section 4.4.2. of this document.

4.3.5. Results summary

A summary of the results of the tests on each of the upright sections has been tabulated below. \bar{X} is defined as the distance of the centroidal axes from the front face of the upright and has been used as the optimum position for loading in the upright compression tests.

Upright	Characteristic Failure Load (KN)	\bar{X} (mm)	A_{eff} (mm ²)
SD17	75.62	20.26	302.48
SD25	108.36	20.99	433.44
SD25T	143.80	21.49	410.86
HD25	146.00	29.36	584.00
HD30	191.73	28.55	766.92
HD25T	199.01	29.86	568.6
HD30T	236.92	28.96	676.91

Table 4.2. Summary of stub column compression test results

4.4. Compression Tests on Uprights

4.4.1. General Outline

The purpose of this test is “ to determine the axial load capacity of the upright section for a range of effective lengths in the down-aisle direction, taking account of out of plane buckling effects and the torsional restraint provided by the bracing and its connection to the uprights ” (FEM-CI.5.4.1). This test is considered to be crucial as far as the load capacity of the racking system is concerned, as these results, together with those obtained from the stub column compression tests form the basis of the design column curves. “ Rack structures are designed to carry predominantly the vertical loads from the stored material ” [18], and as a consequence uprights that support relatively high axial loads in these tests, will allow significant performance advantages to be carried over into the design of the full racking system.

4.4.2. Test Arrangement

A total of 182 tests were performed on sections across the product range, in accordance with FEM CI.5.4. The frames were manufactured with standard Z-form bracing section (see Appendix A) and using the maximum frame width in the product range (1500mm). The diagram overleaf in Fig. 4.9., has been included here to illustrate the test arrangement and the method by which the specimens were tested.

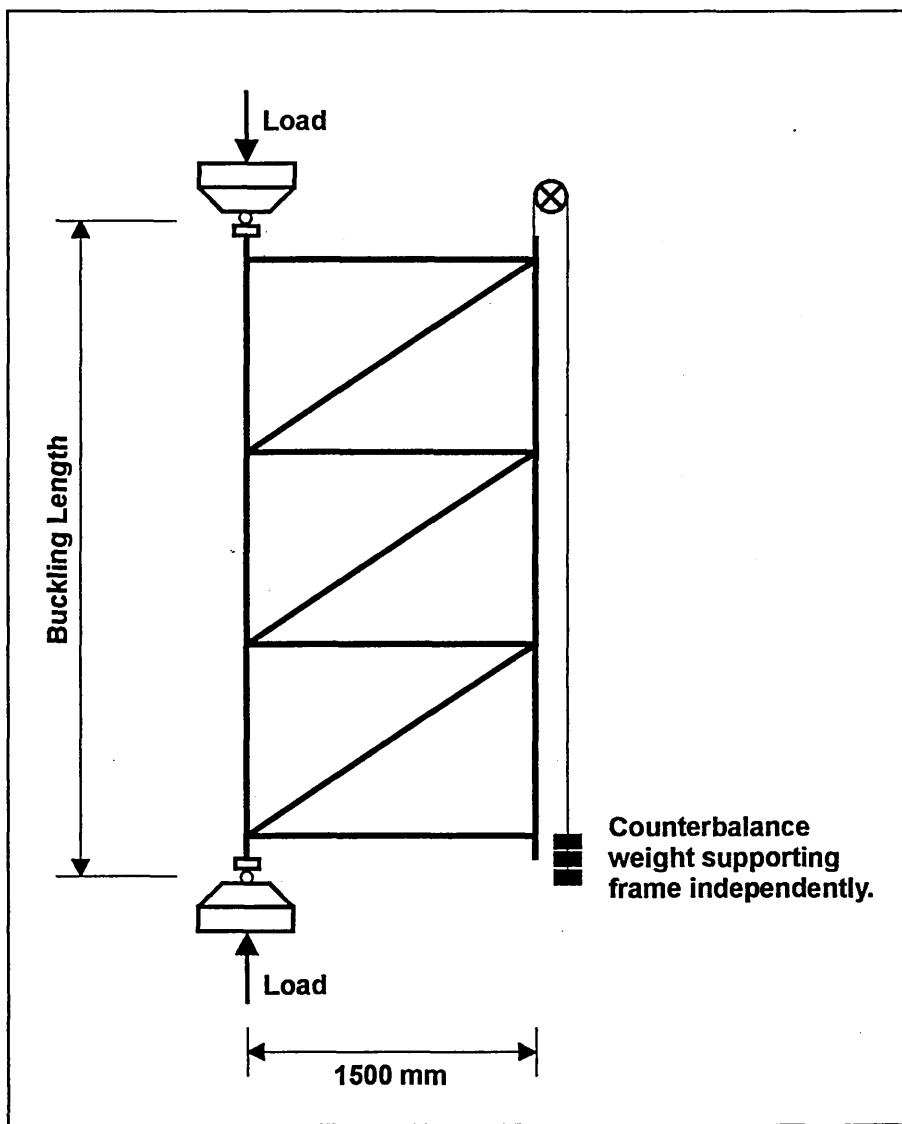


Fig. 4.9. Upright compression test - set up

During testing, an axial load was applied down a single upright from frames between 900mm and 2925mm in length, using a 2500KN Schenck compression testing machine. The mass of the untested portion of the frame was supported independently of the test apparatus using a number of weights acting as a counterbalance. They were loaded through their centroidal axes, the co-ordinates of which had been determined previously from the stub column compression test. The load was applied through two 50mm diameter ball bearings, which were positioned above and below each specimen on ball

seats that were rigidly fixed to the test frame. A diagram of the 'seating' arrangement has been produced below showing the relevant dimensions.

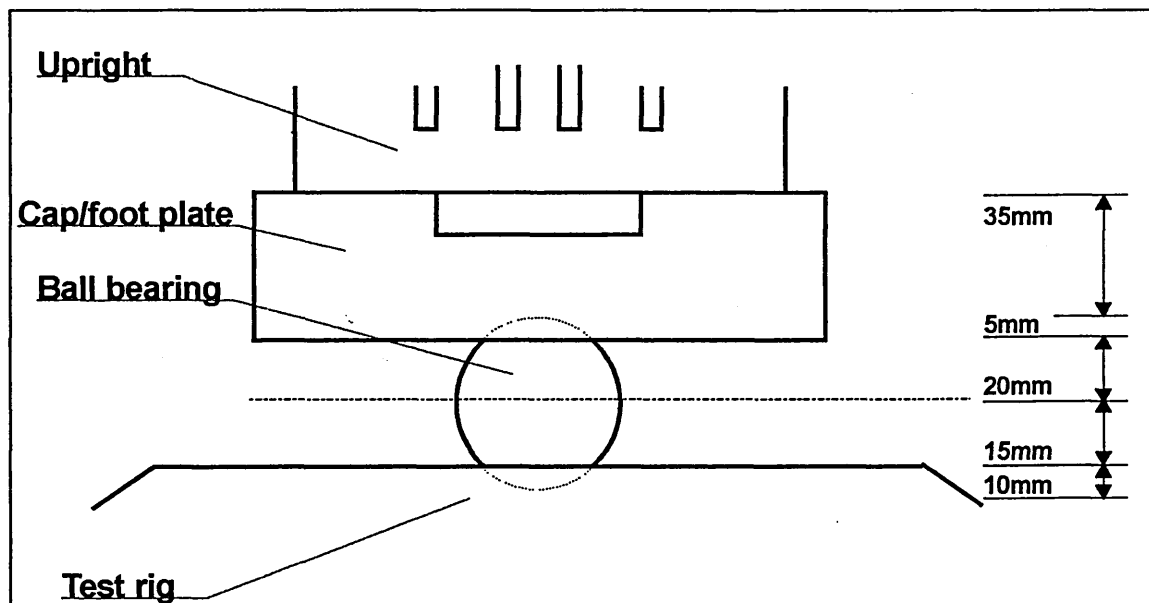


Fig. 4.10. Load application detail

Uprights were located in the test rig using cap/foot plates. These consisted of two identical steel plates (150mm x 100mm x 40mm) which were indented to a depth of 5mm on one side to seat a 50mm ball bearing. A groove was machined into the opposite side of the plate, allowing a steel insert to maintain a position of symmetry about the indent (see Fig. 4.10).

The inserts were manufactured in two sizes, one to fit heavy duty and one for the standard duty uprights. During testing, they were attached to each frame through the standard section holes, using two 12mm diameter cap head screws (ref. Plate 4.6.). The screws were positioned 40mm (to centre) from the end of each upright and once tightened, held the steel inserts firmly against the inside front face of the section. In this way, it was possible to position the inserts along the line of symmetry of each section with a high degree of accuracy.

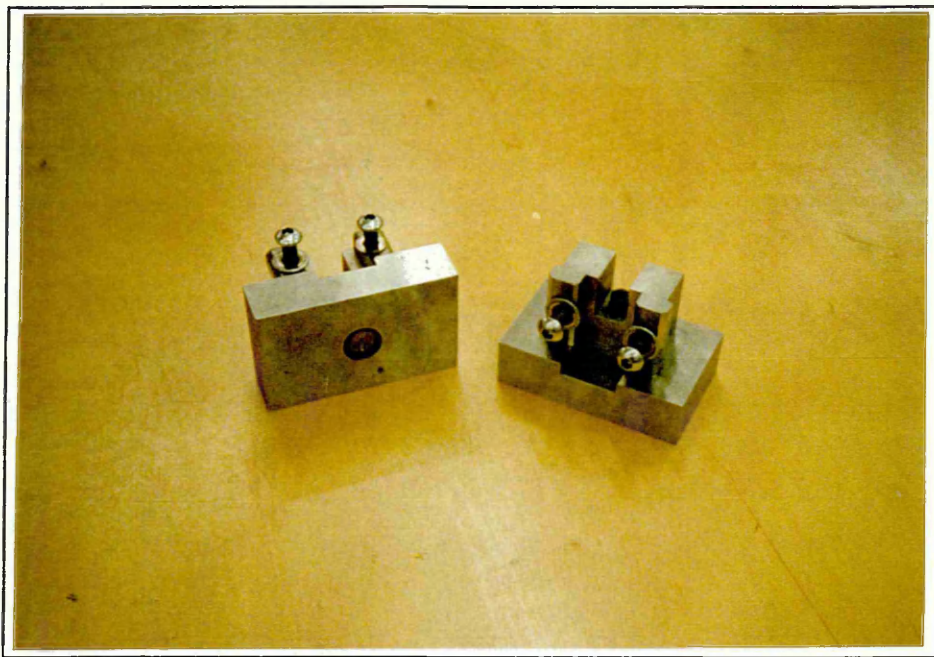


Plate 4.6. Cap/Foot Plates

Prior to being attached to the upright, the inserts were bolted to the cap/foot plates. The groove in the plates ensured that symmetry about the ball bearing indents was always maintained. In addition, a depth micrometer was used to establish with a great degree of certainty (0.01mm), the exact position of the insert (and by implication the upright) with respect to the ball bearings. Uprights were not adjusted for springback.

The following two plates illustrate how the upright compression test was organised in practice. Plate 4.7. is a front elevation showing the cap/foot plates in use on a 900mm long standard duty (SD25) frame. In contrast, Plate 4.8. shows a 2925mm heavy duty (HD25T) frame. The cross head and support plinth of the compression testing machine, together with the upright inserts are clearly visible. Also in evidence, is the counterbalance system, supporting the untested portion of the frame.

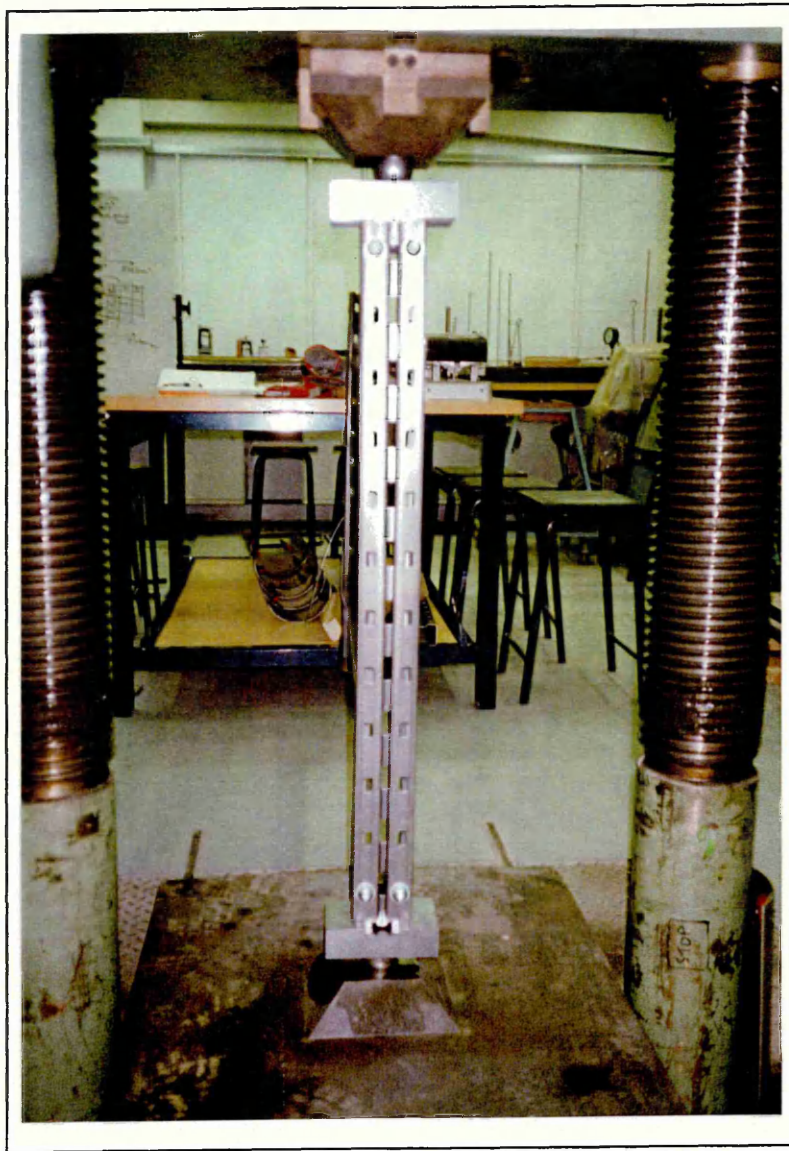


Plate 4.7. SD25 (900mm) frame compression test



Plate 4.8. HD25T (2925mm) frame compression test

4.4.3. Test Measurement

Prior to testing, actual material thickness' were determined using a standard micrometer accurate to 0.01mm. Two tensile tests were also performed on each coil of material used to manufacture the uprights, to determine the actual yield stress of the samples being tested.

The compressive load was applied manually and as far as possible, in a linear fashion to failure. The upright was deemed to have failed when either (see FEM Cl.5.1.3(a)) :

- 1) the applied test loads reached their upper limit, and/or
- 2) deformations occurred of such a magnitude that the upright could no longer perform its design function.

In practice, the first of these conditions always occurred before deformations became severe enough to inhibit the ability of the upright to perform its design function. The highest load was therefore recorded as the failure load using a visual display on the actuator control panel.

4.4.4. Discussion

Generally, upright collapse occurred in two distinct and separate ways. Frames of 900mm in height failed about the Z-Z axis, in the vast majority of cases. This type of failure, which can be seen in Plate 4.9., was characterised by an inward bulging of the section's rear lips, in conjunction with a bulging outward of the web in the central portion of the upright, between bracing connections. Occasionally, this effect was reversed and the upright buckled inwards with the lips splayed out.

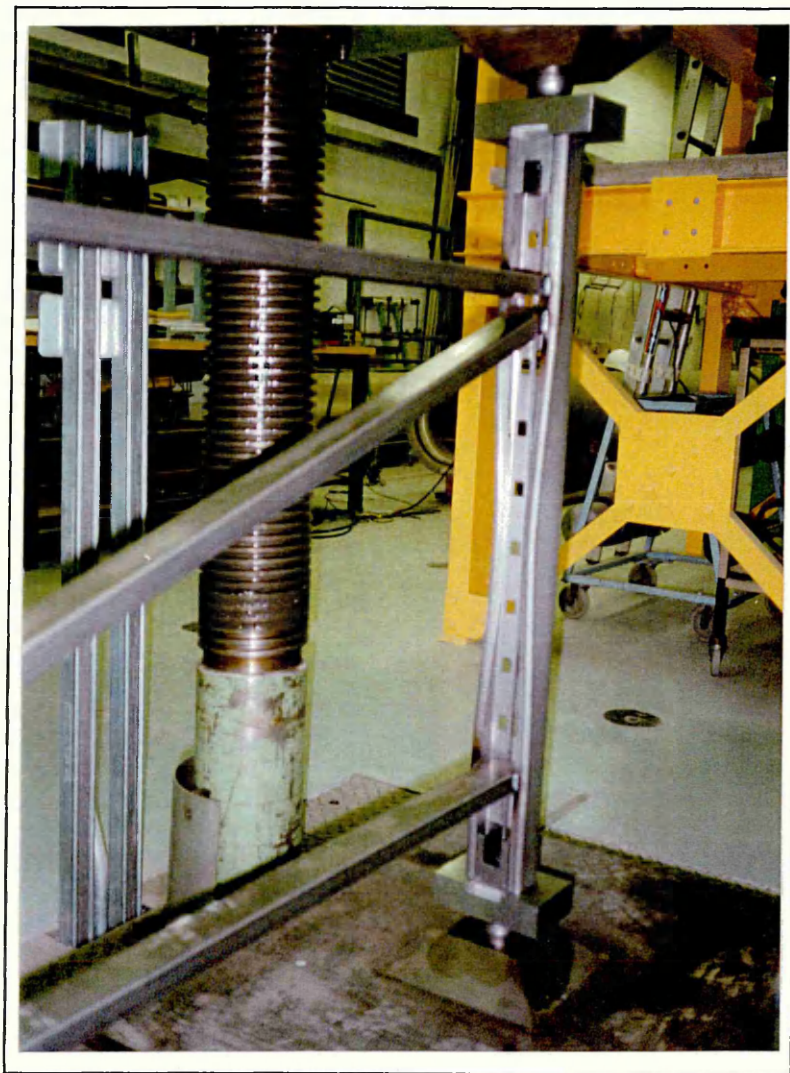


Plate 4.9. Typical upright failure (900mm in length)

Since the section was not doubly symmetric, bending failure was a primary factor in collapse, although local buckling of the upright due to high compressive stresses was also apparent during a number of tests. The upright in Plate 4.10. demonstrates the way in which local buckling and bending behaviour combined together to fail sections during this series of tests.



Plate 4.10. Compressive/bending failure in a 900mm long frame

Frames exceeding 900mm in height (in the range 1725mm to 2925mm) invariably failed in bending about the Y-Y axis. In sections of this height, the slenderness ratio has increased to the point where failure of the steel through yielding or crushing is no longer a factor. Instead, general instability of the upright as a whole is more critical to the resultant failure load. Plate 4.11. illustrates the deformation that occurred in a typical upright during testing. It should be noted here that the presence of beams attached at intervals down both sides of the upright, would serve to enhance the uprights ability to withstand axial loads.

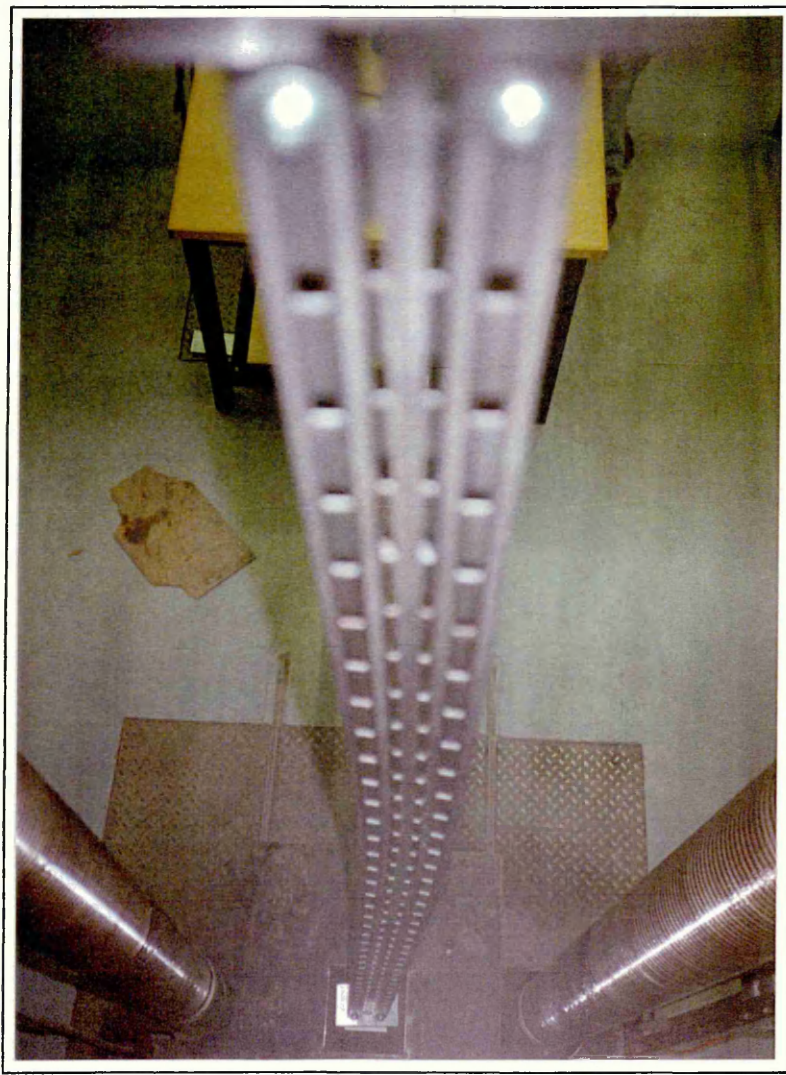


Plate 4.11. Bending failure in a 2925mm frame

4.5. Results and Analysis

4.5.1. Material and geometric corrections

Corrections to the test data were performed in accordance with section 4.3.2. of this document, although the yield stress calculation was modified to reflect the notion that more slender sections are prone to failure prior to reaching their elastic limit. In the following formulae 'C' is the yield stress correction factor :

$$R_{ni} = R_{ti}(C)^{\alpha} \left(\frac{t}{t_t} \right)^{\beta} \quad (4.7)$$

where: for $0 \leq \bar{\lambda} \leq 0.2$ $C = \left(\frac{f_y}{f_t} \right)$ (4.8.a.)

for $0.2 \leq \bar{\lambda} \leq 1.5$ $C = \frac{\bar{\lambda} - 0.2 + \frac{f_y}{f_t}(1.5 - \bar{\lambda})}{1.3}$ (4.8.b.)

It can be shown from this equation that a linear relationship exists between the value of the yield stress ratio (C) and the non-dimensional slenderness ratio ($\bar{\lambda}$) of the test samples between $\bar{\lambda} = 0.2$ and $\bar{\lambda} = 1.5$. Given typical values of nominal and observed yield ($f_y = 250 \text{ N/mm}^2$, $f_t = 280 \text{ N/mm}^2$) values of 'C' are demonstrated in Fig. 4.11. :

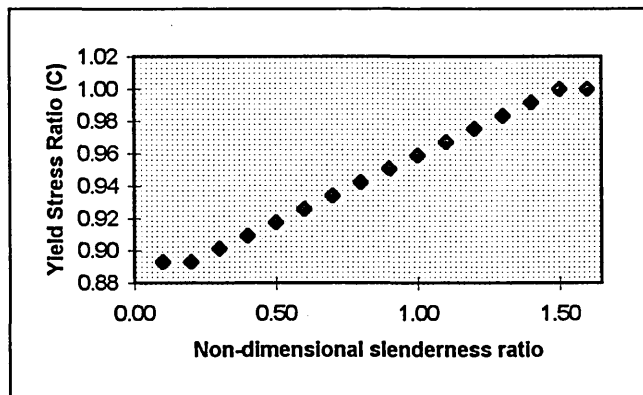


Fig. 4.11. The relationship between yield stress ratio and non-dimensional slenderness for defined values of nominal and observed yield stress.

The implications of this correction are that for very short columns (given here as $\bar{\lambda} \leq 0.2$), where failure is by yielding or crushing and there are no associated buckling or stability considerations, the maximum down-rating of the failure load is applied by the yield stress ratio. At intermediate slenderness ratio's ($0.2 \leq \bar{\lambda} \leq 1.5$) where maximum stresses exceed the proportional limit and the material no longer observes Hooke's law, there is a linear reduction in the effect of yield stress on the failure load until the slenderness of the section is such that elastic stability becomes the governing factor in column failure ($C = \text{unity}$). With high non-dimensional slenderness' ($\bar{\lambda} \geq 1.5$), the

column material remains linearly elastic to failure ($E=210000 \text{ N/mm}^2$), and the column follows the Euler buckling curve. In this case the value of the critical slenderness above which the Euler curve applies is defined as :

$$(\lambda)_c = \left(\frac{\pi^2 E}{\sigma_{pl}} \right)^{\frac{1}{2}} \quad (4.9.)$$

σ_{pl} is the average stress at the proportional limit.

4.5.2. Calculation of column buckling curve

i) Initially, calculations were undertaken for each test (including the stub column compression test) to determine values of stress reduction factor (χ_{ni}) and non-dimensional slenderness ratio ($\bar{\lambda}_{ni}$). χ_{ni} was taken to be the ratio of the corrected failure load for an individual test to the maximum compression resistance of the column, ignoring the effects of perforations. Corrections to the results due to effective area calculations are considered later on in this treatment :

$$\chi_{ni} = \frac{R_{ni}}{A_g f_y} \quad (4.10.)$$

Similarly, $\bar{\lambda}_{ni}$ was taken to be the ratio of the test slenderness to the slenderness of the section at the material yield stress [35]:

$$\bar{\lambda}_{ni} = \frac{\lambda_{ni}}{(\pi^2 E / f_y)^{1/2}} \quad (4.11.)$$

The denominator in this expression has been derived using the following analysis to verify the formula contained within the FEM. This has been done taking the maximum load (centrally applied) on an ideal, pin-ended column to be the critical load for a column with an effective length, 'L_e' :-

$$P_{cr} = \frac{\pi^2 EI}{L_e^2} \quad (4.12.)$$

P_{cr} represents the load just prior to the column buckling, known as the bifurcation point at which the column is in a state of neutral equilibrium (not stable or unstable). The critical stress (σ_{cr}) in the column at this point can be calculated using the formula above, to give :

$$\sigma_{cr} = \frac{P_{cr}}{A} = \frac{\pi^2 EI}{AL_e^2} = \frac{\pi^2 E r^2}{L_e^2} = \frac{\pi^2 E}{\left(\frac{L_e}{r}\right)^2} \quad (4.13.)$$

Assuming the critical stress in the column is taken to be its material yield stress :-

$$f_y = \frac{\pi^2 E}{\left(\frac{L_e}{r}\right)^2} \quad (4.14.)$$

$$\therefore \left(\frac{L_e}{r}\right)_{cr} = \left(\frac{\pi^2 E}{f_y}\right)^{\frac{1}{2}} \quad (4.15.)$$

This equation therefore represents the critical slenderness ratio for a column whose critical stress is the yield stress of the column material.

ii) A graph of χ_{ni} against $\bar{\lambda}_{ni}$ is then plotted and a curve fit chosen. In general, a 6th order polynomial expression was used to define the experimental data set, with the tail of the curve (arbitrarily chosen as any point beyond $\bar{\lambda}_{ni} = 1.5$) being asymptotic from below to the elastic buckling curve (see Fig. 4.12.). This was achieved using the theoretical stress reduction factor values calculated from the formulae in Cl.3.5.2. of the FEM :

$$\chi = \frac{1}{\Phi + \sqrt{\Phi^2 - \bar{\lambda}^2}} \quad (4.16.)$$

$$\Phi = 0.5(1 + \alpha(\bar{\lambda} - 0.2) + \bar{\lambda}^2) \quad (4.17.)$$

A plot of test data, together with the theoretical data calculated using the above equations and a curve fit in the form ($\chi_{cu}(\bar{\lambda}_{ni})$) is presented below for the HD25T upright. Here, the value of $\bar{\lambda}$ is taken to be : 1.5, 1.6 and 1.7.

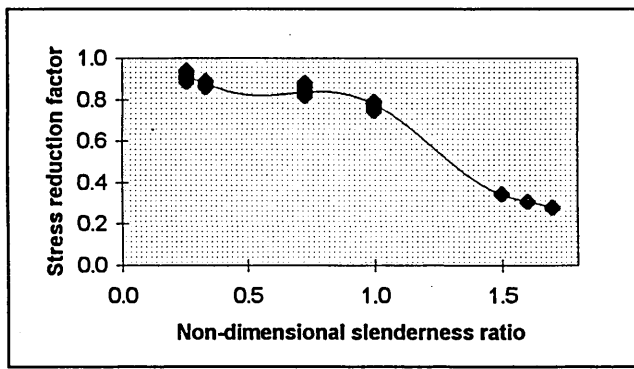


Fig. 4.12. Column curve test results - HD25T

iii) χ_{ni} values were normalised against the associated polynomial value (χ_{cu}):

$$\frac{\chi_{ni} - \chi_{cu}}{\chi_{cu}} \quad (4.18.)$$

and the standard deviation of the normalised values was then calculated. The unadjusted stress reduction value (χ') is then given by :

$$\chi' = \chi_{cu}(1 - k_s s) \quad (4.19.)$$

k_s is based on the total number of tests (n) performed on an individual upright section. This includes stub column tests but as with standard deviation calculations, theoretical values are not taken into consideration. The characteristic value of the stress reduction factor (χ) can then be calculated using :

$$\chi = \chi' \frac{A_g}{A_{eff}} \quad (4.20.)$$

$$\text{where } A_{eff} = A_g \chi'_e \quad (4.21.)$$

and χ'_e is the value of χ' at the stub column slenderness.

Values of non-dimensional slenderness ($\bar{\lambda}$) are also adjusted to take account of the effective area of each section, calculations to this point having been based on the gross cross section :

$$\bar{\lambda} = \frac{\lambda_{ni}}{\left(\frac{\pi^2 E}{f_y}\right)^{1/2}} \left(\frac{A_{eff}}{A_g}\right)^{1/2} \quad (4.22.)$$

Values of A_{eff} could be expected to be identical in this analysis and in that of the stub column test (for the same section). However, this has not proved to be the case (see Table 4.3.). It is reasonable to assume that due to the involved statistical treatment of the results, reflecting and even amplifying the effect of such things as the number of tests performed (e.g. HD25T, 10 stub tests - $k_s = 2.10$, 36 upright tests - $k_s = 1.842$) and the natural variations in any experimental data set, there is likely to be a divergence in the values of effective area between the two tests (A_{eff} from the column compression test has been used in the design formulae). These differences are not markedly significant as can be seen from the table below, with only the SD17 section exhibiting more than a 5% divergence between the results of the two tests:

Upright	Stub test (A_{eff})	A_{eff}/A_g	Column test (A_{eff})	A_{eff}/A_g	Stub/Column (% difference)
SD17	302.48	0.876	286.09	0.829	5.7
SD25	433.44	0.867	436.50	0.873	0.7
SD25T	410.86	0.822	409.00	0.818	0.5
HD25	584.00	0.898	599.95	0.923	2.7
HD30	766.92	0.998	740.35	0.964	3.5
HD25T	568.60	0.875	572.65	0.881	0.7
HD30T	676.91	0.881	692.74	0.902	2.3

Table 4.3. A comparison of effective areas for the stub column and upright compression tests

The ‘ χ vs. $\bar{\lambda}$ ’ results for each upright section undergoing the mathematical treatment outlined above, have been illustrated graphically overleaf. While allowing for a degree of experimental variation, it is apparent that all exhibit the typical S-shaped curve associated with pin-ended column failure over steadily increasing effective lengths. As polynomial curve fits, these plots are used in subsequent chapters of this document to aid in the analyses of racking systems, based on their critical effective lengths (in general treated as the height to the first beam level above the ground).

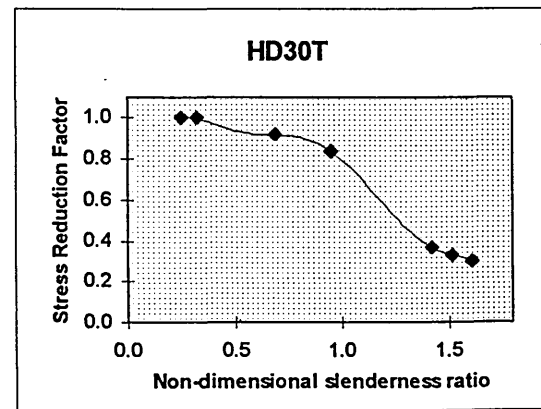
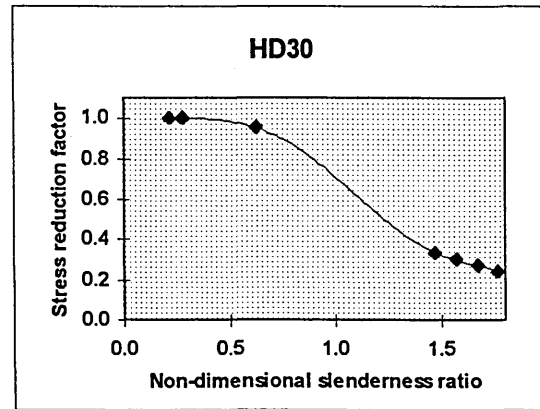
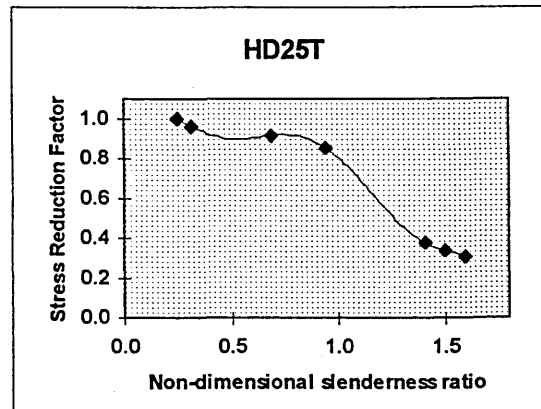
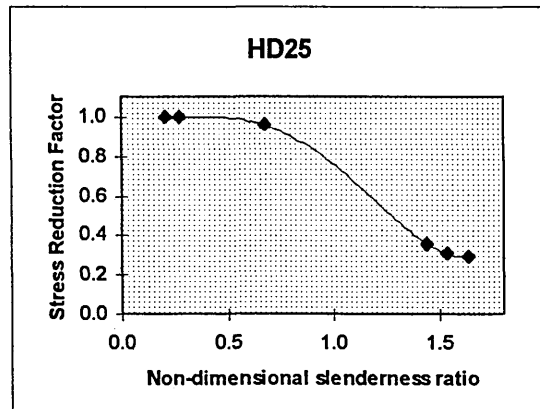
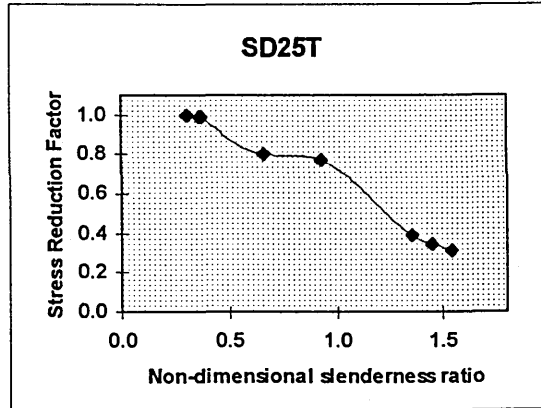
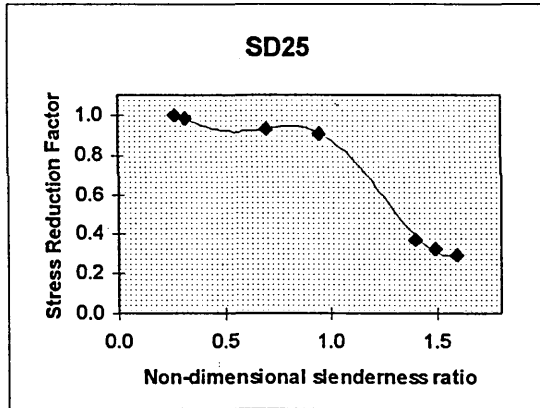
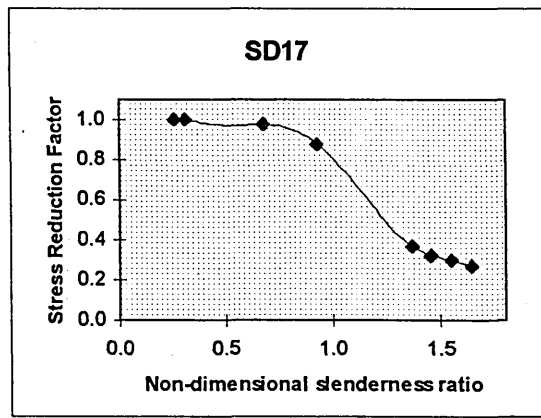


Fig. 4.13. Individual design column curves

4.6. Tests for Shear Stiffness of Frames

4.6.1. General Outline

The purpose of this test is to “determine the shear stiffness per unit length”(FEM-C1.5.9.1) of each frame in the product range. Before testing, it was not anticipated that a frame based on a jig-welded design should have significant problems in terms of shear stiffness in the cross-aisle direction. The results should therefore approximate to the values determined by theoretical calculation found using the formulae in Appendix C and Fig. C2 of the FEM code. With this in mind, the theoretical values of frame shear stiffness have been included in the discussion (4.7.3.) to allow comparisons to be made with the test results.

4.6.2. Test Arrangement

A total of 35 tests were carried out on seven separate upright sections, five tests per section. The frames were placed in the vertical rather than horizontal plane and held in place using rollers that coincided with the points of intersection of the bracing members. In addition, nylon lateral supports were included on the test rig (see Plate 4.9) at the same centres as the rollers to mitigate against sideways movement. The load cell was capable of recording up to 50KN, which was sufficient to fail all the samples (although this was not necessarily a requirement of the test), and the load was applied at a rate of 0.064mm/sec (5mm in 77.62 secs).

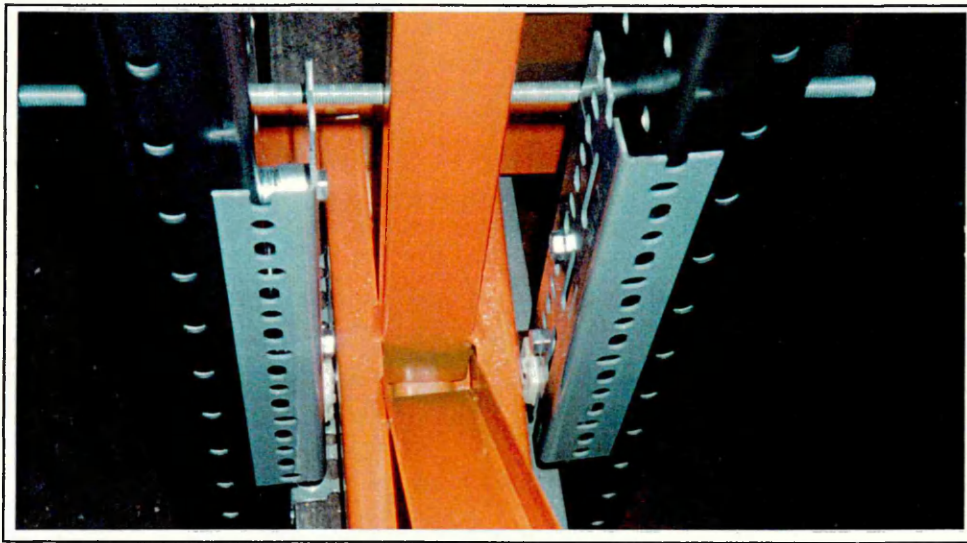


Plate 4.12. Nylon lateral support

Fig. 4.11 demonstrates schematically how each frame was set up for testing. All frames were three panels long and used the standard Z-form bracing pattern. The bracing diagonals were positioned as shown here, going from the bottom left to the top right of each panel, and 'pointing away' from the applied load (see FEM-Fig 5.9.2(a)).

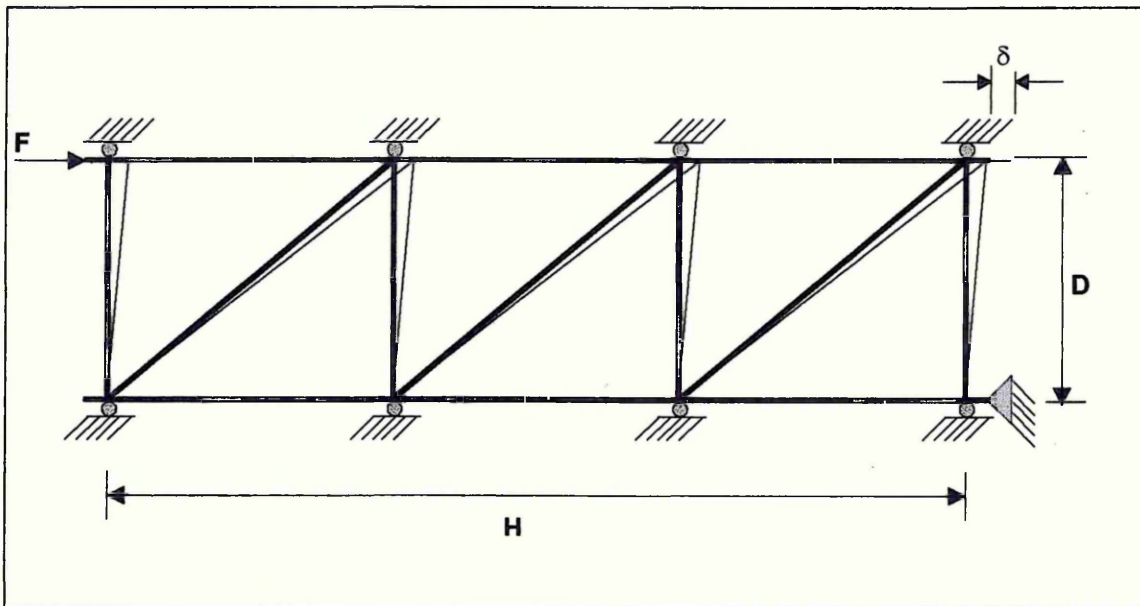


Fig. 4.13. Shear stiffness of frames test - set up

4.6.3. Test Measurement

During each test, both the deflection of the top upright and the loading on the frame were monitored manually. For deflection this was done using a 25mm dial gauge strapped to the test frame and in contact with the upright baseplate (see Plate 4.11). The load was monitored separately using a visual display on the actuator control panel.

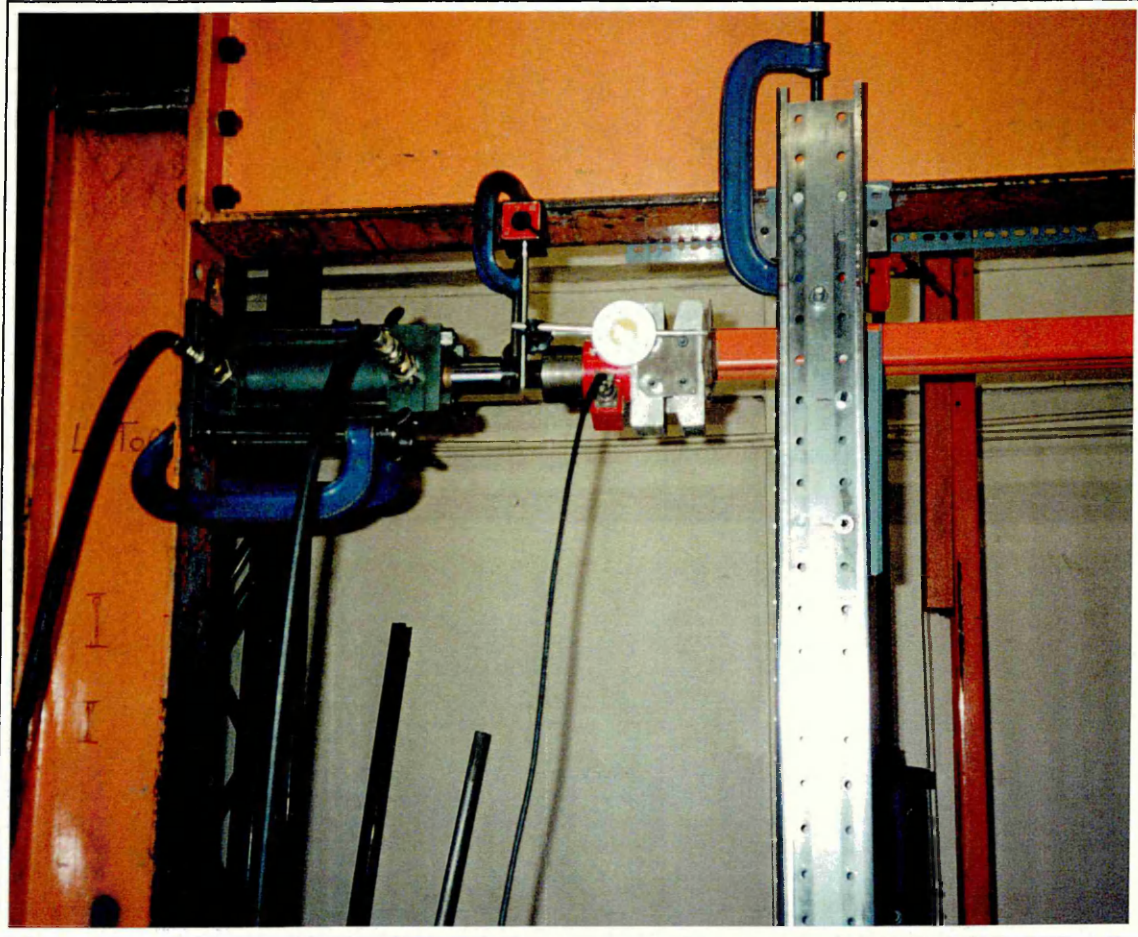


Plate 4.13. Load application and deflection measurement

4.6.4. Discussion

In general, the frames failed due to a catastrophic collapse of the 'end' bracing channel. This mode of failure is most clearly demonstrated by the frame in Plate 4.14. which was typical for all sections of upright tested.



Plate 4.14. HD30T frame - failure occurs centrally in the end bracing channel

4.7. Results and Analysis

4.7.1. Introduction

For each test, experimental data was plotted graphically, and a value of shear flexibility (k_{fi}) determined. This value was arbitrarily taken to be the slope of the linear portion of the curve which included at least three data points. An example of an experimental data set has been produced below for an HD25T upright test, together with the line used to calculate k_{fi} :

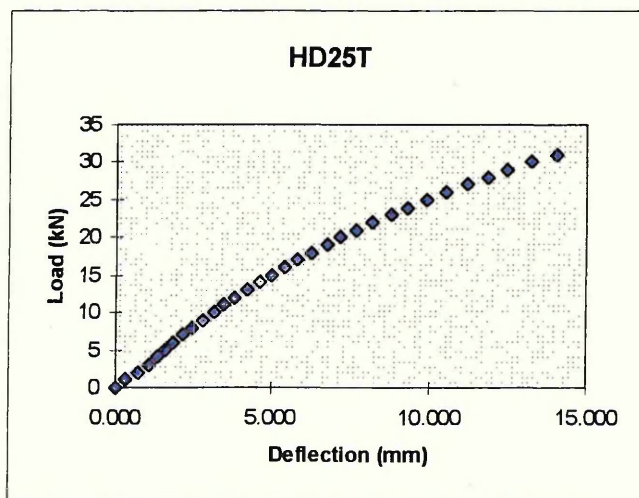


Fig. 4.15. Experimental load vs. deflection curve for HD25T upright.

4.7.2. Calculation of transverse shear stiffness

The transverse shear stiffness of each frame was taken to be :

$$S_{ti} = \frac{k_{ti} D^2}{H} \quad (4.23.)$$

where k_{ti} was the slope of the linear portion of the graph as described earlier and H was the frame length in whole bracing gates (3600mm in all cases). D was the distance between the centroidal axes of the upright sections with all frames being 1500mm wide.

The co-ordinates of these axes were developed from the stub compression test (\bar{X}), and by implication the values of 'D' in table 4.4. take this into account ($D = 1500 - 2\bar{X}$).

Here, the design value of transverse shear stiffness is taken to be the mean value from five tests :

Upright Section	Values of D (mm)	Mean Shear Flexibility, k_m (mm/kN)	Design value of Transverse Shear Stiffness (kNmm/mm)
SD17	1459.5	0.4298	1429
SD25	1458.0	0.2967	2248
SD25T	1457.0	0.2698	2206
HD25	1441.3	0.1933	3302
HD25T	1441.3	0.2289	3058
HD30	1442.9	0.1501	4906
HD30T	1442.1	0.0902	7408

Table 4.4. Summary of shear stiffness of frames test

4.7.3. Calculation of effective area of frame bracing

The effective area of the bracing section was determined based on the ratio of the theoretical to the actual shear stiffness of the member. Theoretical values of shear stiffness for each frame duty per unit length (S_D) were calculated using the following formulae and assuming a 'class 1' bracing system (see FEM, Fig. C2) :

$$\frac{1}{S_D} = \frac{1}{S_{dh}} + \frac{1}{S_{dd}} \quad (4.24.)$$

where
$$\frac{1}{S_{dh}} = \frac{1}{A_h E \tan \Phi} \quad (4.25.)$$

$$\frac{1}{S_{dd}} = \frac{1}{A_d E \sin \Phi \cos^2 \Phi} \quad (4.26.)$$

Using values for the bracing angle (Φ) of $36^\circ 6' 26''$ for SD frames and $36^\circ 40' 7''$ for HD frames, and a cross sectional area for the bracing member ($A_h = A_d$) of 147.58 mm^2 theoretical values of shear stiffness were determined as :- 7805 kNmm/mm SD section; 7854 kNmm/mm HD section. The effective area (A_{eff}) of the bracing section was then calculated using the equation :

$$A_{\text{eff}} = A_g \frac{S_m}{S_D} \quad (4.27.)$$

with S_m as the design value of shear stiffness and A_g the gross area of the bracing section.

Values of effective area were determined as follows :

Frame	SD17	SD25	SD25T	HD25	HD25T	HD30	HD30T
A_{eff} (mm^2)	27.02	42.51	41.71	62.05	57.46	92.19	139.20

Table 4.5. Effective area of frame bracing section

Results developed from this test were found to be considerably lower than had been expected from the theoretical calculations derived from the formulae in Appendix C of the FEM code. As can be seen from Table 4.5., this was particularly true for SD section which had a largely reduced effective area for its frame bracing. It is not entirely clear why a fully welded bracing system should produce such low effective area values, although the use of the largest frame width (1500mm) in the range may have had a significant impact on the moment rotation characteristics of the frame prior to failure. In

this case, improvements might be expected if frame widths were reduced in line with the requirements of the particular rack configuration being designed.

4.8. Bending Test on Upright Section

4.8.1. General Outline

The purpose of this test is “to determine the moment of resistance of an upright section, about its major and minor axes of bending” (FEM-CI.5.10.1). To avoid any misunderstanding that may occur when reading this document, it was thought prudent to clarify the method used for the referencing of axes. This has been done in order to eliminate potential confusion with regard to SEMA design tables, which use an alternative standard axes labelling convention.

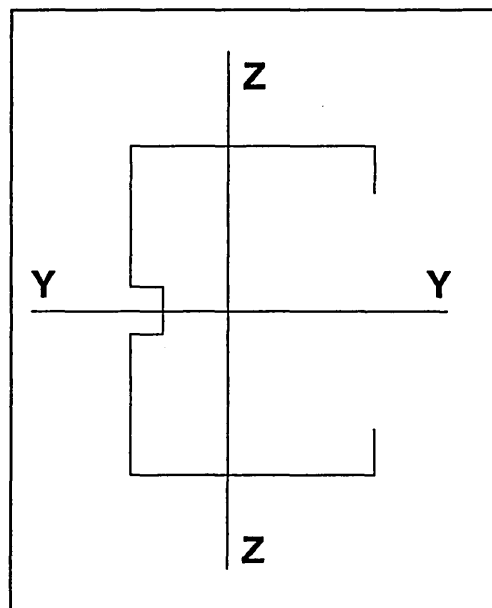


Fig. 4.16. Axes referencing

The nomenclature used in Fig. 4.16. for referencing axes is consistent throughout this document, and in line with FEM recommendations (see FEM-Fig. 3.10).

A total of 36 tests were carried out, and were initially designed to observe the bending behaviour of the samples about the axis of symmetry (y-y axis), allowing lateral torsional buckling effects to occur (see FEM-Fig.5.10.1(b)).

4.8.2. Test Arrangement

Complete frames were tested with two upright sections linked together by the normal bracing system with the section free to twist at the supports (see Fig. 4.17.). Frames 3300mm long ($L=3200\text{mm}$) were positioned on a horizontal testing bed, and the load was applied at quarter points of the span. Choosing this length of section allowed both SD and HD uprights to be tested on the same rig, while remaining in accordance with Cl.5.10.2 of the FEM code ($30 \leq L/D \leq 40$). The ratio 'L/D' for SD and HD sections was calculated to be 38.74 and 32 respectively.

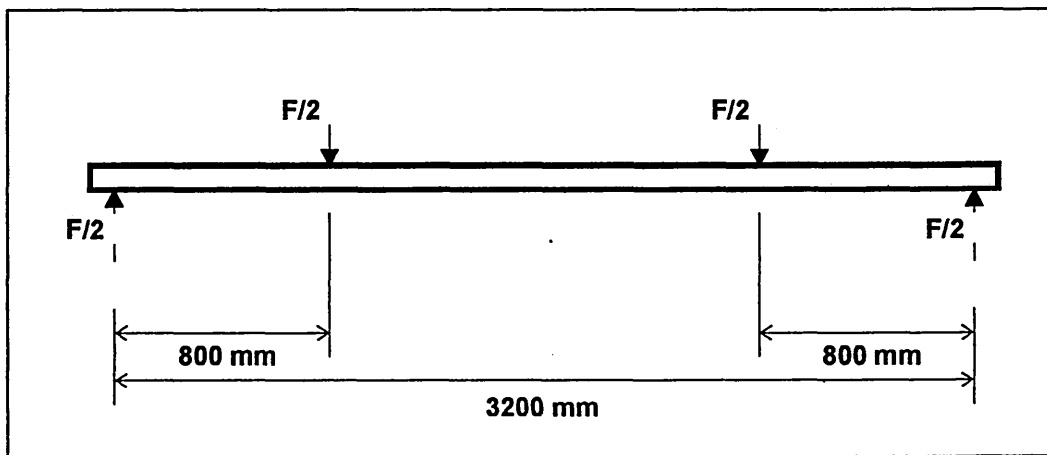


Fig. 4.17. Upright bending test dimensions

A single actuator acted through a ball seat onto I-beam/box-beam spreader system (see Fig. 4.18.) through which load was applied to the section. Load was transferred into the frames via cylindrical rollers and 100mm x 10mm mild steel plate, which prevented localised crushing of the section. Further pieces of plate were also used at the four supports to prevent any localised crushing there.

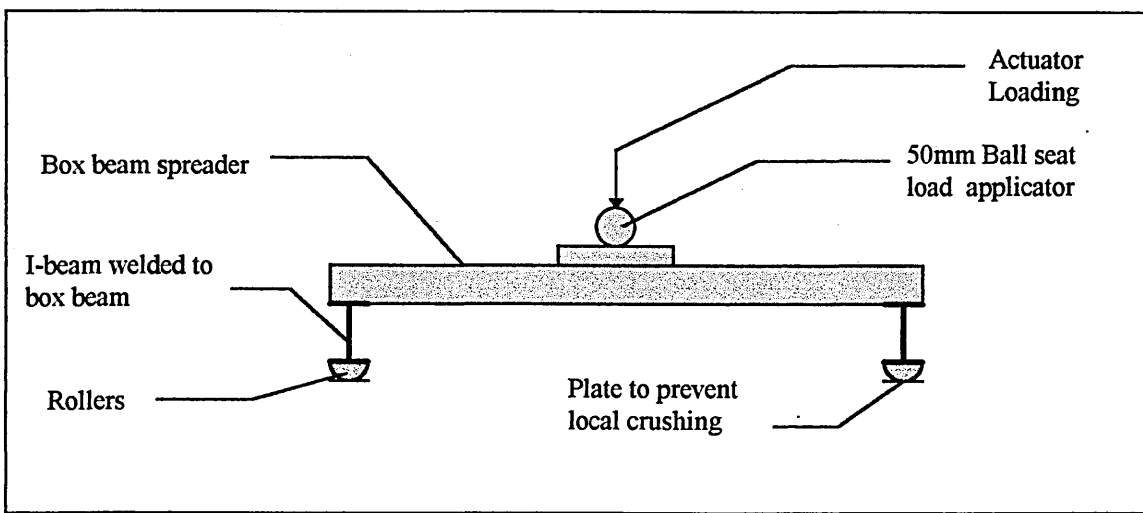


Fig. 4.18. Load spreader system

The loading was applied using a Schenck hydraulic actuator with a displacement capability of $\pm 100\text{mm}$ and a load capacity of 300KN .

4.8.3. Data Capture

All load readings were captured electronically, using in-house data capture equipment and software. Load incrementation and the rate of data capture were determined manually during each test. The plates overleaf have been included to underline some of the points made above and to demonstrate how the tests appeared in practice :

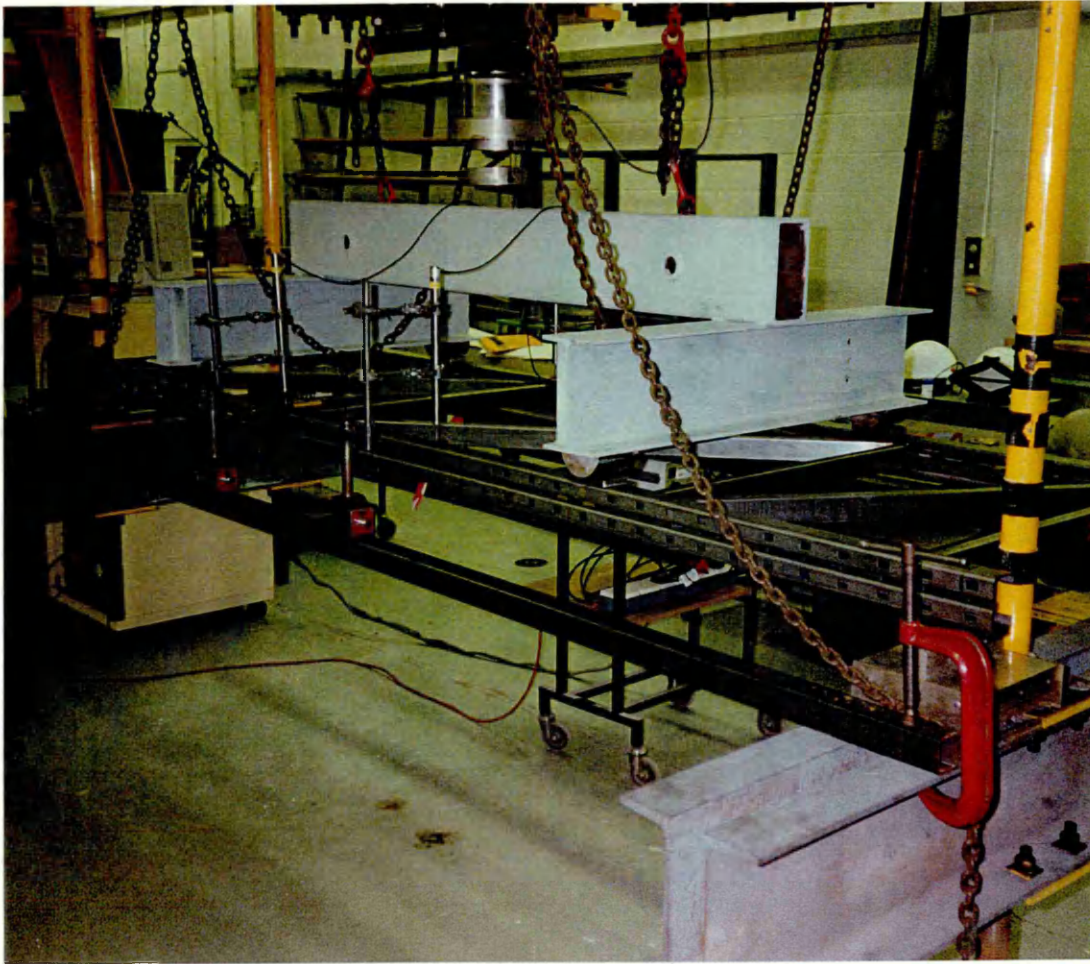


Plate 4.15. Upright bending test - set up

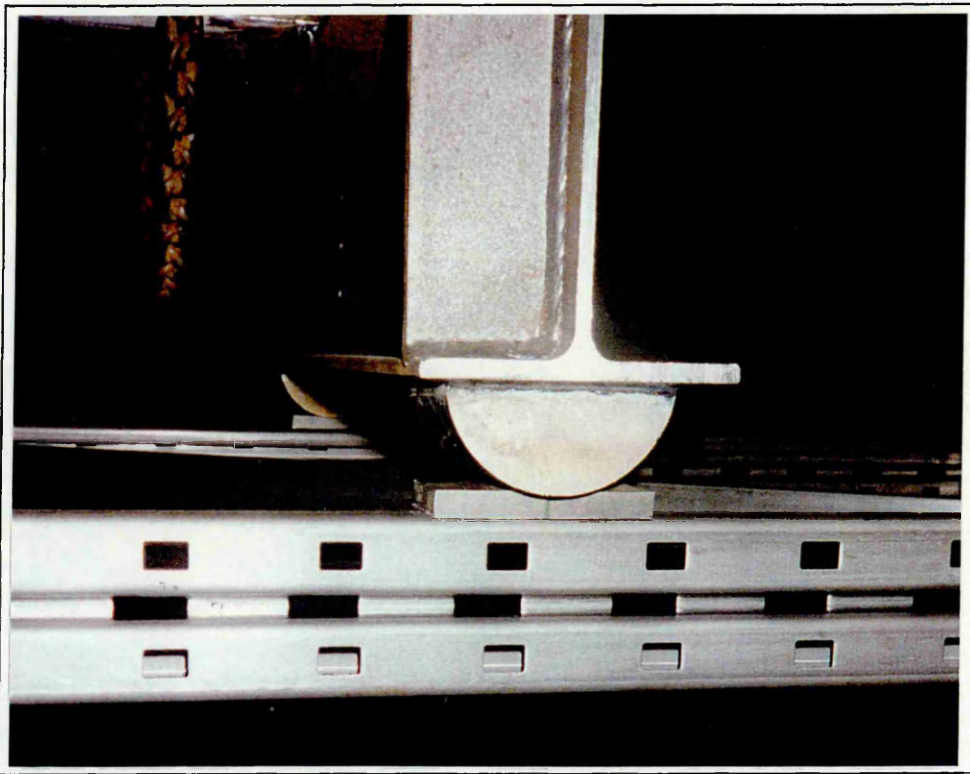


Plate 4.16. Spreader/upright contact detail

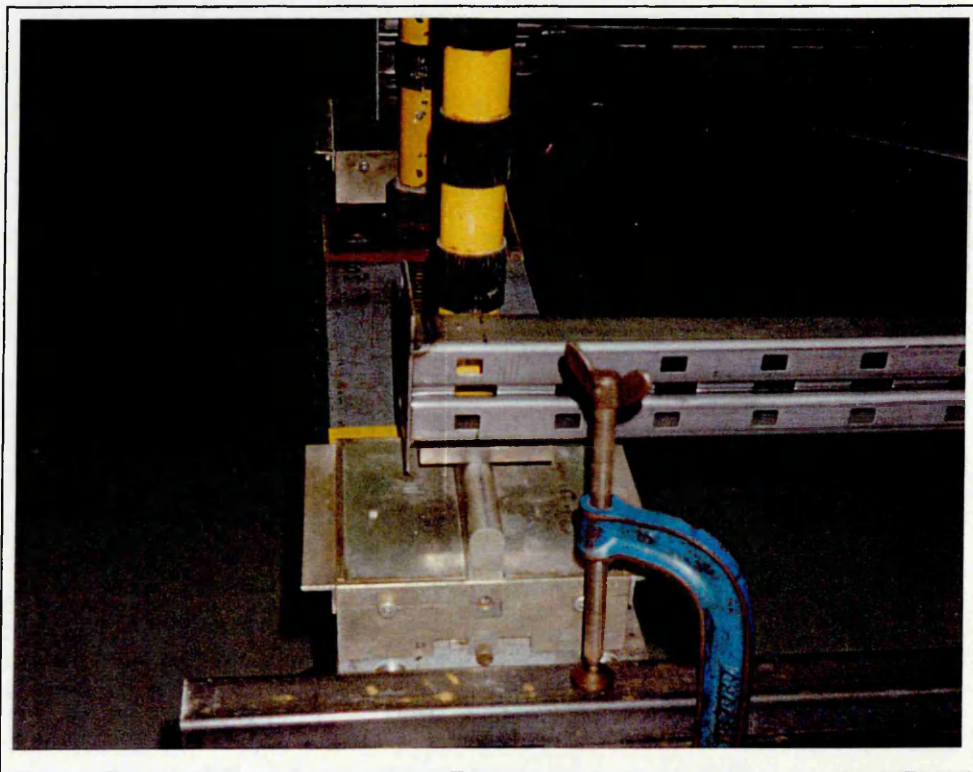


Plate 4.17. Support/upright contact detail

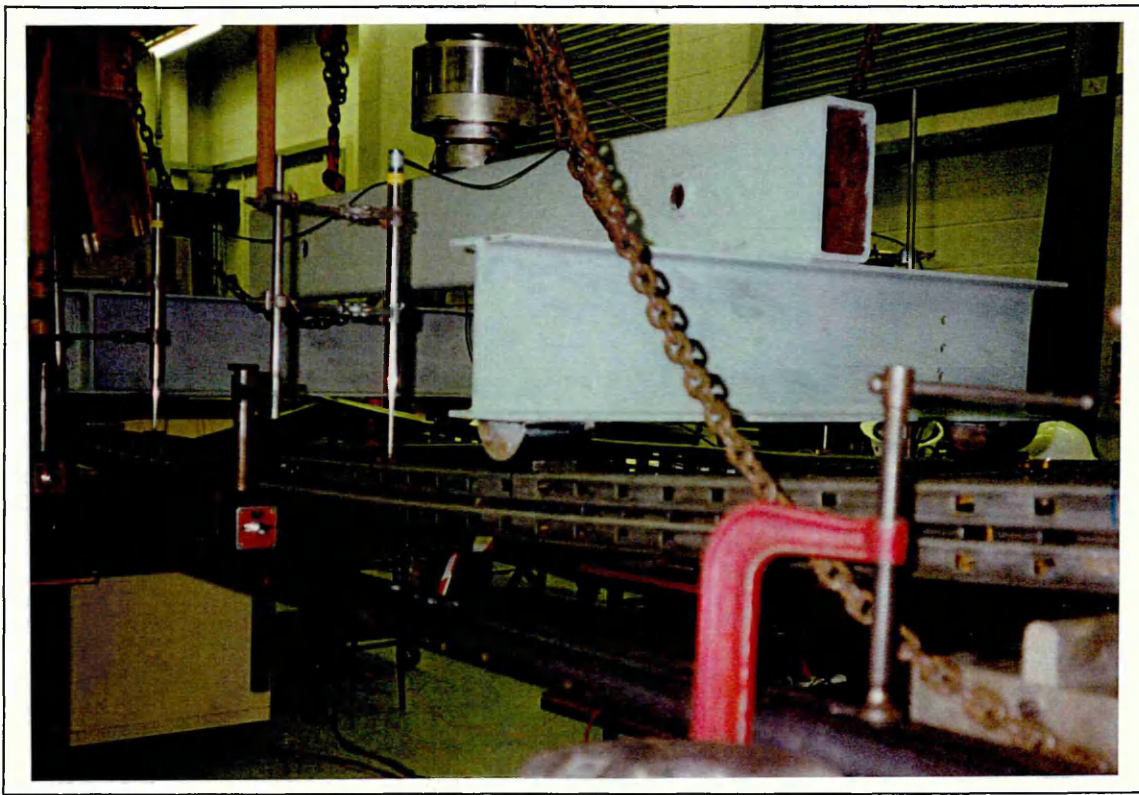


Plate 4.18. Upright sample under four-point bending

4.9. Results and Analysis

4.9.1. Introduction

Uprights failed in the torsional-flexural mode, with torsion in the frame being mediated against in part, by the bracing support. In this series of tests no account has been taken of the restraint provided by the beams (due to the near-infinite variation in their positioning), and as a result the characteristic moments of resistance calculated below are considered to be conservative.

4.9.2. Material and geometric corrections

The failure load (F) taken from the test was converted to a moment using the standard four point bending formula for a simply supported beam. Values at this stage are for a frame rather than a single upright :

$$M_{\max} = M_{ti} = \frac{F_{ti}}{2} \frac{L}{4} = \frac{F_{ti}L}{8} \quad (4.28.)$$

Corrections to the observed failure moment for yield stress and thickness variations were in line with equation 4.1 in section 4.3.2. of this document, with the maximum observed moment calculated from the formula above (M_{ti}) replacing the maximum observed load (R_{ti}). In addition, the value of β determined by the limiting values of width to thickness ratio given in equation 4.2. and 4.3. are determined by the formula :

$$\left\{ \frac{b_p}{t} \right\}_{\lim} = 0.64 \sqrt{\frac{k_\sigma E}{f_t}} \quad (4.29.)$$

with k_σ defined in Appendix D of the FEM code.

4.9.3. Characteristic moment of resistance and results summary

The characteristic moment of resistance for each frame was calculated using the formulae in section 4.3.3. of this document. The value of the effective elastic modulus (W_{effy}) required in the upright design check could then be determined for each upright using the formula below :

$$M_k = 2(W_{effy} f_y) \quad (4.30.)$$

$$W_{effy} = \frac{M_k}{2f_y} \quad (4.31.)$$

The results of the bending test having been analysed as described are presented here in tabular form :

Section	Characteristic Moment of Resistance, M_k <u>frame</u> (KNm)	Effective Section Modulus, W_{effy} <u>single upright</u> (mm³)
SD17	4.09	8180
SD25	4.79	11280
SD25T	7.375	12314
HD25	10.032	23620
HD30	12.278	27360
HD25T	11.523	19229
HD30T	16.371	21229

Table 4.6. Summary table of characteristic moment of resistance (frame) and effective section modulus (upright)

4.10. Floor Connector Test

4.10.1. General Outline

The purpose of this test is to “measure the moment rotation characteristics of the connection between the upright and the floor for a range of axial loads up to the maximum design strength of the upright” (FEM-CI.5.8.1). Two types of baseplate, ‘narrow aisle’ and ‘standard aisle’ are commonly used in rack design (see Appendix A), and consequently each has been tested here. In addition, the geometrically largest and smallest upright sections in the product range (SD17, HD30) were used in this test series, together with a “high carbon” Tenform section (HD30T), in order to identify the extremes of stiffness and failure moment for the product range. A total of 107 tests were performed during this series of tests.

4.10.2. Test Arrangement

The test arrangement involved the use of two 521mm lengths of upright section fitted with baseplates in the standard fashion, and bearing onto a C20 strength concrete cube. The mix design is contained within Appendix B. The cube surfaces were parallel and the dimensions were such (.3m x .3m x .3m) that there was a minimum clearance of 50mm around each baseplate to the edges of the block.

The block itself was confined within a cage and mounted on rollers. It was capable of moving in the horizontal plane, along the line of action of ‘Jack 2’ (see Fig. 4.19.), and was guided on rails, which were designed to prevent rotation in either the vertical or horizontal plane.

Load was applied down the uprights using two cylinders capable of applying upto 250KN. Each of the cylinder rods was fitted with a ‘machine-rounded end’ equivalent to a 50mm ball bearing which located into cap plates attached to the uprights. The cap plates which are described previously in this document (see plate 4.6.) could be adjusted

to ensure that the line of action of the load passed through the centroidal axes of each upright.

Lateral movement of the concrete block was controlled using a third cylinder capable of applying up to 25KN.

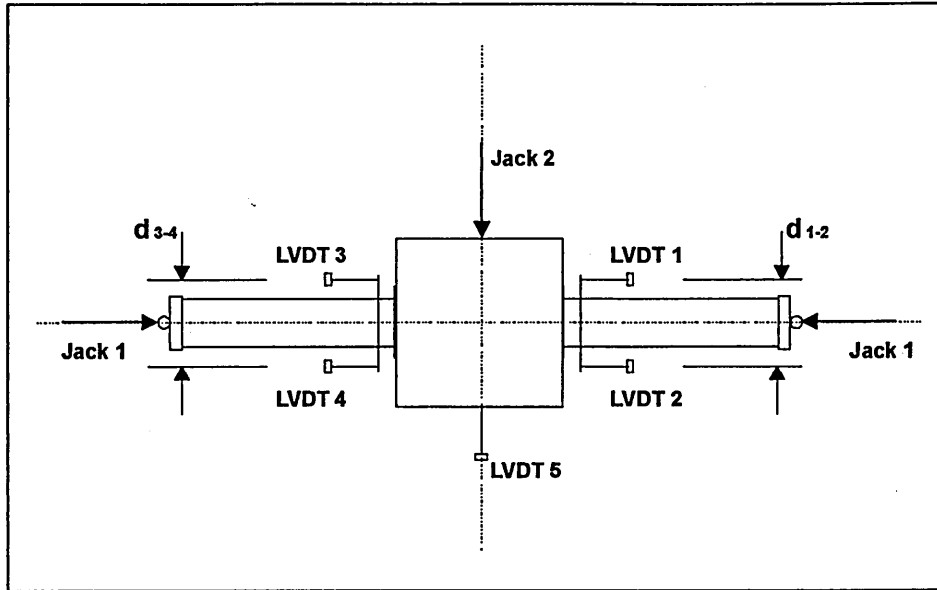


Figure 4.19. Floor connector test schematic

4.10.3. Test Methodology

Initially, Jack 1 was engaged with a load approximating to 20% of the full test load. This allowed the uprights to be held in position on the concrete, while an LVDT was mounted on either side of each upright (four in total) to record rotation. The transducers were able to monitor the rotation of the uprights during testing, using pieces of angled plate attached to the uprights close to the baseplates (see Plate 4.19.). A fifth LVDT was used to measure the lateral movement of the block under loading from Jack 2.

Where movement of the block away from the centreline of the test assembly was detected due to the initial 20% loading, a second cylinder opposite Jack 2, could be employed to take corrective action in the direction of misalignment. However, movement of this kind was rarely in evidence, and the second cylinder proved unnecessary.

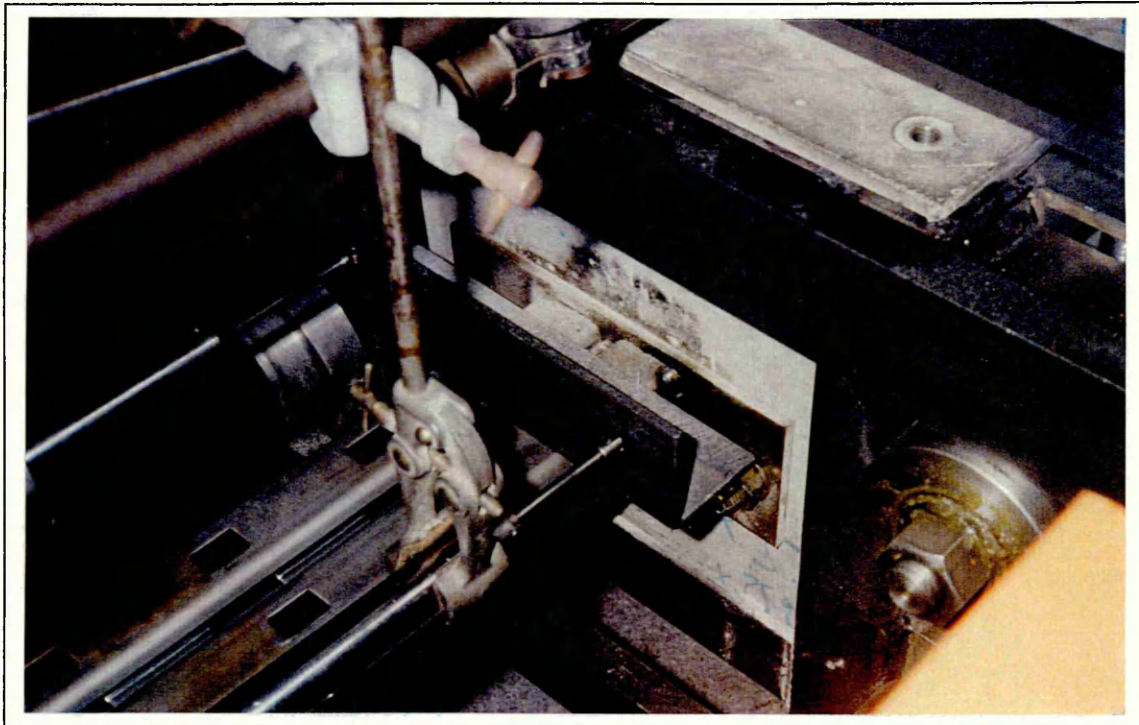


Plate 4.19. Rotation measurement

Once the LVDT's were in position, the load in Jack 1 was re-applied and increased to a pre-determined percentage of the uprights design strength. It was maintained at this level until the completion of the test. The load in Jack 2 was then increased slowly, pushing the concrete block along the guide rails and gradually increasing the moments on the baseplates to failure.

All baseplates were tested, as far as possible, under the same conditions as they would experience in practice. This meant that narrow aisle baseplates were bolted to the concrete 'floor' using standard 12mm diameter holding down bolts torqued to 25Nm. However, in the case of the standard baseplate, which is normally held down by just one bolt in practise (to prevent the rack from moving rather than for any structural purpose), it was decided that no bolts should be used. This conservative approach ensured that no undue influences attributable to the bolts were included in the rotational stiffness' of the baseplates.

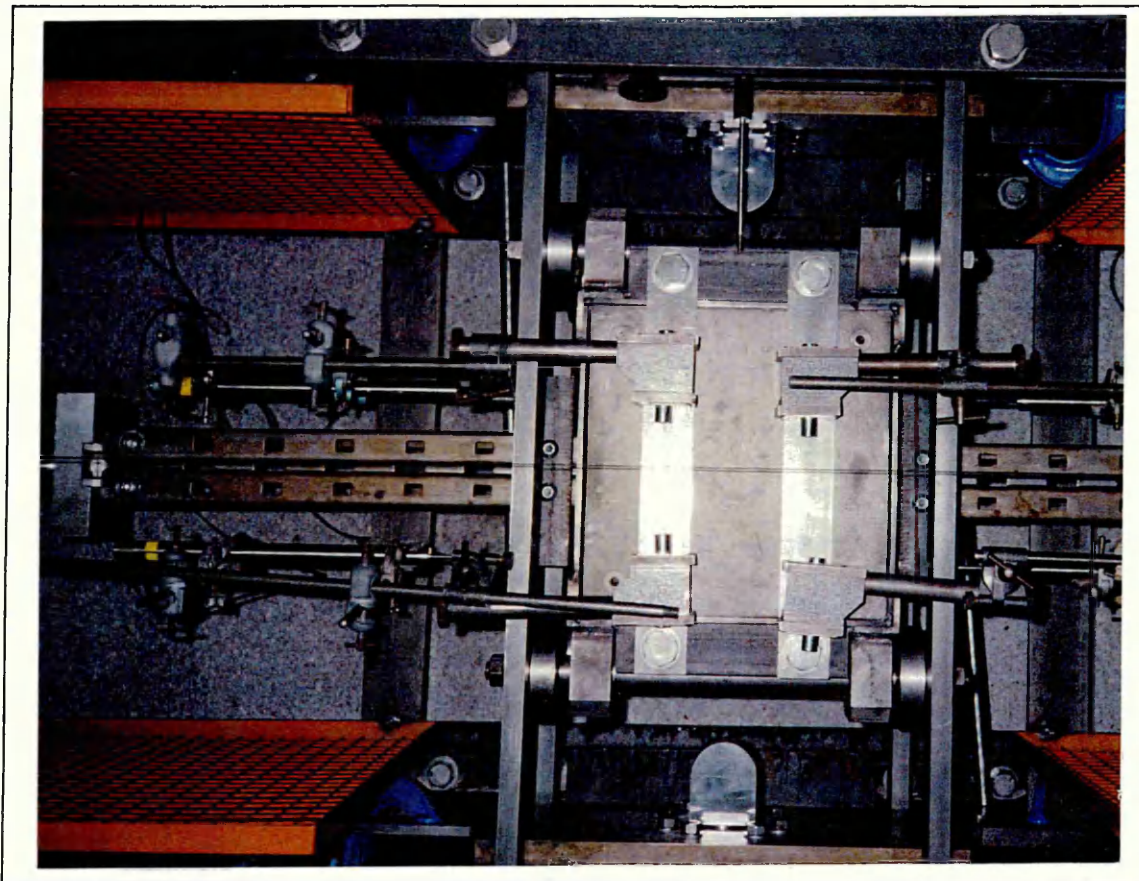


Plate 4.20. Floor connector test on SD17 upright

4.10.4. Data Acquisition

Each floor connector test was monitored using four LVDT's measuring the rotation of the uprights, while a fifth measured the lateral movement of the concrete block. In addition to this, two pressure transducers measured the loads being applied by each set of cylinders. The data acquired was then fed into a Solartron Orion 3530 data logger which scanned all seven channels every 0.5 secs. From the data logger, test information was down-loaded and saved onto a PC using bespoke computer software (PCE 3530).

4.10.5. Design of floor connector test rig

The rig was designed as a bespoke test machine using channel, box and I-section steel to withstand an axial load across the main rams in excess of 250kN and 50kN across the lateral displacement rams. An isometric drawing of the final design is included in Appendix B.

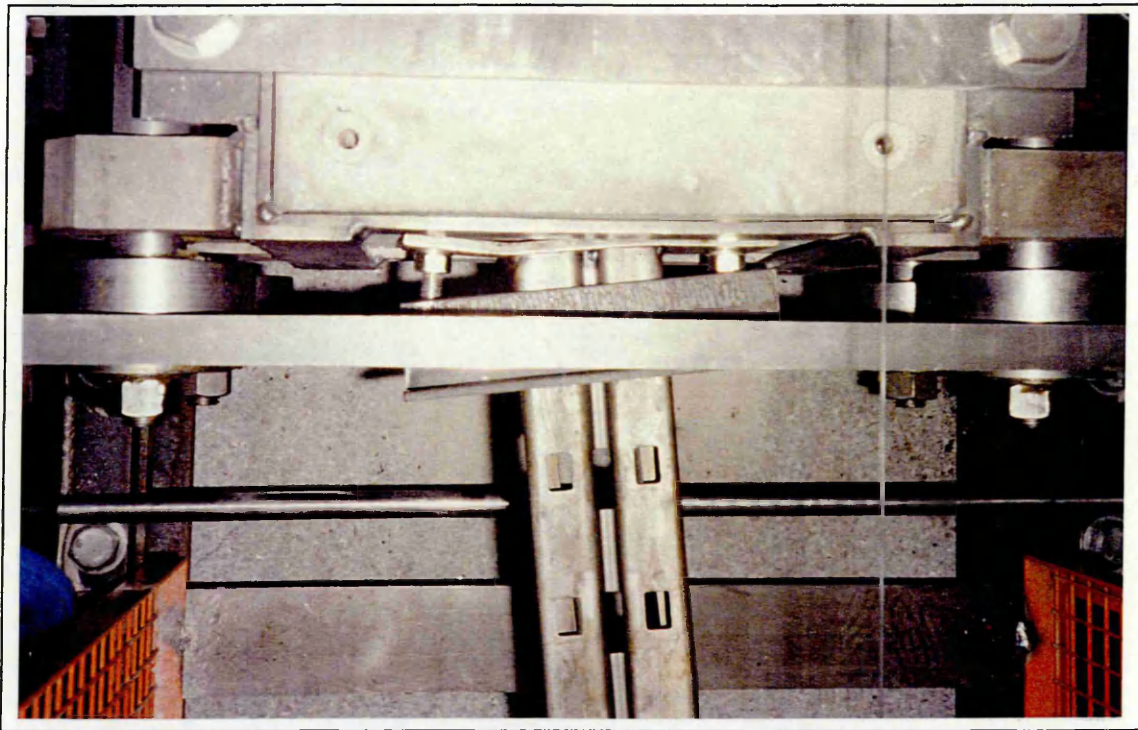


Plate 4.21. Failure of SD17 narrow aisle baseplate

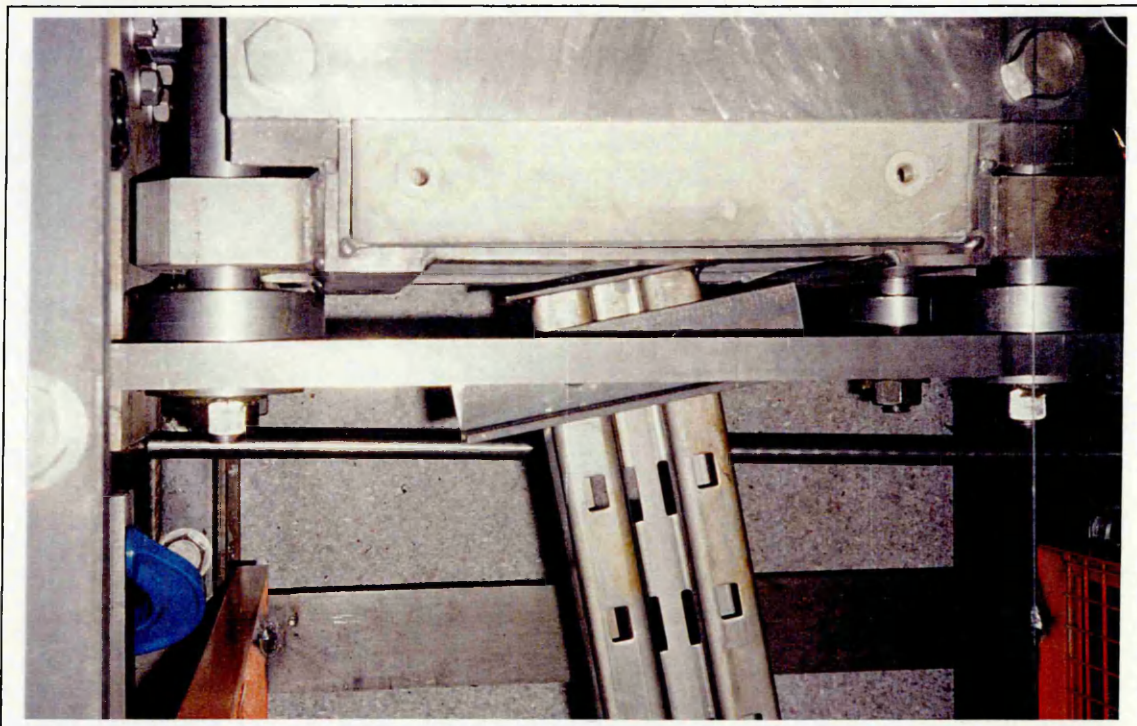


Plate 4.22. Failure of HD30 standard aisle baseplate

4.11. Results and Analysis

4.11.1. Introduction

Moment-rotation curves were developed from test data, in order that stiffness' and failure moments could be determined for axial loads equivalent to 25%, 50%, 75% and 100% of the upright design load. The moment (M_b) applied to each baseplate was established using the formula :

$$M_b = \frac{F_2 l}{2} + F_1 \Delta \quad (4.32)$$

where F_1 was the axial load applied to the columns (each of length $l/2$), F_2 was the lateral load applied to the concrete cube and ' Δ ' was the distance through which the cube was displaced.

The rotation of a single baseplate (θ_b) was taken to be the average rotation for both baseplates in a test, with the equation taking the form :

$$\theta_b = \frac{1}{2} \left[\frac{\delta_1 - \delta_2}{d_{12}} + \frac{\delta_3 - \delta_4}{d_{34}} \right] \quad (4.33)$$

where ' $\delta_1 - \delta_2$ ' was the displacement of one end of the angled bar (shown in Plate 4.19.) relative to the other end, and d_{12} was the distance between the LVDT's measuring that displacement. The equation was based on the arc formula, $S = r\theta$ which allows small angles to be calculated on the basis of linear measurement (see Fig. 4.20.) :

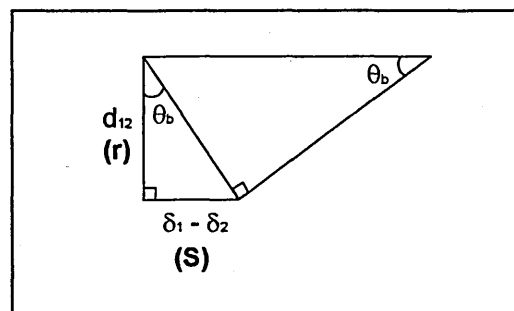


Fig. 4.20. Geometry for determination of baseplate rotation.

4.11.2. Consideration of the statistical treatment of results

The nature of the statistical analysis required by the code had a tendency to amplify any variations between individual test results, particularly when only a small number were performed. This had potentially grave consequences, specifically with regard to the calculation of design values, which could be down-rated very significantly (see table 4.7.). The effect described here was especially relevant to the floor connector test as in general, only three tests were performed on each upright/floor connector/axial load combination (the minimum required by the code), and because the results obtained displayed an unexpected measure of variation that was not anticipated prior to testing. The following example has been provided to demonstrate the potentially anomalous nature of the statistical treatment employed by the code :

For $n=3$, 95% fractile at a confidence level of 75 % (k_s) = 3.15

B/plate	Test failure moment (Nm)	Mean value of test results (Nm)	Standard deviation of test results	Characteristic failure moment (Nm)	Design failure moment (Nm)
A ₁	1400				
A ₂	1500				
A ₃	2100	1667	378.59	474	431
B ₁	625				
B ₂	650				
B ₃	600	625	25	546	497

Table 4.7. FEM statistical treatment of results on a hypothetical data set

It is clear from the example above that for a limited number of tests on two separate baseplates, a higher than ‘normal’ failure moment from an individual test (A₃) can severely affect the resultant design failure moment. In this case for instance, the mean failure moment of baseplate ‘A’ is 267% greater than that of baseplate ‘B’, however, the design moment (upon which each rack design is based) is greater for baseplate ‘B’. This is counter intuitive merely from an examination of the raw test results, and it is clear that the assumption of a normal distribution for any data set can create ‘inconsistencies’ when

a small number of results is being analysed. The floor connector test was particularly vulnerable to this type of statistical anomaly, with only three tests having been performed for each load case, on each upright. It is clear that additional testing could reduce the negative impact of the statistical treatment employed, although this is by no means guaranteed.

4.11.3. Calculation of floor connector design moment and stiffness

Two methods were permitted for determining the floor connector design values. The equal area method (outlined in some depth in section 5.3.) was considered initially, allowing the determination of a design stiffness and moment for a group of tests on each axial load. As a consequence, the results would appear in the form shown in Fig. 4.21.:

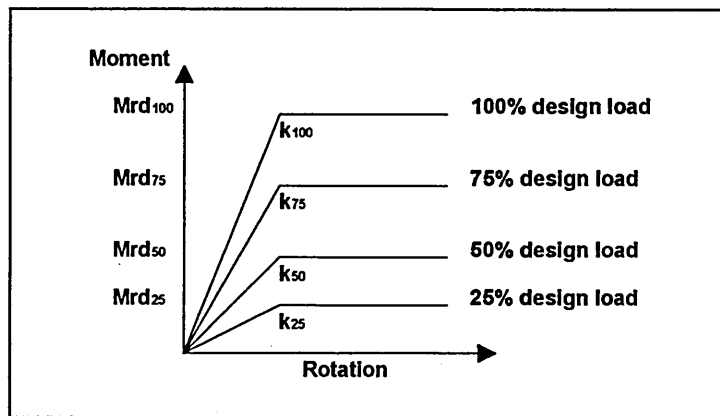


Fig. 4.21. Generalised form of results giving variable stiffness' and moments for variations in design load.

This method had the advantage of increasing the performance of the baseplate in response to increases in the loading on the rack. Inevitably, some measure of design advantage in terms of load capacity, would result from being able to interpolate between these fixed values. Unfortunately, this three dimensional approach to the design of the rack could not be accommodated by the available software, and it was therefore necessary to use a simplified, and by implication, more conservative approach.

This method involved choosing a single stiffness value to be no greater than the maximum slope of any experimental curve from all the tests performed on an upright/baseplate combination. Fig. 4.22. illustrates how a typical set of experimental curves react to an increase in the design load ('DL') applied to the upright. A single stiffness value has been taken from the graph in the manner described above, together with design moments for each quartile of design load. This simplified approach to the behaviour of the baseplate is reproduced in Fig. 4.23. and in Table 4.8. overleaf.

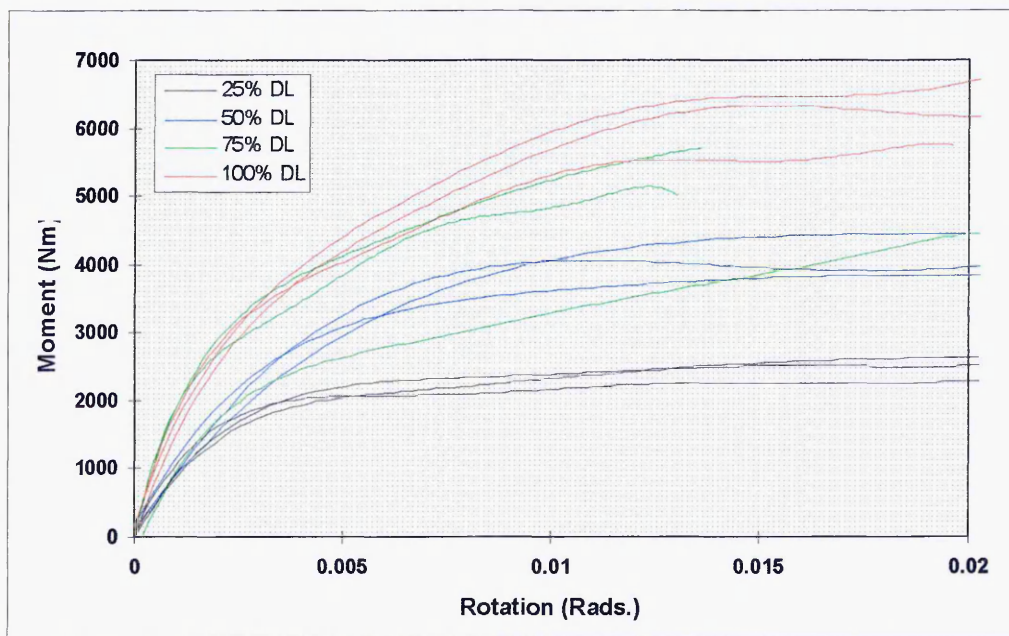


Fig. 4.22. HD30 upright with a standard aisle baseplate

It is clear from the graph above that there is a degree of inconsistency, particularly with regard to tests at 75% of design load. In this case, the statistical treatment outlined in Table 4.7. will have a marked effect on the value of the design moment used. This characterisation reduced the design moment at 75% of upright design load below the value for a 50% design load. The design values outlined in Table 4.8. demonstrate that despite a linear increase in the column design loads, the resultant design moments do not reflect a corresponding proportionality. This can be attributed, at least in part, to the way

in which the statistical treatment of experimental data is designed to influence the results (see 4.10.2.).

Column design load (kN)	Design moment (Nm)
28.2 (25%)	1673
56.4 (50%)	3135
84.7 (75%)	2483
112.8 (100%)	4498

Table 4.8. Design moment summary for HD30 upright with a standard aisle baseplate.

N.B. the design moment was characterised for each axial load case, using the formulae outlined in section 4.3.3. of this document.

The graph in Fig. 4.23. illustrates the moment-rotation characteristics of a standard baseplate on an HD30 upright. A single stiffness was assumed for this combination and incorporated together with the design moments taken from table 4.8. This graph represents the form in which all the results were presented for design, from this test series.

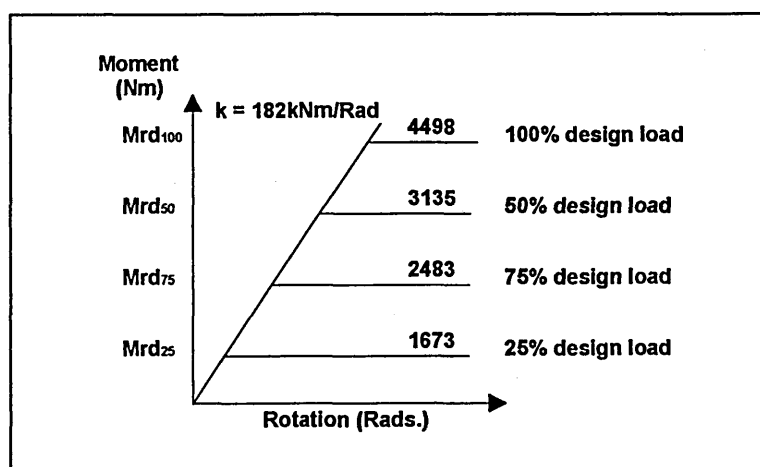


Fig. 4.23. Design moments and stiffness derived for HD30 upright with a standard aisle baseplate.

Clearly the most appropriate solution to the difficulty of a reversal in design moment results would be to perform additional tests in order to ensure as far as possible, that a 'more representative' set of characteristic results could be derived. As an intermediate although not entirely ideal first step however, interpolation was used as a method by which to develop more sensible, initial values of design moment. A summary of these preliminary results for each upright/baseplate combination is contained below in table 4.9. Any interpolated results have been placed within parentheses.

Upright	Baseplate design									
	Standard aisle					Narrow aisle				
	Stiffness (kNm/Rad)	Design moment values at axial load (Nm)				Stiffness (kNm/Rad)	Design moment values at axial load (Nm)			
25%		50%	75%	100%	25%		50%	75%	100%	
SD17	126	447	897	1375	(1375)	161	1824	(1837)	1851	2353
HD30	182	1673	3135	(3816)	4498	194	(2847)	2847	4143	5457
HD30T	182	2631	2829	5896	(5896)	331	3461	4188	4969	(4969)

Table 4.9. Summary of preliminary design moments and stiffness' for tested floor connector/upright combinations at variable axial loads.

It is apparent from these results that the use of narrow aisle rather than standard aisle baseplates, has the effect of increasing the stiffness of the joint interface between the racking system and the floor. This is clearly the case regardless of the type of upright used, and taken together with the general (although not total) increase in design moment values from standard to narrow aisle, gives an indication that small changes in component design in critical areas of the rack, may have a significant influence over the load capacity of a typical system.

Chapter 5

The Determination of Beam End Connector Characteristics through Experimentation

5.1. General Outline

The beam end connector performance is integral to the overall stability of the rack. The semi-rigid nature of the 'joint' in conjunction with the relevant beam and upright, must be considered in some detail so that an accurate model can be constructed of any given racking system. The influence of down-aisle lateral deflection (sway) and associated P- Δ effects (see chapter 6), attributable mainly to the behaviour of the connector in conjunction with the upright, are central to determining the load capacity of the rack. This chapter examines connector performance through a series of five tests, and characterises its' behaviour for each beam and upright combination available. The tests outlined below were exhaustive for the product range supplied:

1. Bending test on beam end connector
2. Looseness test on beam end connector
3. Shear tests on beam end connector
4. Shear tests on beam end connector locks
5. Bending test on beams

5.2. Bending Tests on Beam End Connectors

5.2.1. Introduction

The purpose of this test is to “determine the stiffness and the bending strength of the beam end connector” (FEM-CI.5.5.1) in combination with each beam and upright section in the product range. “The structural behaviour of the upright and beam end connector assembly is critical to the behaviour of the [overall] structure” and as a result the following factors were considered during this series of tests :

- Upright type/thickness (7)
- Beam type (9)
- Connector type (left/right hand only)

Other factors specified in the code that do not feature in this test series, either because they are not covered by the product range or because they are used relatively infrequently include :

- down-welded beams on connectors
- variations in the method of connecting the beam to the connector

5.2.2. Test Arrangement

A total of 676 tests were performed to assess the bending properties of each combination of upright, beam and connector. Each beam was 600mm long and attached to the upright using left or right handed connectors. During testing the load was applied through a Schenck hydraulic actuator, positioned at a distance 400mm from the face of the upright. It had a displacement of ± 50 mm and a load capacity of ± 100 KN. In addition, it was rigidly fixed at the top and a 25mm diameter steel roller was positioned at the point of application of load. A lateral restraint approximately 550mm from the face of the upright was also used to guarantee that each beam remained in position (see Fig. 5.1.).

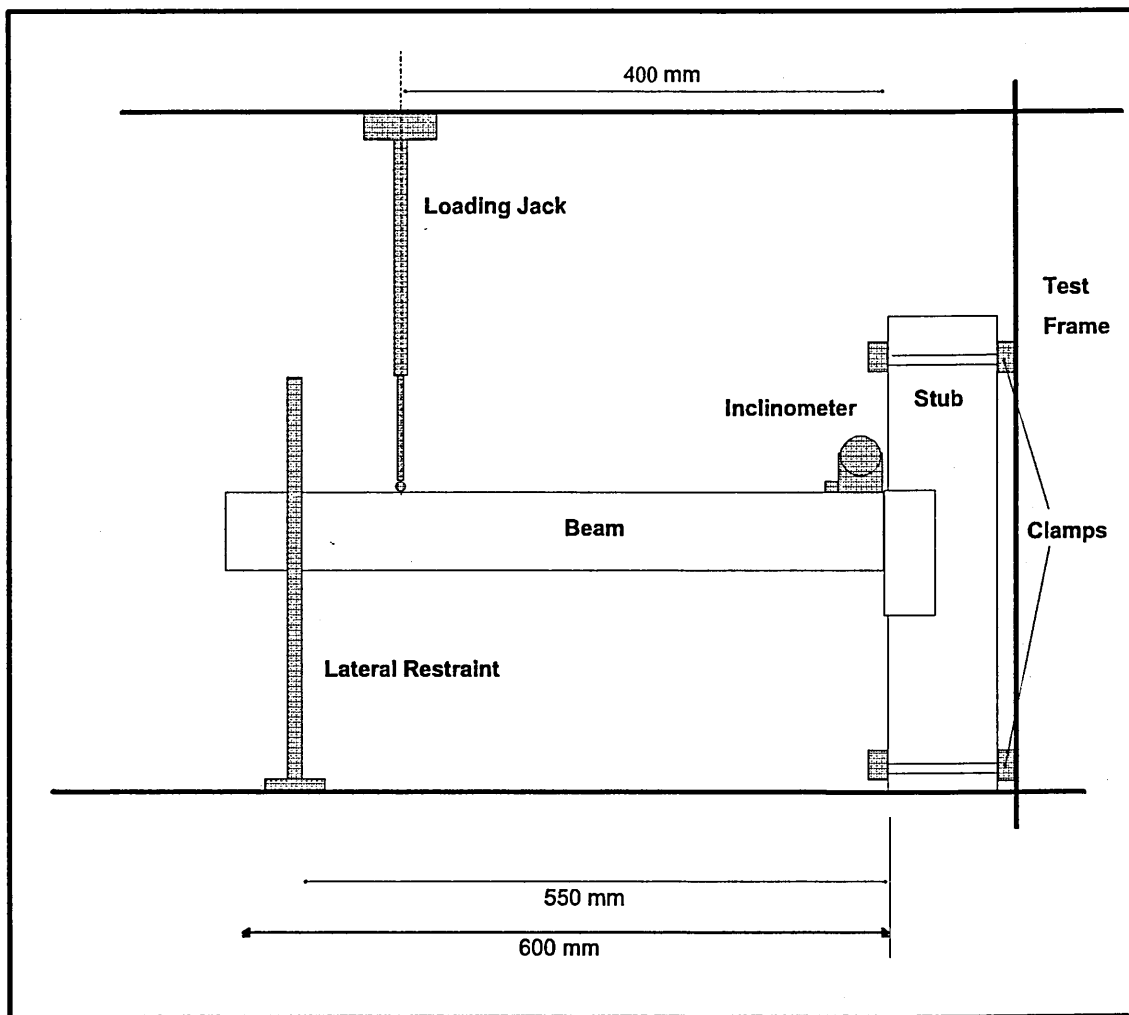


Fig. 5.1. Beam end connector bending test - set up

The upright samples were cut to lengths of 521mm, and clamped “rigidly to a relatively infinitely stiff testing frame” (FEM-CI.5.7.2.) at two points with an appropriate distance between :

- SD $\Rightarrow h_c > 213.5 + 2 \times 50.8 = 315.1\text{mm}$
- HD $\Rightarrow h_c > 213.5 + 2 \times 65.0 = 343.5\text{mm}$

(h_c = the distance between clamps over which there is no contact during the test between upright and testing frame.)

To prevent local crushing due to the clamping action, anti-crush devices were designed to fit inside each type of upright section (see Plate 5.1.). These devices were installed in such a way that during testing the contact length (h_c) was maintained internally.

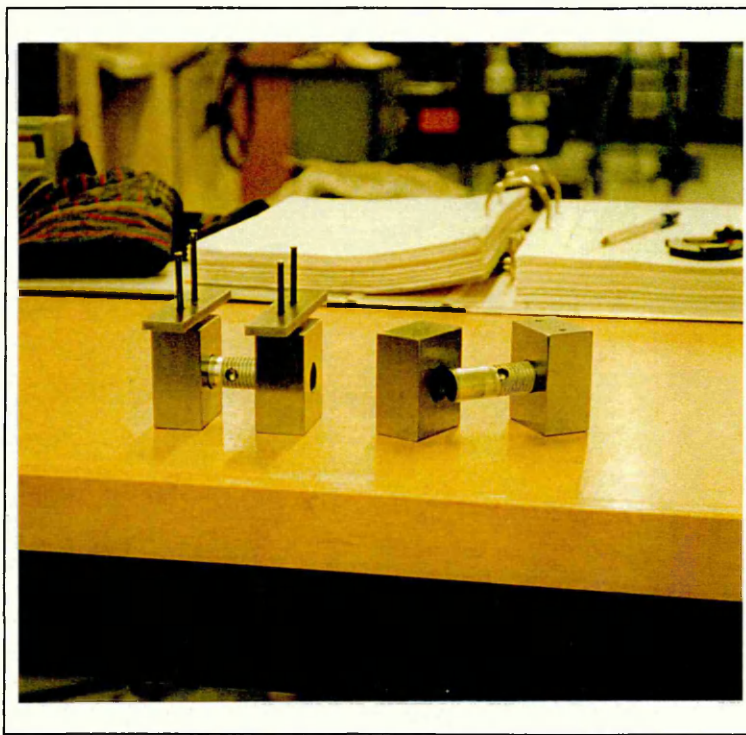


Plate 5.1. Anti-crush devices

5.2.3. Instrumentation

A waveform generator was used to control the rate of displacement with a setting of 333secs/cycle (0.6mm/sec). In addition, the rotation of the beam was monitored using an ES256 - 45° inclinometer. It read to $\pm 45^\circ$ with a tolerance of ± 30 secs. The instrument was attached to the beam in a V-clamp with bar magnets holding the base to prevent movement or slipping (see Plate 5.1.). Checks were made using slip gauges to ascertain the accuracy of the device, and to ensure that the magnets had no undue influence over the test readings.

5.2.4. Data Acquisition

The outputs for load, rotation and displacement were collected on three channels of a Gould (2608 - 20Ms/sec) isolating digital recording oscilloscope in time steps of 0.1 secs, and transferred to PC using Gould's "Transition", data transfer and acquisition program. Plate 5.2. shows the apparatus described above in use on the test rig.

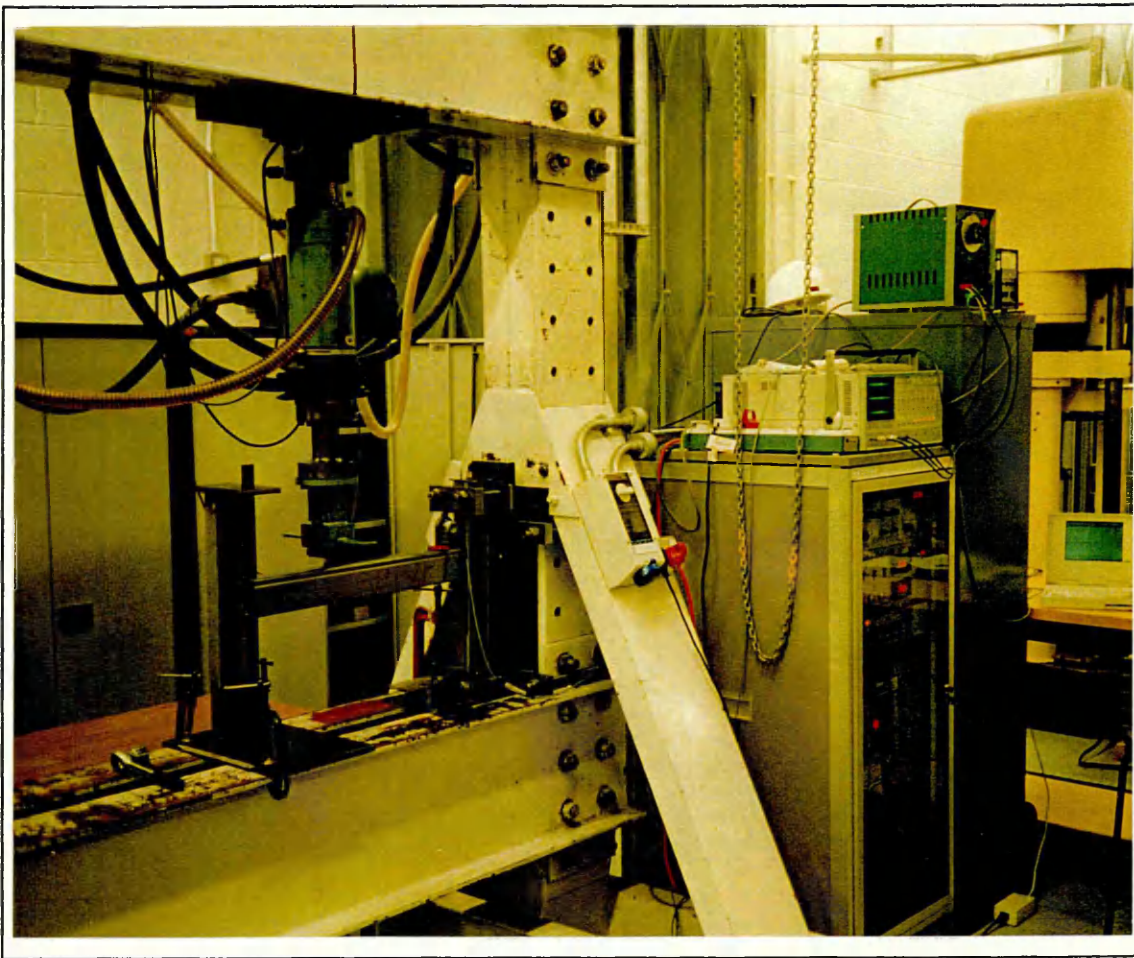


Plate 5.2. Beam end connector bending test - set up

5.2.5. Discussion

In general, failure of samples under bending was characterised by plastic deformation of the connector immediately below the compression flange of the beam. This is demonstrated by plate 5.3. which shows the final stages of a test conducted on a 95(1.6) box beam and SD25 upright.

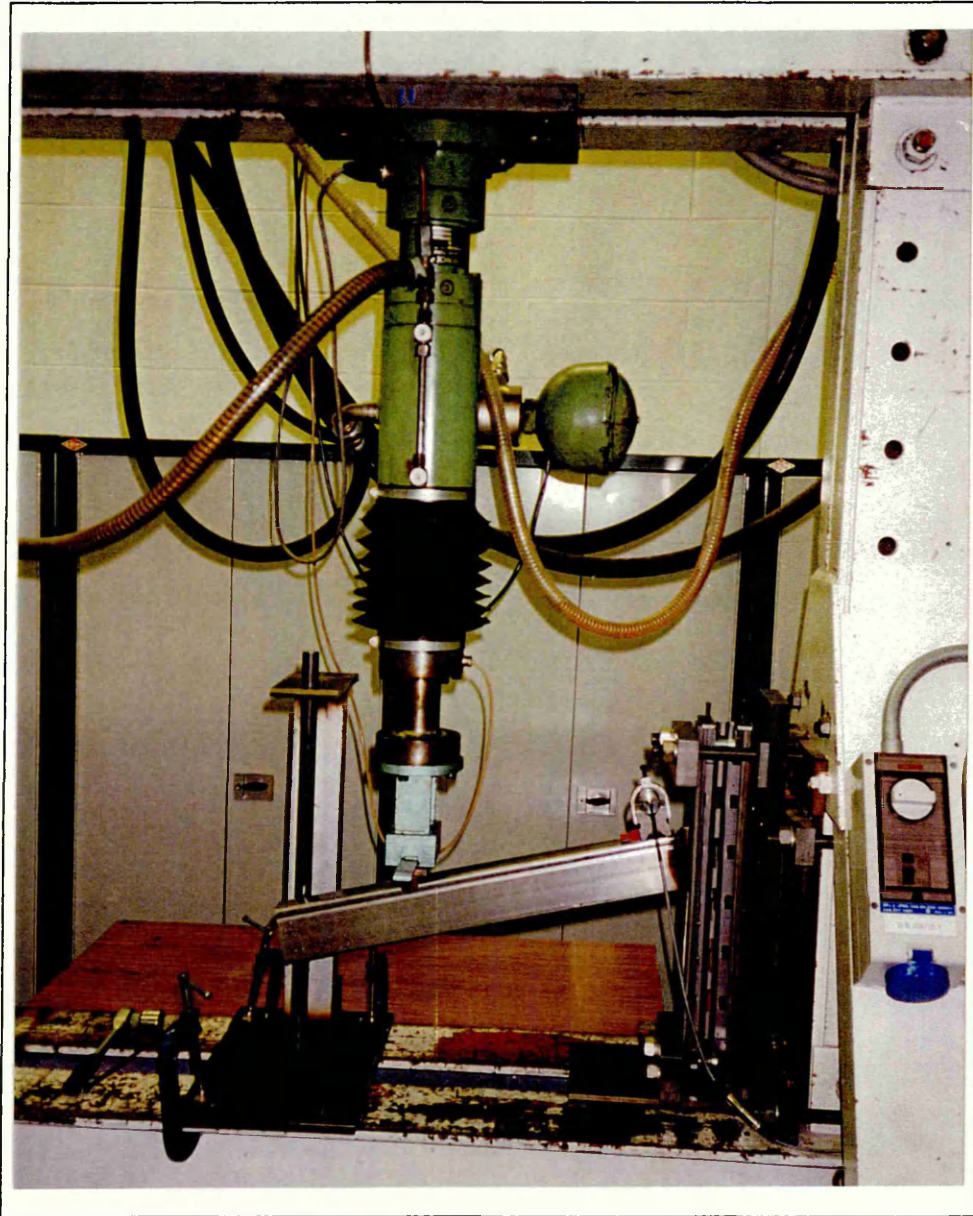


Plate 5.3. Beam end connector bending test in progress

It is clear that yielding of the connector has occurred directly below the bottom of the beam, failure behaviour which was common to the vast majority of sections tested. Additional to this yielding, was an associated widening of the gap between the top of the

connector and the upright sample. Typically, this was accompanied by the shearing off of the top connector 'locating' lug as it moved against the vertical edges of the rectangular web openings in the upright. Significant plastic bending was also experienced in the upper 'load bearing' lug and the effect on the connector is evident from plate 5.4.

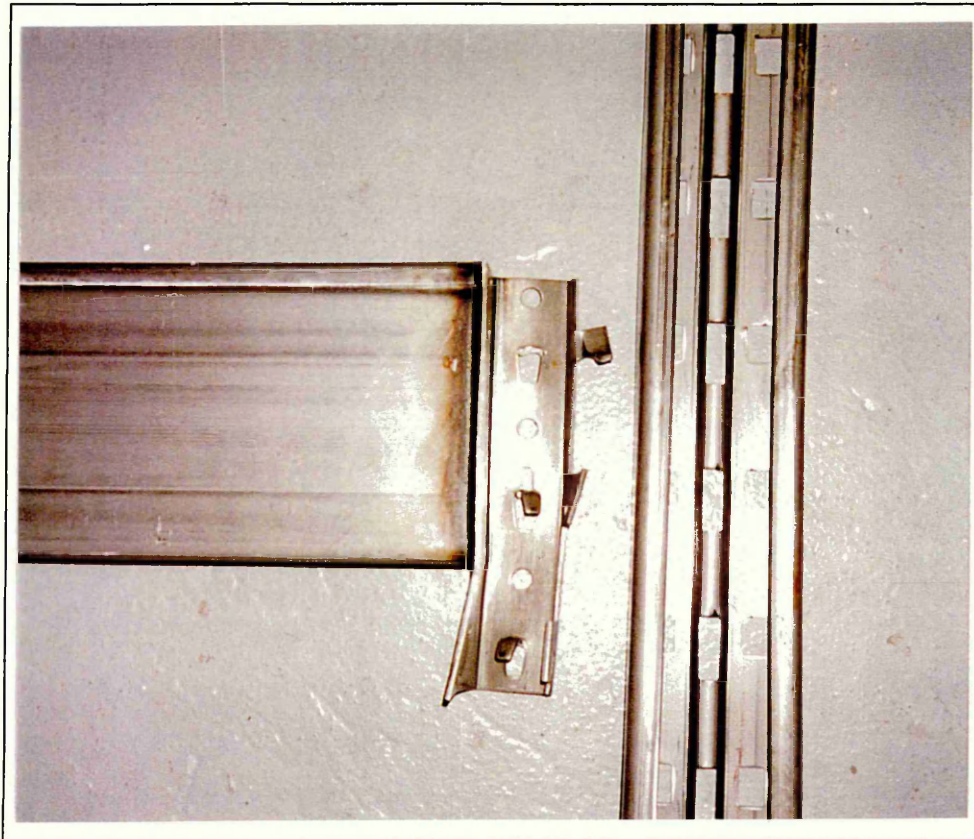


Plate 5.4. Damage to a connector on a 145 box beam

It is apparent from plate 5.4. that the middle and lower locating lugs also experience partial shear failure. In addition, the central load bearing lug has been subjected to a degree of plastic yielding which may have been exacerbated by continuing the test over an extended stroke.

Generally, beam depth was the governing factor in the behaviour of the 'system' to failure. An attempt has been made therefore, to categorise this behaviour within the context of the above discussion, into three distinct groups based on the depth of beam

being tested. It is believed that these groups most accurately reflect the variations in failure mode encountered during testing. They are as follows :

- Failure in tests using 145-110 box beams
- Failure in tests using 110-80(1.6) box beams
- Failure in tests using 80(1.6) and open section beams

145-110 box beams

Typically the mode of failure for this group of beams is defined by the image in Plate 5.4. This was the case when testing with all upright sections, although as the gauge of the upright material decreased, significantly more distortion of the upright web openings was apparent. Horizontal indentations caused as the locating lug sheared off, were particularly extensive in SD17 samples. The middle lug was also prone to shearing although this occurred more infrequently, and usually with 145 box beams.

110 - 80(1.6) box beams

The reduction in the depth of the beam to 110mm, generally resulted in a lessening of plastic deformation for the lower load bearing lugs, and a similar diminution of shear indentations caused by the locating lugs. This was particularly true as the beam depth reduced below 110mm, corresponding to the beam compression flange being roughly in line (or above) the central connector lugs. However, in all other ways the method of failure was consistent with the the 145-110 group of box beams as detailed above.

80(1.6) box and open section beams

The failure characteristics outlined so far in this discussion were not always appropriate, particularly with regard to the open section and a number of 80(1.6) box beams. In these cases, although plastic yielding of the connector below the compression flange still occurred, the effect on the connector lugs was extremely limited. As a consequence, high stresses were placed on the welds between beam and connector. This was particularly

true for the front face weld, which was held rigidly in place by the wrap-around nature of the connector design. In many cases, the weld proved unable to resist the moments place upon it and failed (see Plate 5.5.).

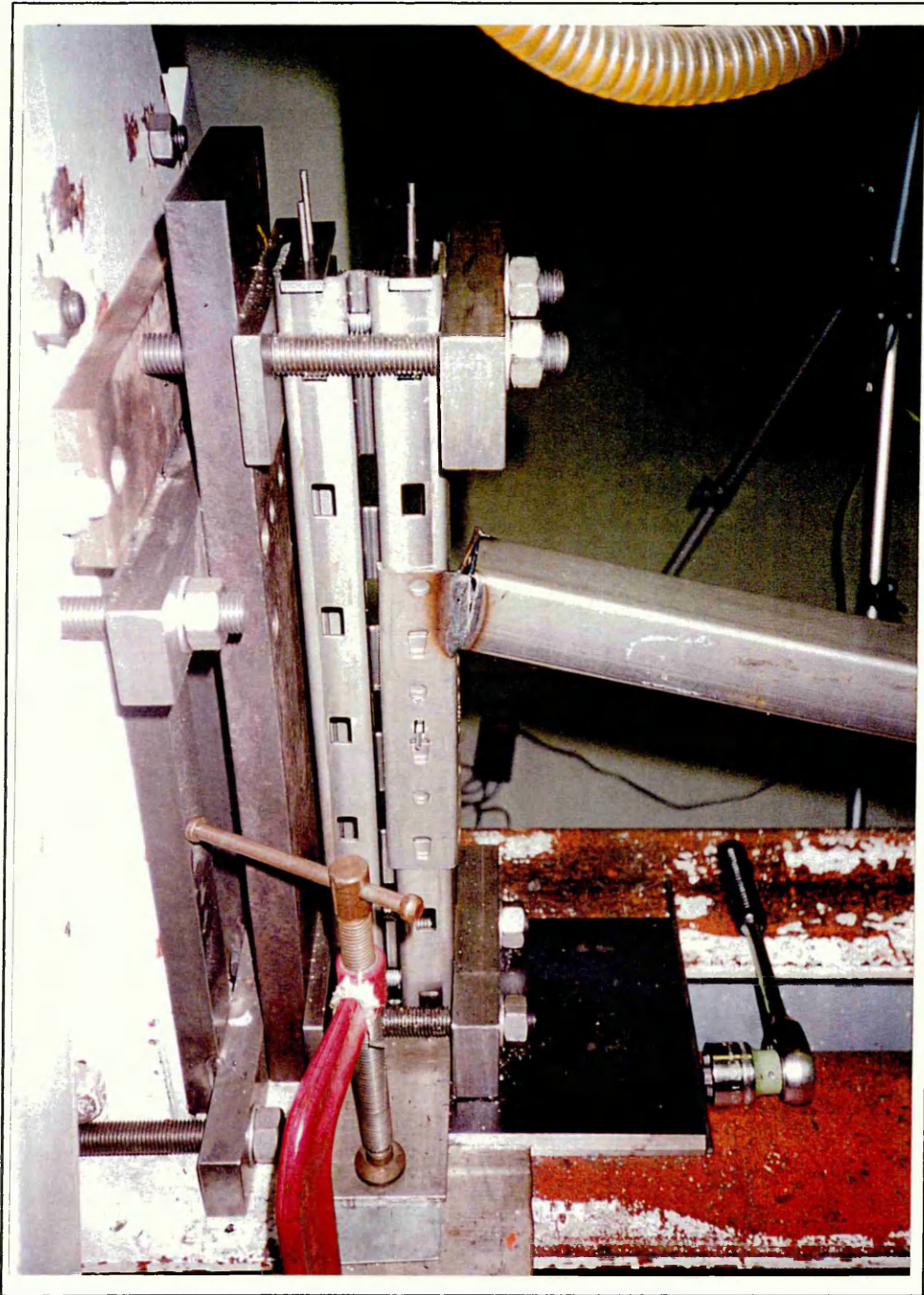


Plate 5.5. Weld failure of 50 open section beam with SD17 upright

5.3. Results and Analysis

5.3.1. Introduction

The moment-rotation behaviour of an individual test regardless of the type of beam, upright or connector used, described a characteristic parabolic curve. A 4th order polynomial fit using least squares regression analysis was then completed on this curve to derive an expression upon which the remainder of the analysis could then be performed.

5.3.2. Material and geometric corrections

Although information on the yield stress and thickness of each component tested was available there is currently no requirement within the FEM code for corrections of this sort to be performed. Engineers should instead be satisfied that these values are “acceptably close to the nominal values before results shall be accepted”.

5.3.3. The relationship between the design moment and stiffness

The implication of this is that since during analysis of the results the failure moment is not reduced, as would be the case if these corrections were implemented, the engineer is given a greater degree of control over the crucial relationship between the design values of moment and connector stiffness. Due to the nature of the curve described above and shown in Fig. 5.2. overleaf, reducing the design moment below the maximum value found by testing (a purely arbitrary decision, see Cl.5.5.4.) will increase the design stiffness of the connector. Global analyses of a racking system using these variations on the test results may have the effect of increasing the load capacity of such a system. However, if the balance between design moment and stiffness is too favourable to one at the expense of the other, there is a risk that the system will under-perform and the capacity may be significantly reduced. Obviously, the use of a multi-linear curve to describe the behaviour of the connector would be the preferred solution to this problem

and is permitted by the code. This would be done by considering an ‘average’ curve based on all the experimental data obtained for a given combination of connector and upright. However, at present the software available to process this type of information is only capable of dealing with a bi-linear curve, and so finding a solution to this problem has been discussed in some detail here, and in subsequent chapters.

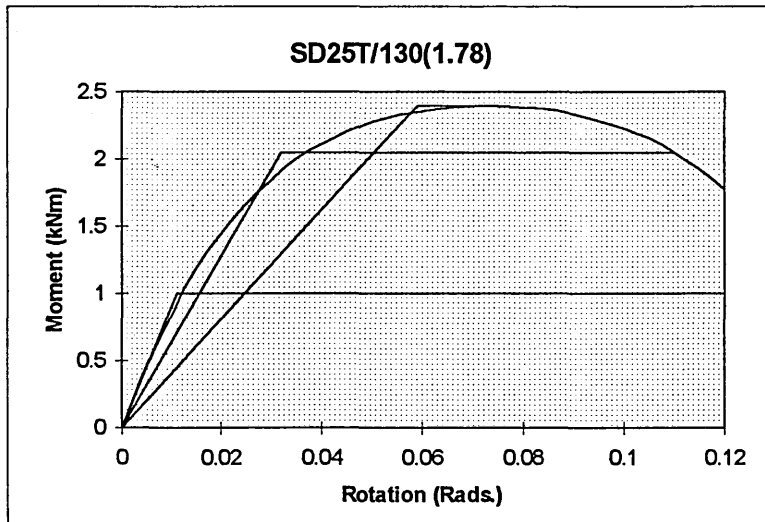


Fig. 5.2. Variations in stiffness in a typical experimental data set, with reducing values of design moment.

Fig. 5.2. above demonstrates the effect of reducing the value of the design moment on the stiffness of the beam end connector/upright combination specified (in this case SD25T and 130(1.78)). The effect on the connector stiffness of varying the design moment is highlighted in table 5.1. Clearly, the final choice for the value of the design moment could have significant implications for the load capacity of the rack and as a consequence must be chosen with some care :

Stiffness values calculated using :	Moment (kNm)	% decrease of moment from (1)	Stiffness (kNm/Rad)	% increase of stiffness from (1)
(1) Failure moment of test	2.39	-	40.51	-
(2) Design moment of test series	2.05	14.2	64.03	58.1
(3) Arbitrary moment chosen to amplify design stiffness	1.00	58.2	87.83	116.8

Table 5.1. Effect of changes in moment on values of stiffness

Table 5.1. demonstrates for a single test, how changes in the value of the moment selected can make a significant difference to the resultant value of stiffness. It is clear that this effect is most evident when the ‘maximum’ design moment is close to the apex of the curve. In such cases, small reductions in the value of the design moment (in Table 5.1. -14.2 %) have an amplified effect on the value of stiffness (increasing by 58.1 %), due to the reduced gradient of the curve at this point. Where the gradient of the curve is greater, the impact of variations in the design moment has a less significant effect on the associated values of stiffness.

5.3.4. Calculation of beam end connector design moment

The test failure moment (M_{ni}) was taken from each experimental curve for a given beam/upright combination. These values were recorded for both the left and right hand connector and a mean ($M_{m/r}$) was taken :

$$M_{m/r} = \frac{1}{n} \sum_1^n M_{ni} \quad (5.1.)$$

Since the statistical treatment of FEM results allows a more favourable characterisation as the number of tests performed increases, left and right hand connector results were grouped together if the following formulae were satisfied :

$$0.9 \leq \frac{M_{ml}}{\left(\frac{M_{ml} + M_{mr}}{2}\right)} \leq 1.1 \quad 0.9 \leq \frac{M_{mr}}{\left(\frac{M_{ml} + M_{mr}}{2}\right)} \leq 1.1 \quad (5.2.)$$

The provisions set out in these equations are no longer a requirement of the code, but have been retained as a guide to establish a single value for either connector type with a given beam/upright combination. If both connectors pass the check (which happened in the majority of cases) the characteristic failure moment is calculated in accordance with equation 4.4, using a confidence level factor (k_s) of 2.10 ($n = 10$). If the connectors fail

the check, a conservative approach is adopted and the lowest mean failure moment is used to determine both connectors characteristic failure moment (M_k) with a confidence level factor (k_s) of 2.46 ($n = 5$).

The design moment for the connector (M_{Rd}) is then given by the formula :

$$M_{Rd} \leq \frac{M_k}{\gamma_m} \quad (5.3.)$$

where γ_m is the material safety factor for the connector, taken as 1.1 (see FEM, Table 2.3). Maximum values of M_{Rd} developed using the formulae above show a strong relationship between increasing beam depth and a rise in the maximum design moment (see Fig. 5.2.). The use of higher yield (tenform) steel and heavier duty uprights also improve the overall connector performance, although this effect is less significant, particularly at lower beam depths.

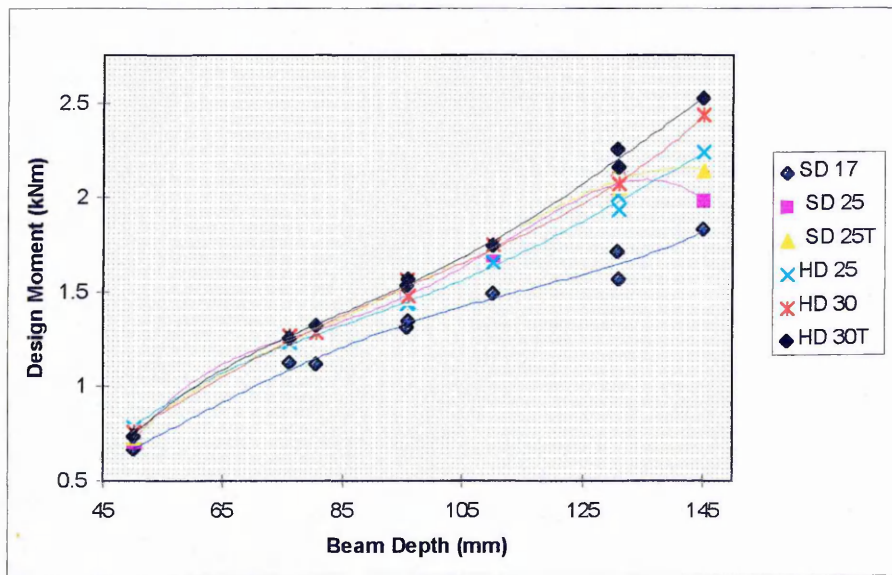


Fig. 5.3. Variations in design moment with increasing beam depth for specified uprights

5.3.5. Calculation of beam end connector design stiffness

The beam stiffness was initially based on the maximum design moment. In subsequent chapters an investigation has been undertaken into ways of varying these two values to

achieve an optimal solution and thereby maximize the load carrying capacity of the rack. The experimental test stiffness' were based on an equal area calculation, with the gradient of the stiffness line passing within 15% of the curve rotation at the design moment (see Fig. 5.4). The method used to calculate the positioning of this gradient is lengthy and has therefore been included within Appendix C.

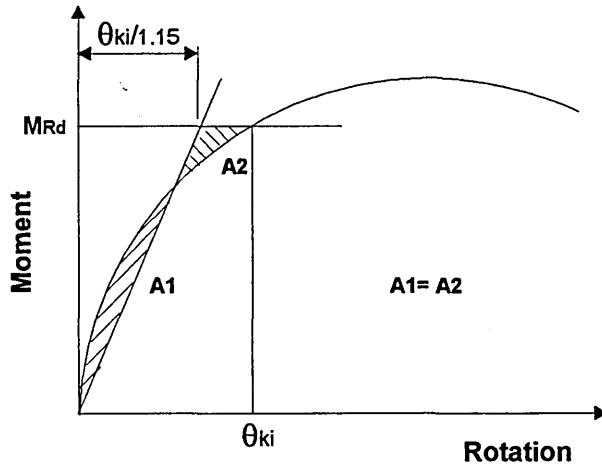


Fig. 5.4. Equal area method of calculating an individual test stiffness.

The design stiffness (k_d) was taken to be the mean stiffness value for a group of tests using a specified upright/beam combination :

$$k_d = \frac{1}{n} \sum_1^n k_{ai} \quad (5.4.)$$

A graph has been produced overleaf (Fig. 5.5.) summarizing the values of design stiffness in relation to beam depth for each upright. The stiffness values in general are only marginally effected by variations in the duty of the upright, the thickness of the cross section or by the yield stress of the upright material. The only exception to this is the SD17 upright (1.7 mm thick) which has a significantly lower performance in terms of stiffness than uprights of 2.5mm and 3mm thickness. This is particularly apparent for beams between 95mm and 145mm in depth. It is possible therefore that a threshold exists

somewhere between 1.7mm and 2.5mm thick, below which the shearing action of the connector lugs moving laterally against the upright has a much more significant impact on the upright itself. This is borne out by notable residual damage found on SD17 uprights following testing. As beam depth increases, higher moments can be applied to the connector and consequently the disparity of performance is amplified (the gap between 1.7 mm and 2.5/3 mm uprights increases).

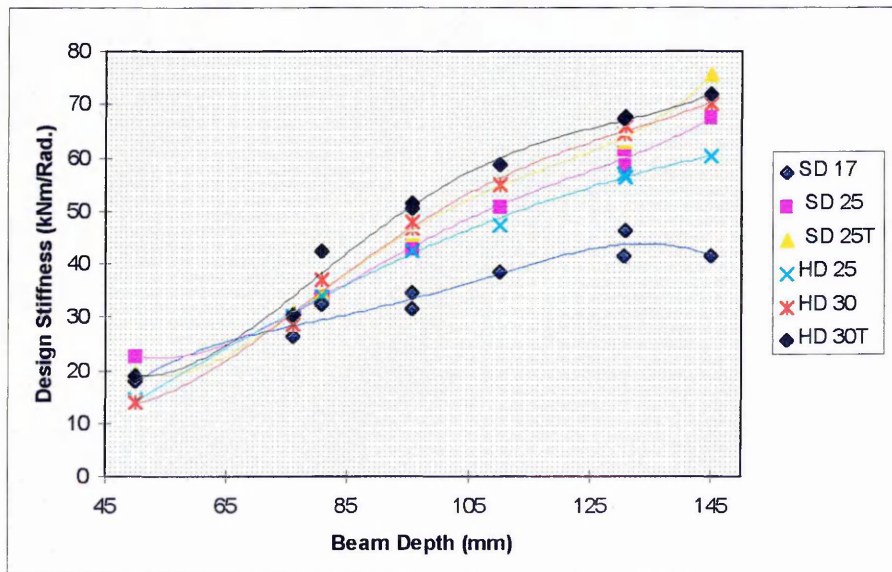


Fig. 5.5. Variations in design stiffness with increasing beam depth for specified uprights.

It should be noted here that, if advantages could be accrued from developing beams of depths not currently manufactured, the near-linear nature of the results for design stiffness and moment would allow interpolation to be performed with a reasonable degree of certainty, and without the need for any more than one or two confirmatory tests.

5.4. Looseness Test on Beam End Connectors

5.4.1. Introduction

A racking structure is characterised by its semi-rigid joints forming connections between beam and upright (as well as upright and floor). As discussed previously the performance of these joints is amongst the factors which dominate the structures design.

Design problems can be exacerbated by the requirement as in 10.2.02, for the inclusion of initial sway imperfections which can manifest themselves as “a closed system of horizontal forces ...” “...proportional to the factored vertical loads at [each beam] level” (FEM-C1.2.5.1).

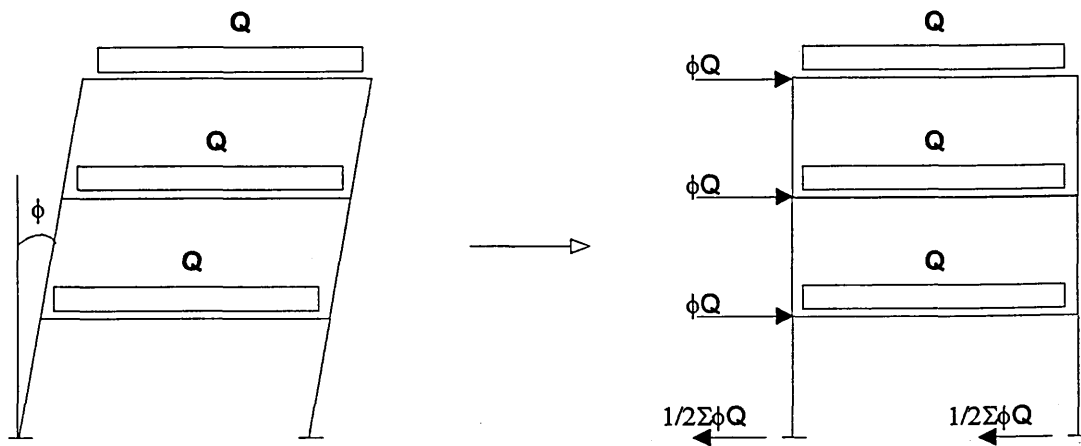


Fig. 5.6 The impact of sway imperfections on design

Clearly, by limiting sway imperfections on a racking system, advantages will accrue in terms of capacity. Since the magnitude of looseness in the beam end connector has a direct bearing on the size of the sway imperfection (see eq. 5.5), it is of the utmost importance that looseness values are small enough to minimise the effect on design, while being large enough to account for manufacturing tolerances and allow ease of construction. The importance of looseness on the stability of a given racking system can be best demonstrated by examining the sway imperfection formula below:

$$\phi = \left[\sqrt{\left(\frac{1}{2} + \frac{1}{n_c}\right)} \cdot \sqrt{\left(\frac{1}{5} + \frac{1}{n_s}\right)} \right] \cdot (2\phi_s + \phi_l) \quad (5.5.)$$

- n_c = number of uprights in the down aisle direction or connected frames in the cross aisle direction
- n_s = number of beams
- ϕ_s = maximum specified out of plumb divided by the height
- ϕ_l = looseness of beam-upright connector determined by test

It is clear that because n_c and n_s are geometry dependent and ϕ_s is effectively a manufacturing tolerance, variations in looseness could have a dramatic impact on the value of ϕ . Obviously a higher looseness value would allow proportionately greater sway in the rack, effectively reducing its capacity.

The purpose of this test is to obtain a value of looseness for the connection ϕ_{li} , for use in the system analysis. As with the shear tests on beam end connector locks, it was considered appropriate for an assessment to be made using beams and uprights from the extremities of the product range. This methodology was expected to provide the most conservative values for looseness while limiting the number of necessary tests. As a result, the combinations of beam and upright type used during testing were restricted to the following :

- HD30 x 145 b/b (left/right hand connector)
- HD30 x 50 o/s (left/right hand connector)
- SD17 x 145 b/b (left/right hand connector)
- SF17 x 50 o/s (left/right hand connector)

This allowed the largest and smallest sections in the standard product range to be combined together in order to identify a maximum value for connector looseness.

and below each beam sample, allowing positive and negative moments to be applied. The rate of displacement was controlled manually.

The rotation of the beam was monitored using an ES256 - 45° inclinometer. It read to $\pm 45^\circ$ with a tolerance of ± 30 secs. The instrument was attached to the beam in a V-clamp with bar magnets holding the base to prevent movement or slipping (see Plate 5.6.). Checks were made using slip gauges to ascertain the accuracy of the device, and to ensure that the magnets had no undue influence over the test readings.

5.4.3. Test Measurements

The load was applied incrementally and read directly off a monitor on the actuator control panel. The rotation was measured as a voltage, and was fed through a Gould (2608-20Ms/sec) Isolating Digital Recording Oscilloscope to a Solartron 7045 digital multimeter reading to 1/10000V for accurate rotation measurement. Plate 5.6. shows the apparatus described above in use on the test rig.

5.4.2. Test Arrangement

A total of 40 tests were undertaken to assess the characteristic looseness of the connector. The tests were performed on a modified version of the beam end connector bending test rig (see Fig. 5.7.) :

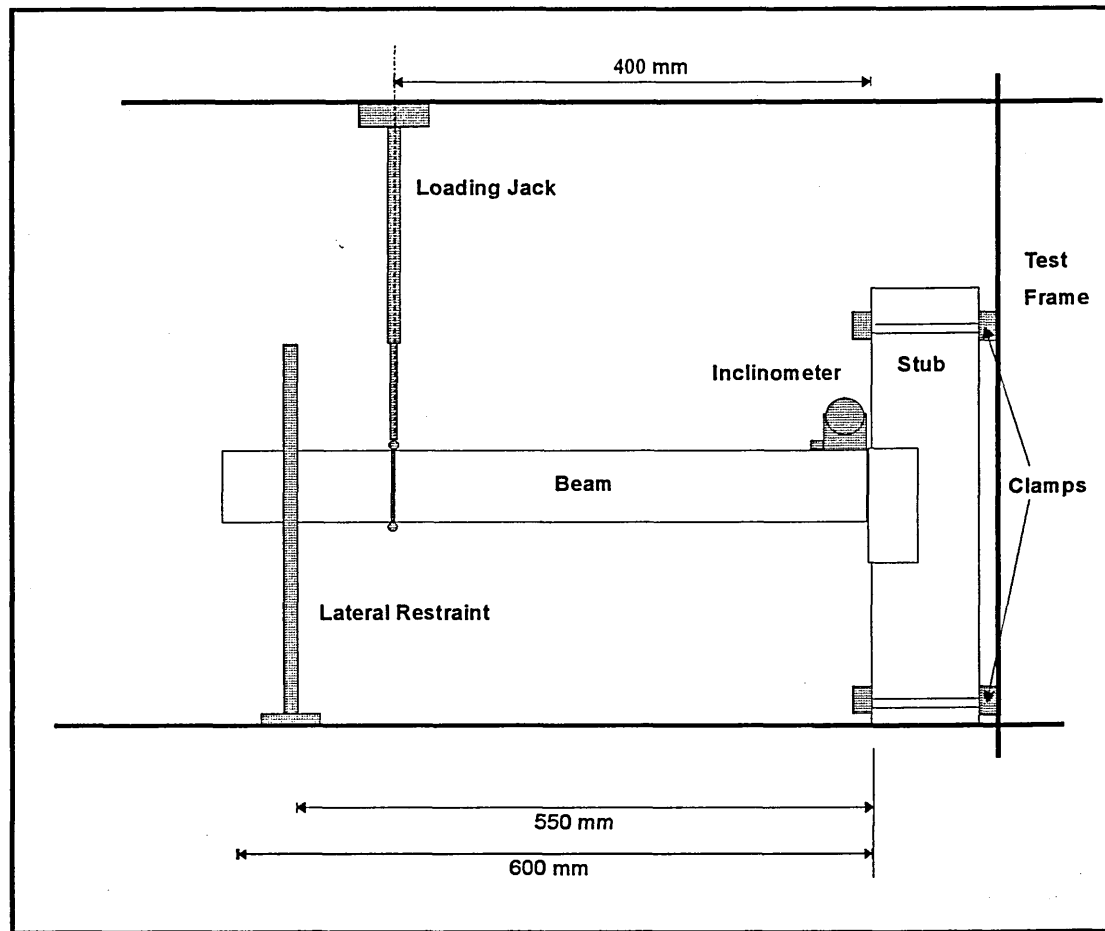


Fig. 5.7. Looseness test on beam end connectors - test rig

The upright samples were clamped “ rigidly to a relatively infinitely stiff testing frame.” Each beam was 600mm long and attached to the uprights using left or right handed connectors. During testing the load was applied through a Schenck hydraulic actuator, positioned at a distance 400mm from the face of the upright. It had a displacement of ± 50 mm and a load capacity of ± 16 KN. In addition, it was rigidly fixed at the top and a 25mm diameter steel roller was positioned at the point of application of load, both above

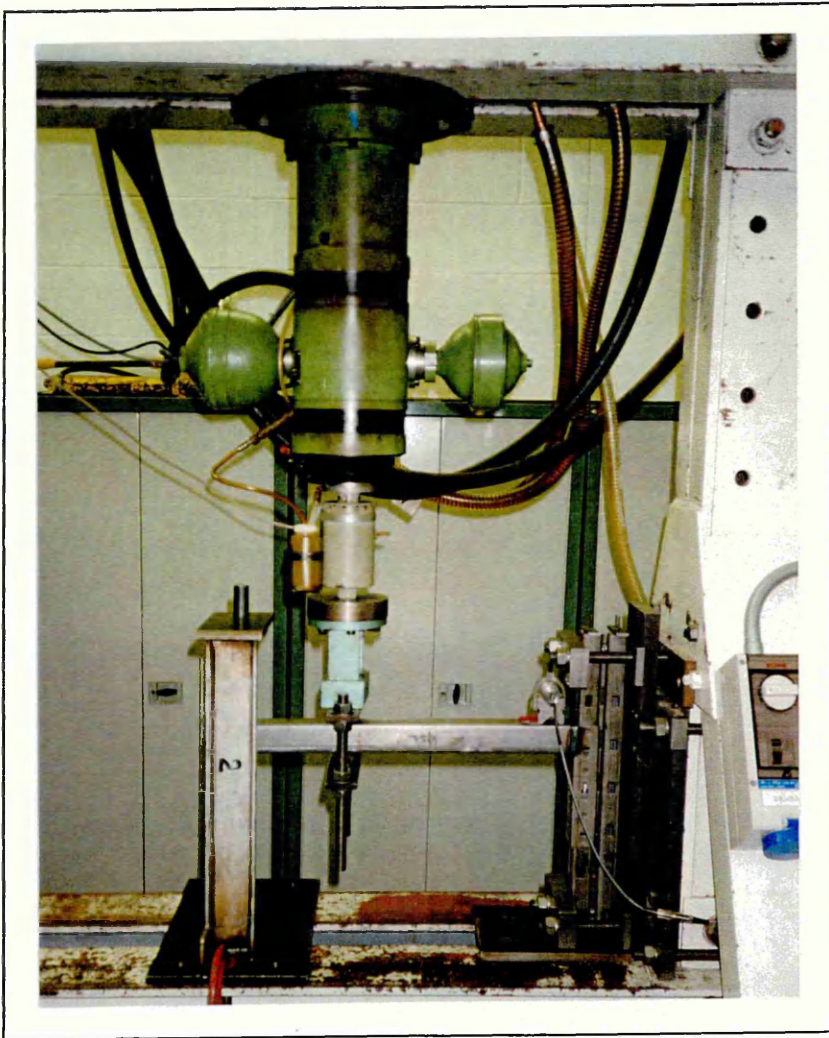


Plate 5.6. Looseness Test on 50 O/S beam with SD17 upright

5.5. Results and analysis

5.5.1. Calculation of design looseness

Test looseness values were taken to be 50% of the rotation of the connector about the upright, as demonstrated by the measurement in Fig. 5.8., while the design value of looseness was taken to be the mean value from the tests performed.

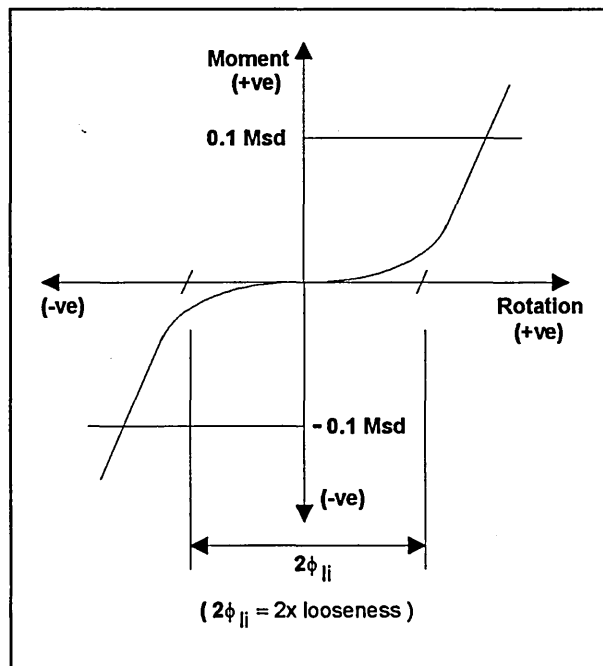


Fig. 5.8. Idealised value for looseness based on FEM generalised interpretation of connector behaviour

The plot above is, as you would expect from a design code, an idealised representation of connector performance for a generalised case. For the connectors tested here however, the curve was offset (see Fig. 5.9.), indicating little or no positive (downward) looseness. Assuming this is an 'accurate' representation of the performance of the connector in practice, then the sway in the rack could justifiably be based only on the positive amount of looseness measured, and would equate approximately to zero. This is the case because for any rack, the lateral deflection is dependent on the minimum

angle (either positive or negative) through which the connector can rotate before moments can effectively be resisted.

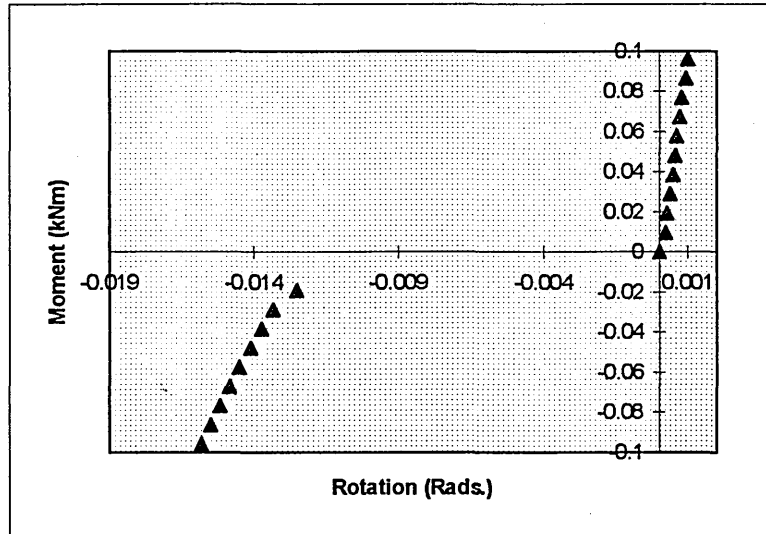


Fig. 5.9. Typical experimental connector looseness (zero positive rotation)

Intuitively however, it is clear that the beam will tend to begin any test at a slight downward angle, and there is therefore a natural tendency for the results to be offset in the way shown. For this reason, the inclination of the engineer to use this lower value of looseness should be resisted. It should also be noted here that, if the curve in Fig. 5.9. was a true representation of the connector's behaviour, then inherent complications arise in modeling beams with non-symmetric connector performance, unless this behaviour is modeled using a multi-linear curve.

Design values of looseness have been summarised in Table 5.2.. Values for beam end connectors with 2.5mm thick uprights have been interpolated from results on 1.7mm and 3.0mm uprights.

	Upright Thickness (mm)		
	1.7	2.5	3.0
Looseness (Rads.)	0.00684	0.00528	0.00431

Table 5.2. Summary of beam end connector looseness against upright thickness

5.5.2. Discussion

Looseness is particularly critical for the design of this type of racking system, and its effect on load capacity has been examined in greater depth in Chapter 7. Two methods of testing were available under the code. Firstly, the cantilever test which was used here to measure values of looseness only, or secondly a portal test which measured bending strength, stiffness and looseness as a single curve and is explored below.

The portal test necessitated the use of an 'average' moment-rotation curve which could be approximated using a multi-linear fit (see FEM Fig. 5.5.4.1/2.). This test was considered to be overly complex to perform and, as discussed previously, the resultant multi-linear curve could not be handled by the software being employed.

The anticipated advantage of this method of testing was that, while the interaction between frames and beams would give similar failure moments and a possible marginal reduction in stiffness when compared with the cantilever test, a much reduced value of looseness would be forthcoming, due to the 'interplay' inherent within a system of connectors. A realistic and desirable 'system value', rather than an overly conservative 'individual value' based on a single connector, would be the result.

It was considered that in order to harness this improved value of looseness it might be possible to use the cantilever test to find values for bending strength and stiffness, and the portal test merely to determine a value for looseness. This solution could not be implemented however, because the values of stiffness calculated using the cantilever test did not allow for looseness. During testing the beam dropped through a small angle due to gravity, thereby eliminating looseness from the test results. If testing could have been performed with the beam perfectly horizontal and at a right angle to the upright, then stiffness may have been measured with an inherent looseness value, although an equal

area calculation could not have been performed and the results could as before, only have been defined using a multi-linear curve.

5.6. Shear Tests on Beam End Connectors

5.6.1. Introduction

The purpose of this test is to assess the shear strength of the beam end connector in combination with each beam and upright section in the product range. The following factors were considered during this series of tests :

- Upright type/thickness (7)
- Beam type (9)
- Connector type (left/right hand only)

5.6.2. Test Arrangement

A total of 555 tests were performed to assess the shear strength of each combination of upright, beam and connector. The upright samples were clamped “rigidly to a relatively infinitely stiff testing frame” (FEM-CI.5.7.2) at two points with an appropriate distance between (see Fig. 5.10). Each beam was 600mm long and attached to the uprights using left or right handed connectors. The screw jack was positioned beneath the beam at a distance of 400mm from the face of the upright.

During testing the load was applied using a Schenck hydraulic actuator, acting at a distance ‘b’ from the upright. In practice this equated to between 76mm and 100mm. It had a displacement of ± 50 mm and a load capacity of ± 100 KN. It was rigidly fixed at the top, and a 25mm diameter steel roller was positioned at the point of application of load. In addition, a test Waveform Generator was used to control the rate of displacement with a setting of 333secs/cycle (0.6mm/sec).

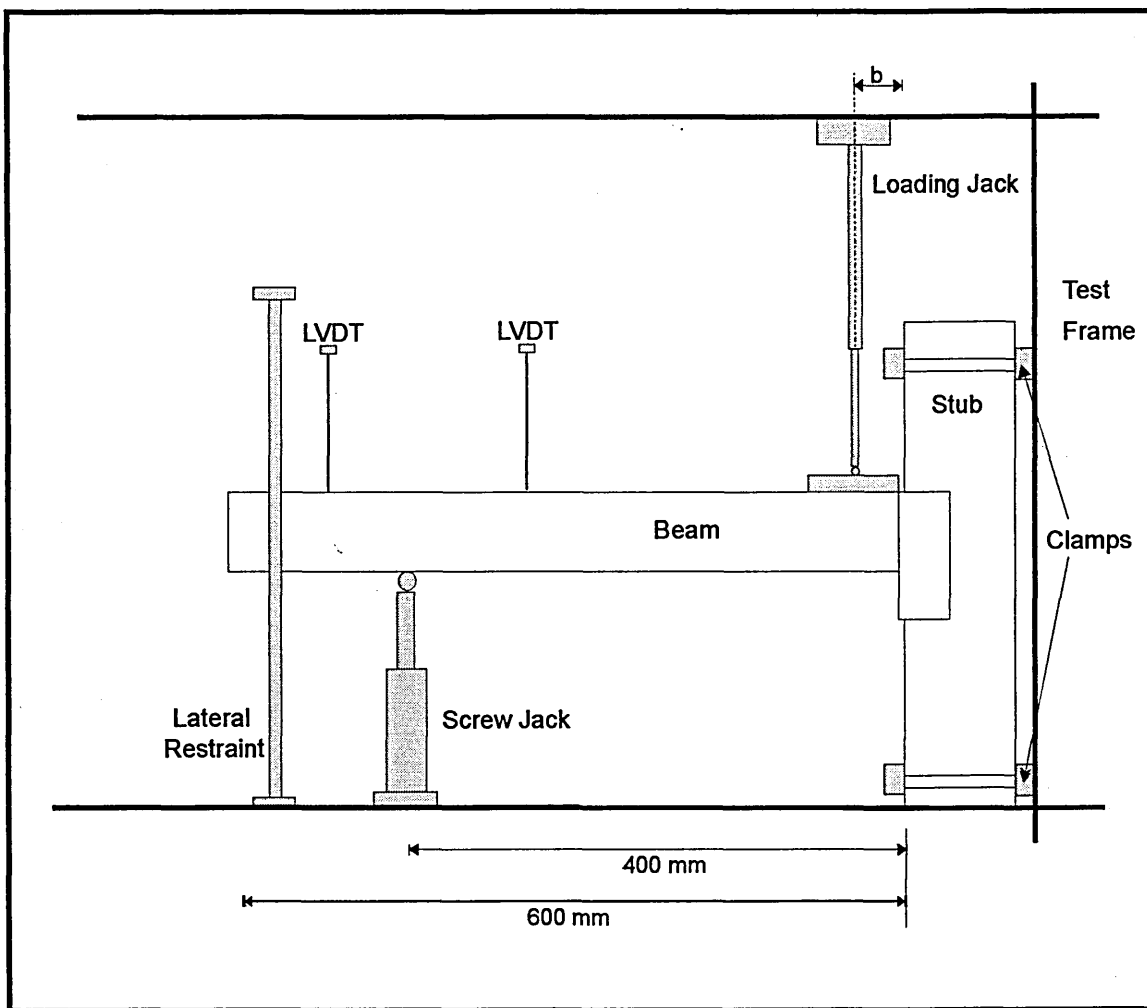


Fig. 5.10. Beam end connector shear test arrangement

To fully develop a shear failure in the connector-upright system a spreader plate was positioned on top of each beam (100mm x 50mm x 25mm) to mediate against local buckling. A second “saddle” plate was also employed during tests involving open section beams to restrict the mode of failure to that of shear. A lateral restraint approximately 500mm from the face of the upright was also used to guarantee that each beam remained in position on the screw jack.

To ensure that each beam tested was maintained in the horizontal plane, two LVDT's (linearly variable displacement transducers) were positioned 250mm apart along its length giving constant visual displacement readings that were kept within 1% of each other (within 2.5mm). As a consequence, the screw jack could be lowered manually,

allowing each beam to remain horizontal throughout testing. Plate 5.7. shows the apparatus described above in use on the test rig. The following equipment is visible (working from left to right) : lvdt displacement displays (x2); lateral restraint; lvdt's above beam (250 mm spacing); screw jack (below beam); loading jack; upright sample.

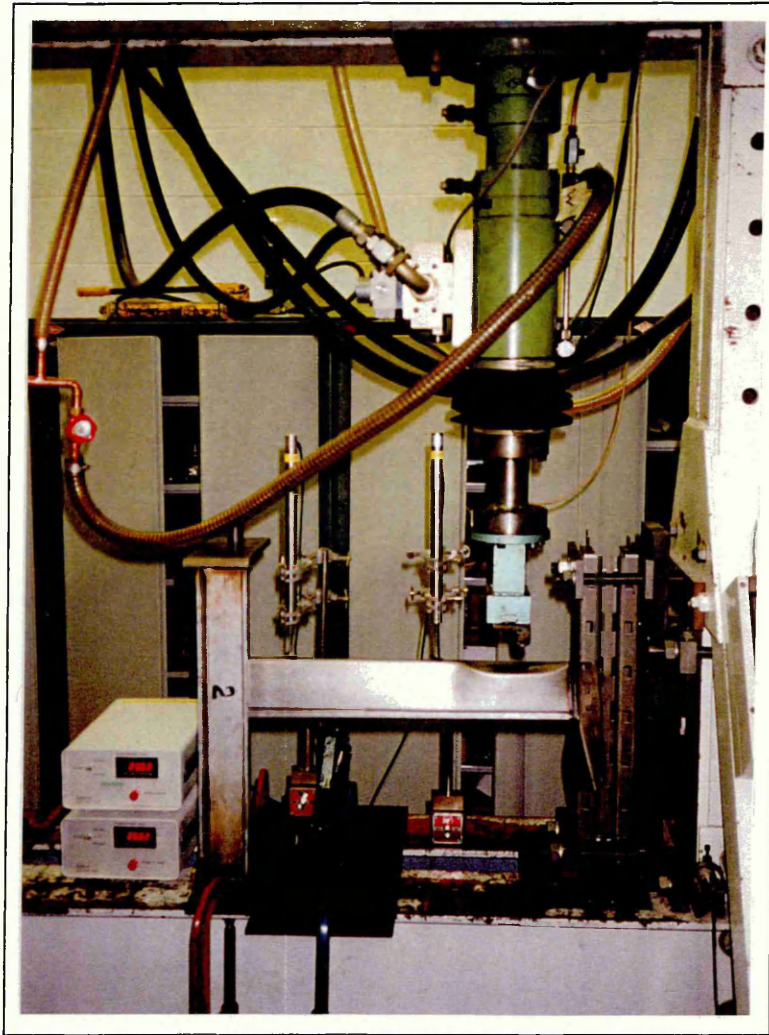


Plate 5.7. Beam end connector shear test apparatus

5.6.3. Data Acquisition

The outputs for load and displacements were collected on two channels of a Gould (2608 - 20Ms/sec) isolating digital recording oscilloscope in time steps of 0.1 secs, and transferred to PC using Gould's "Transition", data transfer and acquisition program.

5.6.4. Discussion

Initially, problems were encountered during testing with respect to the failure mode. Plate 5.8. demonstrates the problem of local buckling around the contact point between the actuator and the beam. This distortion necessitated the use of a 'spreader plate' to mediate against local buckling, allowing shear failures to occur.

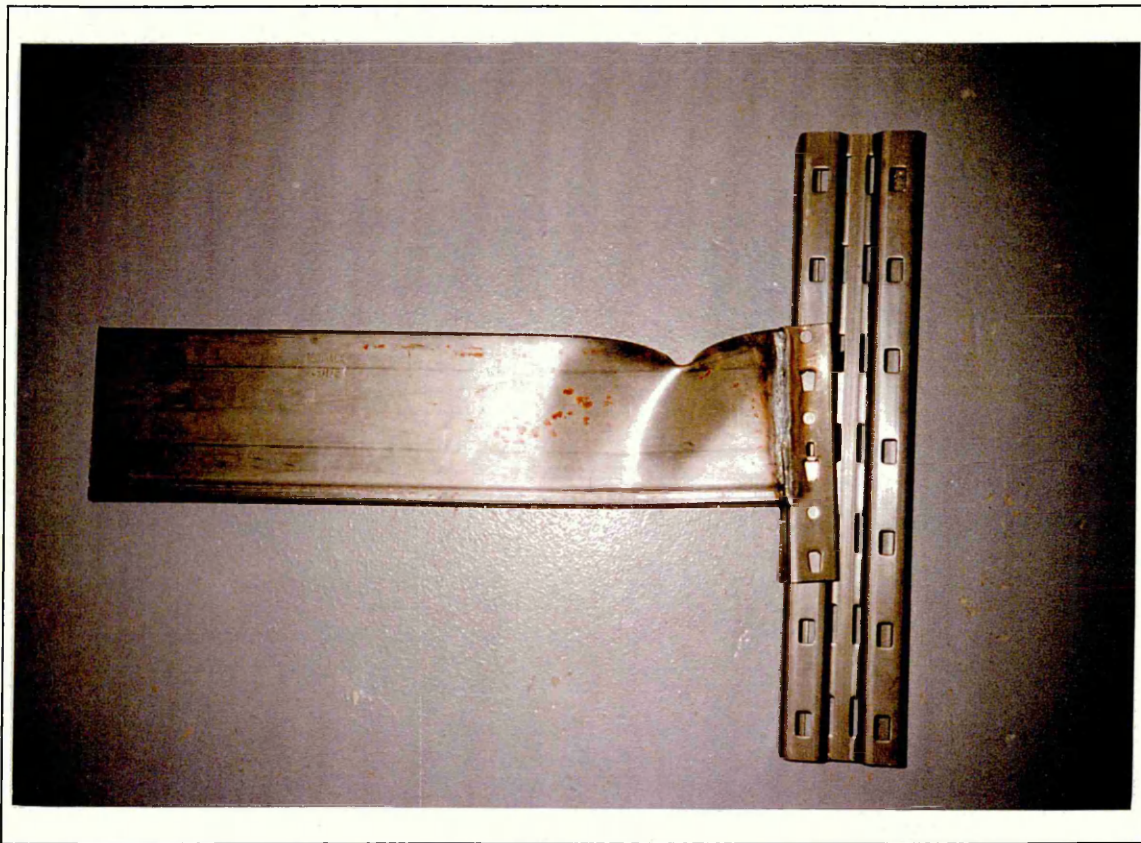


Plate 5.8. Local buckling of 145 box beam resolved by the use of a spreader plate

Typically, under loading the connector lugs were forced upwards and backwards until failure occurred. This behaviour is exemplified by the distortion of the lugs clearly visible in the beam end connector in Plate 5.9. Here a 145 beam with a right hand beam end connector has been tested with an HD30 upright. It is clear that the connector has failed purely in shear.

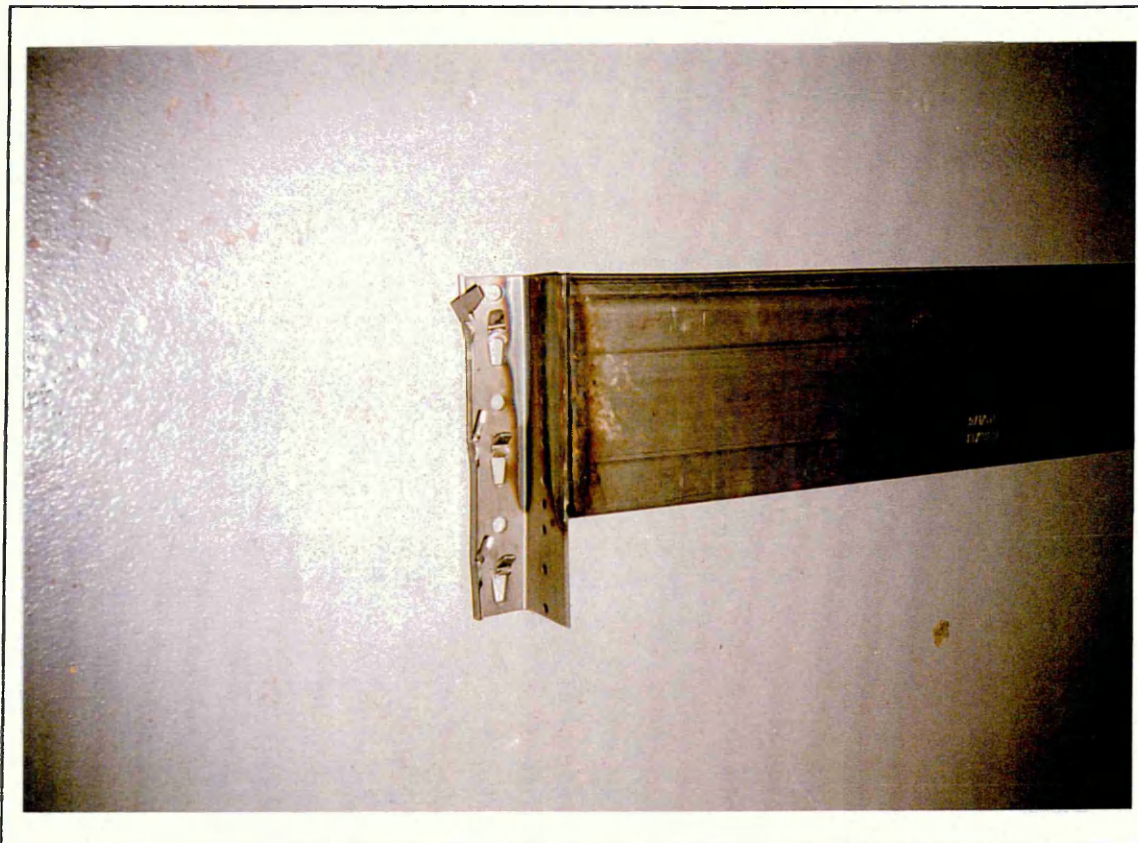


Plate 5.9. Typical beam end connector shear failure

Although connector failure was commonplace during testing some upright section was also prone to shear failure. Plate 5.10. highlights the effect on connector performance of varying the depth of the beam section on SD17 samples. This plate clearly shows the effect of 145 box, 95(1.6) box and 50 open section beams on a section of SD17 upright (SD17 was the only upright to significantly deform or “unzip” during testing). It is apparent that of the 6 lugs on the connector, only the central lugs (designed for load carrying) have had an impact on the uprights. Furthermore, as the depth of the beam gradually decreases (from left to right in Plate 5.10.), it can be demonstrated that the impact of the connector on the stub reduces almost proportionately. The upright (extreme right) is an undamaged section used here for comparison with the tested sections. Generally, upright damage was relatively minor during testing, with the

exception of SD17 uprights, and Plate 5.9. should be seen as indicative of the majority of shear failures in this section of testing.

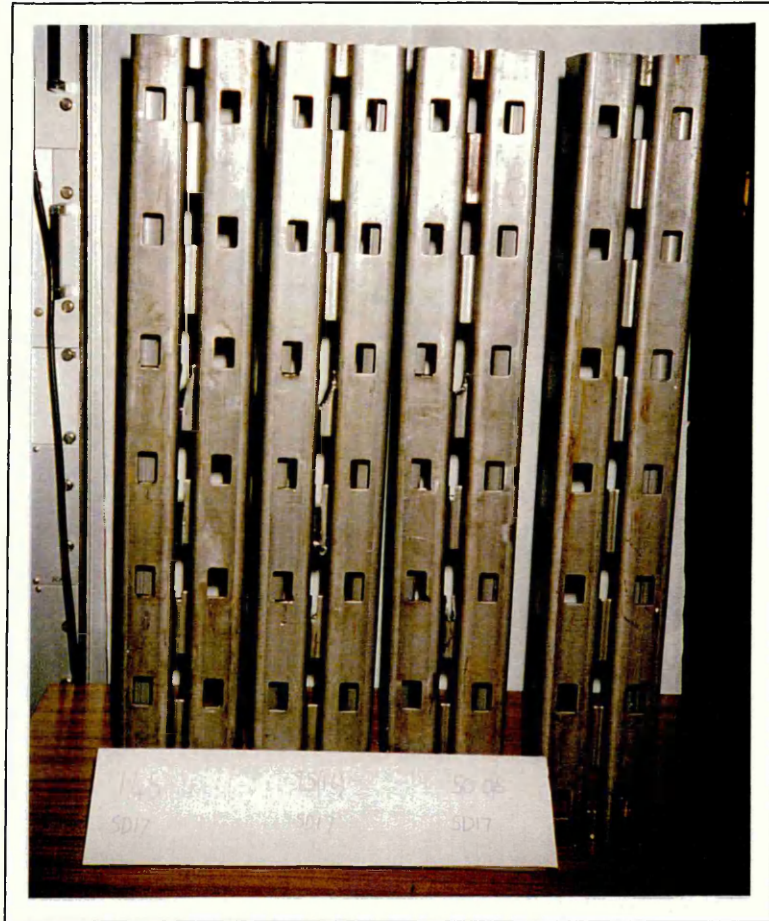


Plate 5.10. Impact of shear testing on SD17 uprights using 145 box, 95(1.6) box and 50 O/S beams (left to right). An untested sample is included for comparison.

5.7. Results and analysis

5.7.1. Evaluation of characteristic shear strength

The individual shear strength of the connector (R_{ti}) was given by :

$$R_{ti} = F_{ti} \left(1 - \frac{b}{400} \right) \quad (5.6.)$$

where F_{ti} was the load applied by the actuator. As with the beam end connector bending test, there was no requirement for geometric or material corrections to the results, and so characteristic values were calculated using eq. 4.4., eq. 5.1. and eq. 5.2. with 'R' (failure load) replacing 'M' (failure moment). The latter two equations, as previously indicated

were used to determine a single value of shear strength for a given beam/upright combination. This reduced the complexities of design, by removing the necessity of having two different values of shear strength for the left and right hand connectors.

The characteristic values of shear strength calculated using the method outlined, have been graphically illustrated below, for every possible beam/upright combination.

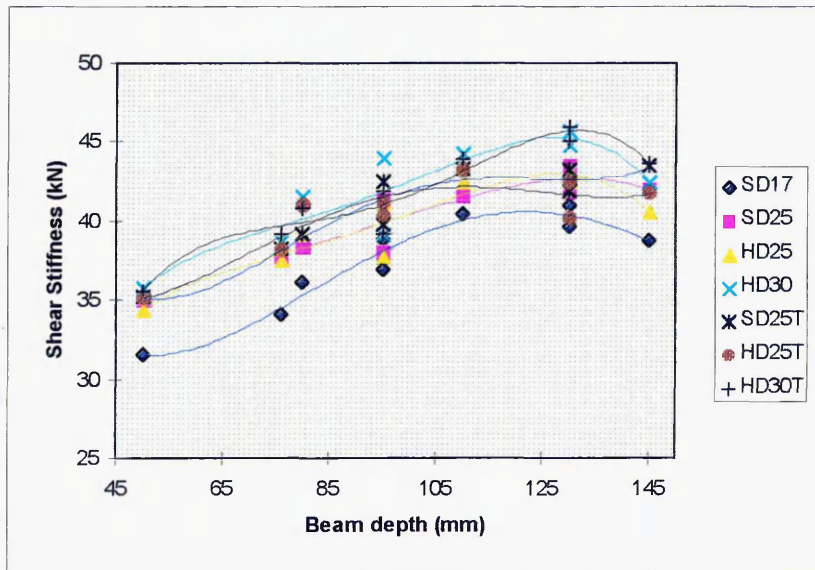


Fig. 5.11. Characteristic shear strength variations with beam depth, for stated upright combinations.

SD17 was the only upright to be considered as the failed component, ‘unzipping’ as increasing load was applied through the connector lugs (see Plate 5.10.). In all other tests it was the connector that was considered to have failed. The effect of this difference in the mode of failure for the SD17 test series is clearly demonstrated in Fig. 5.11., by the gap that exist between the SD17 curve and the other curves. In addition to this, marginal benefits to the shear strength of the system have been accrued by the use of uprights of increased yield stress (250N/mm^2 to 350N/mm^2) and thickness (2.5mm to 3.0mm), although such benefits are by no means distinct or clear cut across the range of beams tested.

5.8. Shear Tests on Beam End Connector Locks

5.8.1. Introduction

The purpose of this test is to measure the shear strength of the connector lock and thereby to determine a characteristic value for resistance to accidental upward force as specified in the FEM code (Cl.2.6.1.). Due to the limited impact that these results were likely to have on the overall analysis and design of the rack, it was considered acceptable for an assessment to be made based on a limited number of tests. As a result, the combinations of beam and upright type used during testing were restricted to the following :

- HD30 x 145 b/b (left/right hand connector)
- HD30 x 50 o/s (left/right hand connector)
- SD17 x 145 b/b (left/right hand connector)
- SD17 x 50 o/s (left/right hand connector)

This allowed the largest and smallest sections in product range to be combined together in order to identify a limiting value for connector lock shear strength.

5.8.2. Test Arrangement

A total of 32 tests were undertaken to assess the resistance of the connector lock arrangement to accidental upward force. To simulate this force, the tests were performed on a modified version of the beam end connector shear test rig, with the test pieces installed in an inverted position (see Fig. 5.12). An additional constant load of 500N was applied to the beam normal to the face of the upright using a pulley system and a number of dead weights. The effect of this extra load, which can be clearly seen in Plate 5.11. overleaf, was to take away any horizontal slop in the assembly of the rack, and to thereby create the worst condition that the connector lock might experience in practice.

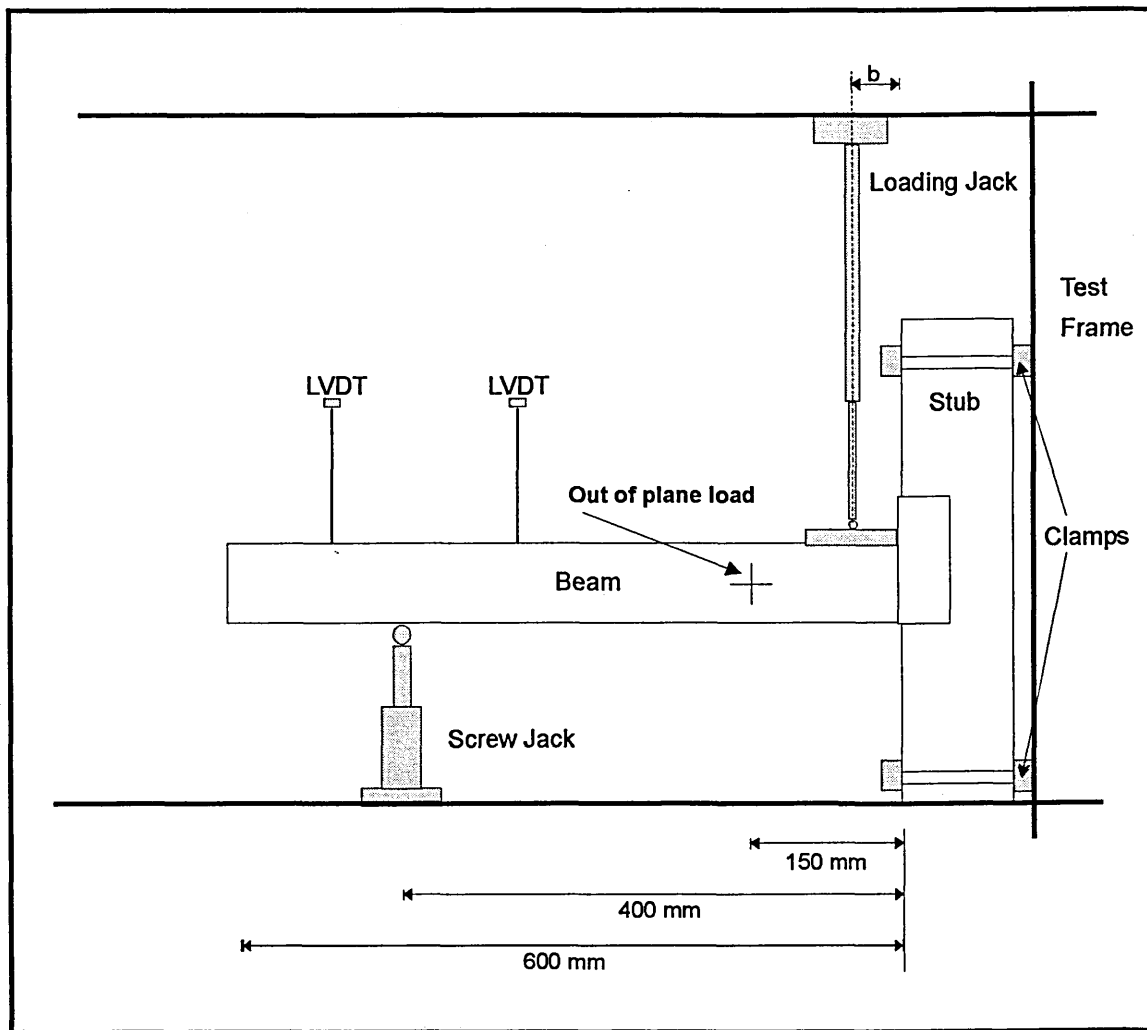


Fig. 5.12. Shear test on beam end connector lock

The upright samples were clamped “rigidly to a relatively infinitely stiff testing frame” (FEM-CI.5.7.2) at two points with an appropriate distance between (see Fig. 5.12.). Each beam was 600mm long and attached to the uprights using left or right hand connectors. The screw jack was positioned beneath the beam at a distance of 400mm from the face of the upright.

During testing the load was applied using a Schenck hydraulic actuator, acting at a distance ‘b’ from the upright. In practice this equated to between 82mm and 100mm. It had a displacement of ± 50 mm and a load capacity of ± 100 kN. The actuator was fixed rigidly at the top with a 25mm diameter steel roller positioned at the point of application

of load. Its rate of displacement being controlled by a test Waveform Generator set to 333secs/cycle (0.6mm/sec).

To fully develop a shear failure during testing a spreader plate was positioned on top of each beam (100mm x 50mm x 25mm) to mediate against local buckling. In addition, to ensure that each beam tested was maintained in the horizontal plane, two LVDT's (linearly variable displacement transducers) were positioned 250mm apart along its length giving constant visual displacement readings that were kept within 1% of each other (within 2.5mm). As a consequence, the screw jack could be lowered manually, allowing each beam to remain horizontal throughout testing.

5.8.3. Data Acquisition

The outputs for load and displacement were displayed visually on the actuator control panel, the maximum load being recorded on individual test sheets.



Plate 5.11.

Shear test on beam end connector lock

5.8.4. Discussion

Two modes of failure were observed during testing, the occurrence of each being directly related to the type of upright section being used (SD17 or HD30). Typically, any tests performed using HD30 section produced a shear failure in the connector above the middle lug. This can clearly be seen in plates 5.12. and 5.13. below.



Plate 5.12. Connector failure - front



Plate 5.13. Connector failure - rear

Although the plates above show the front and rear of a connector on a 145 box beam, the same failure mode is equally applicable to tests employing 50 open section beams with HD30 uprights. Under loading the connector lock is forced against the top of the

central connector lug by the upright until the load becomes critical and the lug is sheared off. Likewise, in the tests involving SD17 upright sections the same process results in a tearing or ‘unzipping’ of the stub proportionate to the displacement of the actuator, rather than a failure of the connector lock. It should be made clear here therefore, that despite the variations in beam and upright section being used during this sequence of testing, no combination in the product range could induce a shear failure in the connector lock.

5.9. Results and analysis

5.9.1. Evaluation of characteristic shear strength of beam end connector lock

The beam end connector lock performance was calculated in the same manner as that used in section 5.7.1. of this document to determine the shear strength of beam end connector. A summary of the characteristic values of shear strength for the connector lock tests has been produced below :-

HD30 (50 O/S, 145B/B), right hand connector	-	11.22 kN
HD30 (50 O/S, 145B/B), left hand connector	-	10.87 kN
SD17 (50 O/S, 145B/B), right hand connector	-	6.13 kN
SD17 (50 O/S, 145B/B), left hand connector	-	5.71 kN

These values are in excess of the limit defined in Cl. 2.6.1. of the FEM code, in which a minimum value of 5kN is set for the amount of accidental upward force that “rack components directly above a load unit should be able to absorb”.

There seems to be no clear explanation as to why the left hand connector results should be lower than those for the right hand connector. Although it may indicate that the punch used to form the left hand connector is leaving slightly less material holding the middle lug (removed at failure) to the body of the connector. This hypothesis could not be confirmed by any practical means, due to the nature and position of the punched shape.

5.10. Bending Test on Beams

5.10.1. Introduction

The purpose of this test is to “measure the bending strength”...“primarily for beams with only one axis of symmetry, which may be subject to lateral torsional buckling” (FEM-CI.5.11.1). Measurement of “beam rotation about its own axis under service load” is also assessed. This test was not mandatory for the open cross section beams supplied, due to the symmetrical nature of the cross section about its vertical axis (see FEM Table 5.1.1.).

Historically, a tack weld at a distance approximately 1m in from the connector has prevented de-nesting of the C-sections which combine to form the box-beams. With the sections welded together at the ends and at ‘mid-section,’ the beams’ ability to rotate is severely reduced. As a consequence, the two open-section beams were of more concern during this series of tests, particularly with regard to rotation, and this was reflected in the choice of beams to be tested. The largest and smallest duty box beams were also chosen to characterise the range within which moments of resistance and beam rotation would lie for these section types. A total of 18 tests were therefore conducted using the following beam duties in conjunction with HD30 frames: 50 open-section; 76 open-section; 80 box beam and 145 box beam.

5.10.2. Test Arrangement

Each beam tested had a span of 3.2m and was attached to two frames at approximately 440mm above the base of the test rig. The frames were 900mm wide, and were bedded onto a combination of 15mm thick ground steel plate and plaster of Paris. These were in turn positioned on rollers or pinned joints (see Fig. 5.13.). The plaster was used to removed any contact imperfections that may have been present beneath the base plates.

A typical support detail has been included below :

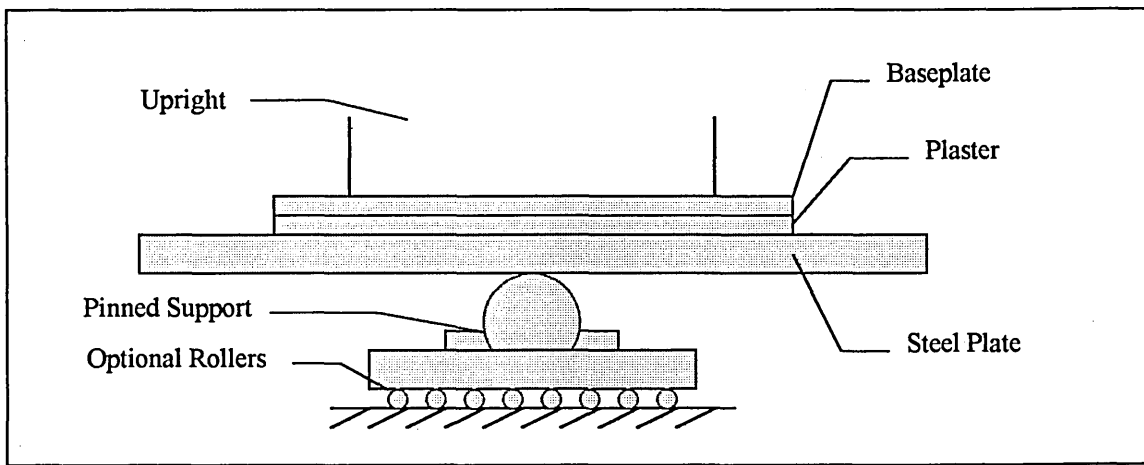


Fig. 5.13. Support detail

The bases that formed the four supports were identical, however during testing the rollers were locked under two of the supports to provide a stationary 'pin', while the other two were left free to move horizontally. Consequently, no horizontal forces or moments could develop in the uprights, in accordance with FEM requirements.

Rotation was measured using four LVDT's with two per beam. These monitored the relative displacements of a 4mm thick, 40mm wide flat steel plate bonded to the side of each beam using 'elastic chemical metal'. During the test programme the chemical metal was used carefully so as to avoid artificial strengthening of the beams at mid-span by holding the C-sections together (see Fig. 5.14.).

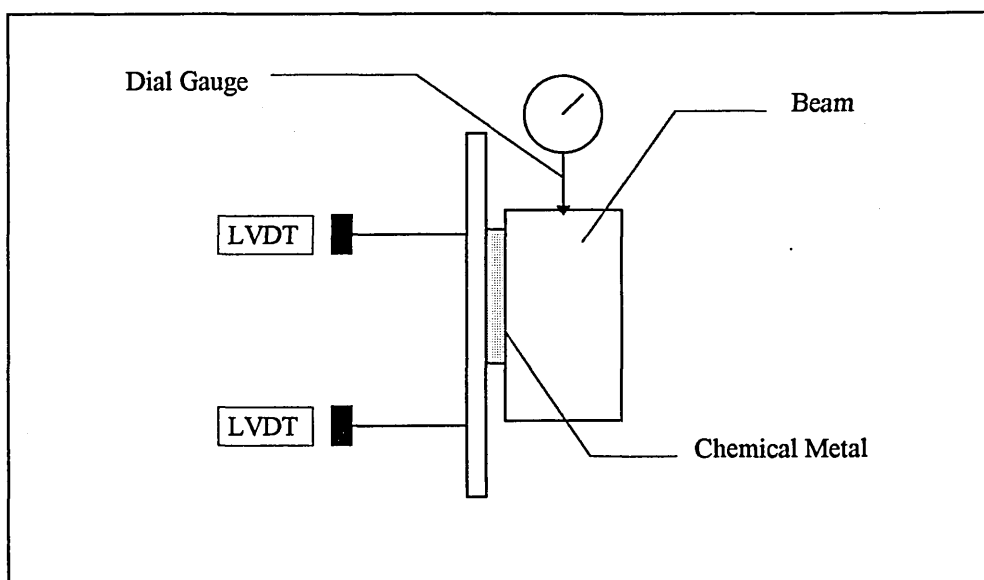


Fig. 5.14. Sketch showing rotation and deflection measurement

Dial gauges were used at mid-span to measure vertical displacements. Readings were taken to the service load of the beam or until the travel on the gauge had been exceeded. The load was applied using a Schenck hydraulic actuator with a displacement capability of $\pm 100\text{mm}$ and a load capacity of 300KN . The actuator acted vertically down through a ball seat onto an I-beam/box-beam spreader system (see Fig. 5.15.).

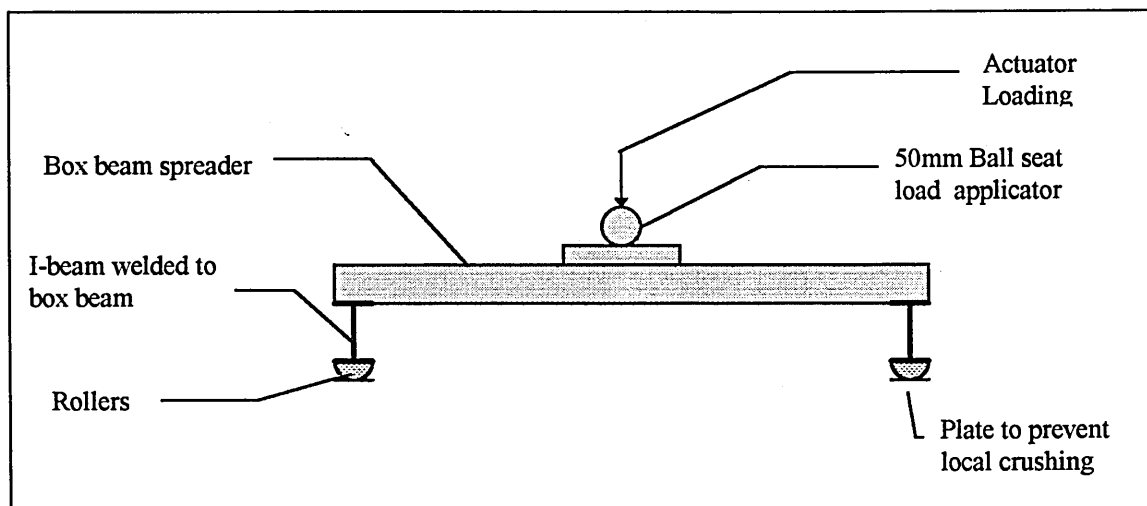


Fig. 5.15. Load spreader system

From there the load was transferred into the sections via cylindrical rollers resting on $100\text{mm} \times 10\text{mm}$ mild steel plate, which were used to prevent localised crushing.

5.10.3. Data Capture

With the exception of the dial gauges, all readings for displacement and load were captured electronically using in-house data capture equipment and software devised specifically for this test rig. Load incrementation and the rate of data capture were determined manually during the course of each test.

5.10.4. Discussion

Plate 5.14. shows the “set up” used during this series of tests. Clearly visible are the LVDT’s and a dial gauge, used for measurement of beam rotation and deflection respectively. This instrumentation is replicated for the other beam. The test was ostensibly designed to assess general stability at service load and as a consequence the load was applied at quarter points (“standard test” FEM-CI.5.11.2). This is reflected by the use of the load spreading system used (see FEM-Fig 5.11.1.).

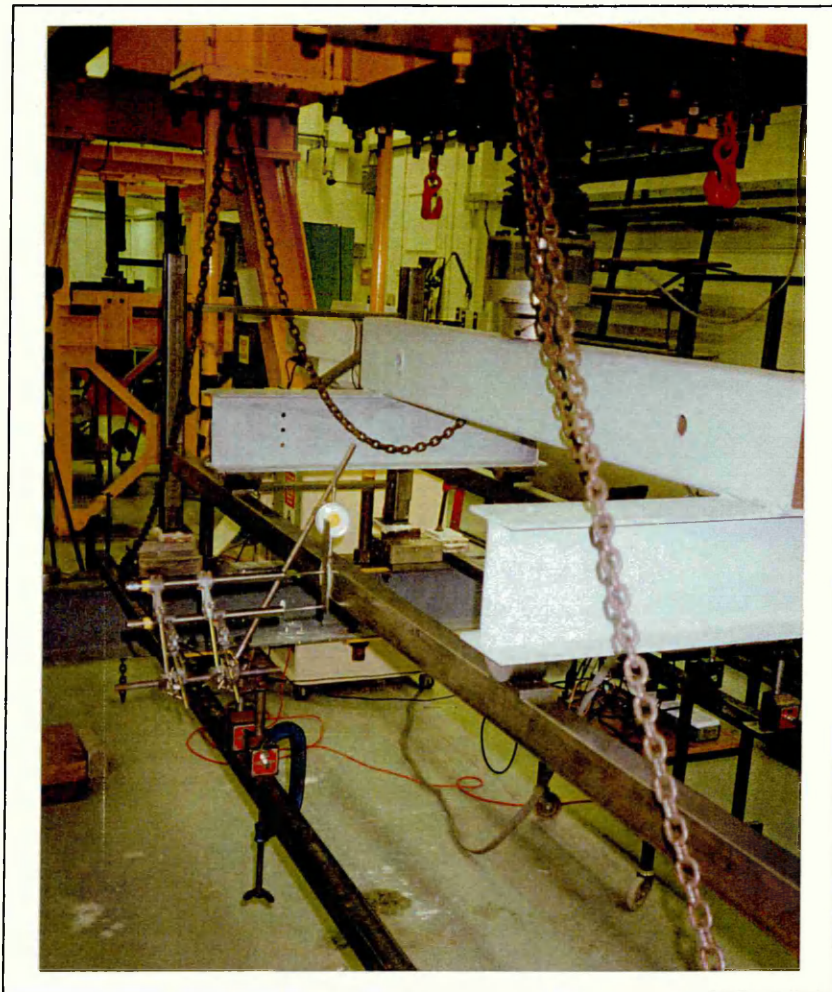


Plate 5.14. Standard test to determine section general stability

Beams were in excess of 50 times longer than their width, with a 3200mm span.

Section	Width (mm)	Minimum Beam Length (mm)	Actual Beam Length (mm)
50 O/S	50	2500	3200
76 O/S	50	2500	3200
80 B/B	48	2400	3200
145 B/B	48	2400	3200

In addition, there was no lateral support between beams using such things as pallet support bars, fork entry bars or beam ties which may have impeded rotation.

Plate 5.15. demonstrates the deflection of an 80 box beam prior to failure. The ability of the uprights to rotate about their supports is also clear.

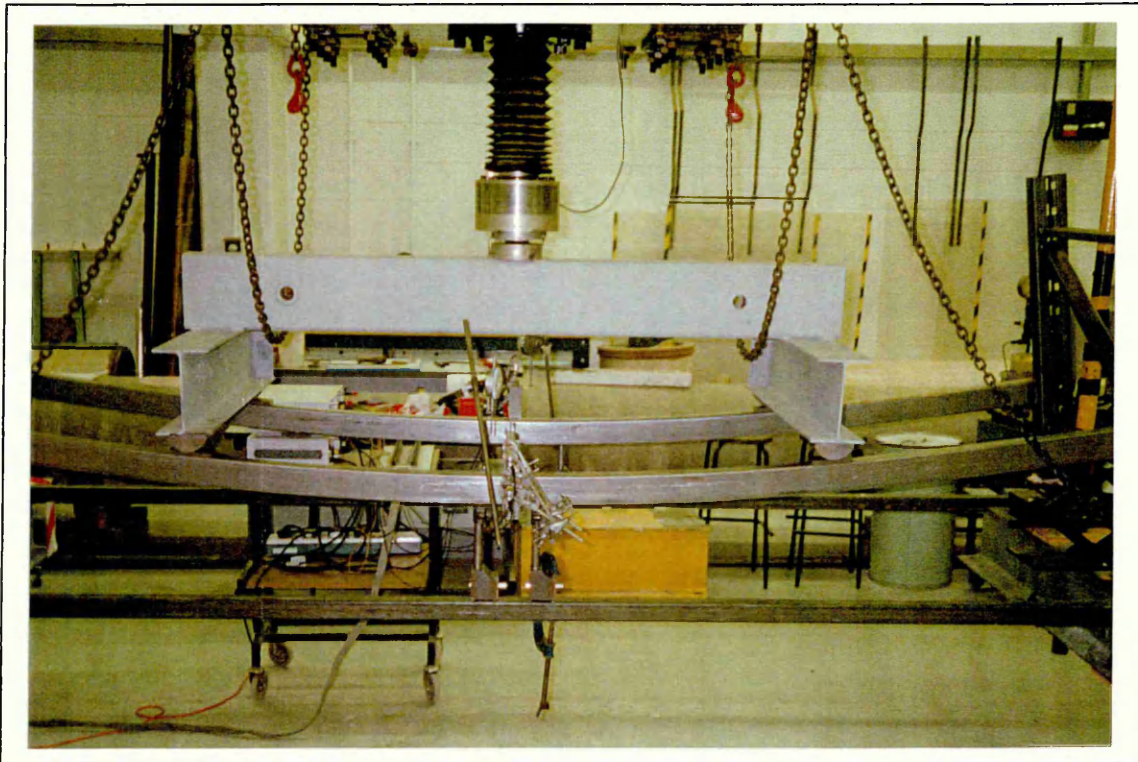
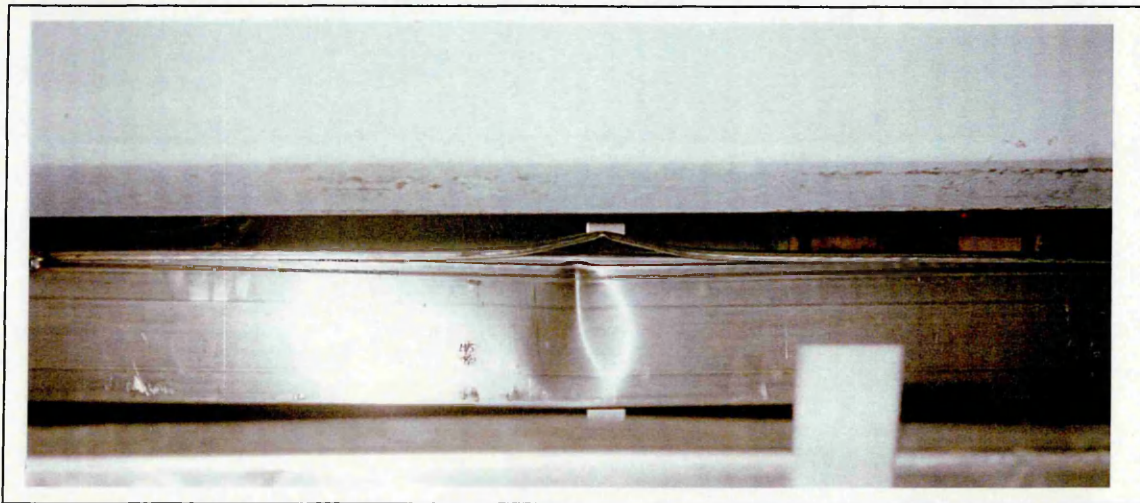
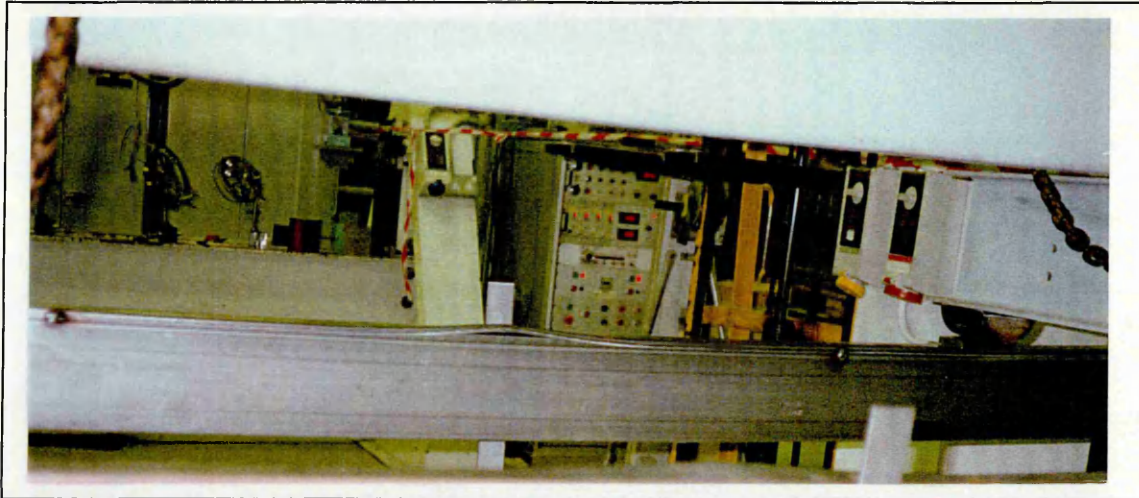
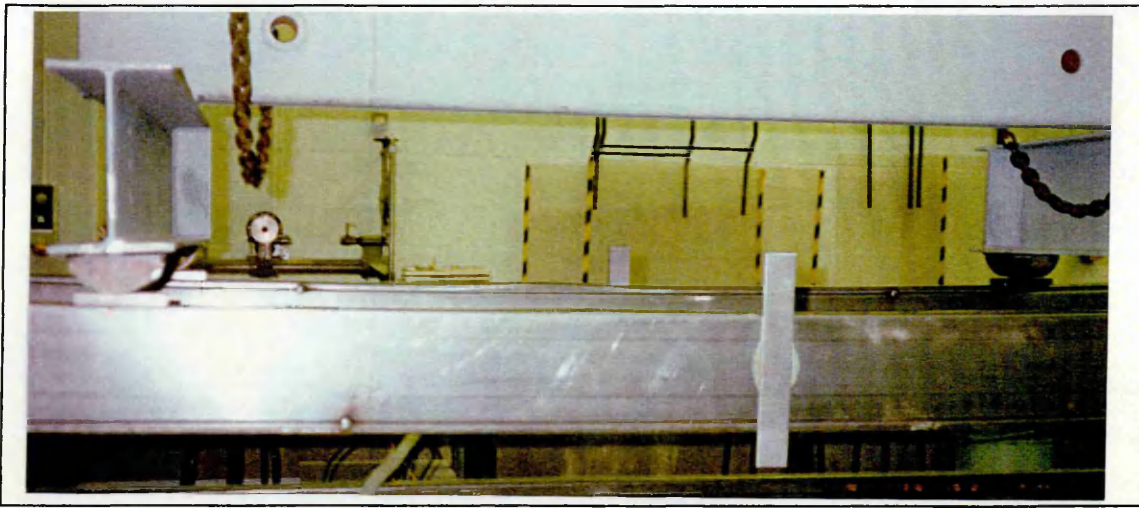


Plate 5.15. Deflection of a 80 (1.6) box beam during testing

The following Plates have been included to characterise how a typical 145 box beam reacted to incremental loading to failure. In contrast to open section beams which were prone to failure through excessive deflection, it is apparent from plates 5.16.-5.18. that

compressive forces in the upper flange of these box beams give rise to progressive deformation until catastrophic failure occurs. It is also evident from these plates that the lip of the flange is effected almost exclusively between the tack welds which are designed to hold the two C-sections together. Further welding to make the connection between these C-sections more fully effective would surely have a beneficial impact on the load to failure.



Plates 5.16.-5.18. Progressive failure of a 145 box beam

5.11. Results and Analysis

5.11.1. Calculation of beam rotation at service load

Test rotations (θ_{ti}) were taken at the mid-span on the beams and corrected as follows :

$$\theta_{ni} = \theta_{ti} \left(\frac{t_t}{t} \right)^3 \quad \text{for open sections} \quad (5.7.a.)$$

$$\theta_{ni} = \theta_{ti} \left(\frac{t_t}{t} \right) \quad \theta_{ni} \geq \theta_{ti} \quad \text{for box sections} \quad (5.7.b.)$$

The design value of beam rotation was then taken to be the mean value from the number of tests performed. Table 5.4. summarises the results obtained for each beam tested :

Beam Section	Design Rotation (Degrees)
50 O/S	2.7554
76 O/S	0.521
80 (1.6)	0.436
145 B/B	0.3368

Table 5.4. Design rotation summary table for beams specified

This test confirms that there was no significant rotation in any of the beams examined, and that although the 50 open section beam showed a much higher degree of rotation than any of the other beam sections it is still well within the limiting value of twist defined in FEM Cl.2.3.4. as 6° .

5.11.2. Calculation of beam characteristic moment of resistance

The treatment of the observed failure moments was equivalent to that used in section 4.3.2. for determining the corrected values of failure loads (see eq. 4.1.), although where the thickness ratio is raised to the power β , the limiting values of width to thickness ratios are treated slightly differently, as follows :

$$\left\{ \frac{b_p}{t} \right\}_{\text{lim}} = 0.64 \sqrt{\frac{Ek_\sigma}{\sigma_{\text{com}}}} \quad \left(\geq \frac{b_p}{t} \right) \quad (5.8.)$$

where k_σ and σ_{com} are defined in Appendix D of the FEM code. The design value of beam moment of resistance was then calculated in accordance with the characterisation described in equation 4.4 of this document. The table below summarises the results obtained for each beam tested :

Beam Section	Characteristic Failure Moment (KNm)
50 O/S	2.050
76 O/S	4.652
80 (1.6)	9.007
145 B/B	14.675

Table 5.5. Design moment of resistance summary table for beams specified.

Chapter 6

Racking System Design to FEM 10.2.02 using Finite Element Analysis

6.1. General outline

A comprehensive design procedure is outlined in this chapter. This includes a full 'global' analysis undertaken in Ansys 5.4 to examine the behaviour of a 'typical' pallet rack using performance values obtained previously in this document. Preliminary checks and calculations have also been detailed together with the loading conditions and load combinations that are considered to be critical in terms of design. In addition, this chapter includes a detailed account of the way in which the finite element model has been generated, describing which F.E. elements have been used and the approach taken when considering the treatment of semi-rigid joints.

To verify the suitability of a racking system to carry a specified load, it is first necessary to appreciate the distribution of its internal forces and displacements. Although racking structures are 3-dimensional, it is permissible under the FEM code to analyse each system as two distinct and separate 2-dimensional models operating perpendicularly to each other. Generally, these consist of a 'down-aisle' sway frame, incorporating the semi-rigid behaviour of the floor and beam end connections, and a 'cross-aisle' welded frame, which is normally less critical in terms of the overall system design. The behavioural characteristics of the various components which go into making up a racking system have been assessed by combining each 2-dimensional model, using interaction formulae where necessary, to verify the structural integrity of the example provided.

6.2. The effect of second order analysis

Generally, first order analyses of linearly elastic structures use equilibrium equations based on undeformed structural geometry together with axial forces which are assumed to act independently of member end moments. Due to the sway frame nature of a racking system however, second order effects may have a significant influence over performance (down aisle) and must therefore be taken into account. This approach requires that equilibrium equations take the deformed geometry of the rack into consideration, together with the interaction between axial forces and member end moments. To illustrate this point, the following example has been provided to demonstrate the general differences between first and second order effects.

The column of length 'L' in Fig. 6.1., is unrestrained at one end and subject to a horizontal load 'H' and a vertical load 'P'. Given that a first order analysis is based on undeformed structural geometry, the deflection at the top of the column is described by the standard cantilever deflection formula, $\Delta_1 = HL^3 / 3EI$. Equally, the moment at the base of the column is defined as, $Mb_1 = HL$.

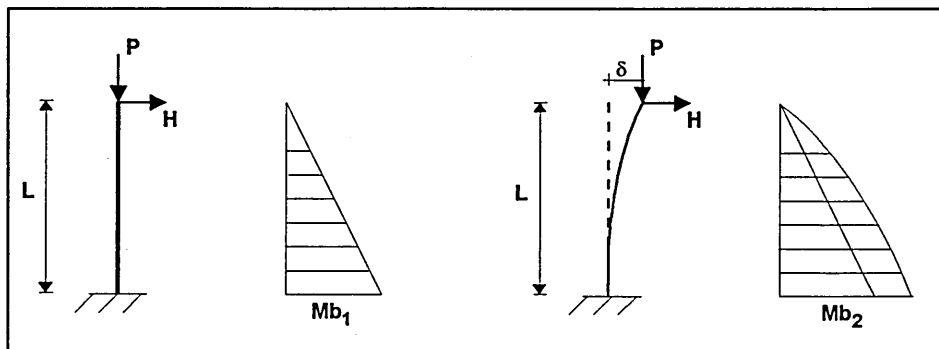


Fig. 6.1. A comparative evaluation of base moment values as a consequence of 1st and 2nd order analysis.

To determine the second order base moment of the same column the lateral deflection due to the horizontal load 'H' is considered together with an additional deflection due to the eccentricity generated with respect to the neutral axis of the column when the vertical

load 'P' is displaced. As a consequence the second order base moment is defined using the formula, $Mb_2 = HL + P\delta$. This second order behaviour is generally referred to as the P- δ effect, and can result in substantial increases in rack moments and deflections when compared with a first order analysis of the same structure.

The complexity of the structural response of a racking system is heightened when the semi-rigid nature of the beam end connector and the floor connector joints is taken into account. As described earlier in chapters four and five, these joints are characterised by a non-linear moment-rotation relationship, but have been simplified here to a bi-linear curve enabling a computerised analysis to be undertaken. A solution is determined iteratively from an initial estimate of the axial forces in each of the members and the joint displacements within the structure. A second order analysis is then performed on this deformed geometry to obtain a more accurate approximation of the behaviour of the structure under loading. This operation is repeated until the convergence criteria have been satisfied, that is to say when the current solution is within a specified percentage of the previous solution. The convergence criteria for the finite element models described here was set to 1%. This allowed a high degree of confidence to be placed in the accuracy of the results, and by implication in the subsequent design checks which were performed on the structure.

6.3. System design using finite element analysis

6.3.1. Model generation

The keystrokes for simulating the down-aisle behaviour of a rack in Ansys 5.3. are detailed in appendix C of this document for a six bay, four level system. Care was taken throughout the preliminary investigation of model generation to ensure that results corresponded with the theoretical calculations. Being thin-walled structures, many racking system configurations can be particularly sensitive to beam deflection checks in

the serviceability limit state. It is important therefore that the maximum deflection of a beam is reliably calculated by the finite element package. Table 6.1. demonstrates the variation in maximum deflections of a simply supported beam 2.7m in length supporting a uniformly distributed load of 1000kg, merely by varying the number of elements in the beam. With a second moment of area (I) of 874757 mm⁴ the anticipated theoretical deflection is :

$$\delta_{\max} = \frac{5}{384} \frac{WL^3}{EI} = 13.686 \text{ mm} \quad (6.1)$$

Beam Elements	3	4	5	6	7	8	9
Maximum Deflection (mm)	11.349	13.686	13.034	13.686	13.353	13.686	13.484

Table 6.1. Maximum central deflection of simply supported beam due to variations in the number of elements used in the beams construction.

Palletised loading methods are standard for racking, and it is generally accepted therefore that a uniformly distributed load can be assumed for analytical purposes, making a central deflection the maximum deflection. Clearly, since using an odd number of elements does not allow a node to be positioned centrally along the length of the beam, it is not possible to generate an accurate picture of the maximum deflection in the beam. The number of elements in each beam was therefore chosen to be four, based on the assessment in Table 6.1. Moments and axial loads were shown to be largely unaffected by the number of elements in the rack, as was the behaviour of the uprights in the system, and as a result of this analysis the uprights were also constructed using four elements.

6.3.2. Treatment of semi-rigid joints in finite element software

The down-aisle interaction between the beams and the uprights is critical to the load bearing capacity of the rack. This interaction is entirely dependent on the performance of

the beam end connector. It has been clearly demonstrated in previous chapters that the experimental behaviour of the connector resembles neither a fully fixed joint or a perfectly frictionless pin. The moment-rotation relationship of the joint is instead characterised by a series of non-linear curves (depending on the beam and upright being used), which have been simplified to bi-linear curves to allow analysis to be undertaken. A number of alternative approaches were available to represent the behaviour of this joint and that of the floor connector (which is also a semi-rigid) using different commercial finite element analysis software . Initially, Cosmos/M 1.65. was considered. In this case the only method of constructing the connector was by using a 3-dimensional torsional bar (see Fig. 6.1.).

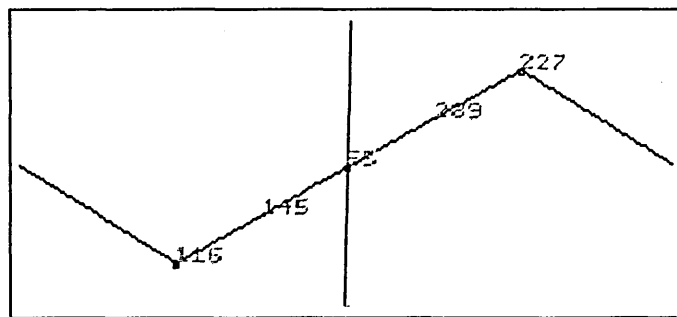


Fig. 6.1. Torsional bar simulating beam end connector.

This permitted a single value of stiffness to be input for the connector, with the design moment being incorporated separately within the subsequent design checks. There was therefore no limitation on the rotation or the moment capacity of the connector within the simulation. In addition to this, since the beams were misaligned about the third (z) axis on opposing sides of the uprights, small, undesirable, additional stresses were present in the uprights. This combined with the extra run time (7 minutes for a single load case which was unacceptable in a commercial design environment) taken for a three dimensional analysis of a two dimensional problem, meant that a more suitable FE package needed to be used.

Ansys (linear plus) 5.4 is capable of generating a two dimensional down-aisle model of a racking system using concurrent nodes, and a specialised non-dimensional spring element (spring-damper 14). This element only requires a specified rotational stiffness (taken directly from the experimental test data) and has the advantage of a much reduced solution time (15 seconds for a single load case) due to a lessening in the complexity of the model geometry.

A subsequent adaptation of this treatment for semi-rigid joints was to use a bi-linear curve element (combin 40), incorporating a value of rotational stiffness and a design moment, within the system model. It is clear from Fig. 6.2. that as the element rotates it will attract moment up to the value of the design moment. Thereafter, the joint will rotate without attracting any further moment until it fails at a predetermined rotational limit. The value of such an element is that the free rotation of the connector enables an automatic redistribution of moment into the attached beam, and potentially into other beam end connectors and floor connections in the racking system.

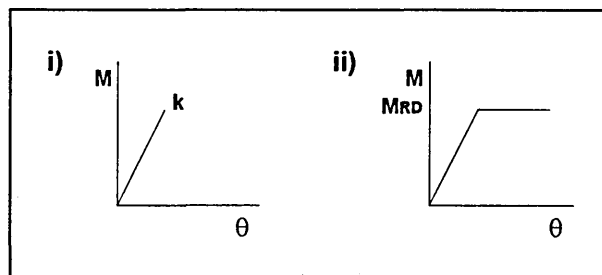


Fig. 6.2. Semi-rigid joint modeling elements
i) spring damper 14 ii) Combin 40

Both of these approaches to modeling joints in FEA allow for a more realistic distribution of moment about the rack, when compared with the standard value of 15% redistribution commonly found in design codes (see FEM Cl.4.4.3.1.). However, as mentioned previously, each element still remains an approximation of the non-linear behaviour of the floor or beam end connector observed during testing. A multi-linear or

polynomial curve which more accurately reflects the actual performance of the connectors would have been more desirable, but has not been possible to model in this way given the limitations of the element library available within the software.

6.3.3. The rotational limit for the Combin40 element

The Combin40 element allowed for the inclusion of a limit on the rotation of a given connection. As described earlier, the connection could rotate linearly, responding to increases in the moment applied to the joint, until a predetermined design moment limit was reached. The joint could then rotate without attracting any further moment until the rotational limit was reached and the connector was deemed to have failed. This is one of the crucial differences between Combin40 and Combin14, with the failure of the Combin14 element being determined only following an Ansys analysis (using design checks), whereas the behaviour of elements modeled using Combin40 being regulated within the analysis itself.

The rotational limit for the beam end connector was determined using the standard characteristic derivation from Cl.5.1.3.(c) of the FEM code, $R_k = R_m - k_{s,s}$. R_m was calculated as the mean of the rotational values from each bending test data set, taken to be the point at which the tail of the test curve fell below the value of the design moment (see Fig. 6.3.).

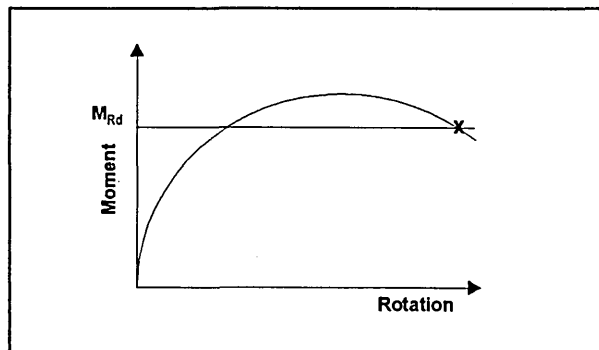


Fig. 6.3. Beam end connector bending curve - individual test rotational limit.

In contrast, it was not possible to determine a rotational limit in the same way for the floor connector. This was due to the differences in the nature of the moment-rotation response (see Fig. 6.4.). The floor connector was therefore modeled using the Combin14 element.

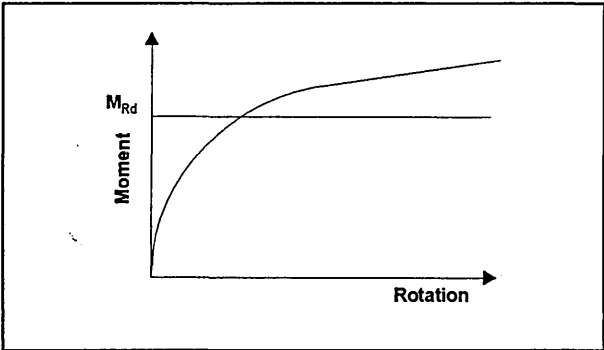


Fig. 6.4. Floor connector bending curve - no rotational limit.

6.4. Design Procedure

6.4.1. Introduction

The following design uses Ansys together with the 2-dimensional modeling techniques described above to determine bending moments, axial loads and deflections for a racking system of beam length 2700mm and a height to first beam of 1575mm. Six bays of racking are analysed in line with recommendations contained in Cl.4.3.3.2. (notes 2) of the FEM code. This clause allows an analysis to be undertaken on a representative number of bays in a rack, with a 'minimum number being five bays or the actual number, whichever is the lesser'. To provide symmetry in the analysis and to allow for a single and potentially critical central upright, it was considered that a six bay system would prove to be the most appropriate 'standard case'. This is particularly true when pattern loading considerations are taken into account. The dimensions of the rack are presented below (see Fig. 6.5. and 6.6) with "system lines coinciding with the centroidal axes of the gross cross-section of the members" (Cl.4.1.). Gross section properties have been used to construct the model, with no allowance being made for perforations in the uprights (Cl.3.2.).

6.4.2. Section Properties

The rack has been modeled using SD25 uprights and 95(1.78) box beams. General section properties have been included in Table 6.1., and are derived from Autocad 12 software :

	Area (mm ²)	I _{yy} (mm ⁴)	I _{zz} (mm ⁴)	r _{yy} (mm)	r _{zz} (mm)	Self weight (kg)
SD25 (gross)	500	540962	170524	32.89	18.47	61.25 (frame)
95 (1.78)	705.5	969059		37.06		15.93

Table 6.1. General section properties

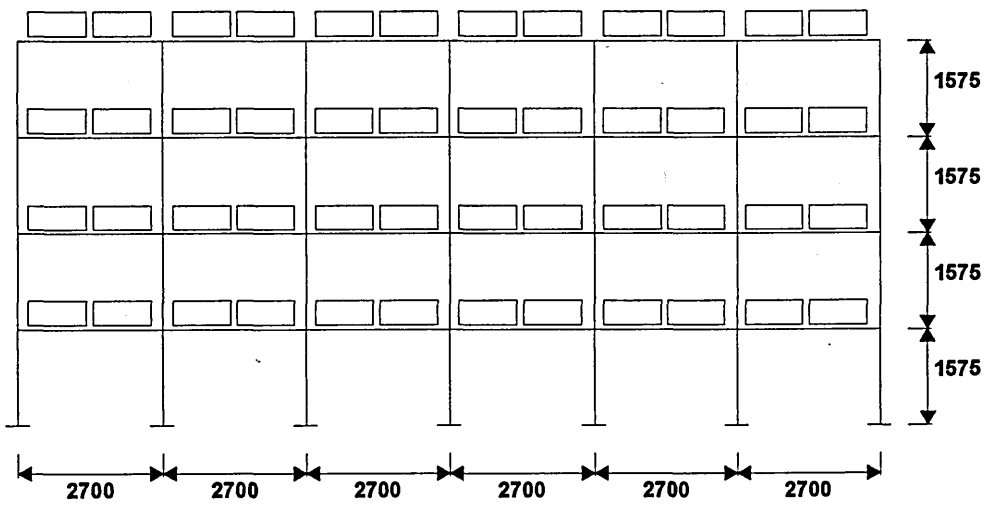


Fig. 6.5. Fully loaded down-aisle rack - dimensioned for F.E.A.

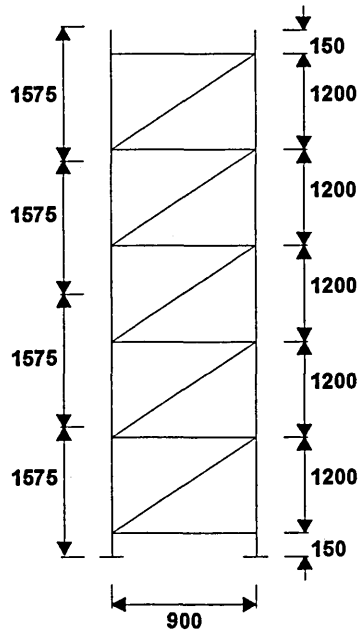


Fig. 6.6. Cross-aisle rack dimensions and bracing pattern

6.4.3. Calculations and considerations necessary for the construction of an F.E. model

Each compartment holds two unit loads of 1100kg (21.58kN in total, 10.79kN/beam) on standard 1200x1000 pallets. Loads are placed by fork lift trucks.

Unless otherwise stated all references to clauses, figures and tables are to be interpreted as references to the FEM code.

- a. Unit pallet load factor, variable actions (Table 2.2.) 1.4
(for systems other than those weighing and discarding pallets over the design load)
Beam design load, uniformly distributed (Cl. 2.4.2.2.)
 $10.79 \times 1.4 = 15.11 \text{ kN}$
Column design load (N_{sd}) $15.11 \times 4 = 60.43 \text{ kN}$
- b. Dead loads, permanent actions (Cl. 2.4.1.)
Self weight of structure (Cl. 2.4.1.2/3) - no fixed service equipment
 $61.25 \times 7 \times (9.81/1000) + 15.93 \times 48 \times (9.81/1000) = 11.7 \text{ kN}$
Total unfactored beam loading $48 \times 10.79 = 517.92 \text{ kN}$
 $(11.7/517.9) \times 100 = 2.26 \%$

The structure self weight is less than 5% of the beam load and is therefore be neglected.

- c. Vertical placement load (Cl. 2.4.5.a.)
(goods placed with mechanical equipment)

Vertical placement loading is only applicable to single unit load systems, and only affects the beam strength, not the beam deflection or the frame design in either the down-aisle or cross-aisle directions. Consequently it is not applicable in this case, although in rack supporting single unit load compartments, beam and connector design should take account of a vertical placement load of 25% of the design load in addition to that design load.

- d. Horizontal placement load (Cl. 2.4.6.a.2.) - for racks over 6m in height

Q_{ph} is the worst of either : i) 0.25 kN applied at the highest beam level
ii) 0.5 kN applied at any beam level up to 3m
Design values of Q_{ph} : i) $0.25 \times 1.4 = 0.35 \text{ kN}$
ii) $0.5 \times 1.4 = 0.7 \text{ kN}$

e. An alternative treatment for horizontal placement loading

An alternative approach to that contained above in section 6.3.3.(d). is outlined in Cl. 2.4.6.1. for down aisle loading and in Cl. 2.4.6.2. for cross aisle loading. Both of these approaches have been summarised below for a rack with loads being placed by manually operated mechanical equipment (case a).

Down aisle :- it is permissible to design for a single load of value $2 Q_{ph}$ distributed uniformly over all beam levels. The placement load is calculated to be the maximum value of Q_{ph} determined from a load applied at the top of the rack. In this case, this translates to a load of $(2 \times 0.25/4 \times 1.4) = .175\text{kN}$ at each beam level. As a result, a reduction of 50% in the number of necessary load case combinations containing horizontal placement loads is achieved.

Cross aisle :- the horizontal placement load may be applied in two distinct ways both of which are required to be checked. Firstly, a point load may be applied at the highest beam level (0.25kN). This load may be distributed over all beam levels but there is no advantage in doing this cross aisle as there is no saving in the number of load cases. Secondly, a bending moment may be introduced midway between bracing nodes as shown in Fig. 6.6. :

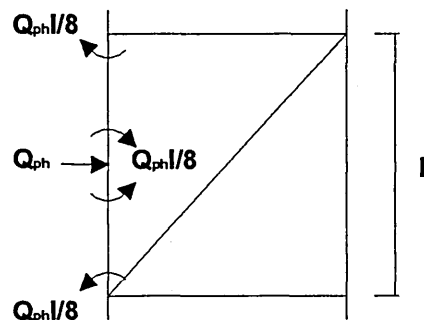


Fig. 6.6. Horizontal placement load bending moment

This will be at the first or second beam level whichever is closer to the middle of a bracing gate. Wherever possible it will also be in the “lowest length of upright” and may

be added to the model without the necessity for carrying out a full, global, cross aisle analysis.

$Q_{ph} = (0.5 \times 1.4 \times 0.9 =) 0.63\text{kN}$ and therefore moments can be added to this example with a value of $(1110 \times 0.63 / 8 =) .087\text{kNm}$.

In the same clause of the code, a load of $0.5 Q_{ph}$ (0.315kN) may be applied at a single beam level. This is required as a local (minor axis) beam check and it is not the intention of the code that this load should be included in the global cross aisle analysis.

6.4.4. Frame imperfections (Cl. 2.5.1.)

The sway imperfection of the rack (ϕ) is calculated using the formula :

$$\phi = \left[\sqrt{\left(\frac{1}{2} + \frac{1}{n_c}\right)} \cdot \sqrt{\left(\frac{1}{5} + \frac{1}{n_s}\right)} \right] \cdot (2\phi_s + \phi_l) \quad (6.2)$$

- n_c = number of uprights in the down aisle direction (7) or connected frames in the cross aisle direction (1)
- n_s = number of beam levels (4)
- ϕ_s = maximum specified out of plumb divided by the height (1/750)
- ϕ_l = looseness of beam-upright connector determined by test (.00528)
($\phi_l = 0$ for braced frames)

$$\phi = .004274 \text{ (down aisle)}$$

$$\text{where } \phi \leq (2\phi_s + \phi_l) \quad .004274 < .00795 \quad \text{ok!}$$

$$\text{and where } \phi \geq (\phi_s + 0.5\phi_l) \quad .004274 > .00397 \quad \text{ok!}$$

$$\text{and where } \phi \geq 1/500 \quad .004274 > .002 \quad \text{ok!}$$

Equivalent down aisle horizontal force applied at each beam level = $\phi \times$ beam level load

$$.004274 \times 6 \times 15.11 = 0.3874 \text{ kN}$$

Considering the rack cross aisle, $\phi = .002191$

where $\phi \leq (2\phi_s + \phi_l)$ $.002191 < .00267$ ok!

and where $\phi \geq (\phi_s + 0.5\phi_l)$ $.002191 > .00133$ ok!

and where $\phi \geq 1/500$ $.002191 > .002$ ok!

Equivalent cross aisle horiz. force applied at each beam level = ϕ x compartment load

$$.002191 \times 15.11 = .0331 \text{ kN}$$

This value is applied to each upright in the frame at each beam level (see Fig.6.8).

6.4.5. Member imperfections (Cl.2.5.)

Member imperfection considerations contained within Cl.2.5.3. may be neglected for (down aisle) global analysis when :

$$\sqrt{\frac{N_{sd}s^2}{EI}} < \frac{\pi}{2} \quad (6.3)$$

for any upright with a design value of axial compression ' N_{sd} ', a gross second moment of area down aisle, I_{yy} and a system length 's' in the plane of buckling which is taken to be the distance between beam levels (MG/FEM/12.42). Member imperfections are not considered in the cross aisle direction because they are only applicable to sway frames with moment resisting connections.

$$\sqrt{\frac{N_{sd}s^2}{EI}} = \sqrt{\frac{60.43 \times 1000 \times 1575^2}{210000 \times 540962}} = 1.149$$

$$1.149 < 1.571 \quad \text{ok!}$$

6.4.6. Bracing system imperfections (Cl. 2.5.2.)

Local bracing imperfections (Cl.2.5.2.2.) in racking systems are taken into account using first order analysis only and have been incorporated into the bracing design check rather than the Ansys model (see section 6.5.5.). Imperfections in the vertical bracing system and its connections (Cl. 2.5.2.1.) have been covered previously in this section (6.3.3.5.).

6.4.7. Accidental vertical load (Cl. 2.6.1.)

“Rack components directly above a unit load should be able to absorb an accidental upward force ...” (A_{pv}) of :

$$A_{pv} \gamma_A = 5.0 \times 1.0 = 5\text{kN} \quad (\text{for manually operated mechanical equipment})$$

γ_A = accidental action load factor from Table 2.2

Experimental data on a single connector lock (see section 5.11.), confirms that the minimum characteristic shear failure of a connector lock system is 5.71kN.

6.4.8. Accidental horizontal load (Cl. 2.6.2.a.)

If pallets are positioned using fork lift trucks as in this case, each upright must be capable of supporting an accidental horizontal overload (A_{ph}) of 2.5kN (cross aisle) and 1.25kN (down aisle), at any height from ground level to 400mm. This additional load can be added into the finite element model, or alternatively, each upright (facing onto an aisle) may be protected over its initial length using a column protector designed to the requirements of Cl.2.6. (*Impact loads*). If accidental loading is to be incorporated within the finite element model, the most critical of the down aisle and cross aisle loading combinations should be considered using the following formula :

$$\sum \gamma_{GA} G_k + \sum_{i \geq 1} \gamma_{QA} Q_{ki} + \gamma_A A_k \quad (6.4)$$

where G_k = characteristic value of permanent action (dead load)
 Q_{ki} = characteristic value of a typical variable action
 A_k = characteristic value of an accidental action applied up to 400mm, Cl.2.6.2. (2.5kN cross aisle, 1.25kN down aisle)
 $\gamma_{GA}, \gamma_{QA}, \gamma_A$ = partial safety factor for each action, = 1.0 (Table 2.2.)

Obviously it is desirable for commercial reasons that if the requirements of this clause can be met without the necessity for column protectors then this should be done, and the accidental loading should in the first instance, be included within the load combinations discussed below.

Equation 6.4. requires that the partial safety factors used should all equate to unity. However, it is the intention of the code that any analysis containing accidental horizontal loading should be done in the ultimate limit state (see Table 2.2). Although this seems contradictory, it was initially envisaged that accidental horizontal loading should be assessed in combination with full vertical loading, imperfection loads and placement loads. This is incompatible with the statement in Cl.4.6. that, “accidental overload shall [not be taken into consideration] at the same time as the horizontal placement load.” Under these circumstances therefore, it has been necessary to omit placement loading from any analysis containing accidental horizontal loading. This is consistent with the formula above and it has therefore been possible to include accidental overload within a serviceability limit state load case (see below).

6.4.9. Load combinations

Finite element models are generated in both the down aisle and the cross aisle direction to determine the most critical combination of loads acting on the three dimensional structure. The large number of potential loading conditions that may occur over the lifetime of a rack have been distilled below (see Fig. 6.7. and 6.8.) into a discrete number of load cases, in accordance with Cl.4.2.2.1. (down aisle) and Cl.4.2.2.2. (cross aisle). These twelve generic cases are considered to form the basis for the majority of racking design. It is recognised however, that there are a number of circumstances under which additional load cases may be required. Such cases may for instance include designs which incorporate braced rack or rack with low level beams. These situations have been examined separately in section 6.4.10.

Where imperfection and placement loading are considered to act on the rack they have been treated as two distinct and separate actions. It is acceptable to consider these loads in one direction only (either down aisle or cross aisle), and when they are taken to act

simultaneously, all 'variable action' loading (including pallet loading) is subject to a reduction factor of 0.9 (Cl.2.7.1.). When considered in the cross aisle direction the imperfection (ϕ) is applied at each beam level as an equivalent horizontal loading. This approach is based on the model appearing in Fig. 4.4.(b) of the FEM code. However, instead of using this method of loading and applying $2\phi w$ to a single upright in the frame, an alternative method has been proposed here with ϕw applied to each upright at each beam level. This has little or no impact on the axial loads and moments around the base of the frame, but more accurately reflects the way in which the application of imperfections may impact on individual bracing gates or members. Additional moments caused locally by 'equivalent' loads are less likely in this instance to have an unwarranted impact on the capacity of the frame.

It is necessary to check the behaviour of a rack design when fully loaded under the various situations outlined above, but in addition pattern loading conditions must also be considered (Fig. 4.1.(a)). This is interpreted as the removal of a central compartment load in the lowest level of the rack and has the effect of increasing the bending moments in the surrounding uprights (down aisle). A conservative approach which has been adopted here, is to assume a maximum value (i.e. a fully loaded condition) for axial load down the upright. This allows the interaction between down aisle and cross aisle analyses to be undertaken at the design checking stage without the problem of combining results which are not in agreement in the lowest levels of the rack. Equally, under these circumstances there is no requirement for any additional pattern load cases in the cross aisle direction which is advantageous in terms of processing time.

When designing a pallet rack, it is not uncommon for the beam deflection limitation ($L/200$, Cl.2.3.4.) to be the overriding consideration in determining its load capacity. In Ansys it is possible to calculate the deflection of a beam in the serviceability limit state by

taking the ultimate limit state deflection from a model and dividing it by the variable action load factor (1.4). This process gives a reasonable approximation of the actual deflection of the beam, although the non-linear nature of the analysis means that complete accuracy cannot be guaranteed. It is clear therefore, that an additional down aisle load case in the serviceability limit state should be included. As well as checking deflection limitations on the beams this load case has been utilised to check the total vertical displacement (sway) at the top of the rack, and the ability of an internal upright to withstand an accidental horizontal placement load. A similar cross aisle load case has also been included to assess the effect of the accidental loading in this direction as well.

All of the points considered in this section have been illustrated graphically in Fig. 6.7. and Fig. 6.8. and these should be regarded as a summary of the minimum number of load cases that are necessary to ensure a satisfactory installation design. An additional point to note when considering these load cases is that cross aisle load case four is not a load case in its own right, but is actually a factored down version of load case two (i.e. $\times 0.9$ to take account of imperfection and placement loads acting together), with additional bending moments simply added to the result in accordance with Cl.2.4.6.2.(2). It is therefore possible to arrive at a solution for this particular case without recourse to an iterative finite element computation.

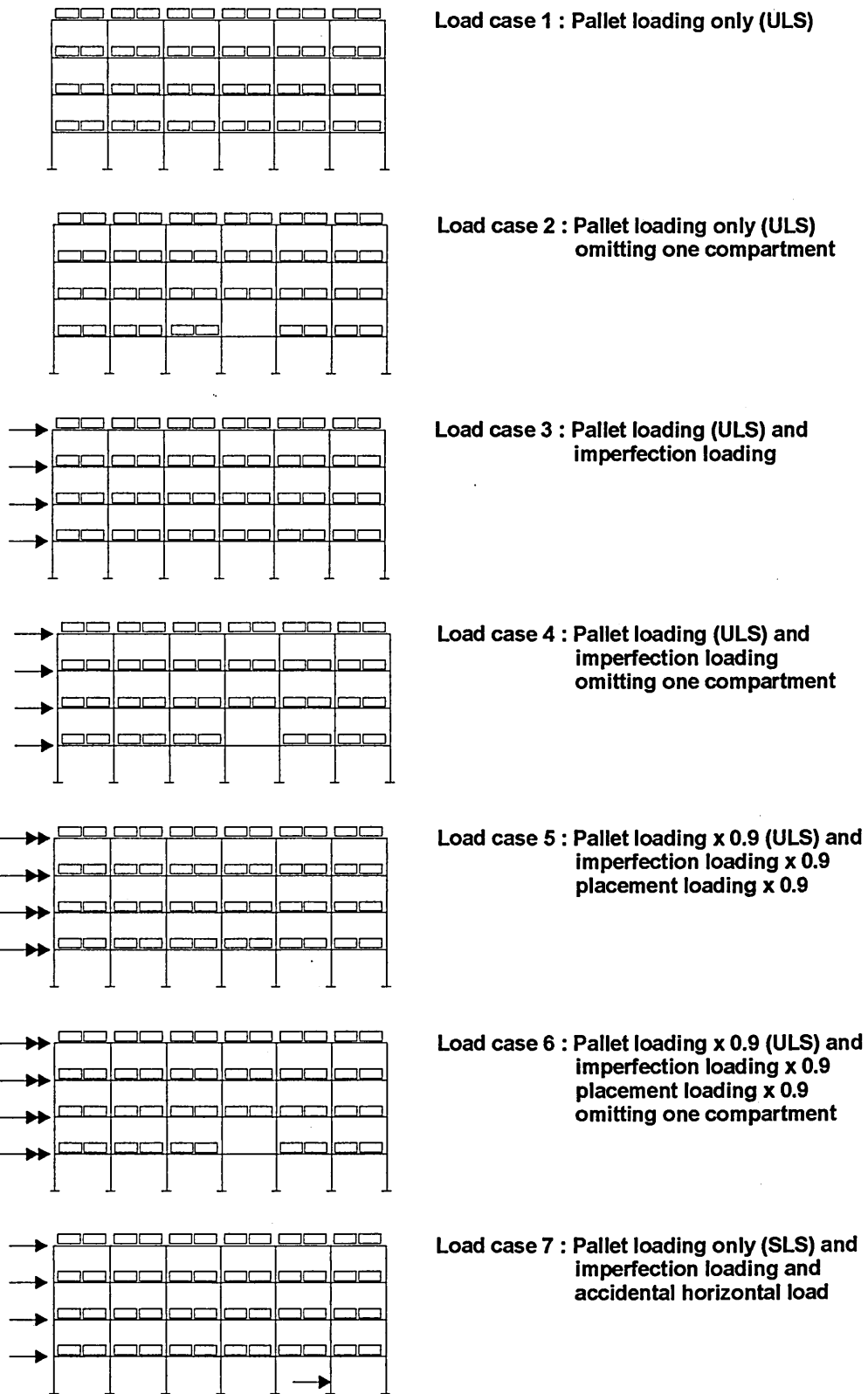
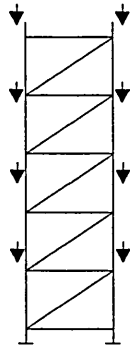
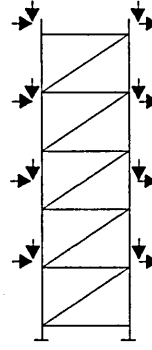


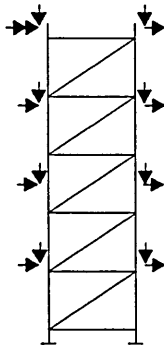
Fig. 6.7. Down aisle load cases - all considered in the ultimate limit state except for load case 7 (serviceability limit state)



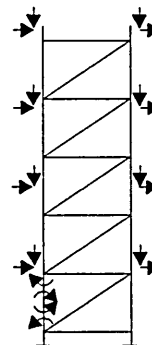
Load case 1 :
Vertical beam loading (ULS)



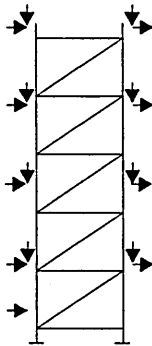
Load case 2 :
Vertical beam loading (ULS)
and imperfection loading



Load case 3 :
Vertical beam loading x 0.9 (ULS)
and imperfection loading x 0.9
and placement loading x 0.9



Load case 4 :
Vertical beam loading x 0.9 (ULS)
and imperfection loading x 0.9
and placement loading x 0.9
(inc. additional mid-gate bending moment)



Load case 5 :
Vertical beam loading (SLS)
and Imperfection loading
and accidental loading

Fig. 6.8. Cross aisle load cases

It is not necessary to consider the interaction between all of the down and cross aisle load cases outlined above. For example, both the imperfection and placement loads only need to be considered in one direction at a time (Cl.2.7.). This ensures that the down aisle load cases three to six can only interact with cross aisle load case one. The combinations which must be examined in order to determine the critical load distribution in the rack can therefore be summarised as follows:

Down aisle load case 1 combined with each load case from :

cross aisle load case 2, 3 and 4.

Down aisle load case 2 combined with each load case from :

cross aisle load case 2, 3 and 4.

Cross aisle load case 1 combined with each load case from :

down aisle load case 3, 5.

Cross aisle load case 1 combined with each load case from :

down aisle load case 4, 6.

Down aisle load case 7 and cross aisle load case 5 are considered independently of other load cases to determine such things as maximum beam deflections, total lateral movement of the rack at its highest point in either direction, and whether the rack can absorb accidental horizontal placement loads in the serviceability limit state.

6.4.10. Additional load cases

As has been mentioned previously, it may be necessary to consider additional load cases to the ones outlined above when, for instance, a low level beam is introduced into the rack. In this instance, “it may be more critical to omit the load from a single beam at the second level” (Cl. 4.2.2.1.notes 1), with the engineer making an assessment as to what constitutes a low level beam. In certain circumstances it may be advisable to perform an

analysis on both alternatives in order that the critical loading condition is not overlooked. The loading pattern which produces this critical loading condition may also be affected by whether the rack is braced. Under these circumstances the pattern load “giving rise to a single curvature in the uprights [see Fig. 6.9.] should also be considered.”

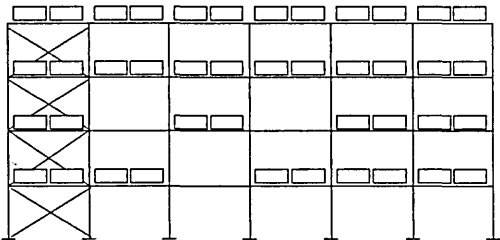


Fig. 6.9. Additional loading pattern - braced rack

6.5. Design checks

6.5.1. Frame design checks

A full set of upright design checks have been included here using the loadings and geometry outlined above. Although a number of down aisle and cross aisle load combinations are normally considered (see section 6.9), only a single interaction has been included here in order to illustrate the methodology. The down aisle analysis includes : pallet loading + imperfection loads + placement loads, and has been combined with a cross aisle analysis supporting design (pallet) loads alone. Significant unity check values from other load case combinations have been commented on where appropriate within the text, and an output of the deformed geometry of the rack is incorporated in App. E.

6.5.2. Bending and axial compression check (Cl. 3.6.1.)

$$\frac{N_{sd}}{N_{c,Rd}} + \frac{M_{ysd}}{M_{c,y,Rd}} + \frac{M_{zsd}}{M_{c,z,Rd}} \leq 1 \quad (6.5.)$$

$$N_{c,Rd} = \frac{f_y A_{eff}}{\gamma_{mc}} \quad (Cl. 3.5.1)$$

$$M_{c,y,Rd} = \frac{f_y W_{effy}}{\gamma_{mc}} \quad M_{c,z,Rd} = \frac{f_y W_{effz}}{\gamma_{mc}} \quad (Cl. 3.4.1)$$

Design value of compressive force in the upright

$$N_{sd} = 54424 \text{ N}$$

As has previously been mentioned, when an analysis in either the down-aisle or cross-aisle direction is performed and placement loading is involved, then all loads acting on the rack in that plane may be multiplied by 0.9. This creates a discrepancy of 10% between cross-aisle and down-aisle solutions with regard to axial loading. In this case, the axial load in the down aisle upright should be used in the interaction formula above, with cross aisle moments added based on the full axial load.

Nominal yield strength

$$f_y = 250 \text{ N/mm}^2$$

Partial safety factor for column material (Table 2.3)

$$\gamma_{mc} = 1.1$$

Effective cross-sectional area (from stub column tests) $A_{\text{eff}} = 436.5 \text{ mm}^2$

The effective section moduli of the cross section are taken from the results of the upright bending tests (see Fig. 3.15(b) and (c) and Cl.3.6.3.(3). Although the test as it has been performed in this document takes lateral-torsional buckling into account and therefore measures $\chi_{\text{LT}} W_{\text{effy}} f_y$ (frames are permitted to twist at their supports), a conservative approach would allow : $M_k = \chi_{\text{LT}} W_{\text{effy}} f_y = W_{\text{effy}} f_y$

$$\begin{aligned} \therefore W_{\text{effy}} &= 11280 \text{ mm}^3 \\ W_{\text{effz}} &= 4915.3 \text{ mm}^3 \end{aligned}$$

Max. down-aisle moment (from Ansys) corresponding with M_{zsd} $M_{\text{ysd}} = 683700 \text{ Nmm}$
 Max. cross-aisle moment (from Ansys) corresponding with M_{ysd} $M_{\text{zsd}} = 8703.9 \text{ Nmm}$

$$\frac{N_{\text{sd}}}{N_{\text{c,Rd}}} + \frac{M_{\text{ysd}}}{M_{\text{c,y,Rd}}} + \frac{M_{\text{zsd}}}{M_{\text{c,z,Rd}}} = 0.823$$

6.5.3. Bending and axial compression without lateral-torsional buckling (Cl. 3.6.2.)

$$\frac{N_{\text{sd}}}{\left(\frac{\chi_{\text{min}} A_{\text{eff}} f_y}{\gamma_m} \right)} + \frac{k_y M_{\text{ysd}}}{\left(\frac{W_{\text{effy}} f_y}{\gamma_m} \right)} + \frac{k_z M_{\text{zsd}}}{\left(\frac{W_{\text{effz}} f_y}{\gamma_m} \right)} \leq 1 \quad (6.6)$$

χ_{min} can be determined using the experimentally derived column curves (Cl. 5.4.5) with the non-dimensional slenderness ratio being calculated from the equations below :

$$\bar{\lambda}_{yy} = \frac{\left(\frac{l_{yy}}{r_{yy}} \right)}{\sqrt{\frac{\pi^2 E}{f_y}}} \left(\sqrt{\frac{A_{\text{eff}}}{A_g}} \right)$$

Elastic Modulus $E = 210000 \text{ N/mm}^2$
 Gross cross sectional area $A_g = 500 \text{ mm}^2$

“The value of $\bar{\lambda}$ is always obtained from the slenderness corresponding to the out-of-plane buckling mode, even when the failure mode is a distortional, torsional flexural or in-plane buckling mode.” This is done to allow “...the column curve to be used in the design and relating buckling loads to down aisle buckling lengths alone.” (Cl.5.4.1.) The

buckling length of an upright (Cl.3.5.2.2.) is equal to its system length, if axial moments and bending moments are determined using second order analysis.

Maximum unsupported down-aisle length of the upright $l_{yy} = 1575 \text{ mm}$

Radius of gyration of the gross section about the relevant axis $r_{yy} = 32.89 \text{ mm}$

$$\bar{\lambda} = 0.4914$$

$$\chi_{\min} = -3.3243\bar{\lambda}^6 + 20.403\bar{\lambda}^5 - 46.927\bar{\lambda}^4 + 50.578\bar{\lambda}^3 - 26.488\bar{\lambda}^2 + 6.1355\bar{\lambda} + 0.5$$

$$\chi_{\min} = 0.922$$

$$\frac{N_{sd}}{\left(\frac{\chi_{\min} A_{\text{eff}} f_y}{\gamma_m}\right)} + \frac{k_y M_{ysd}}{\left(\frac{W_{\text{eff}y} f_y}{\gamma_m}\right)} + \frac{k_z M_{zsd}}{\left(\frac{W_{\text{eff}z} f_y}{\gamma_m}\right)} = 0.870$$

The limiting unity check factor for this design occurs using this interaction formula and combining (see Fig.6.7. and 6.8.) down-aisle load case 3 (pallet + imperfection load) with cross-aisle load case 1 (pallet load only). The unity check factor is 0.98.

Since stress resultants are calculated using second order analysis with global imperfections (both down-aisle and cross-aisle), it is permissible to equate k_y and k_z to 1. Equally, as $\chi_{\min} \leq 1$ it is safe to assume that this check will in all cases produce a more demanding solution than that provided by eq. 6.1. The design check given in Cl. 3.6.1. is therefore superfluous and may be ignored.

It may be possible to enhance the performance of the rack against this design check by determining the value of $W_{\text{eff}y} f_y$ directly, using the test outlined in Fig.5.10.c. - uprights tested with intermittent spacers. Performing these tests is unnecessary however, for reasons that are outlined below in section 6.5.4.

6.5.4. Bending and axial compression with lateral-torsional buckling (Cl. 3.6.2.)

$$\frac{N_{sd}}{\left(\frac{\chi_{\min} A_{\text{eff}} f_y}{\gamma_m}\right)} + \frac{k_{LT} M_{ysd}}{\left(\frac{\chi_{LT} W_{\text{effy}} f_y}{\gamma_m}\right)} + \frac{k_z M_{zsd}}{\left(\frac{W_{\text{effz}} f_y}{\gamma_m}\right)} \leq 1 \quad (6.7.)$$

The design check above is very similar to that contained in eq.6.6., with the exception of the central term which has been modified to take the possibility of lateral torsional buckling into account. $\chi_{LT} = 1$ when $W_{\text{effy}} f_y$ is determined by the frame test contained in Fig.5.10.1(b) of the FEM code. This is considered to be the case for any rack which has a maximum unsupported down aisle length (usually considered to be the height to the first beam level) that is less than or equal to the unsupported length of the test specimen used in the upright bending tests (3.2m). When the maximum unsupported length of upright in the rack is over 3.2m, χ_{LT} should be calculated according to Cl.3.4.4.

The value of k_{LT} which replaces k_y in this formula, must be less than or equal to one. If a conservative approach is adopted and k_{LT} is set to unity, then eq.6.6. and eq.6.7. can be considered to be identical. This assumption is true for any rack having a maximum unsupported upright length of up to 3.2m. For structures beyond this length, k_{LT} and χ_{LT} should be calculated to determine a value for this unity check. The formula above can therefore be evaluated as :

$$\frac{N_{sd}}{\left(\frac{\chi_{\min} A_{\text{eff}} f_y}{\gamma_m}\right)} + \frac{k_{LT} M_{ysd}}{\left(\frac{\chi_{LT} W_{\text{effy}} f_y}{\gamma_m}\right)} + \frac{k_z M_{zsd}}{\left(\frac{W_{\text{effz}} f_y}{\gamma_m}\right)} = 0.870$$

6.5.5. Design of bracing in upright frame

$$\frac{N_{j\text{sd}} + NX_{j\text{sd}}}{\left(\frac{\chi_{\text{min}} A_{\text{eff}} f_y}{\gamma_M}\right)} + \frac{N_{j\text{sd}} e_j}{\left(\frac{W_{\text{effz}} f_y}{\gamma_M}\right)} \leq 1 \quad (6.8)$$

Local bracing imperfections (Cl. 2.5.2.2) are applicable to the rack design based on first order analysis only. The value of additional axial load in the diagonal bracing member ($NX_{j\text{sd}}$) due to these imperfections is :

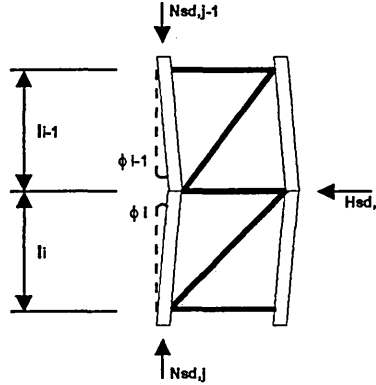


Fig. 6.10. Treatment of local bracing imperfections

Bracing gate height	$l_i = 1200 \text{ mm}$
	$l_{i-1} = 1200 \text{ mm}$
For uprights without splices	$\phi_0 = 2.5 \times 10^{-3}$
Uprights per bracing system	$nu = 2$

When $l_i \leq l_{i-1}$:

$$\phi_{i-1} = \sqrt{\left[\frac{1}{3} + \frac{2}{nu}\right]} \cdot \phi_0 = 2.887 \cdot 10^{-3}$$

$$\text{but } \phi_{i-1} \leq \phi_0$$

$$\therefore \phi_{i-1} = \phi_i = 2.5 \cdot 10^{-3}$$

Partial safety factor for bracing material (table 2.3.)

Design axial load in an upright member (from Ansys)

Initial geometric imperfection applied as a horizontal force

$$\gamma_m = 1.1$$

$$N_{sdi-1} = 54424 \text{ N}$$

$$N_{sdi} = 54424 \text{ N}$$

$$H_{sdi} = N_{sdi-1} \cdot \phi_{i-1} + N_{sdi} \cdot \phi_i$$

$$H_{sdi} = 272.12 \text{ N}$$

Bracing width (horizontal distance between bracing welds, SD)

Bracing height (vertical distance between bracing welds)

Bracing diagonal angle

$$br_w = 798.4 \text{ mm}$$

$$br_h = 1020 \text{ mm}$$

$$br_a = 0.907 \text{ Rads.}$$

Axial force for local bracing imperfections :

$$NX_{j\text{sd}} = \frac{H_{\text{sdi}}}{\cos(\text{br}_s)} = 441.48 \text{ N}$$

Design axial load in critical bracing member (taken from Ansys)
Effective length of critical member (K=0.9, Cl.3.5.2.2.d.)

$$N_{j\text{sd}} = 175 \text{ N}$$

$$l_{\text{eff}} = 1165 \text{ mm}$$

Radius of gyration of the gross section about the relevant axis

$$r_{yy} = 20.32 \text{ mm}$$

$$r_{zz} = 7.9 \text{ mm}$$

Effective cross sectional area (Cl. 5.9.)

$$A_{\text{eff}} = 42.506 \text{ mm}^2$$

Imperfection factor about the relevant axis (from Fig. 3.10)

$$\alpha_{yy} = 0.34$$

$$\alpha_{zz} = 0.34$$

Effective section modulus

$$W_{\text{effzz}} = 524.4 \text{ mm}^3$$

Distance between load centre and centroid

$$e_j = 21.95 \text{ mm}$$

$$\bar{\lambda}_{yy} = \frac{\left(\frac{l_{yy}}{r_{yy}}\right)}{\sqrt{\frac{\pi^2 E}{f_y}}} \left(\sqrt{\frac{A_{\text{eff}}}{A_g}}\right) = 0.436 \quad \text{and} \quad \bar{\lambda}_{zz} = \frac{\left(\frac{l_{zz}}{r_{zz}}\right)}{\sqrt{\frac{\pi^2 E}{f_y}}} \left(\sqrt{\frac{A_{\text{eff}}}{A_g}}\right) = 1.123$$

To calculate the minimum value of χ (Cl. 3.5.2.):

$$\chi_{yy} = \frac{1}{\phi_{yy} + (\phi_{yy}^2 - \bar{\lambda}_{yy}^2)^{0.5}} \leq 1$$

$$\phi_{yy} = 0.5 \left[1 + \alpha_{yy} (\bar{\lambda}_{yy} - 0.2) + \bar{\lambda}_{yy}^2 \right]$$

$$\chi_{yy} = 0.912$$

(similarly) $\chi_{zz} = 0.522$

\therefore use $\chi_{\text{min}} = 0.522$

$$\frac{N_{j\text{sd}} + NX_{j\text{sd}}}{\left(\frac{\chi_{\text{min}} A_{\text{eff}} f_y}{\gamma_M}\right)} + \frac{N_{j\text{sd}} e_j}{\left(\frac{W_{\text{effzz}} f_y}{\gamma_M}\right)} = 0.093$$

\therefore ok!

6.5.6. Sway limit in the down aisle direction at serviceability limit state

Limiting values of deflection for sway (down aisle) are defined in Cl.2.3.4. and reiterated in Cl.4.2.3. for the load combinations detailed in Cl.2.7.2. Sway is defined as total lateral movement of the structure from the vertical, taking the actions arising from the application of imperfection loads (but not placement loads) and the effect of the initial out of plumb of the rack into account on the fully loaded structure. The maximum out of plumb of the structure in any direction shall be height/350 “in the unloaded condition immediately after erection” (Cl.1.13.1.). This is an upper limit and therefore, if it can be shown that a higher measure of verticality is achieved consistently in practice, then this revised value may be used. In general, rack structures should be analysed in the serviceability limit state taking second order effects into account.

Maximum height of rack (h)		= 6300 mm
Limiting value of sway at the top of the rack (S_{lim})	= h/200	= 31.5 mm
Total horizontal movement in top of the structure (S_{act})		= 31.36 mm

$$\frac{S_{act}}{S_{lim}} \leq 1$$

$$\frac{S_{act}}{S_{lim}} \leq 0.996 \quad \therefore \text{ok!}$$

6.5.7. Floor connector check

When a racking structure is considered (conservatively) to be pinned at its base, it will clearly ‘attract’ zero moment to its floor connectors. Under these circumstances the moment that is generated within the rack under load, may be ‘absorbed’ by the beam end connectors and will be taken into consideration in the beam design checks. Clearly, there is no need for a moment capacity check on the floor connector under these circumstances. Equally, when a rack is designed using combin40 elements within the

finite element model, the base moments are taken into account within that analysis and a limitation on the moment capacity of the base is therefore inherent within the design. A separate floor connector design check in this case is also unnecessary. However, when the behaviour of the baseplate is considered within Ansys using the spring damper element (combin 14) as in this example, a single stiffness is attributed to the baseplate performance. Under these circumstances, it would seem appropriate to have a moment limitation check on the value of the connector design moment. A design check has been added here therefore to compare the value of design bending moment that the model develops against the floor connectors bending resistance, despite such a check having been omitted from the code of practice.

The moment of resistance of the floor connector is axial load dependent and a polynomial expression for axial load against moment resistance has been derived from experimental information in Chapter 4, and used here to calculate a design resistance moment.

Design bending moment - floor connector (from Ansys)
 Design resistance moment (Cl. 5.8.)

$M_{sdfc} = 320840 \text{ Nmm}$
 $M_{Rdfc} = 0.897 \cdot 10^6 \text{ Nmm}$

$$\frac{M_{sdfc}}{M_{Rdfc}} \leq 1$$

$$\frac{M_{sdfc}}{M_{Rdfc}} \leq 0.35$$

∴ ok!

6.6. Beam design checks

6.6.1. Beam end connector check (Cl. 4.5)

Re-distribution of bending moments in the case of elastic analysis (Cl. 4.4.3.1) assuming linear behaviour of the connector may be undertaken if necessary. This bending moment may be redistributed into the connected beam by anything up to 15%, with an allowance made for a corresponding increase in the beams design bending moment. As with the floor connector, using the combin 40 element type for the finite element model allows an automatic re-distribution of moments about the structure. The use of this element obviates the need to take an arbitrary value of 15% into account and as a result it may be assumed that a more accurate assessment of the behaviour of the rack may be determined.

Design bending moment (from Ansys)
Design resistance moment (Cl. 5.5.)

$$M_{sdbec} = 968635 \text{ Nmm}$$
$$M_{Rdbec} = 1.507 \cdot 10^6 \text{ Nmm}$$

$$\frac{M_{sdbec}}{M_{Rdbec}} \leq 1$$

$$\frac{M_{sdbec}}{M_{Rdbec}} \leq 0.643 \quad \therefore \text{ok!}$$

with 15% re-distribution included (combin 14) :

$$\frac{M_{sdbec}}{1.15 \cdot M_{Rdbec}} \leq 0.559$$

Design shear force (from Ansys)
Design shear resistance (Cl. 5.7)

$$V_{sdbec} = 7029 \text{ N}$$
$$V_{Rdbec} = 38100 \text{ N}$$

$$\frac{V_{sdbec}}{V_{Rdbec}} \leq 1$$

$$\frac{V_{sdbec}}{V_{Rdbec}} \leq 0.184 \quad \therefore \text{ok!}$$

6.6.2. Moment of resistance of members not subject to lateral buckling (Cl. 3.4.1)

$$M_{sd} \leq M_{cRd}$$

Bending moment due to design load (from Ansys)
Section modulus of effective cross section

$$\begin{aligned} M_{sd} &= 3950000 \text{ Nmm} \\ W_{\text{effmax}} &= 19817 \text{ mm}^3 \\ W_{\text{effmin}} &= 7818 \text{ mm}^3 \end{aligned}$$

The calculation of the section properties of non-perforated members shall, in general be based on the effective cross section determined from appendix D of the FEM code.

Bending moment resistance of the section : $M_{cRdmax} = f_y \frac{W_{\text{effmax}}}{\gamma_{mb}} = 7.5 \times 10^6 \text{ Nmm}$

$$\frac{M_{sd}}{M_{cRdmax}} \leq 0.527 \quad \therefore \text{ok!}$$

This check should be used when the beam end connector design bending moment has been found to be lower than the design resistance moment ($M_{sdbec} < M_{rdbec}$), or when the multi-linear spring element (combin40) is in use in Ansys, thereby redistributing moment from the connectors automatically. However, if $M_{sdbec} > M_{rdbec}$ then a redistribution of 15% of the connector moment is permitted (see section 6.6.1.) leading to a corresponding increase in beam design moment (Fig. 4.6.) as follows :

$$M_{sd} + 0.088M_{Rdbec} \leq M_{cRdmax}$$

$$4.08 \times 10^6 \leq 7.5 \times 10^6 \quad \therefore \text{ok!}$$

6.6.3. Beam design with respect to shear (Cl. 3.4.5)

$$\frac{V_{sd}}{V_w R_{db}} \leq 1$$

Design shear force (from Ansys)

$$V_{sd} = 7029 \text{ N}$$

Design shear resistance (Cl. 3.4.5.1) for a single web subject to shear force

$$V_w R_d = \frac{\tau_w S_w t}{\gamma_{mb}} = 41.1 \text{ kN}$$

Design shear resistance for beam

$$V_w R_{db} = 2V_w R_d = 82.2 \text{ kN}$$

Values of characteristic mean shear stress (τ_w) are taken from table 3.1 of the code “for web with stiffeners at support”, the beam end connector having been designed to prevent distortion of the web and to carry the full support reaction force. τ_w is dependent on the value of $\bar{\lambda}_w$ calculated using the equation :

$$\bar{\lambda}_w = 0.346 \frac{S_w}{t} \sqrt{\frac{f_y}{E}} = 0.840$$

Yield strength of beam material

$$f_y = 417 \text{ N/mm}^2$$

Design thickness of the web

$$t = 1.78 \text{ mm}$$

Distance between the points of intersection of the system lines of the web and flanges (Fig 3.7)

$$S_w = 97 \text{ mm}$$

as $0.84 < \bar{\lambda}_w < 1.38$ then

$$\tau = 0.48 \frac{f_y}{\bar{\lambda}_w} = 238.23$$

Partial material safety factor for beams (Cl. 2.7.4)

$$\gamma_{mb} = 1.0$$

$$\frac{V_{sd}}{V_w R_{db}} = 0.09 \quad \therefore \text{ok!}$$

6.6.4. Design strength of beams with respect to web crippling (Cl.3.4.6)

$$\frac{R_{sd}}{R_s R_d} \leq 1$$

Design force due to concentrated load or support reaction (from Ansys) $R_{sd} = 7029 \text{ N}$

Design crippling resistance of a section with more than one web 3.4.6.3

$$R_s R_d = \frac{\alpha_i t^2 \sqrt{f_y E} \left(1 - 0.1 \sqrt{\frac{r}{t}}\right) \left(0.5 + \sqrt{0.02 \frac{la}{t}}\right) \left(2.4 + \left(\frac{\phi}{90}\right)^2\right)}{\gamma_{mb}}$$

Internal bend radius adjacent to the point of application of load

$$r = 3.17 \text{ mm}$$

Angle between the plane of the web and that of the bearing surface

$$\phi = 90^\circ$$

Overall web depth (see Table 3.2)

$$h_w = 95 \text{ mm}$$

Values of a_i and l_a depend on the category of load defined in Cl.3.4.6.3(4)

Bearing length $l_a = 10 \text{ mm}$
 Imperfection factor $\alpha_i = 0.57$

$$\frac{R_{sd}}{R_a R_d} = 0.169 \quad \therefore \text{ok!}$$

Guidance in Fig. 3.6(a) indicates that beam sections (open and box) are not likely to suffer critical lateral torsional buckling

6.6.5. Beam design with respect to horizontal placement loading (Cl. 2.4.6.2.(3))

In the cross-aisle direction, a load of $0.5Q_{ph}$ may be carried by a single beam in the horizontal plane through the neutral axis. Interaction with the vertical load causing Q_{ph} may be ignored. It is not a requirement of the code that this load should be included in the global analysis.

$$\frac{M_{S_{dym}}}{M_{cR_{dmin}}} \leq 1$$

Design strength moment due to point load (minor axis) :

$$M_{S_{dym}} = \frac{0.5Q_{ph}\gamma_Q L}{4} = 0.236 \text{ kNm}$$

Beam span

$$L = 2700 \text{ mm}$$

Load factor for variable actions (table 2.2)

$$\gamma_Q = 1.4$$

Horizontal placement load

$$Q_{ph} = 500 \text{ N}$$

Bending moment resistance of the beam (minor axis) :

$$M_{cR_{dmin}} = \frac{f_y W_{effmin}}{\gamma_{mb}} = 3.26 \text{ kNm}$$

$$\frac{M_{S_{dym}}}{M_{cR_{dmin}}} = 0.072 \quad \therefore \text{ok!}$$

6.6.6. Combined bending moment and shear force (Cl. 3.4.7)

$$\left(\frac{M_{sd}}{M_{cRdmax}}\right)^2 + \left(\frac{V_{sd}}{V_{wRd}}\right)^2 \leq 1$$

$$\left(\frac{M_{sd}}{M_{cRdmax}}\right)^2 + \left(\frac{V_{sd}}{V_{wRd}}\right)^2 = 0.286 \quad \therefore \text{ok!}$$

6.6.7. Combined bending moment and concentrated load (Cl. 3.4.8)

It shall be verified that :

$$\frac{M_{sd}}{M_{cRdmax}} \leq 1 \quad \text{when} \quad \frac{R_{sd}}{R_s R_d} \leq 0.25$$

$$\frac{M_{sd}}{M_{cRdmax}} = 0.527 \quad \text{when} \quad \frac{R_{sd}}{R_s R_d} = 0.09 \quad \therefore \text{ok!}$$

6.6.8. Beam deflection check in the serviceability limit state (Cl. 2.3.4)

Maximum allowable vertical deflection (Cl. 2.3.4.) $\delta_{all} = \frac{L}{200} = 13.25 \text{ mm}$

(In a cantilever the deflection limit may be increased to L/100.)

Maximum beam deflection (from Ansys) $\delta_{max} = 12.27 \text{ mm}$

$$\frac{\delta_{max}}{\delta_{all}} \leq 1$$

$$\frac{\delta_{max}}{\delta_{all}} = 0.926 \quad \therefore \text{ok!}$$

6.7. Summary and conclusions

This chapter summarises the major considerations necessary for the successful analysis of a racking system to the requirements outlined in the FEM code. An exploration into the most suitable way in which to create a finite element model using the experimental properties developed in chapters four and five has been undertaken. This has been completed in conjunction with an examination of second order analysis techniques, in order to generate appropriate moments and deflections to be used in subsequent design calculations. Of particular concern has been the treatment of semi-rigid connections, both at the base of the structure and also at the beam / upright interface, and this has been examined in some detail.

A full design procedure has been completed using a specified rack as an example. This has allowed full consideration to be given to the various load conditions and calculations that need to be addressed prior to the initiation of an analysis. Consideration has been given to pallet loads, placement loads, imperfections and associated loads, and accidental loading conditions. In addition to this, a discussion of the load combinations necessary for a full analysis has been undertaken, together with some conclusions on the manner in which they should be combined, particularly with regard to the interaction formulae. Additional load cases for 'special' designs has been examined briefly.

Following on from this, is a full summary of the design checks that are necessary for a satisfactory design. Although all load combinations outlined previously were completed, it was not thought practical to annotate more than a single design case. The one chosen includes pallet loading, imperfection loading and placement loading in the down aisle analysis, and was chosen for its slightly greater complexity in comparison to other combinations (with a 0.9 load factor). A similar rack has been examined in chapter 7, using the SEMA code in order that appropriate design comparisons may be drawn.

Chapter 7

A Comparison of Rack Performance based on Limit State and Permissible Stress Design Code Methodologies

7.1. General outline

This chapter examines the major differences in the approaches adopted by both the SEMA and FEM code. This has been done initially by considering the way in which experimental performance data has been obtained and subsequently analysed. Particular scrutiny has been given to an examination of the behaviour of the beam end connector with respect to moment capacity, rotational stiffness and looseness, to the floor connector, and to the performance of the upright.

To permit a full comparison of the design methodologies, a rack design has been included in line with SEMA guidelines. This has enabled consideration to be given to the major design and analysis differences that exist between the codes and they have been summarised here. A Visual Basic programme has also been written by the author (see App. E), with the intention of optimising load capacities for SEMA designed racking against variations in the material, geometric or cross sectional properties of the rack. The programme has been used in this chapter to allow a comparison between maximum load carrying capacities determined by each code, for a select number of racking configurations. Fifty six analyses have been completed, from which an assessment has been made as to the impact of the FEM code on the UK racking industry. This is the only analysis currently available which demonstrates the efficacy of the new code.

In addition, a sensitivity analysis has been performed on (24) FEM designed racks, in order that a greater appreciation can be made of the significance of changes to key aspects of the rack. These include variations to the upright yield stress, beam connector looseness, moment capacity and rotational stiffness, and floor connector stiffness. An

assessment has been made of the effect of these variations on the capacity of the rack, in order that any future re-design of components can be targeted judiciously.

7.2. Treatment of experimental data

7.2.1. Introduction

There are key differences between the approach adopted by the FEM and that adopted by the SEMA code. This is not merely limited to the way in which the design itself is analysed, but also extends to the consideration and treatment of experimental data. In addition to this, a number of tests required by the FEM are either assessed in a different manner by SEMA or not included at all. This section is intended to present an examination of some of the key differences between the codes, and highlight the effect of the change in emphasis on the design of future racking systems.

7.2.2. Beam end connector performance

It has already been demonstrated in this document that the behaviour of the beam end connector has an important bearing on the determination of the load carrying capacity of a racking system. It is clear therefore that the way in which the experimental data is interpreted may have a significant impact on the subsequent analysis. A comparison has been made here between what has been seen as acceptable practice to date, and the methodology that is intended to supersede it. Initially, consideration has been given here to the determination of the beam end connector design moment. In Fig. 7.1. and 7.2. below, experimental data has been interrogated using the approach adopted by each code, to produce design values for a range of beams tested with standard duty (SD17) and heavy duty (HD30) uprights. Conclusions have been drawn on the basis that during the time that has elapsed since the latest SEMA test program was initiated and the present day, there have been no significant or discernible alterations in either the

geometry of the system, the materials used in its production or in the methods employed for the manufacture of its component parts.

In comparing the design moment values established within this document for the FEM code (marked FEM in the legend overleaf) and those for the SEMA code (marked SEMA), it is clear that the former has benefited substantially from the new methodology. The improvement in performance values is in the order of 15% to 29% for beams on SD17 uprights and 23% to 36% for beams on HD30 uprights. This can be explained largely as a result of variations in the approach adopted by each code. A determination of the allowable moment required under SEMA design rules is calculated as the lesser of “half of the failure moment or two-thirds of the moment at which harmful or objectionable distortions occur”. This ensures that the allowable moment can have a maximum value equivalent only to 50% of the ultimate moment. In contrast, the FEM treatment which has been examined in some detail in section 4.10.2., allows design values to be determined using statistical analysis to characterise results with a greater degree of certainty than has previously been possible. The implication of this is that a substantial number of tests (10 per upright/beam combination in this case) are required to be carried out in order that the full benefits of this approach may be appreciated. In the case of the SEMA test procedure there is a specified minimum number of tests (3) that must be performed to determine a mean failure moment, but no statistical benefit can be accrued from doing any further tests. The result is that an equivalent connector may be permitted to develop much higher moments before a design is deemed to have failed.

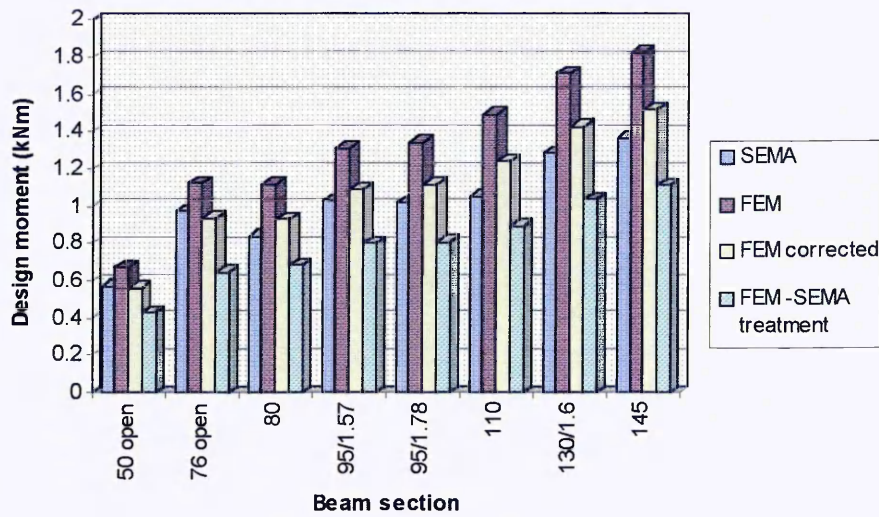


Fig. 7.1. Beam end connector design moment comparisons (kNm) for a range of beams tested with SD17 uprights.

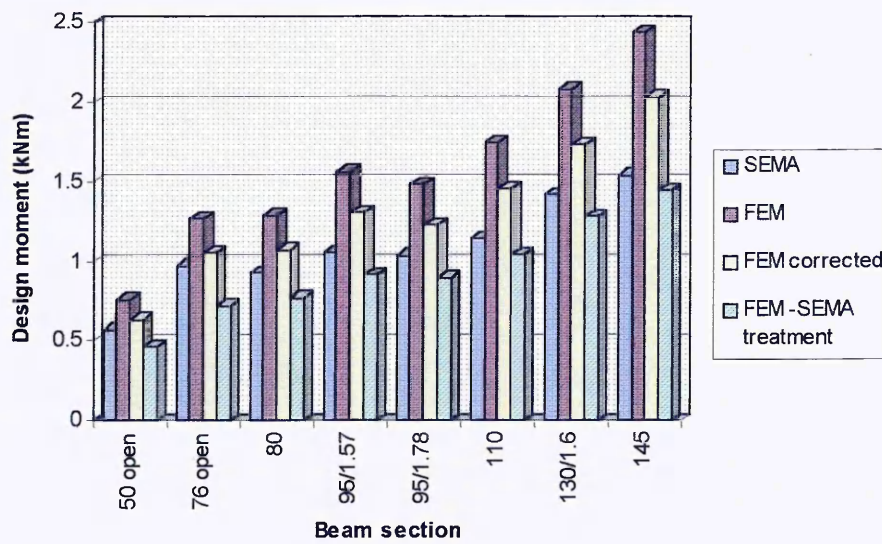


Fig. 7.2. Beam end connector design moment comparisons (kNm) for a range of beams tested with HD30 uprights.

A third column on the graph (marked FEM corrected) represents the result of yield stress and thickness corrections on the experimental data. This has been done using formula 4.1.

Although this approach was included in the original draft of the code, it has been omitted from the final version, with the authors preferring to remain consistent with the SEMA code in allowing engineering judgment to govern the analysis of the results. “The Engineer shall be satisfied that ...” [the yield and thickness of the test sample] “... are acceptably close to the nominal values ...”. A further consideration which reinforced the decision to omit the equation above from the code, was the degree of confidence which could be placed in the identification of the failed component in a system, and as a result which yield stresses should be used for the purposes of correction.

The greatest impact on the value of M_{ni} in equation 4.1., and consequently on the design moment will in general be the potential variation in actual yield stress of each sample in relation to its nominal value. The lack of guidance in the code may mean that a ratio of actual to nominal yield stress in the region of 250/280, which effectively translates to a 10% reduction in the corrected failure moment value, may be interpreted as ‘acceptable’ and therefore ignored when a determination is being made of the value for the design moment. In essence, this may lead to variations in the approach of individual engineers to the design of racking and by implication inconsistencies in the performance of individual structures. If engineering judgment is to be used, it may be more appropriately employed to determine which component has failed during testing, in order that corrections may be applied to results in a consistent manner.

An examination of the ‘FEM corrected’ columns in Fig. 7.1. and 7.2. demonstrates that there is a marked decrease in the performance of the connector across the range of beams tested in comparison with the uncorrected FEM values. In addition, there is much

greater correspondence between these results and the SEMA results, and while this not necessarily desirable, it is clear that only a treatment which incorporates a reduction in design moment values for variations in the thickness and yield of test samples can be considered to be conservative in its approach.

The final column on the graphs (marked FEM-SEMA treatment) indicates the value of FEM results calculated using SEMA design rules. These values are approximately 30% to 40% lower than if they were considered using FEM design recommendations, and in addition are in every case lower than the equivalent SEMA values by between 7% and 35%. This may be accounted for by differences in sample yield stresses between the two sets of test results and demonstrates the value of using equation 7.1. for the purposes of analysis. These differences may have been exacerbated by the small sample size tested under the SEMA code (3 tests per beam/upright combination), giving a less representative outcome than the relatively large sample size tested under the FEM experimental design procedure (10).

An examination of the connector stiffness values displayed in Fig.7.4. and Fig.7.5. demonstrates that due to the non-linear nature of the moment-rotation response, the method by which the respective codes calculate these values tends towards higher design stiffness' for lower values of design moment. The comparison between SEMA and FEM results confirms this to be the case, with results analysed using the SEMA code being between 2% and 29% greater than their FEM equivalents using SD17 uprights, and 5% and 22% with HD30 uprights.

This tendency is moderated against to some extent by the methodology employed in each code to determine the individual test stiffness values as demonstrated below in Fig.7.3. :

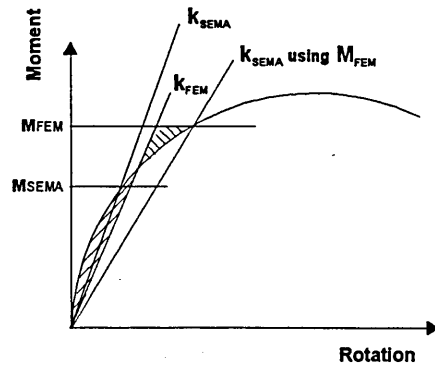


Fig 7.3. SEMA and FEM approach to the determination of beam end connector stiffness

The FEM adopts an ‘equal areas approach’ (see section 5.3.3.) which allows higher values of stiffness to be determined than the SEMA code for comparative design moments. The determination of experimental stiffness ‘k’ using the SEMA approach can be summarised as follows :

“...k may be found from the slope of a line drawn from the origin which intersects the moment-rotation curve at a working moment equal to half the failure moment...”

It is therefore possible for some of the advantages in terms of higher stiffness values gained as a result of the lower levels of design moment under SEMA, to be diminished by an FEM code which adopts a more ‘sympathetic’ approach to determining design stiffness values.

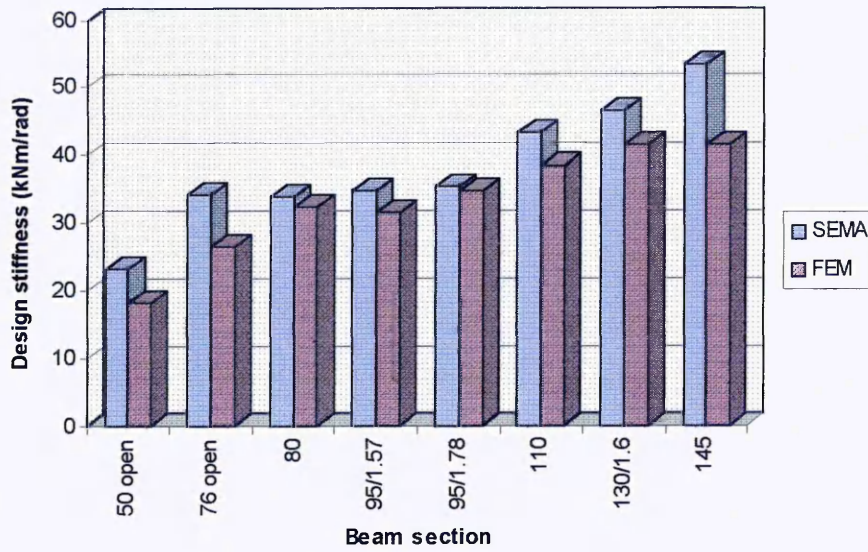


Fig. 7.4. Beam end connector design stiffness comparisons (kNm/rad) for a range of beams tested with SD17 uprights.

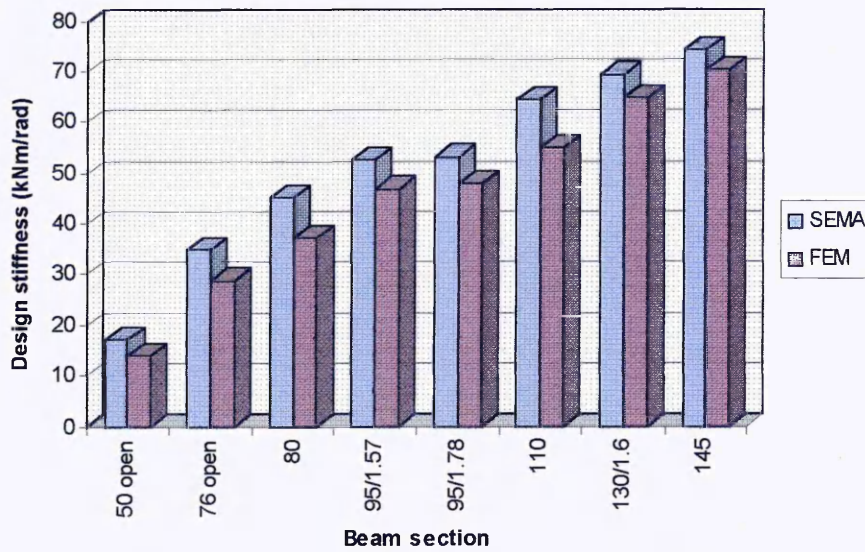


Fig. 7.5. Beam end connector design stiffness comparisons (kNm/rad) for a range of beams tested with HD30 uprights.

Indications are from the test results, that this procedure develops much lower looseness values for the same beam-upright combinations when compared with results determined using the FEM test methodology. An examination of respective results reveals that, for combinations of HD30 upright with any beam, the FEM looseness value is taken to be 0.00431 rads which compares unfavourably with the corresponding SEMA value of 0.0012 rads. This inequity, which is typical across the entire range of uprights examined, leads to inconsistencies in the value of imperfection loads applied to the rack, and a consequent and possibly overly conservative reduction in the load capacity of the FEM designed rack. The relationship between looseness variations and rack payload is explored in more depth in section 7.6.2. of this chapter.

The reason for this anomaly between looseness values is due to a divergence of approach between the codes when consideration is given to what constitutes the true behaviour of the rack. Under the SEMA code looseness is assessed, as has already been demonstrated, on the basis that two connectors around an upright constitute the most appropriate predictor of the actual behaviour of the joint. 'Interference' between left and right hand connectors which may reduce looseness is therefore taken into consideration, together with variations in the positive and negative rotational capacity of the connectors about the upright, which may also effect the degree of looseness. However, the SEMA value for looseness, while taking account of each of these behavioural characteristics is potentially unconservative in one respect. This concerns racking with a limited number of bays (one or two for instance). Under these circumstances the looseness of a single connector attached to an end upright may be the predetermining factor when consideration is being given to the initial imperfections in the rack. As a result, the FEM test on a single connector can be seen as a more appropriate reflection of the practical situation. Consequently, the 'interference fit' described above which concerns itself with

the geometric variations and manufacturing tolerances of the connector, will clearly not be as applicable. Under circumstances such as these therefore, the design might be considered to be unconservative using the SEMA model.

In contrast, the FEM code which examines the behaviour of individual connectors around an upright (see section 5.4.2.) may be seen as being overly conservative in general design. No consideration is given to the effect of the interaction between connectors at a given joint on lessening the looseness at that joint, and as a result, for the majority of joints in a structure (except the end frames) the looseness is unnecessarily large. If the comparison made here between the results of tests using each codes method is indicative of the disparity of performance then looseness is being over estimated by in excess of 300%. Obviously, this will have an impact on the load carrying capacity of the rack.

It would seem appropriate under these circumstances to take aspects of the looseness test from each code and incorporate them into the design procedure. Using Ansys 5.4., it is possible to develop a design with values of looseness appropriate to the characteristics of each joint (i.e. one or two connectors), so that internal joints will display the behaviour associated with connectors whose looseness had been measured using the SEMA test model, while end uprights would display behaviour associated with FEM tested connectors. This process can be modeled using the same design procedure identified in Chapter 6, but with Combin40 elements having an additional 'Gap' element associated with them. This new element would allow variable looseness values to be present within a single rack, thereby permitting the rotation of uprights and beams under load in a way that is appropriate to those looseness values (see Fig.7.7.).

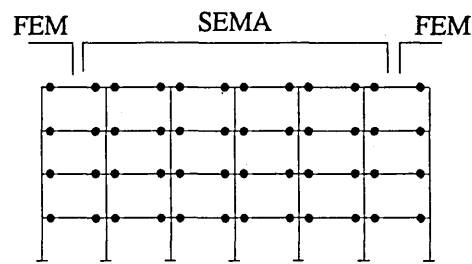


Fig. 7.7. Proposed treatment of looseness for internal and external beam end connectors based on test values determined under specified test conditions.

Using this technique, no moment can be transmitted through the connector until it has rotated sufficiently to absorb all of its inherent looseness. The variability of looseness in the rack would not cause any difficulties as far as the calculation of the imperfection loads is concerned as a sentence addressing this approach was submitted by the author of this document for inclusion in the FEM code. This reads :

“If the effect of the looseness of the beam to upright connector is included in the modelling of the connection used in the global analysis, [the value of looseness] may be set to zero in the [sway imperfection calculation].”

Despite this, at present it is not possible to include the SEMA test data within the existing FEM design code. It is hoped that following the 18 month assessment of the code that is presently ongoing, a submission to the FEM technical committee along the lines outlined above will allow the introduction of this approach to design.

7.2.4. Floor connector performance

The performance of the base of the rack in terms of its rotational stiffness, and the relationship between the axial loading on the upright at its interface with the floor and its moment capacity, are not specifically addressed within the SEMA code. Any consideration of the effect of altering the baseplate design has been limited to the incorporation of a variable slenderness ratio in the determination of the permissible axial

stress on an upright. In general, this is based on a perceived fixity between the baseplate and the floor, and is conditional only upon whether there is one fixing at either side of the upright ($k=1.25$), or whether there is a single fixing or no fixing present ($k=1.5$). The value of 'k' in this context is the ratio of the effective column length to its actual unbraced length, and represents the influence of restraint against rotation and translation at both ends of the column. For a single bay of racking k increases to 2.

Clearly, a more detailed examination of the performance of the baseplate and its response to variations in axial loading, as required by the FEM, must be advantageous in the accurate determination of rack behaviour. This is particularly true with the development and incorporation of second order analysis techniques into rack design.

It is also clear that the FEM treatment of the baseplate overcomes one of the major difficulties of the SEMA code, by designing out the use of the 'k' value altogether. The permissible axial stress is a function of the slenderness of the section ($\lambda=Le/r$), with the effective length being a function of the end fixity. In reality, as demonstrated by this thesis in section 4.3.10., the moment capacity and the rotational stiffness of the base-column connection vary in response to changes in the axial load down the column. In essence, the end condition at the base of the column is redefined relative to the applied axial load during the design process, so that under SEMA rules a higher axial load should be expected to lower the value of k with the connection tending towards fully fixed behaviour. This is not reflected in the SEMA code of practice, which permits the use of effective lengths based on end fixity alone and takes no account of axial loading in the evaluation of permissible axial stress'.

It is clear therefore that SEMA values of 'k' can only ever be approximate, particularly under conditions of analysis which take second order effects and pattern loading into account (where variable axial loading is a design factor). This may have a significant

bearing on load capacity on many racks, in particular in higher, heavily loaded, multi-storey structures where sway stability can become a critical failure criterion. Under these circumstances the notional behaviour of the rack in response to p - δ effects for instance, may differ significantly based on the methodologies adopted by each code for the treatment of the base of the structure.

7.2.5. Upright capacity

As with the FEM, SEMA generation of column curves for perforated sections is derived from test data. The experimental procedure is similar in nature with the exception of the requirement for the bracing section to be simulated (under SEMA) using minor axis supports rather than actual frames as is the case with the FEM.

SEMA column curves are calculated based on a determination of the permissible axial stress for the compression member at specified slenderness ratios. The mean ultimate compressive stress of at least three tests is calculated. A statistical interpretation of the results is limited to re-testing if any individual test is $\pm 10\%$ from the mean. Under these circumstances a further three tests should be performed with the lowest three values from all of the results being used to calculate the mean ultimate axial stress value. In some circumstances this approach is much less conservative than the statistical treatment adopted by the FEM. This statistical approach has been dealt with in some detail previously, in section 4.10.2.

The permissible stress is then determined as the failure stress multiplied by 0.59, a single effective safety factor of 1.69 on the unit load of a pallet, which has been substituted for by partial safety factors and a limit state design approach in the replacement code. A slenderness ratio against permissible axial stress column curve may then be devised with the test results being joined to a permissible Euler stress curve above a slenderness ratio of 80.

The Euler stress values are derived using the following formula :

$$= 0.59 \cdot \frac{\pi^2 E}{\left(\frac{l}{r}\right)^2}$$

An equivalent safety factor for the FEM, 'comparative' to SEMA's 1.69 may be considered to be 1.54. This is derived by combining the variable action load safety factor (1.4) with the column material safety factor (1.1). However, these figures are not directly comparable, and ignore the influence of the statistical treatment of FEM test results (SEMA uses mean values), and more crucially, the use of second order analysis techniques for FEM designs. Both of these variations effectively down-rate FEM upright performance in comparison with the SEMA code. It is clear therefore, that an accurate assessment of the load carrying capacity of the upright is inextricably linked (particularly under the FEM) to the overall performance of the rack. Consequently, a comparative, rack performance evaluation (including upright unity checks) has been undertaken in section 7.4.

7.3. SEMA design

7.3.1. Introduction

Adjustable pallet racking design to the SEMA code is well established, and has a proven record in a commercial environment over the past thirty years. The brevity of this code is in marked contrast to the voluminous detail contained within the FEM, although it was not intended to be a 'stand alone' document.

This section contains the major calculations and assumptions necessary for a SEMA design of the racking system outlined in Chapter 6. Comparisons with FEM analysis have been made wherever possible.

7.3.2. Rack dimensioning and section properties

The rack dimensions are described in Fig.6.5. and Fig. 6.6. of this document. General section properties are equivalent for the beams, but adherence to the SEMA code ensures that minimum net (rather than gross) cross section properties are used for upright design (Cl.2.3.1.,SEMA). The revised general section properties are therefore :

	Area (mm ²)	I _{yy} (mm ⁴)	I _{zz} (mm ⁴)	r _{yy} (mm)	r _{zz} (mm)	Self weight (kg)
SD25 (min)	433.7	497846	141609	33.88	18.07	61.25 (frame)
95 (1.78)	705.5	969059		37.06		15.93

Table 7.1. General section properties

For this example the load on the beams has been increased from 1100kg (used for the FEM example) to 1200kg. This loading is more appropriate to the rack when considered under the SEMA guidelines, and as will be seen in due course in this chapter, a reduction in capacity from SEMA to FEM of 10% or more (on identical systems) is not untypical.

7.3.3. Beam Design

Maximum load per beam (Wb) : 11772 N (1200 kg)
Beam span (L) : 2700 mm (to hooks = L + 38)

Nominal yield stress of beam steel (f_y):	417	N/mm ²
Permissible beam bending stress (P_{bcb}):	271.05	N/mm ² ($f_y \times 0.65$)
Elastic modulus (Z_b):	19817	mm ³
Maximum vertical spacing (h):	1575	mm
Beam end connector stiffness (k):	35.21 x 10 ⁶	Nmm/rad
Beam end connector design moment (M_f):	1017.3 x 10 ³	Nmm (from test = 2034.7/2)

Beam moment capacity check

Effective connector stiffness (k_e):

$$k_e = \frac{k}{1 + \frac{k \cdot h}{3 \cdot E \cdot I_{yy_u}}}$$

$$k_e = 29.92 \times 10^6 \text{ Nmm/rad}$$

Beam load capacity (W_{max1}):

$$W_{max1} = \frac{8 \cdot Z_b \cdot P_{bcb}}{(L + 38) \cdot \left[1 - \left(\frac{\frac{2/3}{1 + \frac{2 \cdot E \cdot I_{yy_b}}{k_e \cdot (L + 38)}}}{1} \right) \right]}$$

$$W_{max1} = 17668 \text{ N}$$

Beam connector load capacity (W_{max2}):

$$W_{max2} = \frac{12 \cdot M_f}{(L + 38)} \left[1 + \left(\frac{2 \cdot E \cdot I_{yy_b}}{k \cdot (L + 38)} \right) \right]$$

$$W_{max2} = 23283 \text{ N}$$

Beam unity check (<1):

$W_b/W_{max1} = 0.666$	\therefore ok!
$W_b/W_{max2} = 0.506$	\therefore ok!

Beam shear capacity check

Beam end connector shear capacity (S):	13350	N	(26700/2)
Actual shear (S_a):	$W_b/2 = 5886$	N	
Beam shear unity check (<1):	$S_a/S = 0.441$		\therefore ok!

Beam deflection check

Allowable beam deflection (δ_{all}):	$L/200 = 13.5$	mm
Actual beam deflection (δ_{act}):		

$$\delta_{act} = \frac{5 \cdot W_b \cdot (L + 38)^3}{384 \cdot E \cdot I_b} \left[1 - \left(\frac{\frac{4/5}{1 + \frac{2 \cdot E \cdot I_{yy_b}}{k_e \cdot (L + 38)}}}{1} \right) \right]$$

	$\delta_{act} = 13.39$	mm
Beam deflection unity check (<1):	$\delta_{act} / \delta_{all} = 0.992$	\therefore ok!

7.3.4. Frame Design

Number of beam levels (n) : 4
 Maximum load on frame (W_{bay}) : $n \cdot W_b = 4 \times 2 \times 11772 = 94176 \text{ N}$
 Maximum load on upright (W_u) : $W_{\text{bay}}/2 = 47088 \text{ N}$
 Nominal yield stress of upright steel (f_y) : 250 N/mm²
 Permissible upright bending stress (P_{bcu}) : 162.5 N/mm² (f_y x 0.65)

Determination of permissible axial stress (P_a)

Effective length factor between ground and first beam level, standard baseplate (k) : 1.5

$$\text{Slenderness ratio } (\lambda) : \lambda = \frac{k \cdot h}{r_{yy}} = 69.73$$

The permissible axial stress is taken from the column curve outlined in section 7.2.5.

$$P_a = 143 \text{ N/mm}^2$$

Frame imperfections

Looseness (θ) : 0.0012
 Horizontal stability factor, Cl.7.2.2. (α): 0.005
 Total imperfection factor (φ) : θ + α = 0.0062

Load case i) Fully loaded rack

Side force moment applied at first beam level (M) : $W_u \cdot h \cdot \phi = 459814 \text{ Nmm}$

Combined bending and axial compression unity check :

$$S_c = \frac{W_u}{A_u \cdot P_a} + \frac{M}{Z_u \cdot P_{bcu}} < 1$$

$$S_c = 0.994 \quad \therefore \text{ok!}$$

Load case ii) Pattern loaded rack (one central, first level beam unloaded)

$$\text{Out of balance moments : } M_w = \frac{W_b \cdot L}{12} \cdot \left(\frac{1}{1 + \frac{2 \cdot E \cdot I_b}{k_e \cdot L}} \right)$$

$$M_w = 438656 \text{ Nmm}$$

$$S_b = \frac{4 \cdot E \cdot I_b}{L} \cdot \left[\frac{3 \cdot \left(1 + \frac{3 \cdot E \cdot I_b}{k_e \cdot L} \right)}{4 \cdot \left(1 + \frac{3 \cdot E \cdot I_b}{k_e \cdot L} \right)} \right]$$

$$S_b = 26513943 \text{ Nmm}$$

$$S_u = \frac{E \cdot I_u}{h} = 66379467 \text{ Nmm}$$

$$M_u = M_w \cdot \left(\frac{3 \cdot S_u}{7 \cdot S_u + 2 \cdot S_b} \right)$$

$$M_u = 168739 \text{ Nmm}$$

Axial load on central upright (W_{u2}) : $W_u - W_b$
 $W_{u2} = 35316 \text{ N}$

Combined bending and axial compression unity check :

$$S_c = \frac{W_{u2}}{A_u \cdot P_a} + \frac{M_u}{Z_u \cdot P_{bcu}} < 1$$

$$S_c = 0.656 \quad \therefore \text{ok!}$$

Frame Bracing check

Frame bracing is required to resist a total transverse shear force (F_q) equal to 2% of the maximum axial force in the frame (Cl.7.2.3.).

Total transverse shear force (F_q) : $0.02 \cdot W_{bay} = 1884 \text{ N}$
 Length of bracing member (d) : 1340 mm
 Width of bracing member (l) : 800 mm
 Axial load in bracing member (F_{q1}) : $F_q \cdot d/l = 3155 \text{ N}$

Determination of frame bracing permissible axial stress (P_a)

Effective length factor for welded bracing (Cl.6.6.c.) (k_b) : 0.85
 Radius of gyration for bracing section (r_{zz}) : 7.9 mm
 Cross sectional area (A_b) : 154.2 mm^2

Slenderness ratio (λ) :

$$\lambda = \frac{k_b \cdot d}{r_{zz}} = 144.2$$

The permissible axial stress is taken from the column curve outlined in section 7.2.5.

$$P_{ab} = 49.3 \text{ N/mm}^2$$

The bracing unity check is performed assuming no bending stresses are developed :

$$S_b = \frac{F_{q1}}{A_b \cdot P_{ab}} < 1$$

$$S_b = 0.415 \quad \therefore \text{ok!}$$

Welding check

The bracing members are connected to each upright using a 4.76mm (leg length) fillet weld with a minimum effective weld length of 13mm. Design is in accordance with Addendum No. 1 (1975) to BS449 : Part 2 : 1969 which states (Cl.127.b.) : “ The stress in a fillet weld, calculated on a thickness of 0.7 times the leg length, shall not exceed $0.46.[fy]$ for the parent material.”

Design weld area (A_w) : $0.7 \times 4.76 \times 13 \times 2 = 86.63 \text{ mm}^2$
Design stress (σ_w) : $F_{q1}/A_w = 3155/86.63 = 36.42 \text{ N/mm}^2$
Allowable stress in weld = $0.46.fy = 115 \text{ N/mm}^2$

Welding unity check :
$$W_b = \frac{F_{q1} / A_w}{0.46.fy} < 1$$

$$W_b = 0.317 \quad \therefore \text{ok!}$$

7.3.5. Overall rack stability

The stability criteria for a rack designed using the SEMA code is confined to a relatively simplistic first order analysis approach. This is based on the requirement for the overturning moments induced by an initial out of plumb (assumed to be 0.5% or 0.005 rads.) in combination with the initial connector looseness to be resisted by the ‘safe’ moment of resistance for one quarter of all the joints on an upright (see SEMA Cl.E1.3.).

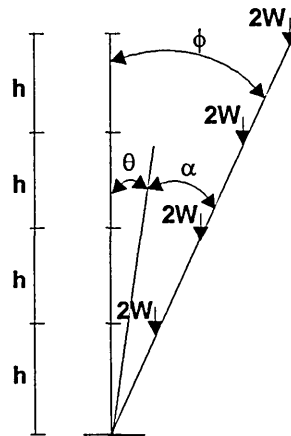


Fig. 7.7. Consideration of loading and offset for stability check on rack.

Moments are taken about the base assuming a fully loaded rack :

$$\begin{aligned}M_{\text{base}} &= 2 \cdot W_b \cdot h \cdot \sin\phi \cdot [n/2 \cdot (n+1)] \\M_{\text{base}} &= 2 \times 11772 \times 1575 \times \sin 0.0062 \times [4/2 \cdot (5)] \\M_{\text{base}} &= 2299057 \text{ Nmm}\end{aligned}$$

With W_b as the load on a single beam, h as the height between beam levels or the distance between the first beam level and the ground, n being the number of beam levels in the rack and ϕ being the sum of the horizontal stability factor for the upright (α) and the looseness of the beam end connector (θ).

This overturning moment is resisted by $0.25 \cdot \sum M_{\text{rd}}$ with M_{rd} being the safe moment of resistance of the beam end connectors on an upright ($0.25 \times 4 \times 4 \times 2067500 =$) 8270000 Nmm . This gives rise to the stability unity check below :

$$\begin{aligned}\frac{M_{\text{base}}}{0.25 \cdot \sum M_{\text{rd}}} &< 1 \\&= 0.278 \quad \therefore \text{ok!}\end{aligned}$$

7.3.6. Summary of the major design and analysis differences between codes

The following considerations summarise some of the major differences in the approach to design and analysis adopted by each code. These have been discussed previously in greater depth in this chapter and in chapter 6.

- Within the FEM gross section properties are used for upright model generation and global analysis in F.E.A. and effective section properties are subsequently used in the design calculations. SEMA permits only the use of minimum section properties throughout.
- There is no interaction in the SEMA code between down aisle and cross aisle frames, with the unity checks lacking any consideration of cross aisle moments. The only check of significance is a cross aisle bracing check assuming a fully effective bracing

section. This is at variance with the FEM, which takes account of the interplay between down aisle and cross aisle behaviour.

- There is no consideration of placement load cases under the SEMA code, and although horizontal forces are considered as part of the imperfection load applied to the rack, the loadings imposed by mechanical equipment (excluding cranes) as a result of normal usage have not been considered. 'Accidental' horizontal forces applied to the uprights have also been omitted.
- The effect of the lack of consideration for both cross aisle behaviour and placement loading conditions under SEMA has served to significantly reduce the number of load combinations (3 minimum) necessary for a satisfactory design when compared with the FEM (12 minimum).
- The performance of the floor connector and its impact on the overall performance of the rack, is only very loosely taken into account in the SEMA code with the use of the k-factor in determining slenderness ratios and permissible axial stresses. It is not possible therefore to adequately reflect the response of the base to variations in axial loading, or to include the moment rotation characteristics in the analysis made possible by the development of iterative finite element solutions.
- The sway imperfection factor contained in SEMA is significantly higher, based on a looseness and a horizontal stability factor (0.0062), than the FEM values. These are based on looseness, out of plumb, the geometry of the rack and the thickness of the upright used. Values for the rack geometry contained within chapter 6 using a 1.7mm thick upright and a 3mm upright are 0.00511 and 0.00375 respectively. This difference is mitigated against by the use of second order analysis in the FEM which has not been incorporated into the SEMA code. Therefore, the additional moments and deflections associated with these p-d effects are not taken into account within the

SEMA code. It is possible under the FEM to incorporate a sway limitation into the code based on the FE response of the model rack, whereas no such governing factor exists within the SEMA code, as there is only a limited appreciation of the degree to which the rack may sway.

- There is no opportunity for redistribution of beam end connector moments into connected beams using the SEMA code. This must, by implication mean that under certain circumstances structures may be designed for reduced capacities unnecessarily. Under the FEM this redistribution can be undertaken either directly in Ansys, or alternatively within the design checks.
- A comparison of the general safety factors in each code, demonstrates a degree of continuity. The FEM ultimate limit state safety factor of 1.54 (variable actions, 1.4 x material safety factor, 1.1) is comparable with the SEMA safety factors of 1.54 on permissible beam bending stress (nominal yield x 0.65) and 1.54 on permissible upright bending stress (nominal yield x 0.65). This comparison can only be made in isolation and without consideration for additional factors in the codes such as second order effects and deflection limitations which also significantly effect the design of racking.

7.4. Racking system design comparisons

The nature of adjustable pallet racking structures means that there are potentially almost infinite variations in the layout of a given rack. Variables include : upright and beam type; number of beam levels; maximum height between beams or between the lowest beam and ground level; length of beam (clear entry); cross-aisle frame width; baseplate type. This ensures that any comparison conducted here must be selective and cannot therefore be entirely comprehensive. Despite this however, the comparisons made below give the clearest and only indication currently available, of the impact of the new FEM code on

industrial pallet racking in relation to the current SEMA code of practice. In general, this has been done by analysing variations in load carrying capacities for specified rack configurations under each code, with 'critical' unity checks included where appropriate.

The SEMA results (including unity checks) within this section are based on a Visual Basic program written by the author to optimise the load carrying capacity of any specified rack configuration within the guidelines of that code. The FEM results have been processed in Ansys 5.4. and maximised using the analysis and design procedures outlined in Chapter 6.

The racking system configurations detailed in Table.7.3.-7.6. overleaf, incorporate a disparate range of geometric variations to allow a general assessment of the effect of the FEM code on racking design. This has been achieved while maintaining a sufficiently high level of continuity between examples in order that trends, where they exist, can be identified.

Beam lengths have been chosen to represent the typical requirement for standard (GKN/Shep - 1200 x 1000) pallet numbers per compartment. This translates to 1150mm for one pallet per compartment, 2700mm for two and 3900mm for three. The associated (cross aisle) frame widths are :

Beam length (mm)	Frame width (mm)
1150	1100
2700	900
3900	900

Table 7.2. Frame widths for associated beam lengths

The number of beam levels chosen (3, 5 and 7) together with variations in the vertical distance between each of these levels (900mm, 1800mm and 3000mm), provides for total system heights and beam configurations covering a range consistent with the majority of rack designs required by industry. A heavy duty (HD25) and a standard duty (SD17)

Test No.	Upright Beam	No. of beam levels	Height to 1st beam (mm)	Clear entry (mm)	Beam moment capacity check	Beam defn. check	Beam shear capacity check	Frame check load case (i)	Frame check load case (ii)	Load capacity per beam pair (kg)
1a	SD17 80 b/b	5	900	1150	0.26	0.20	0.27	1.00	0.71	1488
2a	SD17 80 b/b	5	900	2700	0.54	0.94	0.27	1.00	0.80	1488
3a	SD17 80 b/b	5	900	3900	0.56	1.00	0.15	0.56	0.50	833
4a	SD17 80 b/b	7	1800	1150	0.14	0.11	0.15	1.00	0.67	821
5a	SD17 80 b/b	7	1800	2700	0.30	0.53	0.15	1.00	0.72	821
6a	SD17 80 b/b	5	1800	1150	0.20	0.16	0.21	1.00	0.63	1149
7a	SD17 80 b/b	5	1800	2700	0.42	0.74	0.21	1.00	0.69	1149
8a	SD17 80 b/b	5	1800	3900	0.55	1.00	0.15	0.71	0.54	812
9a	SD17 80 b/b	3	3000	1150	0.19	0.15	0.20	1.00	0.54	1092
10a	SD17 80 b/b	3	3000	2700	0.41	0.72	0.20	1.00	0.58	1092
11a	SD17 80 b/b	3	3000	3900	0.53	1.00	0.15	0.72	0.46	789
12a	SD17 80 b/b	5	3000	3900	0.44	0.83	0.12	1.00	0.70	655
13a	SD17 80 b/b	5	3000	2700	0.25	0.43	0.12	1.00	0.66	655
14a	SD17 80 b/b	5	3000	1150	0.12	0.09	0.12	1.00	0.63	655

Table 7.3. Rack configurations with maximised loads using SEMA design approach

Test No.	Upright Beam	No. of beam levels	Height to 1st beam (mm)	Clear entry (mm)	Beam design strength (6.6.2.)	Beam deflection (6.6.8.)	Connector mmt capacity (6.6.1.)	Frame check (6.5.3.) end i	Frame check (6.5.3.) end j	Load capacity per beam pair (kg)	% reduction in load capacity from SEMA
1b	SD17 80 b/b	5	900	1150	0.22	0.18	0.19	0.99	0.91	1355	8.9
2b	SD17 80 b/b	5	900	2700	0.45	0.79	0.54	1.00	0.95	1280	14.0
3b	SD17 80 b/b	5	900	3900	0.41	1.00	0.61	0.88	0.80	833	0.0
4b	SD17 80 b/b	7	1800	1150	0.10	0.08	0.28	0.99	0.83	600	26.9
5b	SD17 80 b/b	7	1800	2700	0.21	0.36	0.42	1.00	0.84	560	31.8
6b	SD17 80 b/b	5	1800	1150	0.15	0.13	0.28	1.00	0.85	920	19.9
7b	SD17 80 b/b	5	1800	2700	0.31	0.56	0.48	0.99	0.82	880	23.4
8b	SD17 80 b/b	5	1800	3900	0.41	1.00	0.73	0.99	0.87	812	0.0
9b	SD17 80 b/b	3	3000	1150	0.16	0.17	0.31	1.00	0.83	940	13.9
10b	SD17 80 b/b	3	3000	2700	0.32	0.57	0.51	1.00	0.83	910	16.7
11b	SD17 80 b/b	3	3000	3900	0.40	1.00	0.71	0.97	0.80	789	0.0
12b	SD17 80 b/b	5	3000	3900	0.24	0.57	0.59	1.00	0.80	450	31.3
13b	SD17 80 b/b	5	3000	2700	0.18	0.32	0.48	1.00	0.83	480	26.7
14b	SD17 80 b/b	5	3000	1150	0.09	0.07	0.36	0.99	0.82	500	23.7

Table 7.4. Rack configurations passing FEM design checks with reduced loads (from SEMA) where necessary

Test No.	Upright Beam	No. of beam levels	Height to 1st beam (mm)	Clear entry (mm)	Beam moment capacity check	Beam defn. check	Beam shear capacity check	Frame check load case (i)	Frame check load case (ii)	Load capacity per beam pair (kg)
15a	HD25 110 b/b	5	900	1150	0.34	0.20	0.58	1.00	0.73	3174
16a	HD25 110 b/b	5	900	2700	0.77	0.94	0.58	1.00	0.79	3174
17a	HD25 110 b/b	5	900	3900	0.80	1.00	0.32	0.55	0.48	1757
18a	HD25 110 b/b	7	1800	1150	0.19	0.12	0.33	1.00	0.71	1812
19a	HD25 110 b/b	7	1800	2700	0.44	0.55	0.33	1.00	0.74	1812
20a	HD25 110 b/b	5	1800	1150	0.27	0.16	0.47	1.00	0.67	2537
21a	HD25 110 b/b	5	1800	2700	0.62	0.76	0.47	1.00	0.72	2537
22a	HD25 110 b/b	5	1800	3900	0.79	1.00	0.32	0.68	0.52	1726
23a	HD25 110 b/b	3	3000	1150	0.30	0.18	0.51	1.00	0.55	2771
24a	HD25 110 b/b	3	3000	2700	0.68	0.85	0.51	1.00	0.59	2771
25a	HD25 110 b/b	3	3000	3900	0.77	1.00	0.31	0.61	0.39	1690
26a	HD25 110 b/b	5	3000	3900	0.76	0.98	0.31	1.00	0.71	1662
27a	HD25 110 b/b	5	3000	2700	0.41	0.51	0.31	1.00	0.68	1662
28a	HD25 110 b/b	5	3000	1150	0.18	0.11	0.31	1.00	0.65	1662

Table 7.5. Rack configurations with maximised loads using SEMA design approach

Test No.	Upright Beam	No. of beam levels	Height to 1st beam (mm)	Clear entry (mm)	Beam design strength (6.6.2.)	Beam deflection (6.6.8.)	Connector mmt capacity (6.6.1.)	Frame check (6.5.3.) end i	Frame check (6.5.3.) end j	Load capacity per beam pair (kg)	% reduction in load capacity from SEMA
15b	HD25 110 b/b	5	900	1150	0.37	0.23	0.29	1.00	0.96	3580	-12.8
16b	HD25 110 b/b	5	900	2700	0.77	0.99	0.73	1.00	0.90	3340	-5.2
17b	HD25 110 b/b	5	900	3900	0.56	1.00	0.66	0.60	0.52	1757	0.0
18b	HD25 110 b/b	7	1800	1150	0.15	0.09	0.49	1.00	0.88	1420	21.6
19b	HD25 110 b/b	7	1800	2700	0.32	0.42	0.66	1.00	0.86	1380	23.8
20b	HD25 110 b/b	5	1800	1150	0.23	0.14	0.46	1.00	0.89	2150	15.3
21b	HD25 110 b/b	5	1800	2700	0.48	0.63	0.73	1.00	0.88	2100	17.2
22b	HD25 110 b/b	5	1800	3900	0.56	1.00	0.79	0.70	0.60	1726	0.0
23b	HD25 110 b/b	3	3000	1150	0.25	0.15	0.58	1.00	0.83	2340	15.6
24b	HD25 110 b/b	3	3000	2700	0.53	0.70	0.85	1.00	0.81	2280	17.7
25b	HD25 110 b/b	3	3000	3900	0.54	1.00	0.75	0.52	0.47	1690	0.0
26b	HD25 110 b/b	5	3000	3900	0.38	0.63	0.94	1.00	0.86	1055	36.5
27b	HD25 110 b/b	5	3000	2700	0.28	0.40	0.73	0.99	0.81	1180	29.0
28b	HD25 110 b/b	5	3000	1150	0.15	0.08	0.59	0.99	0.82	1260	24.2

Table 7.6. Rack configuration passing FEM design checks with reduced loads (from SEMA) where necessary

frame have been chosen and paired with beams (80 box and 110 box) commonly in use with those frames. Beams and uprights have not been varied more widely in order to limit the number of possible combinations necessary to establish trends. In addition, only the standard baseplate has been used here. Variations in floor connector rotational stiffness and its effect on capacity have been scrutinised separately in section 7.5.4. The geometry of the systems together with a select number of associated unity checks and maximum load carrying capacities for each code are as follows :

The consequences of implementing the FEM code based on the interpretation adopted by this document are clearly illustrated by Fig.7.8. This graph summaries the results of the 56 designs illustrated in the two preceding pages, comparing the load carrying capacities established by each code for each of the stated racking system configurations :

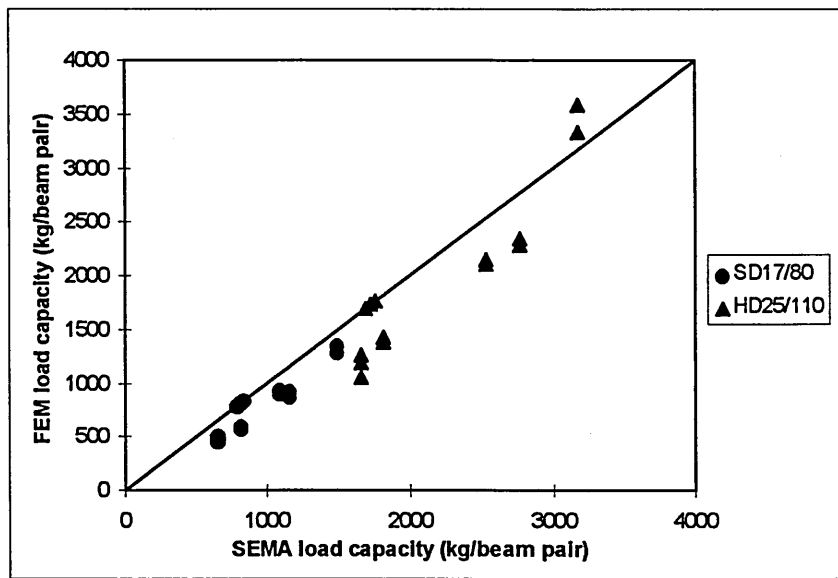


Fig.7.8. A comparison between codes of load carrying capacities for rack configurations specified in Table 7.3.-7.6.

The diagonal line in Fig.7.8. represents equivalence between the resultant load carrying capacities established by each code. It is evident that in the majority of cases, given the same rack geometry and section properties, SEMA designed systems profit from being able to carry higher loads.

There are two exceptions to this general trend. An analysis of the results in Table 7.3.-7.6. and of the graph above demonstrates that there is no advantage to be gained from pursuing a design under the recommendations of either code when load capacities are limited by beam deflection criteria alone. Within this study there are six comparisons that fall into this category, and as a consequence appear on the diagonal line in Fig.7.8. revealing an equivalence in terms of capacity. This is an indication that there is no significant difference between the way in which beam deflection calculations are treated within either code. It is conceivable however, that in circumstances where redistribution of moment into the beam becomes necessary (under FEM recommendations) in order to avoid a unity check failure in the beam end connector (see section 6.6.2.), beam deflection results may vary from code to code.

The second exception highlighted by these results is more easily explained with reference to Fig. 7.9. This figure illustrates the percentage reduction in load carrying capacity of FEM designed rack in relation to SEMA rack, based on increasing total structure heights. It is evident from Fig.7.8. that two of the HD25/110 results benefit from an FEM analysis with higher load capacities than those determined using SEMA.

The graph below (Fig.7.9.) makes clear that there is a tendency for taller racks to be much more heavily penalised by design to the FEM. This can be attributed to the influence of second order effects which increase significantly in response to an increase in height. Conversely therefore, it follows that racks with a reduced total height, and particularly those with higher numbers of beam levels at more frequent intervals (making the structure less slender) are less likely to be penalised by second order sway. The two rack configurations that benefit most significantly from this are made up of heavy duty sections which are more robust down aisle than their standard duty counterparts, with a high number of beam levels (5), and with close vertical spacing (900mm).

With the exception of these two cases, there are no other circumstances identified here under which the design of adjustable pallet racking benefits, in terms of an increase in capacity, from being designed to the new code. Indeed, with reference to Fig. 7.9., it is clear that (excluding the two cases mentioned above) there is a significant and consistent reduction in the carrying capacity of all racking examined by this document.

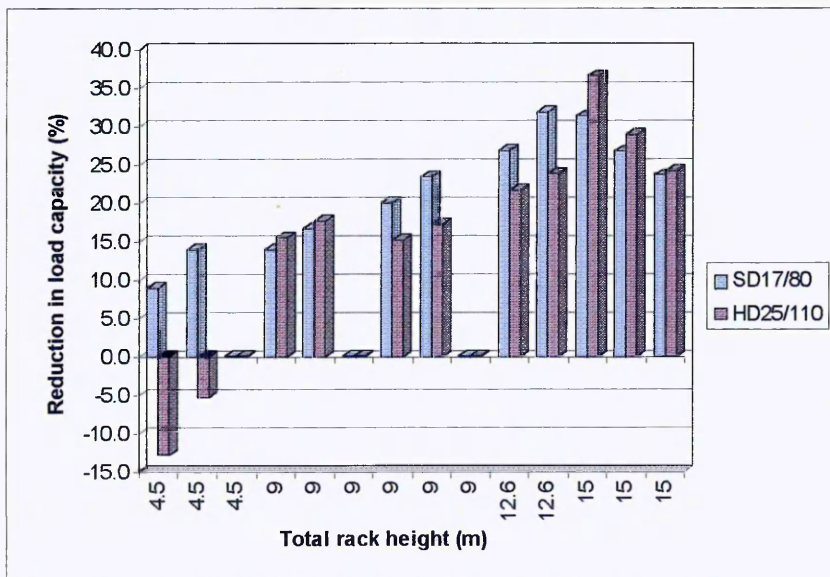


Fig.7.9. A graph illustrating the reduction in load capacity (%) from SEMA rack to FEM rack in relation to increasing total structure heights.

In percentage terms, the reduction in load capacity displayed in Fig.7.9. range between 0% and 31.8% for SD17 analyses, and -12.8% and 36.5% for HD25. The mean reduction in performance of FEM designed rack from SEMA has been tabulated below :

	SD17/80 (%)	HD25/110 (%)	Mean for all tests
Mean values (inc. all tests)	16.95	13.07	15.01
Mean values (excluding deflection limited results)	21.57	16.63	19.10

Table 7.7. Mean reductions in load carrying capacity (%) for FEM designed racking.

The mean reduction in load capacity for all tests examined here is therefore 15.01%, this increases to 19.10% if deflection limited designs are excluded. Clearly, on the basis of these results, the FEM code in its present form will have a significant and negative impact on the design of static pallet racking systems taken as a whole.

7.5. The impact of design changes to the development of the rack

7.5.1. Introduction

A sensitivity analysis has been undertaken here using FEM design rules to assess the impact of variations in a number of key parameters which are considered to be pivotal in the design of racking structures. This impact has been measured in terms of the change in the load carrying capacity of the rack. The parameters considered here are beam end connector looseness, beam end connector moment capacity and stiffness, yield stress of upright material and floor connector stiffness.

In addition, consideration has been given here to the way in which these variations might be achieved in practice, in order that the assumptions that have been made can be interpreted as realistic, and having a basis in reality. It has been demonstrated here that the implementation of any or all of the design alterations incorporated into this section, will increase the capacity of the rack without dramatically changing the rack design. This section therefore provides an understanding of the effect on a specified rack geometry of altering design parameters when using the FEM code, and as a consequence, indicates where improvements can be made to the rack most usefully, to optimise the design opportunities presented by the code.

Racking assessed here consists of HD25 upright and 110 box beams. In the assessment of all of the variables (except moment capacity and stiffness) three rack geometries have been analysed. These include a 4.5m rack with five, 900mm beam levels, a 9m rack with five, 1800mm beam levels and a 15m rack with five, 3000mm beam levels. All beam

were 2700mm long. The moment capacity and stiffness comparisons were performed on a 9m rack with five, 1800mm beam levels and beams of 1150mm 2700mm and 3900mm. Each rack was analysed with three different values for the specified parameter, while all other variables were kept constant, a total of nine analyses per parameter. This ensured that any variations in the response of the rack in terms of load carrying capacity, could be attributed directly to the parameter under consideration.

It must be stressed here, that as with the initial analyses contained in section 7.4. of this chapter, any trends or influences detected here may not entirely represent the 'across the board' performance of the rack. This is due to the enormous number of variables that pertain to this type of analysis, whose specific influences under every possible configuration cannot all be considered individually within the remit of this document. The results obtained here may instead be interpreted as giving a clear indication of what may be true, in general terms, for the majority of racking structures.

7.5.2. Variations in beam end connector looseness

The sensitivity of racking to changes in looseness has been examined here, on structures with variable heights between beam levels. It can clearly be seen from Fig.7.10. that the impact of higher values of looseness is greater when the distance between beam levels, and by implication, the overall height of the rack is increased. This would seem reasonable given the use of second order analysis techniques to determine the moment distribution in the rack. The analysed structures increase in height from 4.5m, where there are no undue effects on the load capacity attributable to any increase in looseness (upto the current looseness value of 0.00528 rads.), to 9m where there is a 7.89% reduction in load capacity from zero looseness to 0.00528 rads., to 15m where there is a 8.02% reduction in load capacity over the same range of looseness. It is evident that the impact of higher values of looseness within the rack, will only be significant in reducing

the load carrying capacity of the system when the horizontal imperfection loads (derived from values of connector looseness) are permitted to act on sufficiently high lever arms in relation to the number of connectors resisting the resultant second order effects. In other words, as the distance between beam levels increases, and the total height of the structure increases proportionately as a result, the rack will become more susceptible to (down aisle) sway. As a consequence, there will be a general and significant reduction in the load capacity of the rack, as is clearly demonstrated by Fig. 7.10.

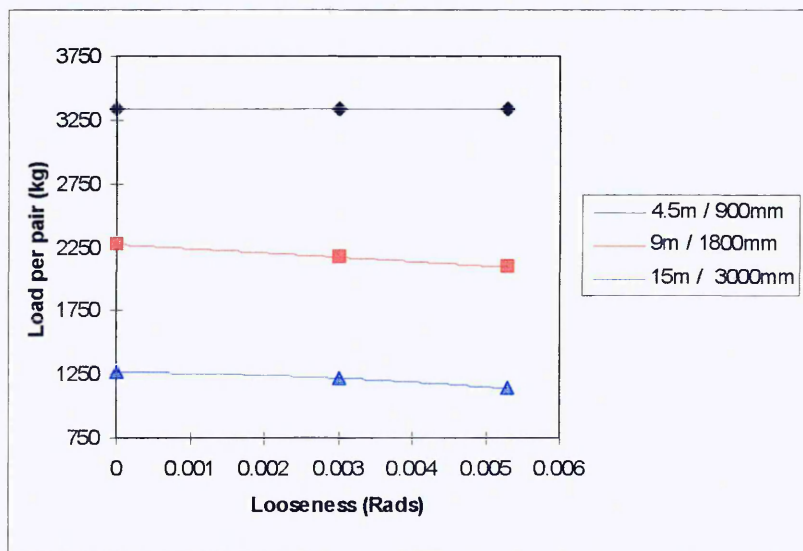


Fig. 7.10. The effect of increased looseness values on rack with progressively increasing distances between beam levels and associated increases in structure height.

Looseness is a function of the interaction between the connector (and its hooks) and the upright. The suitability of this ‘fit’ is based on manufacturing tolerances and may be easily altered. However, the desirability of a ‘non-loose’ interface for the purposes of design conflicts with the need for a degree of looseness to compensate for any variabilities which may be present at the manufacturing stage and to facilitate ease of construction. On the evidence presented here, it is apparent that the removal of a proportion of the looseness at the upright/connector interface may improve the load capacity of rack (particularly taller, more slender structures) without significantly

impinging on the manufacture and construction processes. Reducing the looseness value to something in the order of 0.003 rads - with the use of a double taper in the main upright slots for instance, would (based on the analyses in Fig.7.10.) increase the rack capacity of 9m racking with 1800mm beam levels by 3.4%, and the capacity of 15m racking with 3000mm beam levels by 4.07%.

7.5.3. Variations in beam end connector moment capacity and stiffness

The increases in moment capacity and stiffness in Fig.7.11. are in line with tests performed on experimental four hook, beam end connector samples with a down-weld of 75mm on the beam. These tests (to FEM guidelines) gave improvements in performance of 10% in moment capacity and 80% in rotational stiffness values. The effect of these results on the rack's payload has been demonstrated in the graph below, in which comparisons have been made with the initial load capacities achieved by FEM analyses, and with a connector with a 10% increase in moment capacity but only a 40% improvement in stiffness.

It is clear from Fig.7.11. that very substantial benefits can be gained from any increase in these two properties. This is particularly true with beams of 2.7m or less where a buckling failure in the frame is the critical condition, rather than a deflection failure in the beam as is the case at 3.9m clear entry.

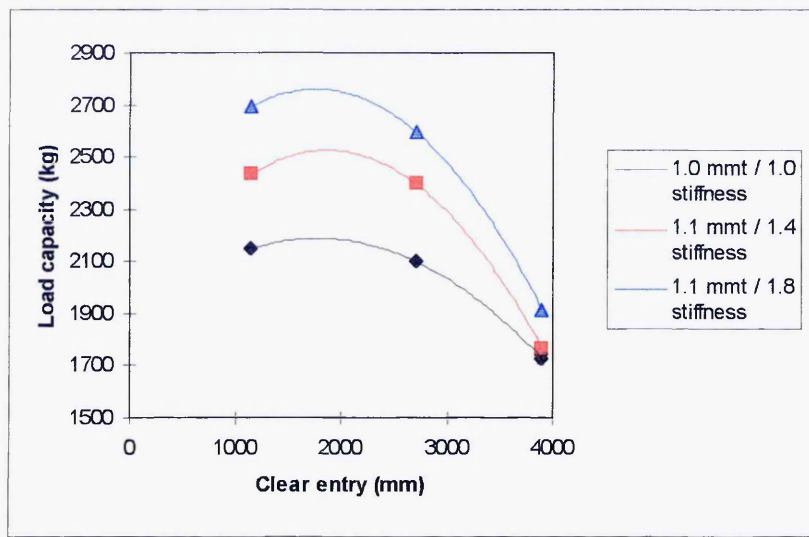


Fig. 7.11. The effect on load capacity of variations in beam end connector moment and rotational stiffness on rack of variable clear entry.

The implications for the design of rack based on the analysis presented above are that, for this rack configuration, there is a 25.58% and 23.81% increase in capacity of rack using 1150mm and 2700mm beams respectively, when considering connectors with an 80% increase in stiffness and a 10% increase in moment capacity. This represents performance improvements on SEMA designed rack (using the original three hook connectors) of 6.4% and 2.48% respectively. Even when consideration is given to deflection limited analyses (at 3900mm beam span) there is an improvement of 11.24% in capacity. Reductions in capacity associated with FEM second order analyses are, at the very least, compensated for by beam end connectors designed specifically to resist these $p-\delta$ effects. Significantly, the load capacity increases are beyond those associated with SEMA, and can be attributed particularly to increases in the rotational stiffness of the connector.

It may be reasonably assumed that further improvements in the rotational stiffness and moment capacity of the connector, limiting the rack in terms of its ability to sway even more substantially, would (upto a point) have an even greater impact in terms of increases in load capacity.

7.5.4. Variations in the nominal material yield strength of uprights

Currently, specifying that higher yield steels should be used in the manufacture of uprights is the only way of improving the nominal yield stress of the parent material. This will have implications not only for the design calculations, which have been examined in Fig.7.12., but should also have an effect particularly on the stub/frame compression test results. The impact on test data has not been assessed here.

It is suggested here however, that a second method of improving the nominal yield of the steel might be to use a modified version of the formula contained within BS5950:Part 5:1987 cl.3.4. and in a similar form in FEM cl.1.9., which enhances the yield of the steel based on the effects of cold forming from f_{yb} , the nominal yield of the material to f_{ya} , the average yield of the cold formed section. The formula is as follows :

$$f_{ya} = f_{yb} + \frac{CNt^2}{A_g} (f_u - f_{yb})$$

'N' is the number of full or partial 90° bends in the section with an internal radius $\leq 5t$, with 't' being the net thickness of the material. ' f_u ' is the minimum ultimate tensile strength, ' A_g ' is the gross cross sectional area of the section and 'C' is a coefficient based on the type of methods used to form the section (C=7 for rolled material).

Although this formula is intended to enhance values of yield strength for non-perforated members, it would seem to be equally applicable to perforated sections such as racking uprights, where it is clear that bends that remain unaffected by perforations will experience similar increases in yield strength as in non-perforated sections. Both types of upright section would therefore be considered to have four 90° bends (instead of seven and eight), taking account of the four corners of the section unaffected by perforations, but ignoring the bends and partial bends forming the central stiffener of the upright. The area of the section would remain conservatively as the value for the gross cross sectional

area. This would seem to be an acceptable and justifiable way of enhancing the yield of the upright material merely by cold rolling the section.

Although this technique has not been used in this document previously, employing the values of yield would raise the nominal yield of the upright material from 250 N/mm² to approximately 260 N/mm² (depending on which upright is considered), giving a small but significant increase in the performance of the rack purely as a result of the methods used in its manufacture.

In Fig.7.12. the effect of an increase in yield strength can be fully appreciated, with improvements in performance of between 11.33% and 4.42% for rack (4.5m and 9m high respectively) with yield values rising from 250 N/mm² to 300 N/mm², and between 3.39% and 2.86% for rack (9m and 15m high respectively) with yield values rising from 300 N/mm² to 350 N/mm². The improvement in frame capacity in the 4.5m high rack has forced failure due to deflection limitations at 350 N/mm², and it can therefore be concluded that there is a discernible benefit in adopting higher values of upright yield (by whatever means are available) to take full advantage of frame performance. This seems to be particularly true for lower level racking.

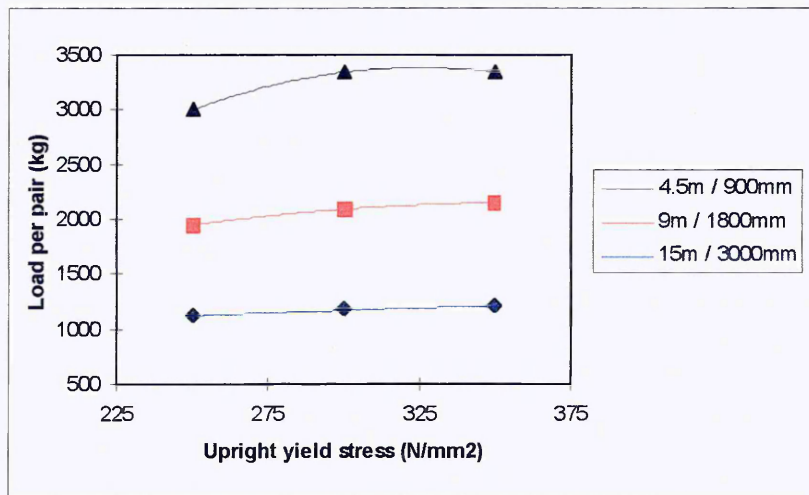


Fig.7.12. The effect on load capacity of variations in nominal yield of upright steel on rack of variable height and beam spacing.

7.5.5. Variations in floor connector stiffness

As has been discussed previously, it is possible to consider the connection between the rack and the floor as a pinned joint, having a zero stiffness value. The consequences of this assumption are apparent in Fig.7.13., with a marked drop in the capacity of the rack when compared with similar structures with base stiffness values of 182 kNm/rad. It is clear from this graph that this increase in stiffness facilitates an improvement in rack performance of between 33.6% (4.5m rack) and 118.52% (15m rack), with the intermediate 9m rack showing an increase of 77.97%. However, although there is clearly a significant improvement in load carrying capacity up to this point, further increases in rotational stiffness of the base produce relatively little benefit, with the greatest increase of 5.9% (70kg) coming, from the structure most vulnerable to sway, the 15m rack. It is apparent therefore that baseplates with higher stiffness' than those analysed here are unlikely to provide much improvement in rack performance. Fig.7.13. seems to indicate the presence of a plateau (around 200 to 300kNm/rad.) beyond which little is to be gained from improving the stiffness of the floor connection.

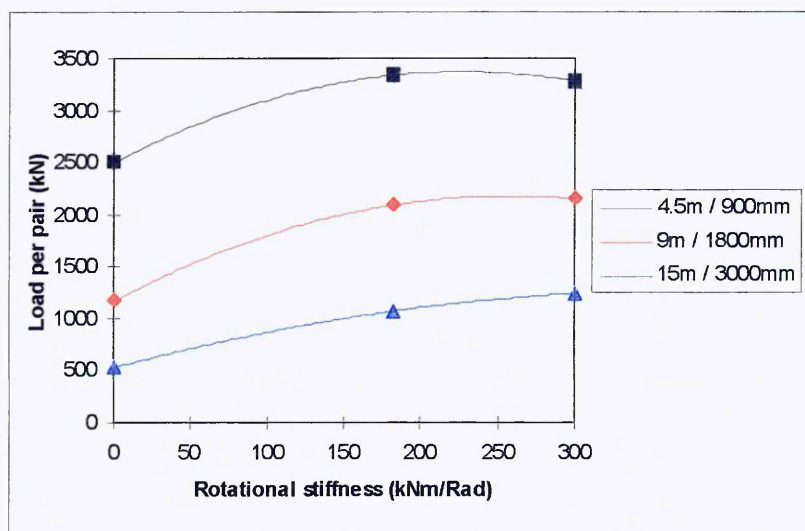


Fig. 7.13. The effect on load capacity of variations in rotational stiffness of the floor connector on rack of variable height and beam spacing.

7.6. Summary and conclusion

This chapter has brought together all the analyses and results determined and described during the course of this document to permit a direct comparison between the current UK and future European pallet racking codes. It is clear that current rack designs will be penalised under the new FEM guidelines and the degree to which this happens has been explored in depth here.

In addition, a sensitivity analysis has been presented in order to further understand the impact of variations in component design values on load carrying capacity. This has produced some clear conclusions as to where improvements can be made to the design of racking to reduce the deficit in capacity caused by the new code, and increase the efficiency of the rack. Taken together, it is clear that alterations to these variables may have a dramatic positive effect on the capacity of racking installations regardless of the guidelines used to design them. However, the fact that these measures are needed at all, encourages the idea that the code, taken as a whole, is overly conservative in its approach and may need to be reassessed in the light of this work.

In the UK over the past thirty years, experience has shown that SEMA designed racking installations are safe and adequately designed for the purposes to which they are put. Seen from this perspective, it would seem that the UK code can be taken as a useful benchmark with which to measure the success of the new code (in terms of its design approach). Many comparisons have been made in this document to identify the differences in approach that make each code different. However, the load capacity comparison contained within this chapter highlights the inequity between what is acceptable (in terms of load) when comparing SEMA and the FEM. Unless there is a degree of parity (or an improvement) in terms of performance between rack designed by the old code and the new, it is clear that rack designed by the FEM will be seen as 'over

designed' and the code will be in danger of becoming irrelevant. It is inconceivable that the racking industry (and its customers) will accept a code that raises prices without increasing performance.

Although no work has been included here to examine its effect, it is clear that a variable action load factor reduction from 1.4 to 1.35, or even 1.3, may be the simplest and most appropriate way in which to achieve parity in terms of load capacities (this has been included in suggestions for future work). This develops a principle which is already established within the FEM, and which has reduced the value of the variable action load factor from 1.5 (for live loads), to 1.4 (for unit pallet loads), based on the limited variation in pallet loads typical in racking installations. The notion that a further reduction in this load factor would permit a closer relationship between load capacities determined by each of the codes would seem to be a desirable outcome for this exercise. In short, this document has highlighted weaknesses in the overall approach of the new code which must be addressed if it is to be adopted by the European racking industry.

Chapter 8

Conclusions and Further Work

8.1. General outline

The consequences of developing a new and more rigorous approach to static pallet racking design have been examined in this thesis in some detail. It is clear from the work that has been done here that the impact of a new code may have far reaching implications for the industry, and although it should be remembered that this investigation has been limited to a single type of rack design, the variations in geometry, material properties, manufacture and construction of other types of racking in the industry are small enough to allow general trends to be extrapolated. It is likely therefore that what is found to be true for one type of racking design, will invariably be true (at least in part) for the majority of racking in the industry.

8.2. Summary and Conclusions

The impact of a new approach to the design and analysis of static pallet racking systems has been investigated in this thesis. This involved an examination of the structural behaviour of cold-formed, perforated and non-perforated thin-walled steel sections through the design and application of experimental testing procedures, within the guidelines of the FEM code. A sufficient number of tests have been completed in order that a reliable statistical characterisation for individual racking components and for combinations of components forming semi-rigid joints could be generated. Raw test data from approximately 2000 tests has been analysed, and the failure modes and methods adopted by the code, particularly with regard to statistical treatment of the results, have been discussed in detail.

An approach has been established, based on the recommendations contained within the new code, to the design of static pallet racking using this characteristic data. This has been documented here in detail, and consists of a two stage design process in order that the loading capacity of a rack structure may be anticipated.

The initial stage is a global, second order, finite element analysis of two distinct 2-dimensional models operating perpendicularly to each other. These have been developed in Ansys, and consist of a down-aisle sway frame incorporating the semi-rigid behaviour of the floor and beam end connections, and a cross aisle welded frame which is normally less critical in terms of overall system design. The generation of the F.E. models, including the treatment of the semi-rigid joint behaviour, the choice of software, and the type and number of elements used, have been investigated here to determine the most appropriate design approach. The legitimacy of the distribution of internal forces and displacements in Ansys was confirmed by comparison with Cosmos.

A typical racking structure has been provided in order that a full design procedure based on the FEM code could be outlined. This example contains all the necessary design information and considerations which must be taken into account for the satisfactory construction of a finite element model within FEM guidelines. Calculations have been performed to establish the methodology behind the development of values for imperfection, placement and accidental loads, and an investigation has been made into the number and type of load cases necessary as a minimum requirement for the 'general design case'. The use of a number of additional load cases under 'specialised' circumstances (for instance racking containing low level beams) has also been considered.

The second stage in the design process was to combine down-aisle and cross-aisle load cases, in interaction formulae where necessary and to highlight and perform the relevant

member unity checks required to assess the structural integrity of the rack. This was accomplished with reference to the example structure, in order to provide a full design procedure for design to the FEM code.

In addition to the work above, an investigation has been undertaken comparing the existing national (SEMA) code with the new European code. This includes an investigation into the key differences between test methodologies and the interpretation of experimental results. A Visual Basic program has been written to optimise load carrying capacities for SEMA rack. The calculations and assumptions that this is based on are outlined briefly in order that a clear and detailed comparison can be made between designs performed by each code.

The nature of adjustable pallet racking means that there are potentially almost infinite variations in the layout of a given rack. This ensures that any comparisons made between the respective codes, in terms of load capacity for instance, cannot be entirely comprehensive. Despite this however, the comparisons that have been made here give the clearest and only indication currently available, of the impact of the new FEM code on the industrial pallet racking industry. Twenty eight structures have been analysed using design guidelines established by this document, and show a mean reduction in load carrying capacity of approximately 15.2% for FEM designed racking. The results distribution was between a 12.8% increase in capacity to a 36.5% reduction. When deflection limited results are excluded (as beam deflections tend to be equivalent under each code), this mean reduction rises to 19.4%. Although there are significant variations in these figures as a result of changes in the geometry, the material properties and section properties of the rack, the effect of the introduction of the new code will be a general reduction in the load carrying capacity of racking systems of the order suggested here.

A sensitivity analysis has also been undertaken using a further 24 structures to identify the critical factors that produce significant improvements in the load carrying capacities of the rack. These included variations to the upright yield stress, beam end connector looseness, moment capacity and rotational stiffness, and floor connector stiffness. Clearly, alterations that are easy to incorporate into the rack design without significant geometric alterations or cost implications are preferable. However, it is clear that the implementation of any or all of the suggestions contained within this document would have a beneficial impact on the capacity of the rack.

Finally, it has been made clear that as a result of this work, and using the tried and tested analyses contained within the SEMA code as benchmark against which to judge the FEM code, some form of amendment to the new code is essential in order that current load carrying capacities are not unduly downrated. It has been suggested that this might take the form of a reduction in variable action load factor from 1.4 to 1.35, or even 1.3. Although no work has been done within this document to validate this proposal it has been included as a future work suggestion. Clearly however, shortfalls in design loads in comparison with the previous code are likely to prove unacceptable to the European racking industry and will need to be addressed if the FEM code is to be adopted in perpetuity.

8.3. Further work

Of great benefit in future might include work to develop a 3-dimensional finite element model. A comparative analysis could then be made to examine whether any differences are apparent between the results obtained from the direct interaction between down-aisle and cross-aisle models as compared with those established using the methods adopted within this document. In addition, the production of a greater number of design examples is desirable, in order to permit a much more detailed assessment of the impact of the new

code (when compared with SEMA) for a much increased range of uprights, beams and rack geometry. This should also include an assessment of the performance of racking with spine and plan bracing. An investigation should also be made into methods by which the disparity between load capacities based on FEM design and those for SEMA designed rack can be minimised. This should include variations to the variable action load factor and justifiable reductions in the value of the imperfection factor. Finally, it is clear that some degree of redesign of the rack along the lines suggested by the sensitivity analysis outlined in this document would clearly be of benefit, and should be investigated in greater depth.

References

1. C.K. Chen, R.E. Scholl and J.A. Blume, Seismic Response of Industrial Steel Storage Racks, *Structural Engineer*, Vol. 53, No 6, June 1975.
2. Recommendations for the Design of Steel Static Pallet Racking and Shelving, 10.2.02., Federation Europeenne de la Manutention, Section X, October 1998.
3. Code of Practice for the Design of Static Racking, Storage Equipment Manufacturers' Association (SEMA), 1980.
4. BS449 : Part 2 : 1969, Specification for the use of Structural Steel in Building.
5. Addendum No.1 (April 1975) to BS 449 : Part 2 : 1969, Specification for The use of Cold-Formed Steel Sections in Building.
6. ENV 1993-1-3 : Eurocode 3 : Design of Steel Structures Part 1.3 : Cold-Formed Steel Sheeting and Members, pub. Euro. Committee for Standardisation (CEN).
7. J.M. Davies and S.J. Cowen, Pallet racks using cold-reduced steel, 12th International Speciality Conference on Cold-formed Steel Structures, St. Louis, Missouri, USA, Oct., 1994.
8. BS5950 : Structural use of Steelwork in building : Part 5 : Code of Practice for the Design of Cold-Formed Sections, 1987.
9. M. Crosbie, Column Curve Design using Stub Column Compression Test Data, Internal report, Redirack UK Ltd., 1997.
10. ENV 1993-1-1 : Eurocode 3 : Design of Steel Structures Part 1.1 : General rules and rules for buildings, pub. European Committee for Standardisation (CEN).
11. Specification for the Design Testing and Utilization of Industrial Steel Storage Rack, Rack Manufacturers' Institute, USA, 1997.

12. Specification for the Design of Cold-Formed Steel Structural Members,
American Iron and Steel Institute, Washington, DC, 1996 Edition.
13. Specification for Structural Steel Buildings, Allowable Stress Design and Plastic
Design, American Institute for Steel Construction, Chicago, Ill., June 1989.
14. Load and Resistance Factor Design Specification for Structural Steel Buildings,
American Institute for Steel Construction, Chicago, Ill., Dec. 1993.
15. Cold-Formed Steel Design Manual, American Iron and Steel Institute,
Washington, DC, 1996 Edition.
16. G.M. Lewis, Stability of Rack Structures, Thin-Walled Structures 12, 163-174,
1991.
17. J.W.B. Stark and C.J. Tilburgs, Frame instability of Unbraced Pallet Racks,
Int. Conference on Thin-Walled Structures, Univ. of Strathclyde, April 1979.
18. J.M. Davies, Down-aisle Stability of Rack Structures, 11th International
Speciality Conference on Cold-formed Steel Structures, St. Louis, Missouri,
USA, Oct 20-21, 1992.
19. J.M. Davies, Stability of Unbraced Pallet Racks, 5th Int. Speciality Conference
on Cold-formed Steel Structures, St. Louis, Missouri, USA, Oct 20-21, 1980.
20. M.R. Horne, An approximate method for Calculating the Elastic Critical Loads
of Multi-Storey Plane Frames, Structural Engineer, Vol. 53, No 6, June 1975.
21. X. Feng, M.R.H. Godley and R.G. Beale, Elastic Buckling Analysis of Pallet
Racking Structures, 5th International Conference on Civil and Structural
Engineering Computing, Edinburgh, Aug 17-19, 1993.
22. S.W. Jones, P.A. Kirby and D.A. Nethercot, The Analysis of Frames with Semi-
Rigid Connections - A State-of-the-Art Report, Construct. Steel Res., Vol. 3, 2-
13, 1982.

23. J.H. Howlet, W.M. Jenkins and R. Stainsby, (ed.), Joints in Structural Steelwork, Pentech Press, 1981.
24. K.M. Romstad and C.V. Subrumaniam, Analysis of Frames with Partial Connection Rigidity, J. Struct. Div., ASCE, Vol.96, 2283-2300, 1970.
25. C.H. Yu and N.E. Shanmugam, Stability of Frames with Semi-Rigid joints, Computers and Structures, Vol.23, 639-648, 1986.
26. G.R. Monforton and T.S.Wu, Matrix Analysis of Semi-Rigidly Connected Frames, J. Struct. Div., ASCE, Vol.89, 1963.
27. K.M. Ang and G.A. Morris, Analysis of three-dimensional frames with flexible beam-column connections, Canadian J. Civ. Eng, Vol.11, 245-254, 1984.
28. M.H. Ackroyd and K.H. Gerstle, Strength of Flexibly Connected Steel Frames, Engineering Structures, Vol.5, Part 1, Jan. 1983.
29. E.M. Lui and W.F. Chen, Analysis and Behaviour of Flexibly-Jointed Frames, Engineering Structures, Vol.8, Part 2, Apr. 1986.
30. X. Feng, The Influence of Baseplates and Semi-Rigid Joints on the Behaviour of Slender Structures, PhD thesis, Oxford Brookes University, 1993.
31. Redirack Interlake, Making a Success, 1979, internal document.
32. BS1449: Part1: Specification for Carbon and Carbon-Manganese Plate, Sheet and Strip, 1983.
33. BS EN 10002 Part 1 : Tensile Testing of Metallic Materials : Annex A, 1990.
34. Wei-Wen Yu, Cold-Formed Steel Design (2nd ed.), John Wiley and Sons Inc., 1991.
35. J.M. Gere and S.P. Timoshenko, Mechanics of Materials (3rd ed.), PWS-Kent publ., 1990.

Appendix A

This appendix contains standard drawings for the product range and has been divided up into three sections for ease of reference. The sections together with their drawing numbers are listed below :

Appendix A1.

Beams/connector/connector lock

Dwg No.	Dwg. Title
PD.040-1/C	Standard beam section 50 & 76 open section 80/1.6, 95/1.6 and 95/1.78 boxed sections.
PD.040-2/C	Standard beam section 110/1.78, 130/1.6, 130/1.78 and 145/1.78 boxed sections.
PD.049-A	Assembly drawing - beam.
SD.002-E	Beam bracket.
SD.007-C	Lock-in pin.

Appendix A2.

Upright/baseplates

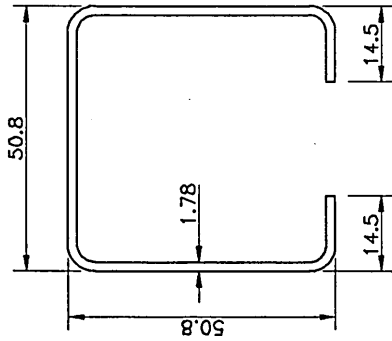
Dwg No.	Dwg. Title
SD.006 - 01/E	Post punched SD17 standard duty upright section.
SD.006 - 02/E	Post punched SD25 & SD25T standard duty upright section.
SD.015-A	SD upright slot pattern elevation.

SD.004 - D	Heavy duty upright section - punched.
SD.016 - A	HD upright slot pattern elevation.
SD.008 - C	Standard baseplate.
SD.010 - E	Drive-in baseplate. (aka 'narrow aisle')

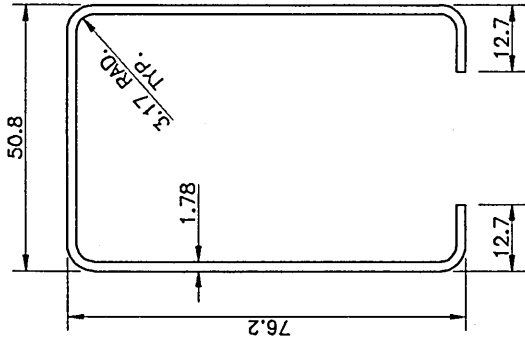
Appendix A3.

Bracing

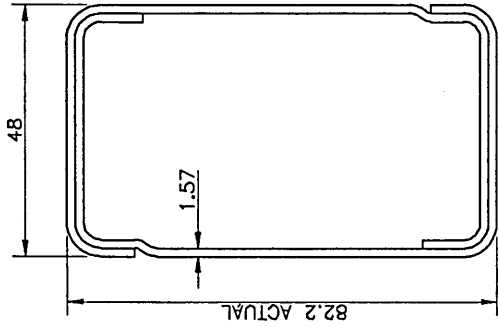
Dwg No.	Dwg. Title
SD.012 - F	Bracing channel section.
PD.059 - D	Standard frame dimension tolerances.
PD.035 - 1-3/B	Frame bracing details.



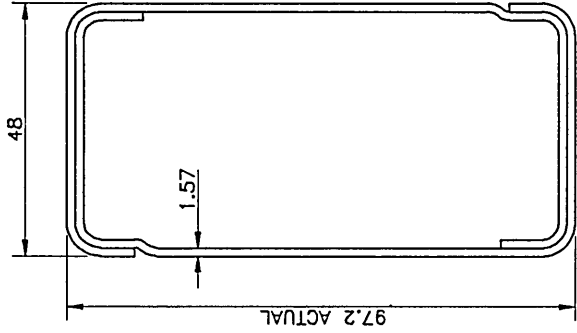
50 OPEN



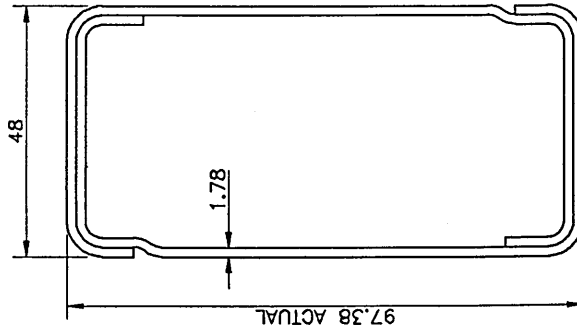
76 OPEN



80/1.6 BOXED



95/1.6 BOXED



95/1.78 BOXED

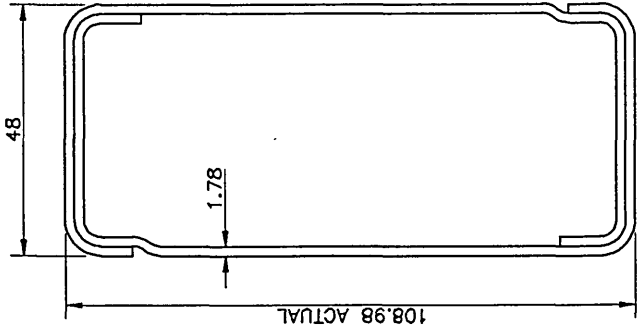
NOTE

1. VIEW ON ARROW INDICATES FRONT OF BEAM.
2. SEE DRG. No. PD.054 FOR ROLLED SECTION TOLERANCES.

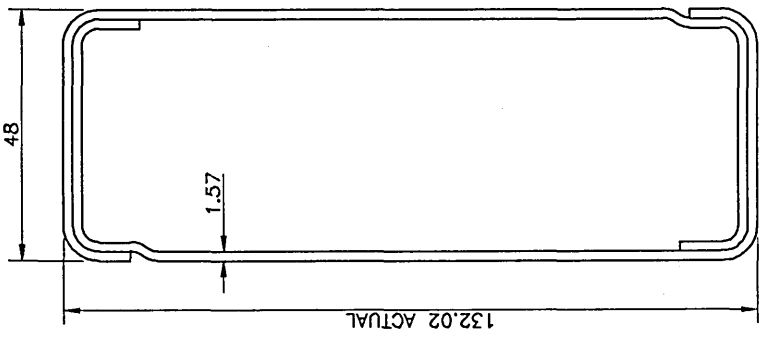
C 13/1/97 DIMENSION 1.6 CHANGED TO
 B 10/7/95 REDRAWN ON CAD.

REVISION	DATE		REDIRACK LTD. WILMOROCK KILNURBERT ROTHENHAM NOTTINGHAM S42 2SU TEL - 01709 FAX - 01709
DRAWN BY D. BIRBLE		TITLE STANDARD BEAM SECTIONS 50 & 76 OPEN SECTIONS 80/1.6 95/1.6 AND 95/1.78 BOXED SECTIONS	
SCALE DO NOT		DRAWING NUMBER PD.040-1	
		DATE 7/7/95	

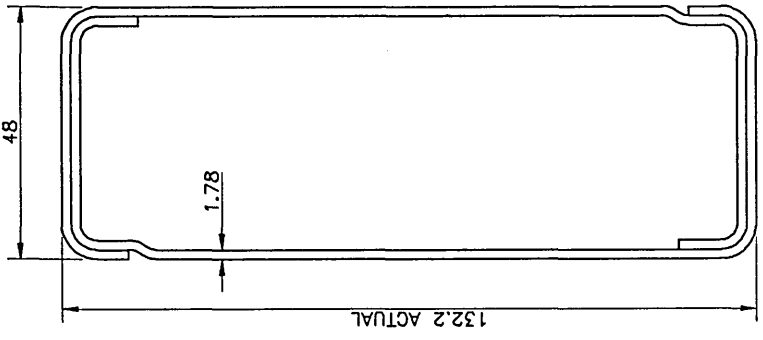
THE MAXIMUM IMPOSED POINT LOAD FROM PACKING UPRIGHTS WILL BE kg/s. THROUGH A BASE PLATE AREA OF mm.² REDIRACK ADVISE INDEPENDENT VERIFICATION OF THE CAPACITY OF THE SUPPORTING STRUCTURE TO SUSTAIN SUCH LOADINGS.



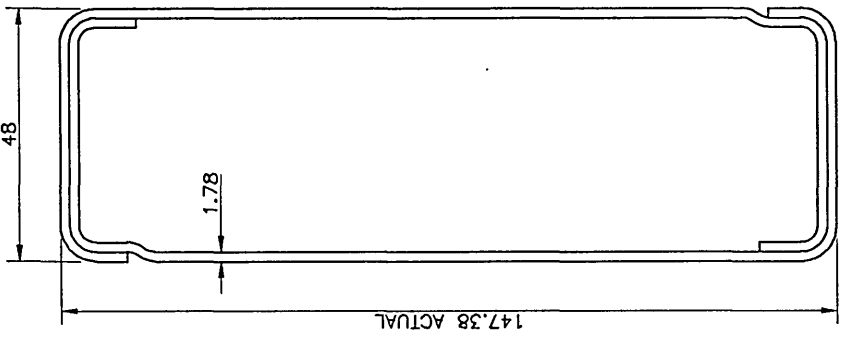
110/1.78 BOXED



130/1.6 BOXED



130/1.78 BOXED



145/1.78 BOXED

NOTE

- 1. VIEW ON ARROW INDICATES FRONT OF BEAM.
- 2. SEE DRG. No. PD.054 FOR ROLLED SECTION TOLERANCES.

- C 13/1/97 DIMENSION 1.6 CHANGED TO 1.78
- B 10/7/95 REDRAWN ON CAD.

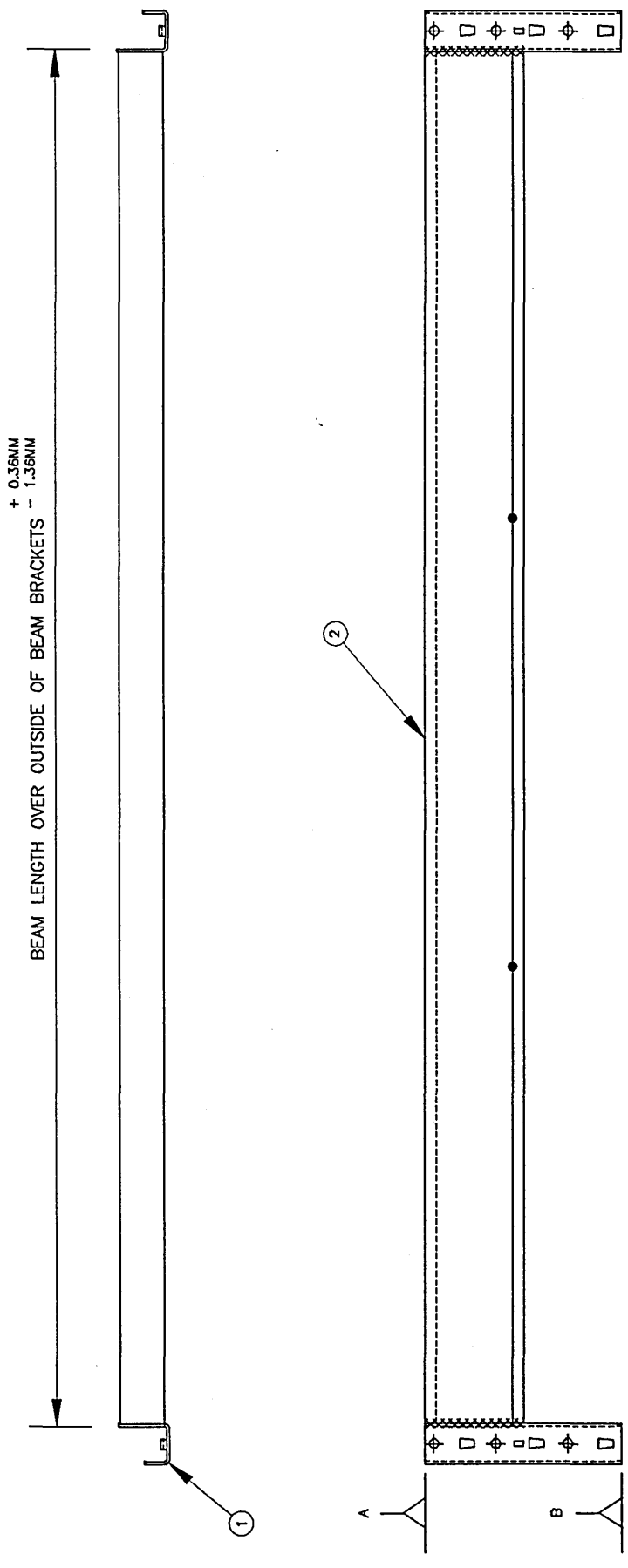
REVISION	DATE	Redirack REDIRACK LTD WHARF RD ROTHWAY SOUTH YK SOUTH YORKS YO21 2JG TEL: 01773 821076 FAX: 01773 821077						
		TITLE STANDARD BEAM SECTIONS 110/1.78 130/1.6 130/1.78 145/1.78 BOXED SECTIONS						
		<table border="1"> <tr> <td>DRAWN BY D.BREWER</td> <td>DATE 7/7/95</td> <td>DRAWING NUMBER PD.040-2</td> </tr> <tr> <td>SCALE</td> <td>DO NOT</td> <td></td> </tr> </table>	DRAWN BY D.BREWER	DATE 7/7/95	DRAWING NUMBER PD.040-2	SCALE	DO NOT	
DRAWN BY D.BREWER	DATE 7/7/95	DRAWING NUMBER PD.040-2						
SCALE	DO NOT							

THE MAXIMUM IMPOSED POINT LOAD FROM RACKING UPRIGHTS WILL BE _____ kgs. THROUGH A BASE PLATE AREA OF _____ mm.² REDIRACK ADVISE INDEPENDENT VERIFICATION OF THE CAPACITY OF THE SUPPORTING STRUCTURE TO SUSTAIN SUCH LOADING.

DO NOT SCALE - WORK TO DIMENSIONS - IF IN DOUBT ASK

© REDIRACK LTD. THE INFORMATION ON THIS DRAWING IS THE PROPERTY OF REDIRACK LIMITED. IT MUST NOT BE COPIED WITHOUT WRITTEN CONSENT AND MU

FACTORY USE ONLY



- NOTES:**
1. WELD ITEMS 1 & 2 AS SHOWN USING A 3MM FILLET WELD DOWN FRONT & BACK FACES
 2. THE BEAM LENGTH MEASUREMENT IS TAKEN AT DATUM A.
 3. WHEN THE BEAM LENGTH MEASUREMENT IS TAKEN AT DATUM B. IT MUST NOT VARY FROM THAT TAKEN AT DATUM A. BY +/- 0.5MM
 4. FOR INSPECTION PURPOSES BEAM LENGTH = THE CLEAR ENTRY DIMENSION (+ 6MM).
 5. THE TOLERANCE ON THE BEAM SECTION LENGTH (AS CROPPED) = +0 - 1MM

ITEM No	DRG No	DESCRIPTION	QTY
1	SD002	BEAM BRACKET	2
2	PD040	BEAM SECTIONS	1

THIRD ANGLE PROJECTION

REVISION A DATE 13/1/97 SPOT WELDS ADDED



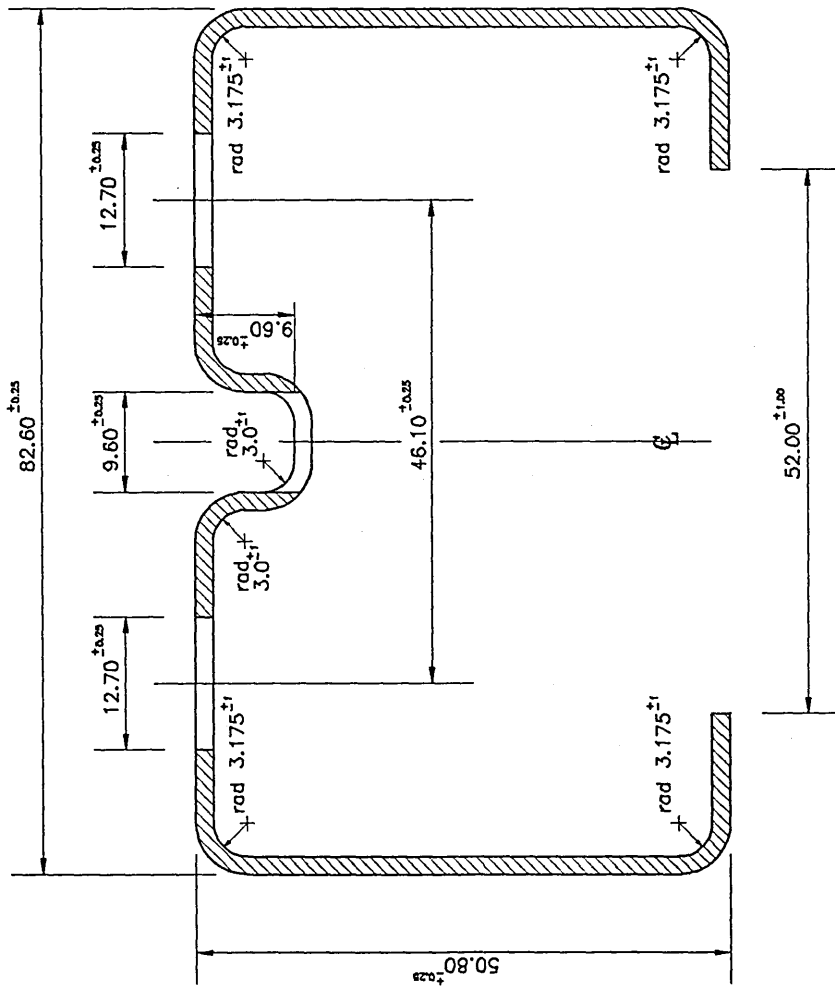
REDIRACK LTD
WHARF ROAD
ROTHERHAM
SOUTH YORKSHIRE
S64 6TJ
TEL-01709
FAX-01709

TITLE BEAM ASSEMBLY DRAWING



DRAWN BY B. LOBERTSON DATE 21/8/98
SCALE N.T.S.
DRAWING NUMBER PD.049-A

THE MAXIMUM IMPOSED POINT LOAD FROM RACKING UPRIGHTS WILL BE kgs. THROUGH A BASE PLATE AREA OF mm.² REDIRACK ADVISE INDEPENDENT VERIFICATION OF THE CAPACITY OF THE SUPPORTING STRUCTURE TO SUSTAIN SUCH LOADING.



MATERIAL

HR4. TO BS.1449 PART ONE 1983
OR
TENFORM TO BS.1449 PART I.

NOTE

GENERAL ANGULAR TOLERANCE $\pm 0.5^\circ$.

ANGULAR TOLERANCE INCREASED TO $\pm 5^\circ$
OVER BOTTOM AND TOP 150 ± 3 OF UPRIGHT
LENGTH DUE TO SPLAY ON CUT-OFF.

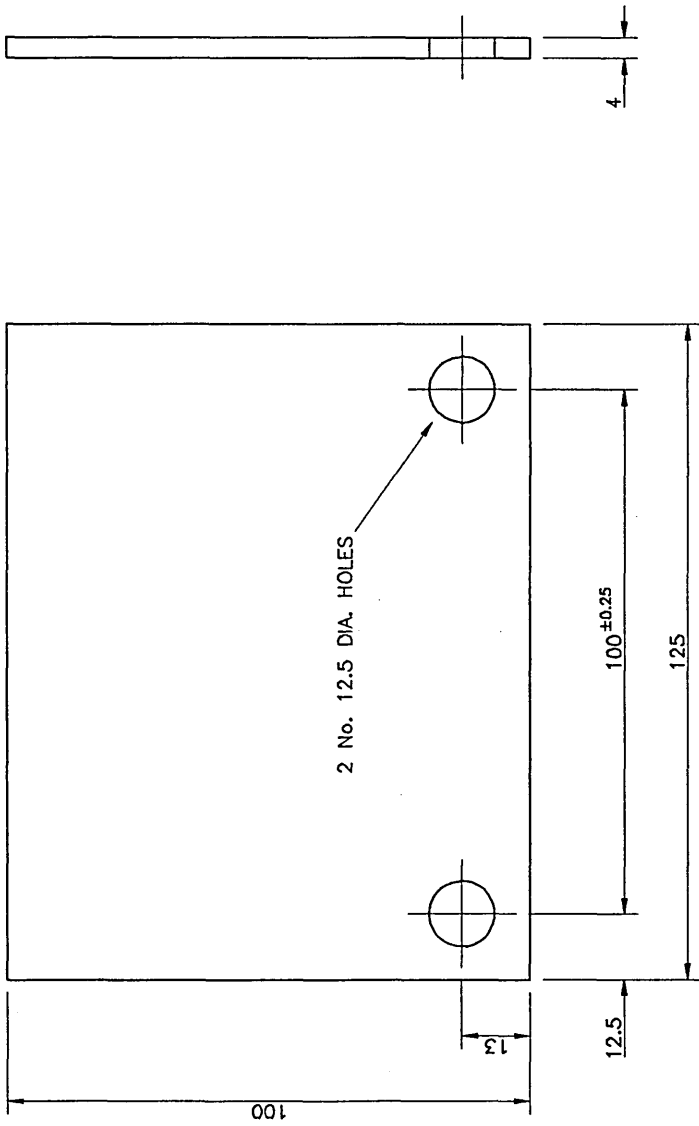
E 6/1/97 STEEL SPECIFICATION REVISED
D 2/2/95 REDRAWN ON CAD-TOLERANCES UPD.

	REVISION	DATE		Redirack <small>REDIRACK LTD MILLWAY BROTHERVA SAKASSU TEL-01706 FAX-01706</small>
			SD17 UPRIGHT SECTION. PUNCHED.	
		DRAWN BY D. BIRBLE	DATE 25/1/95	DRAWING NUMBER SD.006-0
		SCALE	Do Not	

THE MAXIMUM IMPROVED POINT LOAD FROM PACKING UPRIGHTS WILL BE kg. THROUGH A BASE PLATE AREA OF mm². REDIRACK ADVISE INDEPENDENT VERIFICATION OF THE CAPACITY OF THE SUPPORTING STRUCTURE TO SUSTAIN SUCH LOADS.

DO NOT SCALE - WORK TO DIMENSIONS - IF IN DOUBT ASK

© REDIRACK LTD. THE INFORMATION ON THIS DRAWING IS THE PROPERTY OF REDIRACK LIMITED. IT MUST NOT BE COPIED WITHOUT WRITTEN CONSENT AND MUST BE RETURNED ON



MATERIAL

P&O MILD STEEL SLIT COIL
TO BS 1449 1983 GRADE HR4
COIL SIZE 125 X 4
TOLERANCE ON COIL WIDTH +0 -0.25

GENERAL TOLERANCE ±0.5MM

**PACKING PLATES AS DRAWN EXCEPT THICKNESS
PACKING PLATE THICKNESSES 1, 2, 3MM**

C 6/1/97 MATERIAL SPEC. & TOLS. ADD
B 12/6/95 REDRAWN ON CAD.



REVISION DATE
Redirack
REDIRACK
WARRANTY
DEPARTMENT
SOUTH YD
S252SU
0176
FA-0176



TITLE
STANDARD BASEPLATE
125 X 100 X 4



DRAWN BY DATE 12/6/95
D. BIDDLE
SCALE DO NOT
DRAWING NUMBER
SD.008-C

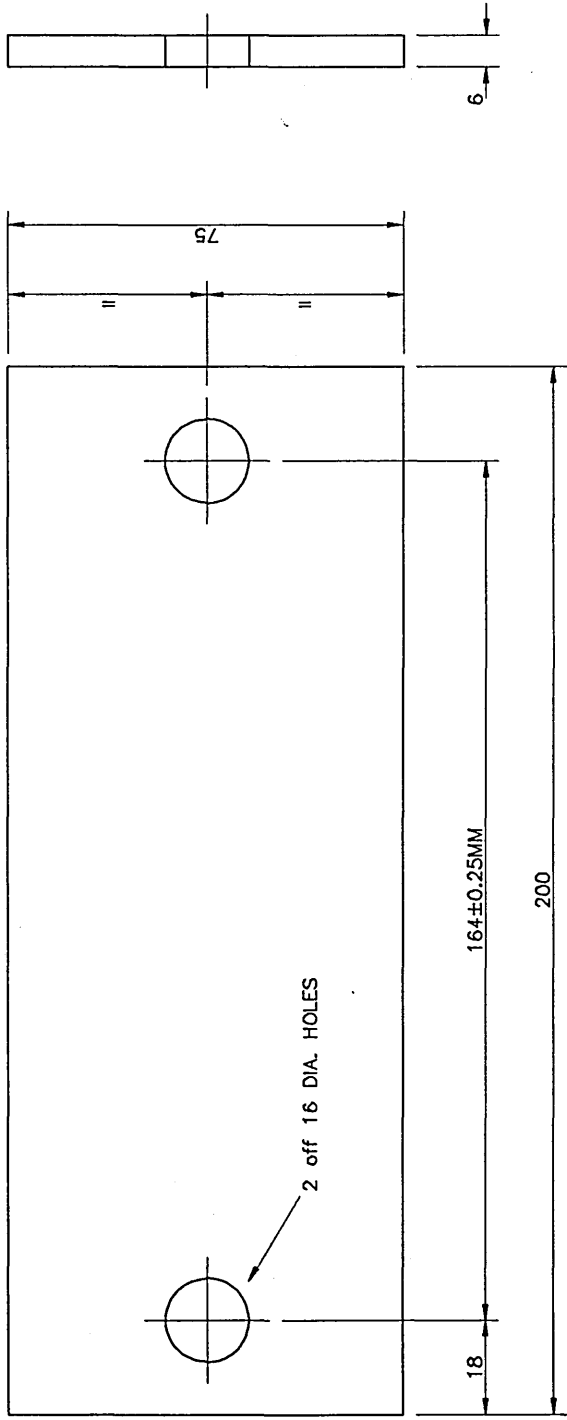
THE MAXIMUM IMPOSED POINT LOAD FROM PACKING UPRIGHTS WILL BE kg. THROUGH A BASE PLATE AREA OF mm.² REDIRACK ADVISE INDEPENDENT VERIFICATION OF THE CAPACITY OF THE SUPPORTING STRUCTURE TO SUSTAIN SUCH LOADING.

DO NOT SCALE - WORK TO DIMENSIONS - IF IN DOUBT ASK

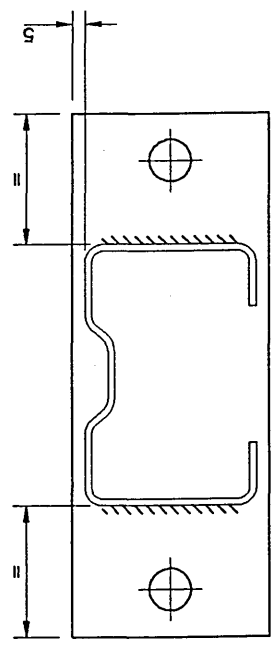
© REDIRACK LTD. THE INFORMATION ON THIS DRAWING IS THE PROPERTY OF REDIRACK LIMITED. IT MUST NOT BE COPIED WITHOUT WRITTEN CONSENT AND MUST BE RETURNED ON

MATERIAL
P80 MILD STEEL SHEARED STRIP
TO BS 1449 1983 GRADE HR4
TOLERANCE ON 200 WIDE STRIP +0

GENERAL TOLERANCE ±0.5MM



PACKING PLATES AS DRAWN EXCEPT THICKNESS
PACKING PLATE THICKNESSES 1, 2, 3MM



WELDING DETAIL (HD UPRIGHT SHOWN, SD UPRIGHT SIMILAR)

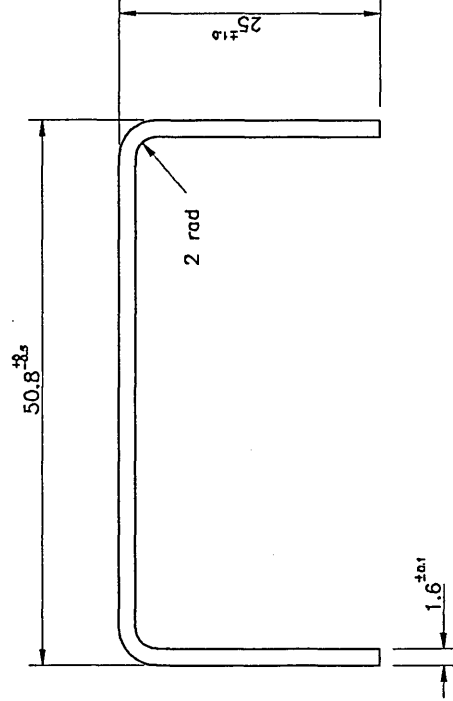
- E 28/10/98 THICKNESS CORRECTED
- D 6/1/97 MATERIAL SPECIFICATION ADDED
- C 12/6/95 REDRAWN ON CAD.

	Redirack DRIVE-IN BASEPLATE 200 X 75 X 6	DRAWN BY D. BIRRELL
REVISION DATE	DRAWING NUMBER SD.010-E	SCALE DO NOT

THE MAXIMUM IMPOSED POINT LOAD FROM PACKING UPRIGHTS WILL BE _____ kgs. THROUGH A BASE PLATE AREA OF _____ mm². REDIRACK ADVISE INDEPENDENT VERIFICATION OF THE CAPACITY OF THE SUPPORTING STRUCTURE TO SUSTAIN SUCH LOADING.

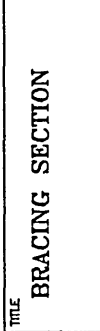
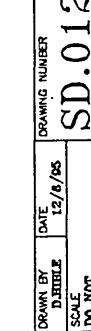
DO NOT SCALE - WORK TO DIMENSIONS - IF IN DOUBT ASK

© REDIRACK LTD. THE INFORMATION ON THIS DRAWING IS THE PROPERTY OF REDIRACK LIMITED. IT MUST NOT BE COPIED WITHOUT WRITTEN CONSENT AND MUST BE RETURNED ON



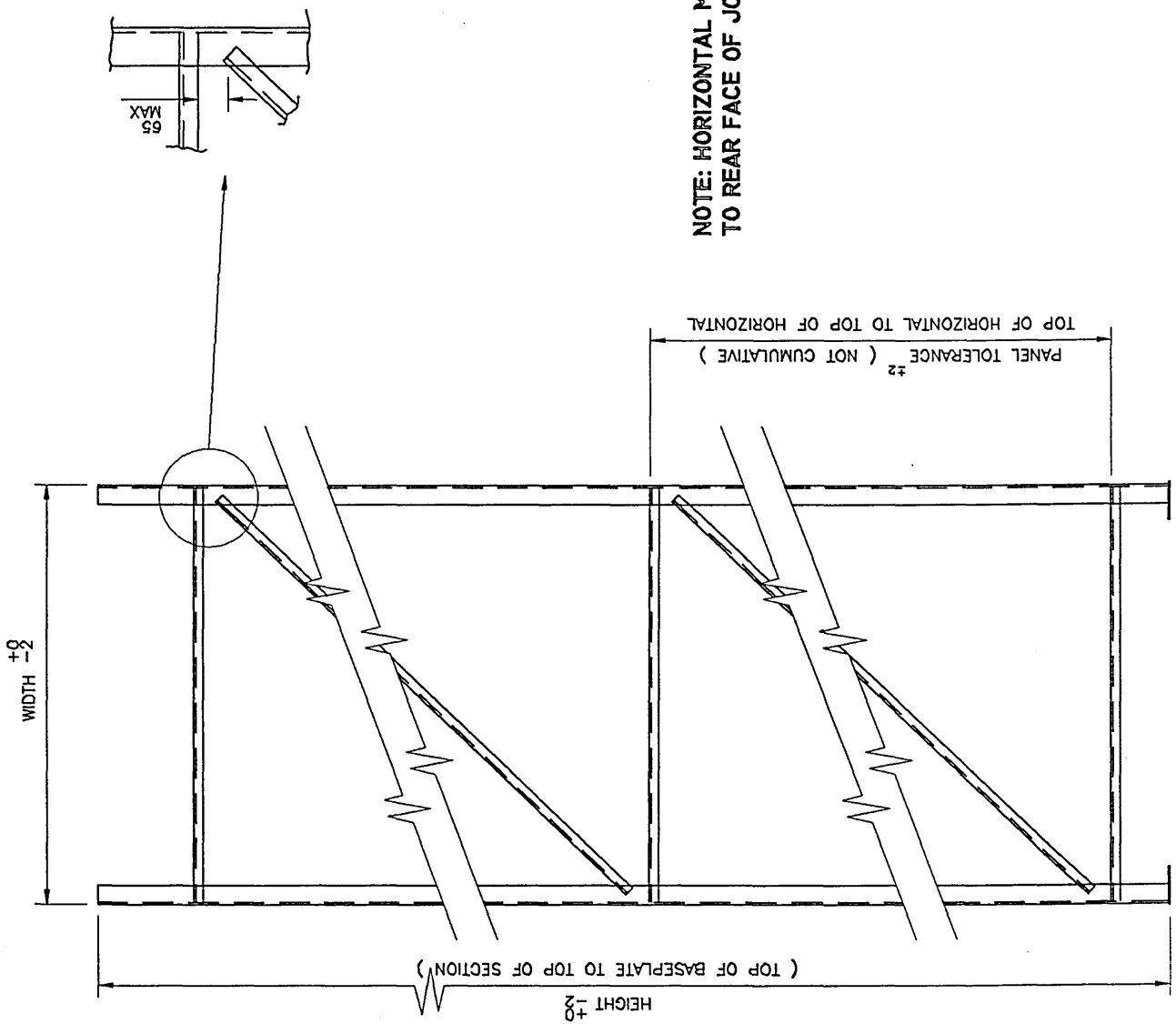
MATERIAL
 P&O MILD STEEL SLIT COIL
 TO BS 1449 1983 CS4
 TEMPER ROLLED TO 27/33 TONNES YIELD
 WITH 6% ELONGATION ON 50MM
 FORMING TOLERANCE ±0.5
 COIL SIZE 94±0.127 X 1.57±0.03

F 4/2/98 50.8 WAS 52
 E 6/1/97 MATERIAL SPECIFICATION N
 D 12/6/95 REDRAWN ON CAD.

	REVISION	DATE	
			
			
DRAWN BY D. BEHLE		DATE 12/6/95	DRAWING NUMBER SD.012-F
TITLE BRACING SECTION		SCALE DO NOT	

THE MAXIMUM IMPOSED POINT LOAD FROM RACKING UPRIGHTS WILL BE _____ mm. REDIRACK ADVISE INDEPENDENT VERIFICATION OF THE CAPACITY OF THE SUPPORTING STRUCTURE TO SUSTAIN SUCH LOADING.

kg. THROUGH A BASE PLATE AREA OF _____



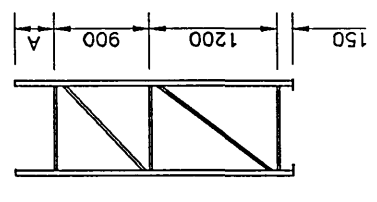
NOTE: HORIZONTAL MAY NOT ALWAYS EXTEND TO REAR FACE OF JOGGLE.

- D 21/1/98 WIDTH TOLERANCE WAS +1 -
- C 13/1/97 DIMENSIONS UPDATED
- B 24/6/96 REDRAWN ON CAD

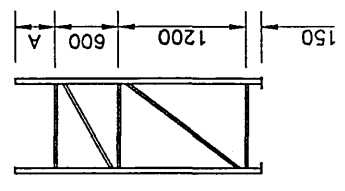
REVISION	DATE	
REDIRACK MILLHURST ROTHERHAM S70 2JW TEL: 01709 522251 FAX: 01709 522252		Redirack STANDARD FRAME DIMENSIONAL TOLERANCES

DESIGNED BY	DATE	DRAWING NUMBER
BLUNDELL	24/8/98	PD.059-D
SCALE		
DO NOT		

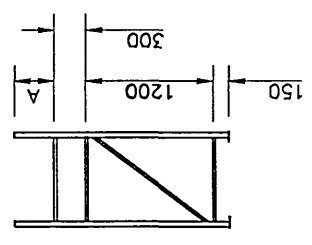
THE MAXIMUM IMPOSED POINT LOAD FROM RACKING UPRIGHTS WILL BE kg. THROUGH A BASE PLATE AREA OF mm. REDIRACK ADVISE INDEPENDENT VERIFICATION OF THE CAPACITY OF THE SUPPORTING STRUCTURE TO SUSTAIN SUCH LOADING.



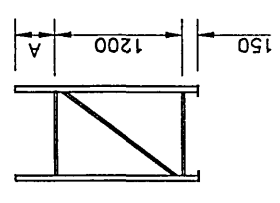
FRAME HT.	A
2400	150
2475	225
2550	300
2625	375



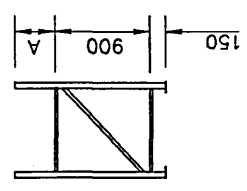
FRAME HT.	A
2100	150
2175	225
2250	300
2325	375



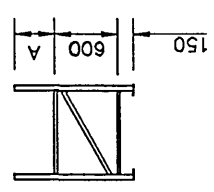
FRAME HT.	A
1800	150
1875	225
1950	300
2025	375



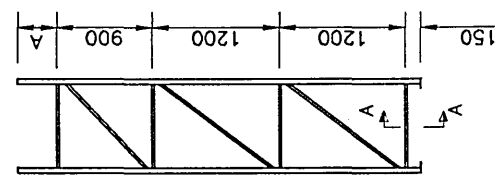
FRAME HT.	A
1500	150
1575	225
1650	300
1725	375



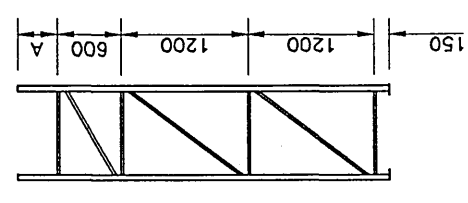
FRAME HT.	A
1200	150
1275	225
1350	300
1425	375



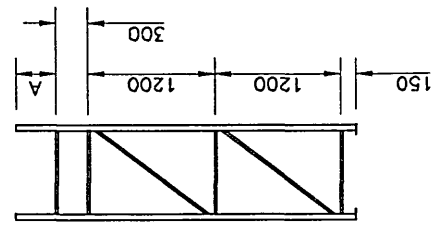
FRAME HT.	A
900	150
975	225
1050	300
1125	375



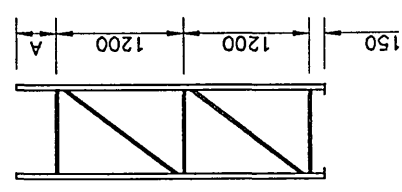
FRAME HT.	A
3600	150
3675	225
3750	300
3825	375



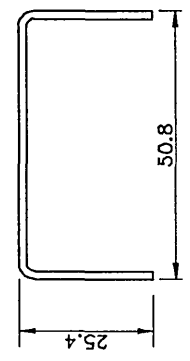
FRAME HT.	A
3300	150
3375	225
3450	300
3525	375



FRAME HT.	A
3000	150
3075	225
3150	300
3225	375



FRAME HT.	A
2700	150
2775	225
2850	300
2925	375



SECTION 'A-A'
(TYPICAL THROUGHOUT)

REVISION DATE 28/3/95 REDRAWN ON CAD

REDIRACK 1
WHARF ROAD
ROCHDALE
GROVE SOUTH YORK
S252SU
01623 708
FAX-01706

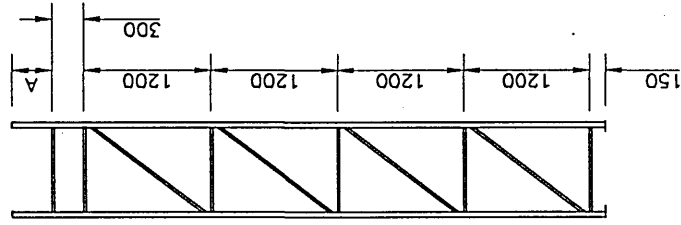
TITLE
FRAME BRACING DETAILS
FRAME HEIGHTS 900 - 3825

DRAWN BY D.HITTE DATE 28/3/95
SCALE DO NOT
DRAWING NUMBER PD.035-1

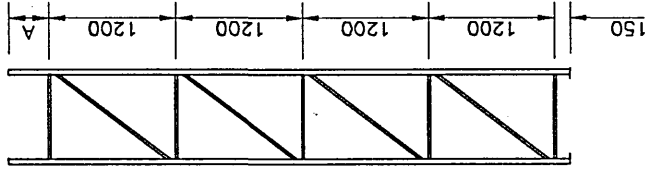


THE MAXIMUM IMPOSED POINT LOAD FROM PACKING UPRIGHTS WILL BE kg/s THROUGH A BASE PLATE AREA OF mm.² REDIRACK ADVISE INDEPENDENT VERIFICATION OF THE CAPACITY OF THE SUPPORTING STRUCTURE TO SUSTAIN SUCH LOADING.

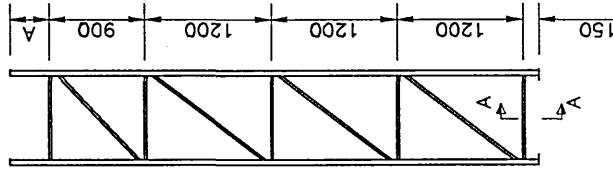
DO NOT SCALE - WORK TO DIMENSIONS - IF IN DOUBT ASK © REDIRACK LTD. THE INFORMATION ON THIS DRAWING IS THE PROPERTY OF REDIRACK LIMITED. IT MUST NOT BE COPIED WITHOUT WRITTEN CONSENT AND MUST BE RETURNED ON



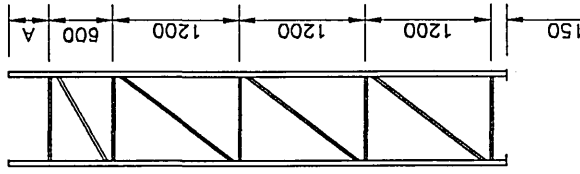
FRAME HT.	A
5400	150
5475	225
5550	300
5625	375



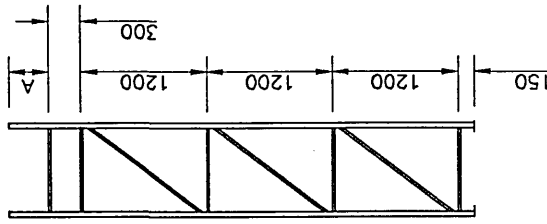
FRAME HT.	A
5100	150
5175	225
5250	300
5325	375



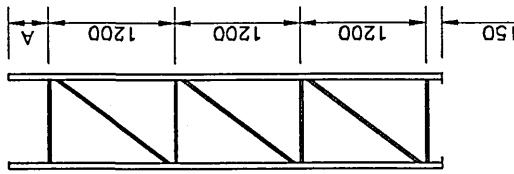
FRAME HT.	A
4800	150
4875	225
4950	300
5025	375



FRAME HT.	A
4500	150
4575	225
4650	300
4725	375



FRAME HT.	A
4200	150
4275	225
4350	300
4425	375



FRAME HT.	A
3900	150
3975	225
4050	300
4125	375

B 28/3/95 REDRAWN ON CAD



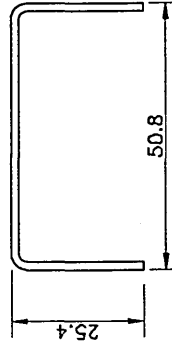
Redirack



TITLE
FRAME BRACING DETAIL
FRAME HEIGHTS 3900 - 5625

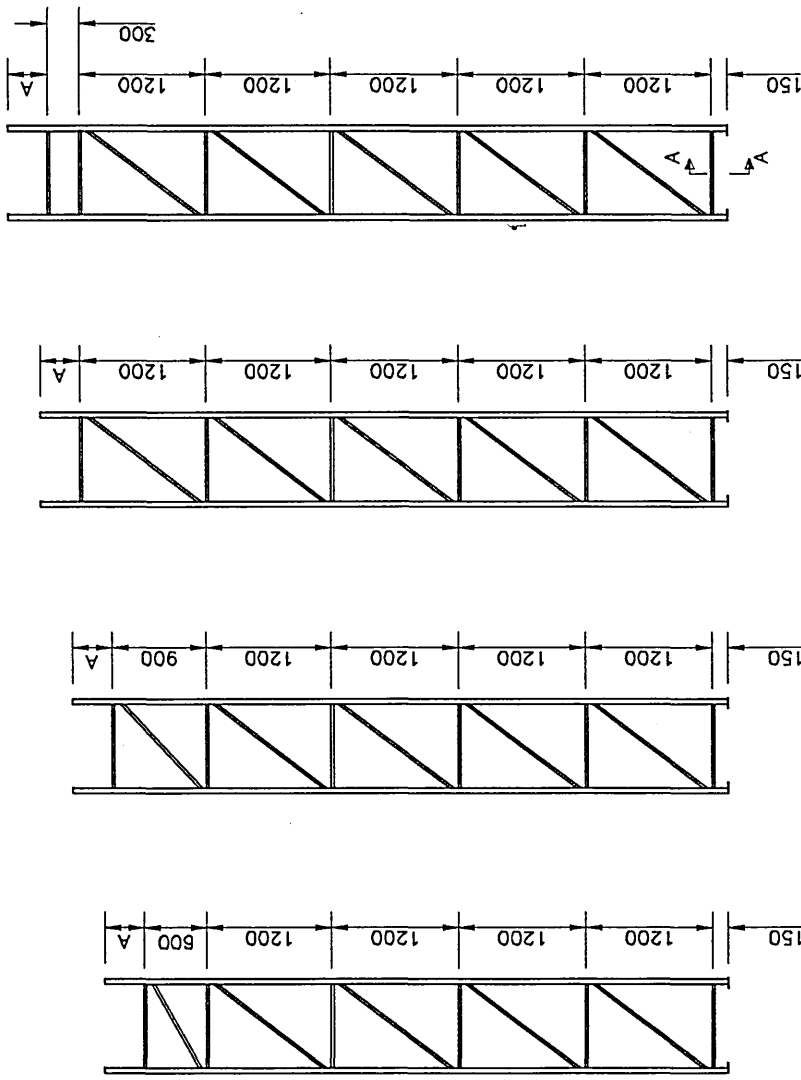


DRAWN BY D. JIBBLIZ DATE 28/3/95
DRAWING NUMBER PD.035-2
SCALE DO NOT



SECTION 'A-A'
(TYPICAL THROUGHOUT)

THE MAXIMUM IMPOSED POINT LOAD FROM RACKING UPRIGHTS WILL BE kg. THROUGH A BASE PLATE AREA OF mm.² REDIRACK ADVISE INDEPENDENT VERIFICATION OF THE CAPACITY OF THE SUPPORTING STRUCTURE TO SUSTAIN SUCH LOADINGS.

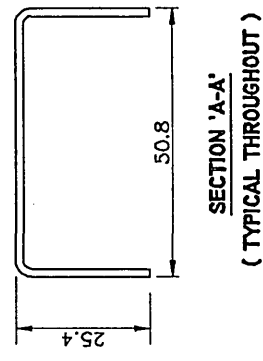


FRAME HT.	A
6600	150
6675	225
6750	300
6825	375

FRAME HT.	A
6300	150
6375	225
6450	300
6525	375

FRAME HT.	A
6000	150
6075	225
6150	300
6225	375

FRAME HT.	A
5700	150
5775	225
5850	300
5925	375



B 28/3/95 REDRAWN ON CAD

	REVISION DATE 28/3/95	REDIRACK LTD MILLHURST ROTHERHAM S62 2JL TEL: 01709 743-01700
	TITLE FRAME BRACING DETAIL FRAME HEIGHTS 5700 - 6825	DRAWN BY D. EBBELZ DATE 28/3/95
	DRAWING NUMBER PD.035-3	SCALE DO NOT

THE MAXIMUM UNPOSED POINT LOAD FROM PACKING UPRIGHTS WILL BE kgs. THROUGH A BASE PLATE AREA OF mm². REDIRACK ADVISE INDEPENDENT VERIFICATION OF THE CAPACITY OF THE SUPPORTING STRUCTURE TO SUSTAIN SUCH LOADING.

Appendix B

Containing :

1. Concrete design mix for floor connector test.
2. Isometric layout of floor connector test rig.

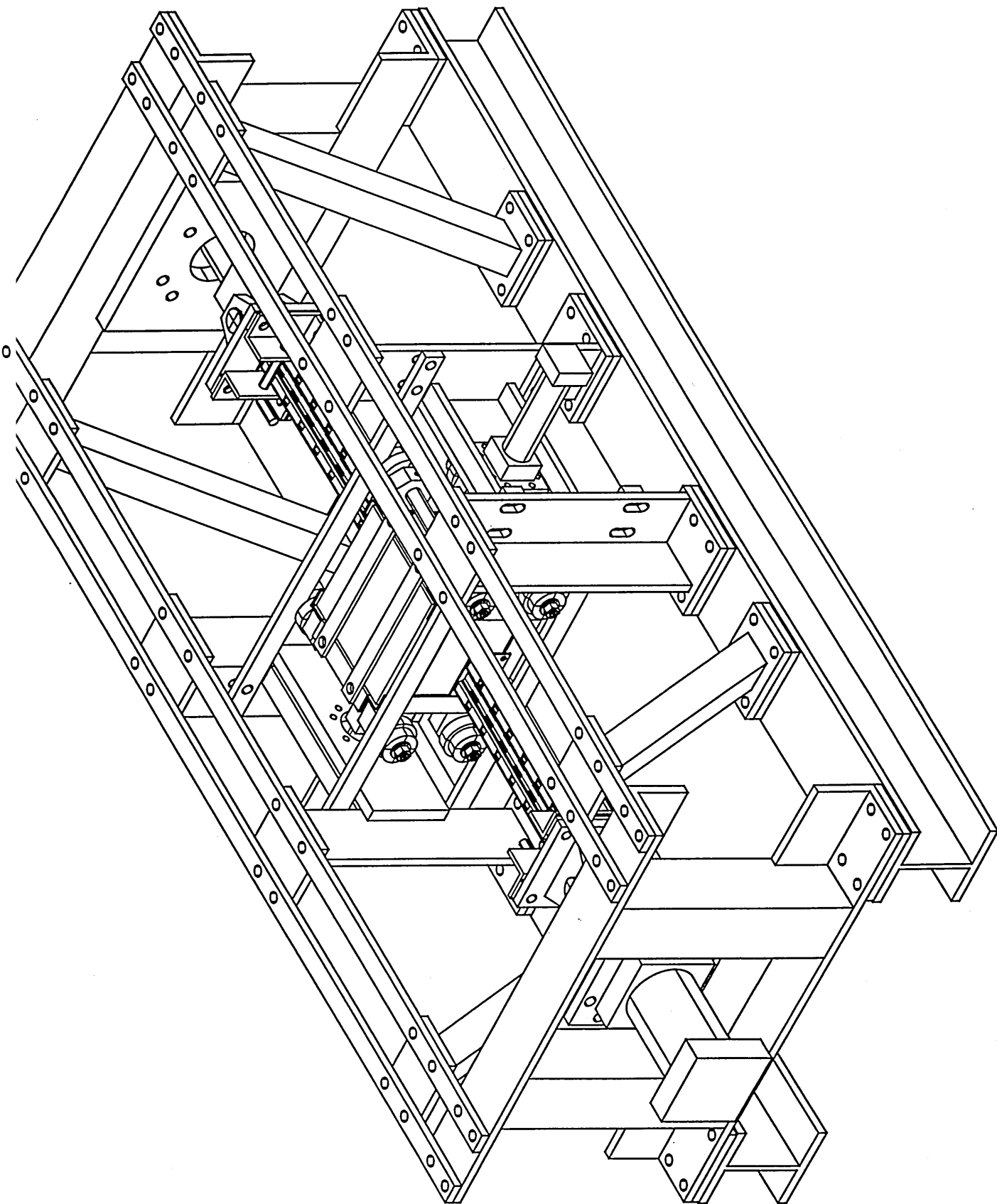
Appendix B

Concrete mix design for floor connector test

Cement content (Portland cement)	-	300 kg/m ³
Fine aggregate Zone M (medium) sand	-	740 kg/m ³ (591 + 25%)
Course aggregate 20mm - 5mm graded gravel	-	1314 kg/m ³
Water	-	195 kg/m ³

Design mix based on 60mm - 180mm slump

Volume : 0.3m x 0.3m x 0.3m / cube



Curve fit equation :

$$x^4 = A := -6072 \quad x^3 = B := 3209 \quad x^2 = D := -670 \quad x = E := 60.6 \quad C := 0.00231$$

Design moment (Mrd) :

$$y1 := 1.232 \quad \text{kNm}$$

Intercept of curve (y-axis) :

$$y2 := 0.003 \quad \text{kNm}$$

Intercept of curve (x-axis) :

$$x2 := 0 \quad \text{Rads.}$$

Initial estimate of x at the intersection of y = Mrd and the curve fit :

$$x := .01 \quad \text{Rads.}$$

$$x1 := \text{root}(A \cdot x^4 + B \cdot x^3 + D \cdot x^2 + E \cdot x + C - y1, x)$$

Calculated value of x at the intersection of y = Mrd and the curve fit :

$$x1 = 0.028$$

Total Area :

$$F := y1 \cdot x1$$

$$F = 0.034$$

Area under curve :

$$G := \int_{x2}^{x1} A \cdot x^4 + B \cdot x^3 + D \cdot x^2 + E \cdot x + C \, dx$$

$$G = 0.019$$

Area of triangle :

$$H := F - G - x2 \cdot y1$$

$$H = 0.015$$

Value of x to determine stiffness :

$$I := \frac{2 \cdot H}{y1 - y2}$$

$$I = 0.025$$

Magnitude check (see Fig. 5.5.2, FEM) :

$$\frac{x1}{1.15} \leq I$$

$$\frac{x1}{1.15} = 0.024$$

Beam connector stiffness :

$$Kti := \frac{y1 - y2}{I}$$

$$Kti = 49.989 \quad \text{kNm/Rad}$$

Appendix D

Statistical treatment of test data (FEM Table 5.1.2.) :

n	k_s
3	3.15
4	2.68
5	2.46
6	2.33
7	2.25
8	2.19
9	2.14
10	2.10
15	1.99
20	1.93
30	1.86
40	1.83
50	1.81
100	1.76
∞	1.64

n = number of tests performed

k_s = statistical correction factor for test data representing the 95% fractile at a confidence level of 75%

Appendix E

Containing :

1. Ansys 5.4. keystrokes - 4 level, 6 bay down and cross-aisle rack.
2. Visual Basic sub-routines for SEMA design program.
3. Deformed down-aisle rack geometry taken from Fig.6.7. (load case 3).

Appendix E

4 LEVEL, 6 BAY DOWN-AISLE RACKING SYSTEM : KEY STROKES

PREP 7

CREATE / NODES / IN ACTIVE CS 1,0,0,0
COPY / NODES COPY / PICK ALL 5,1575,1
COPY / NODES COPY / PICK ALL 7,2700,5
 NODES COPY / PICK ALL 3,,100

ELEMENT TYPE / ADD / BEAM , 2-D ELASTIC / APPLY (TYPE 1)
 COMBINATION, SPRING-DAMPER 14 / OK (TYPE 2)
 OPTIONS / TORSIONAL ROTZ, 3-D TORSIONAL (TYPE 2)
 OPTIONS / (K6) INCLUDE OUTPUT / OK / CLOSE (TYPE 1)

REAL CONSTANTS / ADD / TYPE 1 / 1 (AREA, IZZ, HEIGHT*) / APPLY (UPRIGHT)
 TYPE 1 / 2 (AREA, IZZ, HEIGHT*) / OK (BEAM)
 * FOR UPRIGHTS = FRONT FACE WIDTH, FOR BEAMS = DEPTH
 ADD / TYPE 2 / 3 (STIFFNESS) / APPLY (BEC)
 / TYPE 2 / 4 (STIFFNESS) / OK / CLOSE (FC)

MATERIAL PROPERTIES / ISOTROPIC / 1 / (EX=) 210000 / OK

REAL,1
TYPE,1
MAT,1

E,1,2 (INSERTS ELEMENT BETWEEN NODES 1 AND 2)
COPY / ELEMENTS, AUTO-NUMBERED / PICK-ALL / 4,1 / APPLY
 / PICK-ALL / 7,5 / OK

REAL,2

E,102,107
COPY / ELEMENTS, AUTO-NUMBERED / PICK, SINGLE / 4,1 / APPLY
 / PICK, BOX / 3,10 / OK

E,207,212
COPY / ELEMENTS, AUTO-NUMBERED / PICK, SINGLE / 4,1 / APPLY
 / PICK, BOX / 3,10 / OK

REAL,3
TYPE,2

E,2,102
COPY / ELEMENTS, AUTO-NUMBERED / PICK, SINGLE / 4,1 / APPLY
 / PICK, SINGLE / 6,5 / OK

E,207,7
COPY / ELEMENTS, AUTO-NUMBERED / PICK, SINGLE / 4,1 / APPLY
 / PICK, SINGLE / 6,5 / OK

REAL,4

E,1,101
COPY / ELEMENTS, AUTO-NUMBERED / PICK, SINGLE / 7,5 / OK

FILE / READ INPUT FROM ... / ELEM.MAC (BREAKS BEAMS AND UPRIGHTS INTO 5
ELEMS)

SELECT / ENTITIES / BY ATTRIBUTES / ELEMENTS / REAL SET NUMBER / 2

SOLUTION

LOAD / APPLY / PRESSURE / ON BEAMS / PICK ALL / 1,(*UDL)
 UDL (Nmm) = (PAY LOAD FOR 2 BEAMS (kg) x 9.81/2) / BEAM LENGTH
 NSEL,S,NODE,,2,5 / NPLT
LOAD / APPLY / FORCE,MOMENT / ON NODES / PICK, BOX / FX (Newtons)

NSEL,ALL
CPINTF,UX
CPINTF,UY

NSEL,S,NODE,,1,31,5
LOAD / APPLY / DISPLACEMENT / ON NODES / PICK, ALL / UY / UX
NSEL,S,NODE,,101,131,5
LOAD / APPLY / DISPLACEMENT / ON NODES / PICK, ALL / UY / UX / ROTZ

NSEL,ALL
NPLOT
ESEL,ALL
EPLOT

NEW ANALYSIS / STATIC
ANALYSIS OPTIONS / LARGE DEFORMATION EFFECTS, ON / STRESS STIFFNESS, ON / OK
SOLVE, CURRENT LS / OK

POST PROCESSOR
FILE / READ INPUT FROM / TABLE.MAC (for moments etc.)
LIST RESULTS / ELEM TABLE DATA / AXI, AXJ, MOMZI, MOMZJ
(axial load and moments in upright elements)

LIST RESULTS / ELEMENT SOLUTION / NODAL FORCE DATA / ALL STRUC MOME M
(moments in spring elements)

PLOT RESULTS / DEFORMED SHAPE
LIST RESULTS / NODAL SOLUTION / DOF SOLUTION / TRANSLATION UY / UX
(maximum deflection in beams [SLS only] and sway in top of rack)

4 LEVEL, 6 BAY CROSS-AISLE RACKING SYSTEM : KEY STROKES

PREP 7

CREATE / NODES / IN ACTIVE CS 1,0,0,0 ; 2,0,150,0 ; 3,0,215,0 ; 4,0,1350,0 ; 5,0,1415,0 ;
6,0,1575,0 ; 7,0,2550,0 ; 8,0,2615,0 ; 9,0,3150,0 ; 10,0,3750,0 ; 11,0,3815,0 ; 12,0,4725,0 ; 13,0,4950,0
; 14,0,5015,0 ; 15,0,6150,0 ; 16,0,6300,0 ; 17,900,0,0 ; 18,900,150,0 ; 19,900,1285,0 ; 20,900,1350,0 ;
21,900,1575,0 ; 22,900,2485,0 ; 23,900,2550,0 ; 24,900,3150,0 ; 25,900,3685,0 ; 26,900,3750,0 ;
27,900,4725,0 ; 28,900,4885,0 ; 29,900,4950,0 ; 30,900,6085,0 ; 31,900,6150,0 ; 32,900,6300,0 ;
501,0,0,0 ; 517,900,0,0

ELEMENT TYPE / ADD / BEAM , 2-D ELASTIC / APPLY (TYPE 1)
LINK, 2D SPAR 1 / APPLY (TYPE 2)
COMBINATION, SPRING-DAMPER 14 / OK (TYPE 3)
OPTIONS / TORSIONAL ROTZ, 3-D TORSIONAL (TYPE 3)
OPTIONS / (K6) INCLUDE OUTPUT / OK / CLOSE (TYPE 1)

REAL CONSTANTS / ADD / TYPE 1 / 1 (AREA, IZZ, HEIGHT*) / APPLY (UPRIGHT)
* FOR UPRIGHTS = FRONT FACE WIDTH, FOR BEAMS = DEPTH
ADD / TYPE 2 / 2 (AREA) / OK (BRACING)
ADD / TYPE 3 / 3 (STIFFNESS = 0) / OK / CLOSE (FC)

MATERIAL PROPERTIES / ISOTROPIC / 1 / (EX=) 210000 / OK

REAL,1
TYPE,1
MAT,1

E,1,2 E,31,32 (INSERTS ELEMENT BETWEEN NODES)

TYPE,2
REAL,2

E,2,18; E,3,19; E,4,20; E,5,22; E,7,23; E,8,25; E,10,26; E,11,22; E,13,29; E,14,30; E,15,31

FILE / READ INPUT FROM ... / ELEM.MAC (BREAKS UPRIGHTS INTO 4 ELEMENTS)

TYPE,3
REAL,3

E,1,501 ; E,17,517

CPINTF,UX
CPINTF,UY

SOLUTION

SELECT / ENTITIES / NODES / BY NUM / 1,17 / OK
LOAD / APPLY / DISPLACEMENT / ON NODES / PICK, ALL / UY / UX
SELECT / ENTITIES / NODES / BY NUM / 501,517 / OK
LOAD / APPLY / DISPLACEMENT / ON NODES / PICK, ALL / UY / UX / ROTZ

SELECT / ENTITIES / NODES / BY NUM / 6,9,12,16,21,24,27,32 / OK
LOAD / APPLY / FORCE / ON NODES / PICK ALL / FY, -16800 (Newtons)

ESEL,ALL
EPLOT

NEW ANALYSIS / STATIC
ANALYSIS OPTIONS / LARGE DEFORMATION EFFECTS, ON / STRESS STIFFNESS, ON / OK
SOLVE, CURRENT LS / OK

POST PROCESSOR

FILE / READ INPUT FROM / TABLE.MAC (for moments etc.)

LIST RESULTS / ELEM TABLE DATA / AXI, AXJ, MOMZI, MOMZJ
(axial load and moments in upright elements)

LIST RESULTS / ELEMENT SOLUTION / NODAL FORCE DATA / ALL STRUC MOME M
(moments in spring elements)

PLOT RESULTS / DEFORMED SHAPE

LIST RESULTS / NODAL SOLUTION / DOF SOLUTION / TRANSLATION UY / UX
(maximum deflection in beams [SLS only] and sway in top of rack)

Visual Basic sub-routines for SEMA design program

Sub SEMA1()

```
Sheets("Summary of results").Activate
Range("A2:M250").Select
Selection.ClearContents
Range("A2").Select
Sheets("Uprights and beams").Activate
Cells(26, 11).Value = 0
Sheets("Redirack design to SEMA").Activate
```

End Sub

Sub Optimise_load()

```
With Toolbars(8)
    .Left = 601
    .Top = 9
End With
ActiveWindow.TabRatio = 0.823
```

Dim Reqloadbeam, Reqloadupright, loadincrement As Integer

```
loadincrement = 25
Reqloadbeam = Sheets("Redirack design to SEMA").Cells(3, 3).Text
```

110 If Sheets("Redirack design to SEMA").Cells(7, 7).Text = "Beam failure !" Then

 Do Until Sheets("Redirack design to SEMA").Cells(7, 7).Text = "Beam ok"

```
        Reqloadbeam = Reqloadbeam - loadincrement
        Sheets("Redirack design to SEMA").Cells(3, 3).Value = Reqloadbeam
```

 Loop

```
        Reqloadbeam = Reqloadbeam - 1
```

 Do Until Sheets("Redirack design to SEMA").Cells(7, 7).Text = "Beam failure !"

```
        Reqloadbeam = Reqloadbeam + 1
        Sheets("Redirack design to SEMA").Cells(3, 3).Value = Reqloadbeam
```

 Loop

```
        Reqloadbeam = Reqloadbeam - 1
```

Else

 Do Until Sheets("Redirack design to SEMA").Cells(7, 7).Text = "Beam failure !"

```
        Reqloadbeam = Reqloadbeam + loadincrement
        Sheets("Redirack design to SEMA").Cells(3, 3).Value = Reqloadbeam
```

 Loop

If Sheets("Redirack design to SEMA").Cells(7, 7).Text = "Beam failure !" Then

 Do Until Sheets("Redirack design to SEMA").Cells(7, 7).Text = "Beam ok"

```
        Reqloadbeam = Reqloadbeam - 1
        Sheets("Redirack design to SEMA").Cells(3, 3).Value = Reqloadbeam
```

 Loop

End If

End If

```
Reqloadupright = Sheets("Redirack design to SEMA").Cells(3, 3).Text
```

If Sheets("Redirack design to SEMA").Cells(8, 7).Text = "Upright failure !" Then

```

Do Until Sheets("Redirack design to SEMA").Cells(8, 7).Text = "Upright ok"
    Reqloadupright = Reqloadupright - loadincrement
    Sheets("Redirack design to SEMA").Cells(3, 3).Value = Reqloadupright
Loop
    Reqloadupright = Reqloadupright - 1

Do Until Sheets("Redirack design to SEMA").Cells(8, 7).Text = "Upright failure !"
    Reqloadupright = Reqloadupright + 1
    Sheets("Redirack design to SEMA").Cells(3, 3).Value = Reqloadupright
Loop
    Reqloadupright = Reqloadupright - 1

Else

    Do Until Sheets("Redirack design to SEMA").Cells(8, 7).Text = "Upright failure !"
        Reqloadupright = Reqloadupright + loadincrement
        Sheets("Redirack design to SEMA").Cells(3, 3).Value = Reqloadupright
    Loop

If Sheets("Redirack design to SEMA").Cells(8, 7).Text = "Upright failure !" Then
    Do Until Sheets("Redirack design to SEMA").Cells(8, 7).Text = "Upright ok"
        Reqloadupright = Reqloadupright - 1
        Sheets("Redirack design to SEMA").Cells(3, 3).Value = Reqloadupright
    Loop

End If
End If

If Reqloadupright <= Reqloadbeam Then
    Sheets("Redirack design to SEMA").Cells(3, 3).Value = Reqloadupright

Else

    Sheets("Redirack design to SEMA").Cells(3, 3).Value = Reqloadbeam

End If
End Sub

```

Sub SEMA2()

```

Dim count, Uptype, BType, BPTYPE, Levels, kgpair, firstbeam, Clearentry, Locat As Integer
Dim Bluck, Bsuck, Bduck, Fchk1
Dim Passfail, Fchk2

```

```

count = Sheets("Uprights and beams").Cells(26, 11).Text
If count = 0 Then count = 1
    count = count + 1
    Locat = count

```

```

Sheets("Uprights and beams").Cells(26, 11).Value = count

```

```

Uptype = Sheets("Uprights and beams").Cells(11, 3).Text
BType = Sheets("Uprights and beams").Cells(25, 3).Text
BPTYPE = Sheets("Uprights and beams").Cells(11, 11).Text
Levels = Sheets("Redirack design to SEMA").Cells(2, 3).Text
kgpair = Sheets("Redirack design to SEMA").Cells(3, 3).Text
firstbeam = Sheets("Redirack design to SEMA").Cells(4, 3).Text
Clearentry = Sheets("Redirack design to SEMA").Cells(5, 3).Text

```

Bluck = Sheets("Redirack design to SEMA").Cells(37, 4).Text
Bsuck = Sheets("Redirack design to SEMA").Cells(41, 4).Text
Bduck = Sheets("Redirack design to SEMA").Cells(45, 4).Text
Fchk1 = Sheets("Redirack design to SEMA").Cells(69, 4).Text
Fchk2 = Sheets("Redirack design to SEMA").Cells(76, 4).Text
Passfail = Sheets("Uprights and Beams").Cells(25, 11).Text

Application.Sheets("Summary of results").Activate

Cells(Locat, 1).Value = Uptype
Cells(Locat, 2).Value = BType
Cells(Locat, 3).Value = BPType
Cells(Locat, 4).Value = Levels
Cells(Locat, 5).Value = kgpair
Cells(Locat, 6).Value = firstbeam
Cells(Locat, 7).Value = Clearentry
Cells(Locat, 8).Value = Bluck
Cells(Locat, 9).Value = Bsuck
Cells(Locat, 10).Value = Bduck
Cells(Locat, 11).Value = Fchk1
Cells(Locat, 12).Value = Fchk2
Cells(Locat, 13).Value = Passfail

Application.Sheets("Redirack design to SEMA").Activate

End Sub

ANSYS 5.3
JUN 29 1998
11:33:08
DISPLACEMENT
STEP=1
SUB =1
TIME=1
RSYS=0

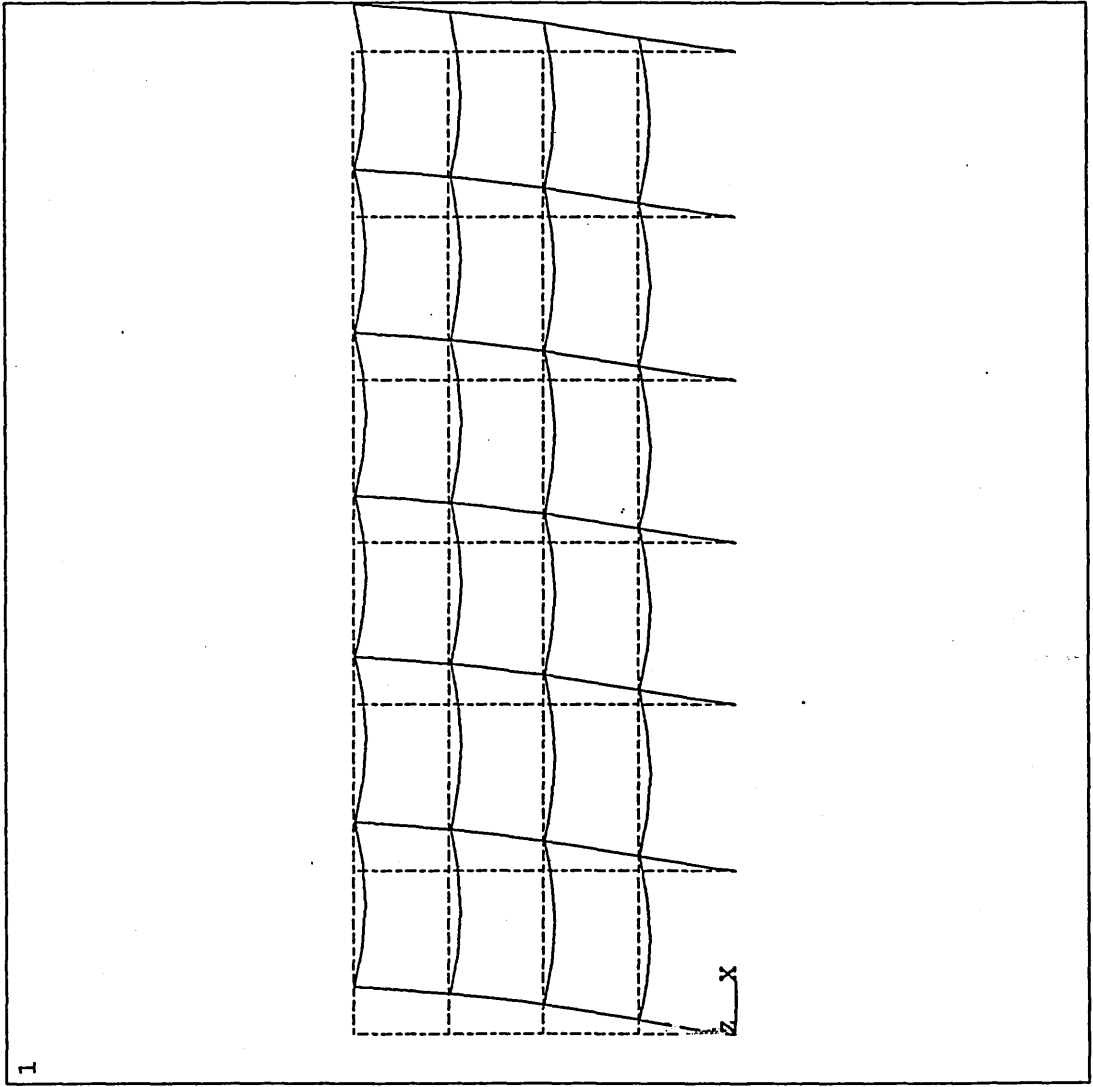


Fig. E.1. Deformed, down-aisle rack geometry from Ansys (load case 3, see Fig. 6.7)